Fluid Mud Modelling

Thesis submitted in accordance with the requirements of the University of Liverpool for the degree of Doctor in Philosophy

by

Martin Cràpper

November 1995

Volume II

Chapter 7: Fluid Mud Modelling Using the Wallingford FLUIDMUDFLOW-2D Software

7.1 Introductory Remarks

This chapter describes in detail the verification of the Wallingford FLUIDMUDFLOW-2D fluid mud modelling software using experimental data from previous investigations and from the Race Track Flume experiments described in chapters 4, 5 and 6.

Despite the fact that clear differences have been identified between fluid mud flow as measured in the field and that reproduced in the Race Track Flume, it is still felt that the verification of the mathematical model against experimental data is a worthwhile exercise, since regardless of differences in the fluid mud phenomena between laboratory and field, the laboratory data still provides sufficient information to thoroughly test the basic transport equations and the explicit layered construction of the mathematical model. It is therefore felt that a successful model test with the available laboratory data should give increased confidence in the performance of the model when applied to field data. Moreover, in addition to assessment of the model itself, use of the Wallingford FLUIDMUDFLOW-2D software to attempt to model laboratory phenomena does shed further light on certain aspects of the experimental results, and may therefore lead ultimately to a greater understanding of the physical processes at the foundation of the fluid mud phenomenon.

The model study described in this chapter was in part conducted in parallel with the analysis of experimental data detailed in the previous chapter. For this reason, some of the discussion of model results is based on information from previous laboratory work described by Georgiadis (1989) and Ali and Georgiadis (1991), whilst the remainder relates directly to Race Track Flume data which became available during the course of the study.

7.2 Model Description

The basic equations which form the Wallingford FLUIDMUDFLOW-2D fluid mud transport model are discussed in section 5.2.1, chapter 5, as consideration of these equations was fundamental to the design of the experimental programme discussed previously. This section focuses on the implementation of those equations as a finite difference algorithm in the form of a series of computer programs, but the discussion here should be read in conjunction with section 5.2.1.

7.2.1 Original Implementation of the Model

The way in which the fluid mud continuity, momentum and associated source and sink terms that form the Wallingford FLUIDMUDFLOW-2D model are set out in discretised, finite difference form is fully described in Roberts (1992). The x-direction velocity of the fluid mud at any given location is calculated according to equation 7.1:

$$u_m^{n+1} = \frac{u_m^n - S\Delta t - \Omega v_m^n \Delta t + \frac{\Delta t}{d_m \rho_m}\left[\frac{\tau_i}{|u^n - u_m^n|}\right]u^n}{1 + \frac{\Delta t}{d_m \rho_m}\left(\frac{\tau_0}{u_m^n} + \left[\frac{\tau_i}{|u^n - u_m^n|}\right]\right)} \qquad (7.1)$$

where the superscript n or n + 1 refers to the timestep. Note, however that in the all model runs carried out during the course of the current investigation, the Coriolis parameter Ω was set to zero, it being reasonable to assume that Coriolis forces were negligible in experiments of the scale of those carried out in the Race Track Flume. The slope terms S are given by:

$$S = \frac{\rho_w}{\rho_m} g \frac{\partial \eta}{\partial x} + \frac{g}{\rho_m}(\rho_m - \rho_w)\frac{\partial \eta_m}{\partial x} + \frac{g d_m}{2\rho_m}\frac{\partial}{\partial x}(\rho_m - \rho_w) \qquad (7.2)$$

with the $\partial/\partial x$ terms being calculated numerically according to the values of the property at adjacent locations at timestep n.

Shear stresses in the model are determined according to equations 5.3 and 5.4; however, values of friction factors f_w and f_m are required for these equations. f_w, the friction factor relating to the overlying water was taken as a constant value of 0.08 in the original implementation of the model, whilst the fluid mud friction factor f_m was determined from Hydraulic Research Wallingford Limited's (1992) smooth turbulence theory according to equation 5.5. However, in the model subroutines acquired by the author from Hydraulics Research Wallingford Limited, equation 5.5 had been altered to the following form:

$$f_m = \begin{cases} \dfrac{24}{R} & 0 \le R \le 46 \\ 1.506x10^6\left(0.01x10^{(\log_{10}R)^{-0.88}}\right)^{4.74} & 46 < R \le 1200 \\ 460\left(0.05x10^{(\log_{10}R)^{-1.23}}\right)^4 & 1200 < R \end{cases} \qquad (7.3)$$

with a trap to ensure that when velocity is zero then shear stress is also zero. This amended form of equation 5.5 was retained for the purposes of the investigations described in this chapter. The Reynolds number is still as given by equation 5.6:

$$R = \frac{u_m d_m}{\nu_m} \qquad (5.6)$$

for which a value of viscosity is required. In the original model this was determined from the formulation:

$$\nu_m = \nu_w e^{\left(\frac{C}{C_0}\log_e\left[\frac{\nu_{m0}}{\nu_w}\right]\right)} \qquad (7.4)$$

where C is the current concentration, C_0 is a reference concentration such that $\nu_m = \nu_{m0}$ at $C = C_0$ and ν_w is the kinematic viscosity of salt water ($1x10^{-6}m^2s^{-1}$).

Having calculated the fluid mud velocities in the x and y-directions, fluid mud flux is determined from:

$$F_{xij}^{n+1} = \begin{cases} u_{mij}^{n+1} \Delta t \Delta y C_{mij}^{n} d_{mij}^{n} & u_{mij}^{n+1} \geq 0 \\ u_{mij}^{n+1} \Delta t \Delta y C_{mi+1j}^{n} d_{mij}^{n} & u_{mij}^{n+1} \leq 0 \end{cases} \quad (7.5)$$

where F_{xij} refers to the fluid mud flux in the x-direction at location (i,j). The total mass of mud in each cell at the new timestep n + 1 is then given by:

$$M = C_{mij}^{n} d_{mij}^{n} - F_{xij}^{n+1} + F_{xi-1j}^{n+1} - F_{yij}^{n+1} + F_{yi-1j}^{n+1} + sources - sinks \quad (7.6)$$

The sources and sinks are determined relatively straightforwardly from equations 5.7 to 5.15; however, in the calculation of settling into the fluid mud layer according to equations 5.7 and 5.9, a factor β is introduced to take account of stratification effects in the mud suspension overlying the fluid mud layer. These are not, of course, modelled directly due to the two-dimensional depth averaged nature of the model algorithm. Equation 5.7 thus becomes:

$$\frac{dm}{dt} = \omega \beta C \left(1 - \frac{\tau_i}{\tau_d}\right) H(\tau_d - \tau_i) \quad (7.7)$$

whilst equation 5.9 becomes:

$$\omega = \begin{cases} \omega_{min}, & \beta C < \dfrac{\omega_{min}}{\omega_s} \\ \omega_s \beta C, & \beta C \geq \dfrac{\omega_{min}}{\omega_s} \end{cases} \quad (7.8)$$

β is defined by:

$$\beta = \frac{C_{nb}}{C} \quad (7.9)$$

in which C_{nb} is the mud concentration immediately above the fluid mud layer, and which influences settling into that layer, and C is the modelled depth averaged concentration of suspended mud.

The formulation of the finite difference algorithm used in the Wallingford FLUIDMUDFLOW-2D programs is fully explicit; however, the program logic is constructed in such a way as to provide what Roberts (1992) describes as a "partially implicit" solution, with shear stresses being calculated twice at each timestep, once for use in the determination of fluid mud velocity and then again, using the newly calculated velocity, for use in evaluating the various source/sink terms. This logic is illustrated in the flow chart in figure 7.1.

It will be seen from the flow chart that the time step sequence ends with the calculation of new concentrations. In the original implementation of FLUIDMUDFLOW-2D, this refers principally to the concentration of suspended mud overlying the fluid mud layer, the fluid mud concentration being taken as a constant value equal to C_0 as used in equation 7.4.

As discussed previously, the FLUIDMUDFLOW-2D programs represent suspended mud in a depth-averaged manner, with suspended mud transport due to convection being modelled using a flux equation similar to equation 7.5, using the water depth and velocities which are input directly into the model. The mass of suspended mud at each location depends on the mud flux and on the vertical exchange of mass with the fluid mud layer as determined from the fluid mud source/sink terms, and the concentration of suspended mud is obtained by dividing the mass of mud at each location by the grid cell area and the depth of water above the fluid mud layer. The model implementation neglects suspended mud transport due to diffusion, it being assumed that this is negligible compared to the convective terms.

The fluid mud thickness d_m at a given location was determined directly from the calculated mass of mud and the value of the constant concentration C_0 assumed for the fluid mud.

Table 7.1: Subroutines Making up FLUIDMUDFLOW-2D

Subroutine Name	Function
BEDSUM	Calculates total mass of mud in settled bed at a given location
CONCENTRATION	Calculates changes in suspended mud concentration due to convective transport
CONSOLIDATION	Calculates bed yield strength at each timestep
BEDSTRESS	Calculates shear stress due to fluid mud layer
INTERFACESTRESS	Calculates shear stress due to water layer
MUDDEPTH	Calculates thickness of fluid mud layer from the mass of mud in the layer and its concentration
MUDEXCHANGE	Calculates vertical exchange of mud between water, fluid mud and settled bed and the resulting changes in suspended mud concentration
MUDFLUX	Calculates flux of fluid mud due to convective transport
MUDVEL	Calculates fluid mud velocities
SETFLAGMUD	Sets flags according to presence or absence of fluid mud at a given location
VDIFF	Calculates difference in velocity between water and fluid mud

The model solved its finite difference equations using a rectangular grid structure in which the location indicator (i,j) increased in the positive x-direction East and the negative y-direction, referred to as South. The grid cells are, however, stored as a one-dimensional array called the k-array, which assigns a numerical index to each cell sequentially according to its location, as illustrated in figure 7.2. The numerical index is set to one for inactive cells such as those representing solid boundaries and increases to the east and south for the other cells. Use of the k-array makes it easy to determine which cells are adjacent to the location under consideration and minimizes the memory requirements for the computation.

The Wallingford FLUIDMUDFLOW-2D programs were not originally implemented as a single stand-alone package, but as a series of subroutines that form part of Wallingford's TIDEFLOW-2D modelling package. This is a complete modelling system which allows the engineer to simulate tide and wave hydrodynamics as well as sediment transport problems. A list of the subroutines making up FLUIDMUDFLOW-2D, the fluid mud section of the TIDEFLOW-2D suite, is included in table 7.1. In the table, the term 'water' refers to the mud/water mixture overlying the fluid mud and settled bed layers. Full listings of all the Hydraulics Research Wallingford Limited subroutines used in the current investigation are included in appendix 3.

7.2.2 Initial Set-Up of the Model for Use in the Current Investigation

The Wallingford software made available for use in the current investigation consisted of the FLUIDMUDFLOW-2D subroutines together with a main program from the TIDEFLOW-2D suite and associated header files. However, the main program could not be run independently of the rest of the TIDEFLOW-2D software, so it was necessary first of all to produce a new main program capable of handling the necessary input to and output from the fluid mud flow routines and of calling those routines in the correct order. This program, called FM101.FOR was written in FORTRAN 77 and a listing of it is included in appendix 3.

FM101.FOR preserves the original FLUIDMUDFLOW-2D logic as described in figure 7.1, making no contribution itself to the actual solution of the fluid mud equations discussed in section 5.2.1, chapter 5 and section 7.2.1 above. FM101.FOR does, however, check the total mass of mud in the system at each timestep so as to ensure that this remains constant, and also averages the output over the number of timesteps between chosen output steps so as to give values representative of the whole output step. This process was necessary, since timesteps were typically of one second or less (see discussion in section 7.3 below), meaning that requesting output at every timestep resulted in a completely unmanageable 1200 or more data lines for each twenty minute simulation.

As mentioned in section 5.2.1, chapter 5, the latest version of the FLUIDMUDFLOW-2D software takes account of wave effects, and it was this version of the subroutines that was made available to the author. It was therefore necessary to remove the statements and subroutines referring to wave action from the programs before implementing them in the current investigation.

A particular upshot of the removal of the wave effects subroutines from the FLUIDMUDFLOW-2D software was an effect on the way in which the programs calculated the fluid mud thickness after each timestep. Whilst in the original implementation of the programs described in section 7.2.1 above, this had been determined on the basis of an assumed constant concentration of fluid mud, the version of the software supplied to the author used a calculated wave boundary layer thickness to determine the fluid mud thickness. It was therefore necessary to change this situation to remove the wave dependent parameter and return the software to something like the version used by Odd and Cooper (1988). This involves changing the subroutine MUDDEPTH (see table 7.1 and listing in appendix 3).

Roberts and his predecessors assumed a single value of $75kgm^{-3}$ for the concentration at which fluid mud existed in its layer. This value, however, is far higher than many of the fluid mud concentrations recorded in the current investigation (including corrections as discussed in section 6.3.1, chapter 6) and in the previous laboratory

experiments carried out by Ali and Georgiadis (1991). It therefore seemed sensible to alter the assumption of a 75kgm^{-3} fluid mud concentration.

Since the initial testing of the FLUIDMUDFLOW-2D software was carried out before the Race Track Flume results described in chapter 6 had been fully processed, an analysis was carried out of the concentrations at which fluid mud formed in Ali and Georgiadis' (1991) experiments. Figure 7.3, taken from Ali and Georgiadis, shows fluid mud to have formed at a concentration varying with the initial density of the suspension and the bed slope. A suggested assumption, based on a simplified interpretation of this figure is that the incipient fluid mud concentration is given by:

$$C_0 = 1.363\,C_i + 4.542 \qquad (7.10)$$

(figure 7.4), where C_0 is the concentration at which fluid mud first forms and C_i is the initial average concentration of the mud suspension (determined from bulk density readings via equation 4.5, chapter 4 with ρ_w = 1025kgm^{-3} and ρ_d = 2323.18kgm^{-3}). This assumption, though far from conclusive, yielded what were felt to be more realistic values of initial fluid mud concentration with which to test the model than did the previous assumption of C_0 = 75kgm^{-3}, and it was therefore incorporated into the model.

The Wallingford FLUIDMUDFLOW-2D programs were, for the purposes of this investigation, implemented on a 486DX IBM-Compatible personal computer with a 33MHz Central Processing Unit and 4Mb of RAM. Some later runs were carried out on a higher grade PC with a 66MHz CPU and 16Mb RAM. The FORTRAN 77 compiler used was FTN77/386 version 2.51 from The University of Salford.

7.3 Testing of the FLUIDMUDFLOW-2D Software

This section describes the basic testing procedures carried out on the author's implementation of the Wallingford FLUIDMUDFLOW-2D software, these having

consisted of testing for numerical stability under various conditions and of testing for sensitivity to changes in timestep, spacestep and various empirical input parameters.

7.3.1 Testing for Convergence, Stability and Consistency

In the implementation of finite difference solutions to differential equations, convergence and consistency concern the conditions in which, and the accuracy with which a finite difference approximation tends to the exact solution of the differential equation it represents. Stability concerns the practical implications of the arithmetical solution of the finite difference approximation, and in particular, of course, the propagation of rounding errors caused by floating point calculations on a computer (Smith 1978). Clearly it is necessary before relying on the results of a finite difference algorithm to ensure that the conditions of convergence, stability and consistency have been met.

For simple, linear equations, it is possible to determine theoretically the precise conditions, ie the lengths of the time and spacesteps, in which convergence, consistency and stability are achieved. However, it will be seen that the fluid mud equations (5.1 and 5.2) are not linear; in particular, 5.1 includes a shear stress term dependent on u_m^2 and 5.2 includes u_m, v_m and d_m, all of which are interrelated in a complex manner. It was not therefore possible to determine simple limits to the values of Δx and Δt that could safely be used with the Wallingford FLUIDMUDFLOW-2D programs.

Hydraulics Research Wallingford Limited offered the advice that the FLUIDMUDFLOW-2D system should function adequately provided that the timestep is less than the time required for fluid mud to traverse a single grid cell; however, in order to more precisely evaluate the conditions under which the model could reliably be used, it was decided to test it using various time- and spacesteps.

Initially, therefore, the model was therefore set up so as to represent laboratory conditions in a relatively arbitrary way, with the intention not of comparing modelled and measured fluid mud data, but solely of comparing model results obtained with different time and spacesteps, all other parameters remaining the same.

The set-up for this part of the investigation was based on the experiments carried out by Ali and Georgiadis (1991). The model geometry consisted of a rectangular grid representing a closed flume 2.0m long by 1 grid cell wide, giving in effect a two dimensional, longitudinal-vertical set up in which the lateral dimension could be neglected. A bed slope of 1:5 was incorporated, with an overlying water depth of 0.4m at the upslope end and an initial situation in which mud was present in suspension only in an evenly mixed concentration of $30kgm^{-3}$. Water flow was set to zero, so the only phenomenon under investigation was the settling of suspended mud to form fluid mud and a settled bed layer. A salt water density of $1025kgm^{-3}$ was used.

A number of unknown parameters were taken from Roberts' (1992) implementation of the FLUIDMUDFLOW-2D software, these being the erosion constant m_e, the bed consolidation rate A and the bed yield strength values ζ. Critical shear stresses for deposition and erosion were set to high values so that these would play no part in the model equations (ie deposition would always occur and erosion would never occur), and the settling velocity parameters were taken from Thorn's (1981) work as expressed by equation 6.17, chapter 6. Here the values for $4 < C < 15.3kgm^{-3}$ were used regardless of the modelled value of concentration, since the FLUIDMUDFLOW-2D subroutines based on equations 7.7 to 7.9 had no way of taking account of hindered settling observed at concentrations above $15.3kgm^{-3}$ (section 5.2.1, chapter 5 and section 7.2.1 above).

The overlying water friction factor f_w was set to the high value of 4000, this value being consistent with fluid mud friction factors encountered for fluid mud profiles measured in the Race Track Flume (see section 6.5.2, chapter 6). This value was chosen since it seemed reasonable to assume that a high friction factor in the moving

fluid mud layer would correspond to a high friction factor in the dense suspension immediately above the fluid mud layer. A much fuller discussion on values of friction factor and critical shear stress is included in section 7.5.2 below.

Further values were based on observations made in the Race Track Flume and discussed in chapter 6. The kinematic viscosity of fluid mud at C_0, the constant concentration used in the model was set to $660x10^{-6}m^2s^{-1}$, this value being taken from Hydraulics Research Wallingford Limited (1992) and corresponding broadly with values encountered in fluid mud velocity profiles measured in the Race Track Flume (see section 6.5.2). The dewatering velocity was maintained at $5x10^{-5}ms^{-1}$, this value taken from Hydraulics Research Wallingford Limited (1992) also being broadly consistent with Race Track Flume results (section 6.4.3).

The value β as defined in equation 7.9 is an important parameter in the depth-averaged modelling of field situations where density variations throughout the depth can be large, meaning that the near bed concentration influencing settling into the fluid mud layer can be much larger than the depth averaged concentration, which is the property modelled directly. However, as discussed in section 6.3.3, chapter 6, such variations are not pronounced in laboratory scale experiments. In the case of the results of Ali and Georgiadis (1991) (figure 6.44), the 1:5 bed slope and $30kgm^{-3}$ concentration case gives a maximum variation in concentration between the water surface and the top of the fluid mud layer at 26mm above the flume bed of approximately 10g/l, corresponding to a β value in the region of only 1.15. In view of this, therefore, and for simplicity, the β value for the initial model testing was set to unity. A helpful discussion on stratification in small scale mud experiments is contained in Teisson et al (1992).

Finally, in order to compare dewatering results for different time- and spacesteps, it was necessary to assign a bulk density to each of the various bed layers included in the model so that the modelled mass of mud in the bed could be converted into an elevation. An arbitrary, constant figure of $1054kgm^{-3}$ was chosen to represent bulk density of all the bed layers in the model testing phase.

Table 7.2: Values of Parameters Used in the FLUIDMUDFLOW-2D Programs for Convergence, Consistency and Stability Testing

Parameter	Description	Value and Units
f_w	Friction Factor	4000
u and v	Water Velocities	ms^{-1}
τ_d	Critical Shear Stress for Deposition	10 000Nm^{-2}
ω_s	Settling Velocity Constant	$5x10^{-5}m^4kg^{-1}s^{-1}$
ω_{min}	Minimum Settling Velocity	$4x10^{-5}ms^{-1}$
v_0	Dewatering Velocity	$5x10^{-5}ms^{-1}$
ρ_w	Salt Water Bulk Density	$1025kgm^{-3}$
m_e	Erosion Constant	$0.00643m^{-1}s$
τ_e	Critical Shear Stress for Erosion	10 000Nm^{-2}
A	Bed Consolidation Constant	$3x10^{-5}s^{-1}$
ζ	Yield Strength of Each Bed Layer	0.38 to 100 000kgm^{-2}
ν_m	Fluid Mud Kinematic Viscosity at $C_m = C_0$	$660x10^{-6}m2s^{-1}$
β	Ratio of Near Bed Suspended Mud Conc. to Average Suspended Mud Conc.	1.0
ρ_{bed}	Arbitrary Bed Bulk Density	$1054kgm^{-3}$

A summary of all the parameters input into the Wallingford FLUIDMUDFLOW-2D software for the purposes of convergence, consistency and stability testing is included in table 7.2.

The timesteps and spacesteps used in testing the model for convergence, consistency and stability were chosen to represent sensible values, bearing in mind that for a given geometry and simulation time, reducing either the time- or the spacestep increases computation time, whilst reducing them results in a loss of precision of output. In the end, timestep Δt values of 0.1, 0.5, 1, 2 and 10 seconds were chosen for testing and spacestep Δx values of 0.01, 0.05, 0.1 and 0.2m. However, the values $\Delta t = 10s$ and $\Delta x = 0.2m$ were not considered as realistic for actual simulation purposes as they offered insufficient precision of output. They were included in this stage of the model testing simply to give a broad picture of the model function. None of the values chosen resulted in excessive or inconvenient computation time, runs typically lasting only two to three minutes.

7.3.2 Model Convergence and Stability

Convergence and stability are in fact quite closely related in a computerised finite difference solution, since one concerns what may be described as 'rounding errors' implicit in the discretisation of the problem's governing differential equations, and the other concerns rounding errors caused by the floating point solution of the discretised equations. Where it is possible to separate these issues, the areas of convergence and stability may be addressed separately; however, in the present case the equations are too complex to be solved except by use of floating point arithmetic on a computer, so it is in general impossible to tell whether the presence or propagation of an error in the computerised finite difference solution is due to lack of convergence or to instability. Thus the two issues must be treated together, with the objective that conditions must be found in which the model equations converge to a sensible solution, at which point it may be assumed that both conditions of convergence and stability have been satisfied.

Various combinations of the time- and spacesteps listed above were tested so as to ascertain combinations leading to a stable solution in which numerical errors did not propagate through the system. When such propagation of errors did occur, it was apparent in that total mass of mud was not conserved but increased rapidly leading to the programs halting with a floating point overflow. Details of the combinations tested and the success or failure of each case are noted in table 7.3.

Whilst, as mentioned in section 7.3.1, it is not possible to determine analytically the conditions required for stability in the fluid mud transport equations 5.1 and 5.2, the ratio $r = \Delta t/\Delta x^2$ is an important one in the finite difference solution of many equations involving time as an independent variable (Smith 1978). Evaluating this ratio for the combinations of Δt and Δx in table 7.3 indicates that, with the various parameters set up as described in section 7.3.1 and table 7.2 above, the FLUIDMUDFLOW-2D model functions in a stable manner in conditions where r is 100 or less, but is unstable when r is greater than 100. It may therefore be concluded that time and spacesteps should be chosen so as to give an r value of less than 100 whilst also providing appropriate precision of output and use of computer resources.

Table 7.3: Results for Various Combinations of Time- and Spacesteps Tested

$\Delta x \backslash \Delta t$	0.1s	0.5s	1.0s	2.0s	10s
0.01m	Unstable	Unstable	Unstable	Unstable	Unstable
0.05m	Stable	Unstable	Unstable	Unstable	Unstable
0.1m	Stable	Stable	Stable	Unstable	Unstable
0.2m	Stable	Stable	Stable	Stable	Unstable

7.3.3 Model Consistency

In order to test for convergence in the FLUIDMUDFLOW-2D programs, model results from the stable combinations Δt and Δx detailed in table 7.3 were compared to see if changes in Δt and Δx affected the modelled values of fluid mud velocity, thickness or elevation.

Plots showing the fluid mud velocity, thickness and elevation for various timesteps with constant spacesteps of 0.1m and 0.2m are included in figures 7.5 to 7.14, these figures having been obtained by fitting a smooth curve through data output at 15 second intervals. Figures 7.5 to 7.10 show output at the mid-point of the model geometry, corresponding roughly to the location of the results quoted in Ali and Georgiadis (1991), and figures 7.11 to 7.14 show variations along the length of the model geometry. It should be noted that the negative fluid mud velocities indicated on figure 7.12 are as a result of the curve fitting procedure; the model results show only zero values at x = 1.333m and 1.667m, with no output having been recorded in between. In this case, the presence of negative velocities, however caused, is not an issue, it being desired only to compare results from different timesteps. It is clear that the differences between results obtained with different Δt values are entirely insignificant.

Modelled fluid mud flow results for various spacesteps with Δt constant are included in figures 7.15 to 7.21, figures 7.15 to 7.17 representing the mid-point of the model geometry and figures 7.18 to 7.21 variations along its length. The comments made above about negative velocities on figure 7.12 apply also to figure 7.19. It is clear in this case, however that there are differences in modelled results obtained using different spacesteps, and these appear to be significant, differences in fluid mud velocity of up to 70.2% being recorded. Details of the differences in fluid mud velocity and thickness caused by variations in spacestep are detailed in table 7.4.

It is possible that the differences in fluid mud velocity and thickness recorded with different Δx values are as a result of a problem with the consistency of the finite

difference solution. This would mean, in effect, that a solution achieved with a different spacestep would be the solution of a different equation, rather than a different solution of the same equation. There is some justification for this possibility in the way the FLUIDMUDFLOW-2D subroutines are put together, with routines such as MUDVEL (see table 7.1 and appendix 3) using fluid mud parameters obtained by averaging the relevant parameters at the current location and the adjacent cells. In such cases the change in spacestep is likely to have a significant effect, particularly at points in the simulation where $\partial/\partial x$ terms are significant.

Table 7.4: Maximum Differences in Results Obtained with Various Spacesteps

Location and Time	$\Delta x = 0.05m$	$\Delta x = 0.2m$	Difference (% of maximum)
u_m at flume mid-point, time 5.75 mins	$0.0005ms^{-1}$	$0.0018ms^{-1}$	70.2
u_m after 2 mins, $x = 0.333m$	$0.0014ms^{-1}$	$0.0019ms^{-1}$	24.5
u_m after 10 mins, $x = 0.333m$	$0.0003ms^{-1}$	$0.0006ms^{-1}$	54.9
d_m at flume mid-point, time 5.75 mins	0.1450m	0.1286m	11.3
d_m after 2 mins, $x = 2.0m$	0.1564m	0.1442m	7.7
d_m after 10 mins, $x = 0.333m$	0.0758m	0.0501m	33.9

However, an important point to note is that in changing the spacestep Δx, the precision with which output can be located is altered, so it may in fact be that the apparently significant differences in results shown in table 7.4 are due solely to the inability to compare like with exact like caused by the change in output precision.

In conclusion, it may be stated that in order to reduce the risk of consistency errors in the equations to a minimum, a spacestep should be chosen so as to give sufficiently precise output and to reduce variations between parameters in adjacent grid cells to a minimum.

7.3.4 Oscillation of the Model Results

The output included in figures 7.5 to 7.21 is taken at 15 second intervals and results from the output averaging procedure included in the new main program FM101.FOR and discussed in section 7.2.2 above.

In order to check that this output averaging was not disguising any undesirable feature of model performance, runs were carried out in which output was obtained at every timestep without, of course, any averaging. Sample fluid mud velocity results from such a run are included in figure 7.22.

The notable feature of figure 7.22 is the oscillatory nature of the model results during the very initial stages of the fluid mud process. The amplitude of the oscillations is quite large, the maximum value recorded being in excess of 50% of the maximum fluid mud velocity recorded during the entire simulation. However, the oscillations were confined to the first twenty seconds of the run, and did not recur after this. Neither were oscillations noted in fluid mud thickness or elevation results. It was therefore concluded that this oscillatory behaviour was insignificant in terms of the overall pattern of results obtained from the FLUIDMUDFLOW-2D software.

7.3.5 Model Sensitivity

An important characteristic of a numerical model such as the Wallingford FLUIDMUDFLOW-2D model is its sensitivity to variations in its various input parameters. In field situations, many parameters are difficult and costly to quantify, and it is important that limited resources are concentrated on the accurate assessment of parameters that have significant effects on model results, rather than on others whose significance is limited. Since no detailed sensitivity analysis of the FLUIDMUDFLOW-2D software has yet been attempted, it was decided to test the model, implemented as described in section 7.3.1, for sensitivity to various input parameters.

The parameters chosen for this analysis were the water friction factor f_w, the critical shear stress for deposition τ_d, the dewatering velocity v_0, the fluid mud viscosity ν_m and the settling velocity constant ω_s. In view of the nature of the experimental results of the current and previous investigations and of the nature of the model set up as described in section 7.3.1 above, it was decided to exclude erosion parameters from the sensitivity analysis. In general it was the intention to test each parameter at a supposed 'sensible' value and at one order of magnitude on either side of the suggested value, so that a general view of the parameter's significance could be obtained. In the case of fluid mud viscosity, however, this two order of magnitude range was extended, with a minimum value of $2x10^{-6}m^2s^{-1}$, twice the viscosity of seawater being considered, this value having been used for fluid mud by Ali and Georgiadis (1991) and by Odd and Rodger (1986). The maximum fluid mud viscosity taken was $200x10^{-3}m^2s^{-1}$, this corresponding to results obtained in the Race Track Flume (see sections 6.4.2 and 6.5.2). In the case of the settling constant ω_s, the variation above the chosen 'sensible' value was limited, as settling velocities in excess of about $3mms^{-1}$ were regarded as implausible under any circumstances. The water friction factor f_w was reduced from the value of 4000 used in the convergence, stability and consistency tests described in sections 7.3.1 to 7.3.4 above, since such a high value generated massive shear stresses in equation 5.4, preventing deposition

from taking place at all unless the critical shear stress τ_d were also set very high as before.

Details of the parameters and their values used in the sensitivity analysis are included in table 7.5. It should be noted that in the first instance, each parameter was tested in isolation, all other parameters being maintained at their 'sensible' values. The simulations described in this section were all run with Δt set to 0.25s and Δx set to 0.1m.

Table 7.5: Parameters and Values Used in Sensitivity Analysis of the FLUIDMUDFLOW-2D Software

Parameter	Minimum Value	'Sensible' Value	Maximum Value
f_w	0.002	0.02	0.2
τ_d	$0.007 Nm^{-2}$	$0.07 Nm^{-2}$	$0.7 Nm^{-2}$
v_0	$5x10^{-6} ms^{-1}$	$5x10^{-5} ms^{-1}$	$5x10^{-4} ms^{-1}$
ν_m	$2x10^{-6} m^2 s^{-1}$	$660x10^{-6} m^2 s^{-1}$	$200x10^{-3} m^2 s^{-1}$
ω_s	$5x10^{-6} m^4 kg^{-1} s^{-1}$	$5x10^{-5} m^4 kg^{-1} s^{-1}$	$1x10^{-4} m^4 kg^{-1} s^{-1}$

Results of the sensitivity analysis for the parameters f_w, τ_d and v_0 are shown in figures 7.23 to 7.31. The data shown represents the modelled fluid mud velocity, thickness and elevation over the ten minute simulation time at the mid point of the model geometry. As with the previous tests described in section 7.3.1 to 7.3.4 above, the fluid mud elevation is derived from a modelled mass of mud in the bed using the arbitrary, constant bed density of $1054 kgm^{-3}$. This does not necessarily produce a realistic model of bed growth, but it does allow clear comparison between the various sets of results.

The results for water friction factor f_w show a much higher peak velocity than those obtained during the convergence tests when f_w was set to 4000 (compare figure 7.23 with, for example, figure 7.5). This suggests that a very large change in f_w has a highly significant effect. However, within the two order of magnitude range tested for the sensitivity analysis, there is limited effect on either fluid mud velocity or thickness. The pattern of bed elevation is altered due to the evaluation of shear stress using equation 5.4; for $f_w = 0.2$, the critical shear stress of $0.07 Nm^{-2}$ is exceeded after about 6 minutes resulting in a cessation of bed growth. The increased difference in results from $f_w = 0.02$ to $f_w = 0.2$ compared with that from $f_w = 0.002$ to $f_w = 0.02$ indicates a non-linear response to changes in f_w. This, when considered with the results obtained previously for $f_w = 4000$ (see for example figures 7.5 to 7.7) suggests that changes in f_w may be highly significant if the values themselves are high; however, at the values indicated in table 7.5, order of magnitude changes are not of great importance.

The only notable effect of changing τ_d, the critical shear stress for deposition, is a change in bed growth as shown in figure 7.28. This is caused by a change in the time during the simulation at which the bed shear stress due to the fluid mud layer falls below τ_d.

The dewatering velocity v_0 has slightly more significance than τ_d, as can be seen from figures 7.29 to 7.31. The most obvious result of changing v_0 is shown in the plot of bed elevation, figure 7.31, where the slopes of elevation against time are clearly dependent on v_0; at the highest value tested, $v_0 = 5x10^{-5} ms^{-1}$, dewatering of the fluid mud layer takes place fast enough to have a significant effect on the layer's thickness and velocity.

Results of the initial sensitivity analysis for fluid mud viscosity ν_m and settling constant ω_s are included in figures 7.32 to 7.37. Over the large range tested, changes in ν_m have a major impact on fluid mud flow, with peak velocities and also the times at which they occur changing radically. There is also a knock-on effect on bed

growth as the changes in flow velocity affect the exceeding of the critical shear stress τ_d.

Changing the settling constant also has a major effect on the peak fluid mud velocity and thickness recorded and the time at which they occur, with a very low settling constant resulting in a delayed start to fluid mud motion (figure 7.35); here also there is an effect on bed formation (figure 7.37), but again this may be regarded as a knock-on feature caused by changes in velocity and hence in the exceeding of the critical shear stress for deposition to the bed.

It is impossible to summarise the results of this sensitivity analysis quantitatively in a table or chart, as this would over simplify the many effects of varying the considered parameters: instead, reference should be made to the figures. However, in conclusion, it may be stated that the above sensitivity analysis shows that the most significant effects on model results are due to changes in fluid mud viscosity and settling constant, though the effect of very large changes in water friction factor f_w have not been considered. It is also clear that there are complex interactions between parameters, particularly in the area of exceeding of critical shear stress for deposition and consequent effects on bed formation. The results of this analysis should not, therefore, be regarded as a reliable means of predicting the response of the FLUIDMUDFLOW-2D software to changes in individual parameters when such changes are not carried out in isolation.

7.3.6 Sensitivity to Fluid Mud Viscosity and Settling Constant when Water Friction Factor is High

In order to extend the model sensitivity analysis described in the previous section to take account of very high friction factors such as those encountered in the Race Track Flume experiments (see sections 6.4.2 and 6.5.2, chapter 6) and used in the model tests described in section 7.3.1 to 7.3.4 above, further runs were carried out. These involved testing the FLUIDMUDFLOW-2D subroutines for their responses to

changes in water friction factor, fluid mud viscosity and settling constant with the water friction factor f_w set high values and the critical shear stress for deposition once more adjusted so as to ensure that deposition would always occur. The values of the various parameters used in this part of the investigation were therefore f_w = 400, 4000 and 40000, $\nu_m = 660x10^{-6}m^2s^{-1}$ and $200x10^{-3}m^2s^{-1}$ and $\omega_s = 5x10^{-5}m^4kg^{-1}s^{-1}$ and $1x10^{-4}m^4kg^{-1}s^{-1}$. The middle value of f_w and the lower values of ν_m and ω_s were used as the base conditions for this test, with only one parameter being varied from these values at once. Values of viscosity and settling constant lower than those stated were not tested in this analysis.

Results of these tests are included in figures 7.38 to 7.46, these results being for the mid point of the flume as with figures 7.23 to 7.37.

Figures 7.38 to 7.40 confirm that when water friction factor is high, an order of magnitude change in its value will have significant effects on modelled fluid mud velocities. It will also be noted that the peak fluid mud velocities achieved with a high water friction factor are very much smaller than those recorded with the friction factor values indicated in table 7.5.

The effect of changing a high value of f_w on fluid mud thickness is limited, and on elevation it is zero; however, it must be remembered that critical shear stress parameter τ_d has essentially been removed from consideration in these tests, so the modelling of deposition phenomena is substantially different from that used in the sensitivity tests described in the previous section.

Figures 7.41 to 7.43 show that with a high friction factor, changes in the fluid mud viscosity still produce a highly significant effect on both the value and timing of the peak fluid mud velocity, though as may be expected from the removal of critical shear stress τ_d from consideration, there is little effect on fluid mud thickness and absolutely none on fluid mud elevation. On the other hand, figures 7.44 to 7.46 show that when the settling constant ω_s is changed, there is a major change in fluid mud

thickness, but no significant change in the absolute value of fluid mud velocity. The timing of the peak fluid mud velocity is, however, substantially altered.

It may be concluded at this point that, with a high water friction factor, changes in water friction factor, fluid mud viscosity and settling constant in the ranges considered have a highly significant impact on modelled fluid mud flow, with fluid mud peak velocity being principally affected by changes in friction factor and viscosity, and fluid mud thickness being affected by changes in settling constant.

7.4 Stationary Fluid Mud

With regard to the modelled patterns of fluid mud thickness, an important point must be made, which is that the FLUIDMUDFLOW-2D subroutines model the phenomenon of stationary fluid mud, ie in the model, a fluid mud layer can exist with zero velocity, but finite mass. This is not the case in the laboratory results obtained in the Race Track Flume, where, as detailed in section 4.5, chapter 4, measurement of a fluid mud thickness depended on visual observation of a *moving* fluid mud layer. Stationary fluid mud, had it existed, could not therefore have been identified in the laboratory experiments but would have been seen either as settled bed or as mud undergoing vertical hindered settling but not lateral motion. Since Ali and Georgiadis (1991) also used visual observation/dye tracking methods for the measurement of fluid mud flow in the laboratory, this consideration may also be taken to apply to their results.

It is possible to re-interpret the model results for comparison with laboratory data in the light of these comments. The minimum absolute value of fluid mud velocity recorded was $0.11 mms^{-1}$ (section E, nominal initial average concentration $30 kgm^{-3}$, see table 6.8, chapter 6). This may be regarded as the minimum measurable fluid mud velocity, and thus in comparing modelled and measured fluid mud flows, modelled fluid mud thicknesses corresponding to modelled velocities of less than $0.11 mms^{-1}$ may for the purposes of comparison with laboratory data, be disregarded.

If a Newtonian fluid flow profile with a zero interface velocity is assumed, this analysis may be extended as follows. The flow profile may be expressed by equation 7.11:

$$u_m(z_m) = \frac{1}{2\rho_m \nu_m}\left(\frac{d_m^2}{4} - z_m^2\right) \tag{7.11}$$

where $u_m(z_m)$ is the fluid mud velocity at distance z_m from the point of maximum velocity (see equation 6.25, chapter 6). Setting $u_m(z_m) = U_{max}$ when $z_m = 0$, this equation becomes:

$$u_m(z_m) = U_{max} - \frac{4 U_{max} z_m^2}{d_m^2} \tag{7.12}$$

Integrating equation 7.12 over the interval $z_m = 0$ to $d_m/2$ and dividing by $d_m/2$ gives the mean fluid mud velocity $\bar{u}_m$ in terms of U_{max}:

$$\bar{u}_m = \frac{2}{3} U_{max} \tag{7.13}$$

Hence, substituting 7.13 into 7.12, rearranging and setting u_m to $0.11 mms^{-1}$ or $0.00011 ms^{-1}$, the apparent thickness of the fluid mud layer d_m' may be determined from the following equation, where d_m is the actual modelled thickness of the layer and $\bar{u}_m$ is the modelled mean fluid mud velocity. The factor of two comes from the fact that z_m is the distance between the maximum flow and the point at which fluid mud motion becomes undetectably slow, ie half the apparent layer thickness.

$$d_m' = 2z_m = 2\sqrt{\frac{d_m^2}{6|\bar{u}_m|}\left(\frac{3|\bar{u}_m|}{2} - 0.00011\right)} \tag{7.14}$$

The modulus signs take account of negative fluid mud velocities. This equation is not rigorously accurate, since it is based on an assumptions of a Newtonian fluid flow profile and of zero interface velocity. However, it gives a guideline against which model results can be interpreted in line with laboratory observations. For a discussion on Newtonian flow profiles as applied to fluid mud flow, see section 6.6.4, chapter 6.

As an example of the use of equation 7.14, the results of figures 7.41 and 7.42 with $\omega_s = 5x10^{-5}m^4kg^{-1}s^{-1}$ were reprocessed and are included as figures 7.47 and 7.48. As can be seen, the model results for fluid mud thickness are still not closely related to the general pattern observed in the laboratory experiments, but application of equation 7.14 does cause the apparent cause fluid mud thickness to decay at times after the fluid mud velocity has begun to subside.

7.5 Application of the FLUIDMUDFLOW-2D Model to the Experiments of Ali and Georgiadis (1991)

On completion of the sensitivity analysis, the general performance of the Wallingford FLUIDMUDFLOW-2D implemented as described in section 7.2.2 was evaluated by comparing model results against data obtained in the relatively simple experiments carried out by Georgiadis (1989) and Ali and Georgiadis (1991) (section 2.3.3).

For this purpose, the model geometry remained much as used for the various tests described previously, since the flume to be simulated was a 2.0m long by 0.1m wide 'box' with solid ends and mounted on a jack so as to allow its bed to be tilted to various different slopes. This flume was assumed to be two dimensional in the vertical/longitudinal sense, so that y-direction motion could be neglected. Further, the solid ends of the flume meant that there were no complex boundary conditions to be represented in the simulation: the modelled area simply terminated with inactive, zero-flow cells on all four sides. All the experiments began with an evenly mixed suspension of mud in salt water, which was then allowed to settle under gravity, during which process the formation and motion of fluid mud was monitored, and since the experiments all took place in still water, there were no overlying water velocities to be included in the model.

Application of the FLUIDMUDFLOW-2D model to the experimental data required the selection of the various empirical parameters as used in the sensitivity analysis in the previous section. It was decided that critical shear stress should be set to a high

value as in the model stability tests described previously, since it was clear from Ali and Georgiadis' (1991) analysis that the fluid mud flow encountered in their experiments was laminar, and therefore that shear stress due to such flow would not be indicative of vertical turbulent motions which could contribute to keeping mud flocs in suspension. It was further decided that fluid mud viscosity and dewatering velocity should remain at the values used by Hydraulics Research Wallingford Limited (1992), since that study provided evidence of their appropriateness and no further evidence was available to support variation from these values. (This analysis was carried out before results from the dewatering velocity analysis of fluid mud in the Race Track Flume as discussed in section 6.4.3, chapter 6, became available.)

Selection of settling velocity constants was a difficult problem, since it was clear that the initial average concentrations of 15.6kgm^{-3} and 30.0kgm^{-3} were both in the hindered settling range as given by equation 6.17 and on figure 6.61, chapter 6, whereas the model algorithm given by equations 7.7 to 7.9 did not take account of hindered settling. Ali and Georgiadis (1991) obtained settling velocity values for the initial average concentrations in question, both from the equivalent of equation 6.17 and from their own analysis of fluid mud flow, as shown in table 7.6. These values of settling velocity were taken as a starting point for the evaluation of the settling constant ω_s to be used in the model.

Table 7.6: Settling Velocities from Ali and Georgiadis (1991)

Initial Concentration / Parameter	ω from equation 6.17 (mms^{-1})	ω from Ali and Georgiadis (1991) (mms^{-1})
30.0kgm^{-3}	1.13	0.55
15.6kgm^{-3}	1.21	2.13

The water friction factor f_w was initially assumed to be high, since it was apparent that fluid mud concentrations were relatively high and therefore likely to result in large shear stresses.

Following some relatively unsuccessful initial runs of the model, it was decided to adjust some of the empirical parameters used so as to obtain a better fit with the measured data as presented by Georgiadis (1989). The parameters chosen for variation were the settling constant ω_s, since the settling algorithm was known to be unrealistic in not accounting for hindered settling, and the water friction factor f_w, on the grounds that there was no objective evidence at all as to what value this should have. The model was therefore tested using various values of these parameters until a reasonable 'best fit' could be obtained. The values of all the empirical parameters finally used in the model for the various initial average concentrations were then as shown in table 7.7.

Table 7.7: Values of Empirical Parameters Used in Initial Model Verification

Initial Concentration/ Parameter	f_w	τ_d (Nm^{-2})	v_0 (ms^{-1})	ν_m (m^2s^{-1})	ω_s ($m^4kg^{-1}s^{-1}$)
$30.0kgm^{-3}$	40	10 000	$5x10^{-5}$	$660x10^{-6}$	$1x10^{-5}$
$15.6kgm^{-3}$	4	10 000	$5x10^{-5}$	$660x10^{-6}$	$2.25x10^{-5}$
$7.0kgm^{-3}$	0.04	10 000	$5x10^{-5}$	$660x10^{-6}$	$3.5x10^{-5}$

The tests to find the best values of ω_s and f_w were all carried out with a slope of 1:5; the model was then run for the remaining slopes of 1:10 and 1:20 without further variation of any parameters, since no justification for such a variation could be found. The model results obtained from this procedure are included in figures 7.49 to 7.51.

For a bed slope of 1:5, there is a reasonably successful fit between experimental data and model results for fluid mud velocity and thickness at initial concentrations 30.0kgm^{-3} and 15.6kgm^{-3}, and for fluid mud thickness at concentration 7.0kgm^{-3}. Fluid mud velocity at concentration 7.0kgm^{-3} is seriously under-predicted by the model, and in all three cases the bed growth is seriously under-predicted, indicating that the dewatering velocity v_0 used was much too small. Changing the v_0 value, however, has a serious effect on fluid mud depth, destroying the successful fits obtained for fluid mud velocity and thickness.

At slopes of 1:10 and 1:20, no successful fits to measured fluid mud thickness were obtained, even when results were processed using equation 7.14, as shown in figure 7.52. This situation can be improved by increasing f_w and reducing ω_s, but this is unhelpful since in fact the model can be made to produce widely differing results by changing a parameter from one plausible value to a different, but still plausible value without any objective evidence to support such a change.

From these results it may be concluded that through judicious selection of certain empirical input parameters, it is possible for the Wallingford FLUIDMUDFLOW-2D software as first implemented by the author to accurately simulate some features of the fluid mud flow as measured by Georgiadis (1989). However, it is clear that the model is not reproducing the overall behaviour of fluid mud flow correctly, since the totality of the relationship between fluid mud velocity, thickness and elevation is not being simulated accurately and the model does not respond realistically to changes in bed slope when all other parameters remain the same. This does not augur well for the model as an engineering tool; however, it must be remembered that in the above analysis, the FLUIDMUDFLOW-2D routines were not set up specifically to represent the laboratory situation to which their results were compared. It is therefore unfair to criticise the model performance on the basis of the results given in this section alone.

7.6 Critical Evaluation of Model Equations

It is clear from the previous section that in order to accurately simulate laboratory fluid mud flow data, and therefore to provide a fair test of its basic transport equations and layered construction, the Wallingford FLUIDMUDFLOW-2D software will be in need of some modification. In particular, the absence from the model algorithm of any way of accounting for the hindered settling phenomenon in high concentrations of suspended mud has already been highlighted. It is, however, important that any modifications to the model are carried out on the basis of a critical examination of key areas of the model equations in the light of experimental data, rather than by continuing to adjust various empirical parameters in the hope that model results can be made to match experimental observations.

The following sections therefore attempt to assess the model equations, and to suggest suitable modifications so as to ensure that the mathematical model is set up in a way that gives it a good chance of successfully simulating the laboratory conditions to which it is to be applied. This discussion also includes some consideration of field situations, since ultimately it is the model's ability to predict fluid mud flow in the field that will determine its value as an aid to engineering design.

The discussion is centred around experimental data from the Race Track Flume; however, as discussed in section 6.2.4, chapter 6, there is sufficient basic similarity between the Race Track Flume data and that from the experiments of Ali and Georgiadis (1991) to suggest that the points made will also apply to the simulation of those authors' results.

7.6.1 Momentum Equations

The momentum equations used to determine fluid mud velocity in the Wallingford FLUIDMUDFLOW-2D software are based on equation 5.1, chapter 5. This equation

can be rearranged as in equation 7.15, so that the relative contributions of the various terms on the right hand side to the evaluation of $\partial u_m/\partial t$ can be considered. In equation 7.15, the Coriolis term has been omitted, since as discussed in section 5.2.1, chapter 5, this was not used in the current investigation.

$$\underset{L.H.S.}{\frac{\partial u_m}{\partial t}} = \underbrace{-\frac{1}{d_m \rho_m}(\tau_0 - \tau_i)_x}_{Term\ 1} \underbrace{- \frac{\rho_w}{\rho_m} g \frac{\partial \eta_w}{\partial x}}_{Term\ 2} \underbrace{- \frac{g}{\rho_m}(\rho_m - \rho_w)\frac{\partial \eta_m}{\partial x}}_{Term\ 3} \underbrace{- \frac{g d_m}{2\rho_m}\frac{\partial}{\partial x}(\rho_m - \rho_w)}_{Term\ 4} \quad (7.15)$$

Considering results from the Race Track Flume, it can immediately be seen that Term 2 always evaluates to zero, since the $\partial\eta_w/\partial x$ term representing the water surface slope was always zero. Term 2 is always likely to be small, since water surface slopes due to tidal propagation are themselves small, typical values measured in the Parrett Estuary by Hydraulics Research Wallingford being approximately $3x10^{-5}$. Nevertheless, Term 2 may still be significant in field situations, since a slope of $3x10^{-5}$ combined with other values similar to those obtained in the Race Track Flume and included in table 7.8 below give a largest Term 2 value of $2.9x10^{-4}$ compared with a maximum absolute value of the left hand side of equation 7.15 of $1.4x10^{-5}$.

Fluid mud concentration data from the Race Track Flume, as discussed in section 6.3, chapter 6, indicates no evidence of any spatial variation in either fluid mud concentration or overlying suspended mud concentration. It may therefore be supposed that in the case of the flume experiments, the term $\partial/\partial x$ of $(\rho_m - \rho_w)$ also always evaluates to zero and hence Term 4 may, for the purposes of the current investigation, be disregarded. In a field situation, however, this term may possibly be significant depending on local conditions.

Term 3 may be evaluated from typical Race Track Flume results such as those for nominal initial average concentration $40kgm^{-3}$, time 9 minutes. Values for this condition are extracted from tables 6.7 and 6.8 and are included in table 7.8.

Table 7.8: Typical Data from the Race Track Flume

Parameter	Section B	Average of Section B and Section E	Section E
u_m (ms^{-1})	0.00274	0.00219	0.00164
d_m (m)	0.022	0.050	0.078
z (m)	0.010	-	0.012
η_m (m)	0.160	-	0.090
C_m (kgm^{-3}) (from equation 6.1)	54.4	-	54.4
ρ_m (kgm^{-3}) (from C_m)	1118.0	-	1118.0
ρ_w (kgm^{-3})	1021.0/ 1092.3	-	1021.0/ 1092.3
$\partial u_m/\partial t$ (ms^{-2}) (forward difference)	$-1.4x10^{-5}$	$-7.1x10^{-6}$	$-1.7x10^{-7}$
R based on ν_m = $660x10^{-6}m^2s^{-1}$	0.091	0.142	0.194

Table 7.8 also includes average values of various parameters between sections B and E where they are to be used in the analysis which follows. It should be noted that η_m refers to elevation above a datum, and for this purpose the datum was taken as the level at the flume base at section E. The flume base at section B is 0.128m higher than this, and this value is therefore incorporated in the determination of η_m at section B. The horizontal distance between sections B and E may be taken as 2.0m. The table

includes two values for ρ_w, the overlying water density at each section. The minimum of these is based on the density of the clear salt water used for the tests, whilst the other is altered to allow for the presence of suspended mud at a concentration of $40kgm^{-3}$.

Using the parameters in table 7.8, it is easy to approximately evaluate the right hand side and term 3 of the left hand side of equation 7.15. The right hand side, in fact is equal to $\partial u_m/\partial t$ included in the table, and is therefore at its maximum magnitude $-1.4x10^{-5}ms^{-2}$. Using the minimum ρ_w of $1021.0kgm^{-3}$, Term 3 evaluates at maximum, to 0.0298. This is clearly a much greater magnitude than $\partial u_m/\partial t$, and leads to the conclusion that, if equation 7.15 indeed applied to the Race Track Flume data, then Term 1 of its left hand side, which includes the shear stresses τ_0 and τ_i, must have a negative sign and an absolute value very slightly greater than 0.0298.

Clearly this analysis is limited in its scope; in particular the evaluation of $\partial/\partial x$ over a range of two metres cannot be very accurate; however, the treatment does give an insight into the relative importance of the various terms in equation 7.15 (and therefore in equation 5.1) against which model performance can be assessed. Further, it may be concluded that Term 1 in equation 7.15 is a very important term in the analysis of fluid mud flow, and therefore the evaluation of the shear stresses τ_0 and τ_i, on which that term depends, will also be very important.

A further point which has been emphasised by the examination of equation 7.15 is that the water density, ρ_w, is, in fact, dependent on the concentration of mud in suspension above the fluid mud layer. In the original implementation of the Wallingford FLUIDMUDFLOW-2D routines and in the model tests described previously, this parameter was set to the salt water density, and no corrections for suspended mud were made. This was justified because in field situations the concentration of mud above the fluid mud layer is generally low enough to have little effect on the local bulk density. However, use of the maximum value of ρ_w from table 7.8 causes a major change to the value of term 3, which reduces from 0.0298 to 0.0079, a drop of some 73%. It may therefore be that in a laboratory or other rapid

settling situation in which the mud concentration above the fluid mud layer is high, the water density ρ_w will have to be evaluated more carefully and corrections for changes in suspended mud concentration will have to be included in the model (see section 6.3.3).

7.6.2 Shear Stresses, Friction Factors and Fluid Mud Viscosity

It is apparent from the discussion contained in the previous section that determination of the bed and interfacial shear stresses acting upon a moving fluid mud layer can be highly significant in the correct modelling of fluid mud flow. This issue revolves around the evaluation of equations 5.3 and 5.4, which are used in the Wallingford FLUIDMUDFLOW-2D programs to determine shear stresses based on the friction factors f_w and f_m.

Term 1 on the right hand side of equation 7.15 may be evaluated on the basis of the analysis carried out in the previous section:

$$-\frac{1}{d_m \rho_m}(\tau_0 - \tau_i)_x = -\frac{1}{0.050 \times 1118.0}(\tau_0 - \tau_i)_x \approx -0.0298 \qquad (7.16)$$

$$\Rightarrow \quad (\tau_0 - \tau_i)_x \approx 0.0298 \times 0.050 \times 1118.0 \approx 1.7 Nm^{-2}$$

The term $(\tau_0 - \tau_i)$ (the subscript indicating the x-direction will henceforth be omitted for simplicity) may be regarded as the net shear stress acting upon the fluid mud layer. It will be remembered from the explanation in section 5.2.1, chapter 5, that equation 5.1 (and hence equation 7.15 above) was derived on the basis of τ_0 resisting fluid mud motion and τ_i assisting it. However, in a situation where the overlying water has zero ambient current, such as the experiments of Ali and Georgiadis (1991), or where ambient water current is perceived to have no effect at the level of the top of the fluid mud layer such as in Race Track Flume experiments carried out during the current investigation (see section 6.2.2, chapter 6), then it is clear that both τ_0 and τ_i will in fact resist fluid mud motion. Further, assuming variations in mud concentration across the fluid mud layer are relatively insignificant, it may be

supposed that the bed shear stress τ_0 is approximately equal to the interfacial shear stress τ_i. Equation 7.16 may then be re-expressed as follows:

$$\begin{aligned} \tau_0 + \tau_i &\approx 2\tau_0 \approx 1.7 Nm^{-2} \\ \Rightarrow \quad \tau_0 &\approx 0.85 Nm^{-2} \end{aligned} \tag{7.17}$$

Now τ_0 may be expressed in terms of the friction factor f_m as in equation 5.3, chapter 5:

$$\tau_0 = \frac{f_m \rho_m u_m^2}{8} \tag{7.18}$$

Re-arranging this equation and inserting the values derived above, the friction factor f_m can be evaluated approximately to 1268.2. This is a very high value, and is comparable with the friction factors derived from the analysis of fluid mud profiles measured in the Race Track Flume, as discussed in section 6.5.2, chapter 6. It must be remembered, however, that the analysis just described includes a large number of assumptions and approximations, so the friction factor value of 1268.2 is not to be regarded as quantitatively accurate to any great degree.

In the runs previously described in this chapter, the friction factor f_m was determined from equation 7.3. It is interesting to compare the friction factors derived from this equation with those obtained from the Couette flow analysis technique using equation 6.7.

The first two data sets included in tables 7.9 and 7.10 show a comparison between fluid mud friction factors obtained from the Couette flow analysis described in section 6.4.2, chapter 6, and those derived from Hydraulics Research Wallingford Limited's (1992) smooth turbulence theory as expressed by equation 7.3. As can be seen, the friction factors derived from the smooth turbulence theory tend to be larger than those determined from the Couette flow analogy according to equation 6.7.

This analysis, however, is somewhat artificial, in that the friction factors obtained from the smooth turbulence theory are dependent entirely on Reynolds numbers, and

hence on viscosities determined from the friction factors already calculated from equation 6.7. A more meaningful comparison is between the Couette flow friction factors (the first data set in tables 7.9 and 7.10) and smooth turbulence theory friction factors based on Hydraulics Research Wallingford Limited's (1992) assumed viscosity value of $660x10^{-6}m^2s^{-1}$, as shown in the third data set of the tables. Friction factors calculated in this way are very much larger than the other two, though of course this would be altered were a smaller viscosity, and hence a larger Reynolds number, assumed.

In order to reduce the friction factor at section E, nominal initial average concentration $40kgm^{-3}$, time 14 minutes from $8.45x10^{2}$, the value obtained from equation 7.3 using $\nu_m = 660x10^{-6}m^2s^{-1}$, to $2.53x10^{1}$, the value obtained from equation 6.7, it would be necessary to reduce the assumed viscosity to $19.8x10^{-6}m^2s^{-1}$, which clearly represents a significant change from viscosity values such as those encountered in laboratory results from the current investigation as discussed in chapter 6. It is interesting to note that a viscosity value of $19.8x10^{-6}m^2s^{-1}$ corresponds quite closely to some of the values determined from the Couette flow analysis for the Parrett Estuary field data, as shown in table 6.30, chapter 6. There is clearly scope for variation of fluid mud viscosity, since none of the analyses presented in this thesis provide an absolute guide to its true value. However, given all the evidence available at present, the author does not believe there is any justification for reducing the fluid mud viscosity for laboratory situations as encountered by Ali and Georgiadis (1991) and in the Race Track Flume to a value as low as $19.8x10^{-6}m^2s^{-1}$.

Tables 7.11 and 7.12 include similar information to tables 7.9 and 7.10, but refer to fluid mud profiles measured in the Race Track Flume (table 7.11) and Parrett Estuary fluid mud data (table 7.12). For the Race Track Flume profile data, the comparison between the various methods of determining the friction factor is different from that described above, the smooth turbulence theory with a viscosity of $660x10^{-6}m^2s^{-1}$ generating f_m values much smaller than those produced by equation 6.7. On the other hand, table 7.12 shows that for the field situation, equation 7.3 as used in the

computer model produces friction factors of approximately one order of magnitude less than those produced by the Couette flow method.

The results upon which table 7.11 is based, the fluid mud profiles measured in the Race Track Flume and discussed in section 6.5.2, are mainly obtained at a very high initial average mud concentration and are also largely dependent on the application of equation 6.1 outside the time range for which it was derived. It is therefore arguable that these results are in some way anomalous, and that the other results, those of tables 7.9, 7.10 and 7.12 provide a more meaningful comparison between different ways of determining fluid mud friction factor. On the basis of these results, it may be concluded that Hydraulics Research Wallingford Limited's (1992) smooth turbulence theory, as expressed by equation 7.3, overestimates the friction factor compared with that derived from the Couette flow analysis. A Couette flow analogy has already been shown to provide a more realistic model of measured fluid mud profiles that the smooth turbulence theory, which fails to reproduce the observed fall in velocity towards the water/fluid mud interface (see section 6.5.2, chapter 6). It may therefore be postulated that the values of friction factor derived from the Couette flow method may be more appropriate for use in fluid mud modelling than values determined from equation 7.3. At any rate, it is clear that within the bounds of evidence presented in this investigation, there remains considerable scope for varying the method by which the fluid mud friction factor f_m is calculated for use in the Wallingford FLUIDMUDFLOW-2D software.

It is possible to replace the model implementation of equation 7.3 by a rearrangement of equation 6.7, allowing friction factor to be determined directly This involves altering only the subroutine BEDSTRESS (see table 7.1 and appendix 3), and has no bearing on the overall logic of the programs.

It should be noted that equation 6.7 depends on a value of the parameter α, which for laminar flow has been estimated as 0.64. For turbulent flow, however, this value changes to 0.43 (Harleman 1961), so it is necessary to estimate whether fluid mud flow is laminar or turbulent before equation 6.7 can be applied to determine f_m.

Table 7.9: Fluid Mud Friction Factors - Section B
Variation with Concentration

Fluid Mud Friction Factor (from eqn 6.5)

Time (mins)	C = 15g/l	C = 20g/l	C = 30g/l	C = 40g/l	C = 80g/l
5					
6					
7			1.08E+00		
8			1.30E+01		
9			2.00E+00	1.08E+00	1.21E+01
10				5.66E+00	
11				7.37E+00	5.38E+01
12		2.54E+00	2.53E+00		8.40E+01
13		8.13E+00	6.36E+00		
14		2.81E+00		5.30E+00	
15	2.16E+00	7.49E+00	6.49E+00	3.99E+01	
16		1.13E+01	1.35E+01		9.20E+01
17		1.36E+01		2.37E+01	
18					
19			1.73E+01	2.67E+01	7.45E+01
20			1.62E+01	9.18E+01	

Friction Factor from HRL's Smooth Turbulence Theory

Time (mins)	C = 15g/l	C = 20g/l	C = 30g/l	C = 40g/l	C = 80g/l
5					
6					
7			1.80E+01		
8			2.45E+00		
9			8.50E+00	1.28E+01	3.46E-01
10				1.60E+00	
11				1.74E+00	3.69E-01
12		7.72E+00	3.60E+00		3.22E-01
13		3.87E+00	7.79E+00		
14		2.07E+01		8.25E+00	
15	5.14E+00	2.48E+00	7.97E+00	1.64E+00	
16		5.82E+00	2.71E+00		3.38E-01
17		3.86E+00		2.00E+00	
18					
19			1.23E+01	2.22E+00	4.74E-01
20			5.88E+00	1.95E+00	

Friction Factor from STT with Viscosity set to 660x10-6m^2/s

Time (mins)	C = 15g/l	C = 20g/l	C = 30g/l	C = 40g/l	C = 80g/l
5					
6					
7			3.71E+02		
8			6.07E+02		
9			3.23E+02	2.63E+02	7.96E+01
10				1.72E+02	
11				2.45E+02	3.77E+02
12		3.73E+02	1.74E+02		5.14E+02
13		5.98E+02	9.43E+02		
14		1.11E+03		8.31E+02	
15	2.11E+02	3.54E+02	9.84E+02	1.24E+03	
16		1.26E+03	6.99E+02		5.91E+02
17		9.97E+02		9.00E+02	
18					
19			4.04E+03	1.13E+03	6.72E+02
20			1.81E+03	3.40E+03	

Table 7.10: Fluid Mud Friction Factors - Section E
Variation with Concentration

Fluid Mud Friction Factor (from eqn 6.5)

Time (mins)	C = 15g/l	C = 20g/l	C = 30g/l	C = 40g/l	C = 80g/l
5			4.13E+00		
6					2.53E+01
7			5.65E+00	3.05E+00	
8		2.61E+00			2.89E+01
9		1.34E+00			
10		2.94E+00	8.32E+00		
11	1.65E+00	1.26E+01			4.92E+01
12	1.65E+01				
13		1.42E+01		2.34E+01	
14	1.50E+00	3.76E+01		2.53E+01	
15			2.63E+01		
16	3.58E+00		3.58E+01		1.02E+02
17				1.44E+02	
18					
19		2.37E+02	5.35E+01		4.87E+01
20					

Friction Factor from HRL's Smooth Turbulence Theory

Time (mins)	C = 15g/l	C = 20g/l	C = 30g/l	C = 40g/l	C = 80g/l
5			1.94E+00		
6					4.02E-01
7			1.25E+00	1.46E+00	
8		8.69E+00			1.22E+00
9		5.04E+00			
10		1.30E+01	1.27E+00		
11	1.94E+01	3.38E+00			1.21E+00
12	1.29E+01				
13		2.93E+00		3.37E+00	
14	1.12E+02	2.55E+00		1.75E+00	
15			2.96E+00		
16	6.55E+00		1.05E+00		5.21E-01
17				9.35E-01	
18					
19		1.68E+00	2.47E+00		1.43E+00
20					

Friction Factor from STT with Viscosity set to 660x10-6m^2/s

Time (mins)	C = 15g/l	C = 20g/l	C = 30g/l	C = 40g/l	C = 80g/l
5			1.53E+02		
6					1.93E+02
7			1.34E+02	8.46E+01	
8		4.31E+02			6.69E+02
9		1.28E+02			
10		7.28E+02	2.02E+02		
11	6.08E+02	8.09E+02			1.13E+03
12	4.04E+03				
13		7.91E+02		1.50E+03	
14	3.19E+03	1.83E+03		8.45E+02	
15			1.48E+03		
16	4.46E+02		7.14E+02		1.01E+03
17				2.55E+03	
18					
19		7.58E+03	2.51E+03		1.32E+03
20					

Table 7.11: Comparison Between Friction Factors Calculated from Couette Flow Analysis and HRL's Smooth Turbulence Theory - Race Track Flume Profile Results

Section/ Speed/ Time	Fluid Mud Friction Factor	Friction Factor from HRL's Smooth Turbulence Theory	Friction Factor from STT with Viscosity set to 660e-6m2/s
B/0/8	1.90E+03	1.31E+03	1.22E+03
B/0/11	7.55E+03	5.22E+03	8.56E+02
B/0/15	3.50E+04	2.42E+04	2.16E+03
B/0/25	1.60E+05	1.11E+05	4.69E+03
B/0/38	1.49E+05	1.03E+05	3.69E+03
B/0/42	1.96E+04	1.36E+04	2.40E+03
B/0/43	9.13E+03	6.31E+03	2.23E+03
B/0/47	1.51E+04	1.04E+04	2.68E+03
B/0/48	1.83E+04	1.27E+04	2.93E+03
B/2/9	7.02E+03	4.86E+03	2.64E+03
B/2/14	2.12E+04	1.47E+04	1.93E+03
B/2/20	2.98E+04	2.06E+04	3.37E+03
B/2/36	1.31E+06	9.07E+05	8.71E+03
B/2/42	2.19E+04	1.52E+04	2.60E+03
B/2/47	2.00E+04	1.38E+04	1.86E+03
B/2/52	1.47E+05	1.02E+05	8.17E+03
B/-2/7	2.49E+04	1.73E+04	3.38E+03
B/-2/12	2.78E+04	1.92E+04	1.88E+03
B/-2/17	1.49E+05	1.03E+05	3.45E+03
E/0/8	3.50E+03	2.42E+03	5.58E+02
E/0/11	1.19E+05	8.25E+04	3.73E+03
E/0/17	2.94E+05	2.03E+05	4.55E+03
E/0/26	1.52E+05	1.05E+05	2.02E+03
E/0/35	1.89E+05	1.31E+05	5.52E+03
E/2/9	6.41E+03	4.43E+03	7.17E+02
E/3.5/27	1.61E+06	1.11E+06	2.49E+04
E/3.5/31	1.77E+06	1.23E+06	1.09E+04
E/3.5/44	5.70E+06	3.94E+06	1.13E+04
E/-2/7	1.51E+04	1.04E+04	2.75E+03
E/-2/11	3.78E+04	2.61E+04	2.02E+03

Table 7.12: Comparison Between Friction Factors Calculated from Couette Flow Analysis and HRL's Smooth Turbulence Theory - Parrett Estuary Results

Date and Profile Number	Fluid Mud Friction Factor	Friction Factor from HRL's Smooth Turbulence Theory	Friction Factor from STT with Viscosity set to 660e-6m2/s
23/7 No 6	1.61E-02	2.92E-03	8.29E-03
23/7 No 7	1.35E-02	2.76E-03	6.73E-03
23/7 No 8	5.00E-02	4.85E-03	6.61E-03
23/7 No 9	1.64E-02	2.94E-03	7.11E-03
24/7 No 7	4.35E-03	2.02E-03	1.03E-02
24/7 No 8	1.45E-02	2.82E-03	1.00E-02
24/7 No 1	2.29E-02	3.31E-03	4.12E-03
19/8 No 4	1.57E-02	2.90E-03	8.68E-03
19/8 No 7	2.18E-03	1.74E-03	8.78E-03

A possible way of checking the fluid mud flow regime is to use a laminar sublayer treatment, calculating the laminar sublayer thickness according to equation 6.22, chapter 6, and assuming fluid mud flow to be laminar if δ/d_m is greater than unity. This procedure requires values of fluid mud viscosity and average shear rate, $\dot{\gamma}$ in equation 6.22. Average shear rate may be estimated by dividing the maximum fluid mud velocity, which for a Newtonian flow pattern may be approximated to 1.5 times the mean velocity (see equation 7.13), by half the fluid mud layer thickness. This procedure would not be absolutely rigorous, but it would provide a guideline as to the fluid mud flow regime in question. In the case of error, where fluid mud flow were really laminar but modelled as turbulent, it will be seen from equation 6.7 that the error in the value of f_m would in any case be only of the order of $1 + 0.43/1 + 0.64$ or about 13%.

There remains, of course the issue of the water friction factor f_w, which at high values was shown to be significant in its effect on model results (section 7.3.6 above). There is no absolutely reliable evidence as to what value should be assigned to f_w in any given situation, and hence there is scope for variation in choosing this parameter. However, in modelling situations such as that encountered in the laboratory, where concentration above the moving fluid mud layer is high, it is suggested that, following the analysis of Harleman (1961), the value of f_w be equated to $0.64f_m$ determined by application of equation 6.7 for laminar fluid mud flow, and to $0.43f_m$ for turbulent flow. This would require an alteration only to the subroutine INTERFACESTRESS. For field situations in which suspended mud concentration is much less than the concentration of the fluid mud, a much lower value of f_w, such as 0.02 as used by Ali and Georgiadis (1991) in their analysis of fluid mud in field situations, might still be more appropriate.

Use of the water friction factor f_w in equation 5.4 assumes, of course, that the interfacial shear stress can be related to the difference between the mean velocities of the fluid mud layer and the overlying water. In this sense, f_w was always an empirical factor of limited physical meaning, since it is clear that in normal field situations, the velocity immediately above the bed or fluid mud layer is not equal to

the depth averaged velocity, which is the parameter used in determining $\Delta u/\Delta v$ in equation 5.4. In the case of the Race Track Flume results, this issue is further complicated in the light of the discussion of 6.2.2. In that section it is shown that the measured fluid mud velocities exhibit no obvious relationship to ambient water current, a fact which is attributed to the dense layer of mud undergoing no longitudinal motion that was generally observed immediately above the moving fluid mud layer.

In view of this, when attempting to model fluid mud flow in the Race Track Flume, there is some justification for removing the mean water velocity altogether from the determination of interfacial shear stress, and instead using a modified version of equation 5.4 as follows:

$$\tau_i = \frac{\rho_w f_w}{8}(u_m^2 + v_m^2) \qquad (7.19)$$

This modification would require a simple alteration to the subroutine INTERFACESTRESS (see table 7.1 and appendix 3).

Note that in the case of zero ambient water current, which applies to all the model test results so far discussed, this suggested modification would make no difference, as in this instance the velocity difference Δu in equation 5.4 is already equal to the fluid mud velocity u_m.

7.6.3 Vertical Exchange of Mass and Settling

In the light of the experimental results from the Race Track Flume, vertical exchange of mass between suspension, fluid mud layer and settled bed has been identified as crucial to the pattern of fluid mud flow in a given situation (section 6.4.2, chapter 6). This conclusion was verified by the application of the FLUIDMUDFLOW-2D model as described in section 7.5 above. Further, the modelling of fluid mud dewatering according to equation 5.10 has been shown in section 6.4.3 of chapter 6 to be at least

broadly in agreement with experimental data. It may therefore be assumed that, leaving aside the erosion situation not considered in this investigation, the successful modelling of vertical exchange of mass using the Wallingford FLUIDMUDFLOW-2D software will depend almost entirely on the success or failure of the modelling of settling of suspended mud into the fluid mud layer according to equations 7.7 and 7.8.

It will be noted, of course, that equation 7.7 depends on shear stress at the fluid mud/water interface, and therefore that the previous discussion on shear stresses and friction factors, and particularly the water friction factor f_w, will be crucial here. However, three further issues critically affecting settling behaviour as modelled by equations 7.7 and 7.8 also need to be discussed. These are the determination of settling velocity ω, the evaluation of the near bed (or more properly near fluid mud) suspended mud concentration in terms of the modelled depth-averaged value, and the dependence of settling rate on a ratio of applied shear stress to critical shear stress.

It will be remembered from the discussion in section 5.2.1, chapter 5, and in section 7.3.1 above that the settling velocity algorithm used in the FLUIDMUDFLOW-2D programs (which occurs in the subroutine MUDEXCHANGE, see table 7.1 and appendix 3) takes no account of hindered settling that was found by Thorn (1981) to occur at concentrations of above $15.3kgm^{-3}$ (see equation 6.17, chapter 6). In the application of the model to field situations, this is not likely to be a serious issue, since suspended mud concentrations this high are regarded as rare. In attempting to model a situation such as that encountered in the Race Track Flume, however, hindered settling will be crucial, since almost all the concentrations encountered above the fluid mud appear to have been above $15.3kgm^{-3}$. It is therefore essential that the MUDEXCHANGE subroutine be modified in line with equation 6.17, so as to include the effects of hindered settling at high concentrations. Such a modification is relatively simple to achieve, however, and has no impact on the overall logic of the programs.

With regard to the choice of the constant values in equation 6.17, there is some scope for adjustment. The figures used represent the 'best fit' line as obtained by Thorn (1981), but the data from which this line was derived includes considerable scatter, so it is possible that actual settling velocities may vary from values given by equation 6.17 as it stands by up to half an order of magnitude. This is illustrated in figure 7.53, which shows the relationship of equation 6.17, chapter 6, together with the data from which it was derived.

The second issue, the value of β as defined in equation 7.9, has already been considered to an extent; it follows from the discussions in section 6.3.3, chapter 6 and in section 7.3.1 that a value of β of close to unity is reasonable for laboratory situations. In field situations, the value of β would clearly have to be chosen quite carefully in order to ensure successful results.

There is another issue surrounding the modelling of suspended mud concentration, which is that at the end of each timestep the new concentration of suspended mud is evaluated by dividing the mass of mud remaining in suspension by the whole depth of water above the fluid mud layer, so as to arrive at a depth averaged concentration. However, it is apparent from the discussion in section 6.3.3, chapter 6, that in the settling column experiments and in the Race Track Flume, the mass of mud in suspension can change quite radically with no change or with a slight increase in the local concentration immediately above the fluid mud layer. As explained in section 6.3.3, this is due to the formation of a hindered settling lutocline above which the water clears of sediment almost totally. Whilst the formation of such lutoclines is particularly emphasised in laboratory experiments, such features do occur in field situations (Ross and Mehta 1989).

The upshot of this analysis is that in a deposition situation such as that produced in the Race Track Flume experiments, near bed/fluid mud concentrations cannot be accurately represented by the suspended mud concentration algorithm in the Wallingford FLUIDMUDFLOW-2D model as it stands. Either the value of β must be allowed to increase with time so as to model a constant or gradually increasing

near fluid mud concentration with a gradually decreasing depth averaged concentration, or the depth averaged suspended mud concentration must remain constant or increase gradually, regardless of water depth, whilst there is any mass of mud remaining in suspension. Either of these alternatives could fairly easily be incorporated into the Wallingford FLUIDMUDFLOW-2D programs, requiring alterations only to the subroutine MUDEXCHANGE. However, in attempting to simulate experimental results such as those from the Race Track Flume, the first case would require the evaluation of a β/time relationship that had little physical meaning, whilst the second alternative would represent in a simple manner the observed phenomena as discussed in section 6.3.3 of chapter 6. It is therefore suggested that the second alternative, that of allowing suspended mud to remain at a constant value or to increase gradually while any mud at all remains in suspension, would be more satisfactory.

It is difficult to recommend a solution to the problem outlined in the previous paragraphs that could easily be applied to field situations. The dynamics of lutoclines in real estuaries can be highly complex (Ross and Mehta 1989) and cannot therefore necessarily be related directly to the experimental phenomena discussed in section 6.3.3. Further, in situations where convective transport of suspended mud were both significant and complex in nature and geometry, care would have to be taken to ensure that modification of the model subroutines as suggested did not lead to errors. A far more satisfactory approach, though one requiring complicated programming and increased computer resources, would be to abandon the depth averaged approach to suspended sediment modelling altogether and use a three dimensional suspended mud algorithm such as that of Nicholson and O'Connor (1986) to determine conditions above a fluid mud layer.

The final issue concerning modelling of settling using equation 7.7 is that when the interfacial shear stress τ_i falls below the critical shear stress for deposition τ_d, the rate of settling is still dependent on the ratio τ_i/τ_d. Implicit in this fact, therefore, is the assumption that the interfacial shear stress τ_i is a turbulent shear stress, since only turbulent shear stress due to eddying motions with a vertical component can resist the

settling of mud flocs under gravity. If, however, the flow situation immediately above the fluid mud layer is laminar, which in the light of the experimental results discussed in sections 6.2.2 and 6.2.4 of chapter 6, seems likely to have been the case in the Race Track Flume, there can be no justification for retaining the $(1 - \tau_i/\tau_d)$ term in equation 7.7, since any ambient shear stress due to laminar flow would not cause a reduction in settling rate.

It would be easy to modify the subroutine MUDEXCHANGE to account for this; however, it would be necessary to include some kind of check for turbulent flow, so that the $(1 - \tau_i/\tau_d)$ could be incorporated where it was relevant. The most satisfactory way of doing this would perhaps be to assume that the flow regime immediately above the fluid mud layer corresponded to that in the fluid mud layer, which could be checked by means of the laminar sublayer treatment suggested in the previous section.

7.6.4 Concentration Within The Fluid Mud Layer

It will be remembered from the discussions in section 7.2.2 above that (in the absence of wave effects) the Wallingford FLUIDMUDFLOW-2D software is set up to use a constant fluid mud concentration, C_0, which in the author's runs of the model previously described was defined by equation 7.10. It is apparent, however, from the experimental results discussed in section 6.3, chapter 6, that in laboratory conditions such as those encountered in the Race Track Flume experiments, the fluid mud concentration does not remain constant, but increases with time according to equation 6.1. It is therefore essential that, when attempting to simulate such laboratory conditions, the FLUIDMUDFLOW-2D routines be amended to account for this fact.

Since equation 6.1 includes no dependence on anything except the initial average suspended mud concentration and the elapsed time, it is relatively easy to incorporate it into the FLUIDMUDFLOW-2D programs; it can be placed in the main program

FM101.FOR, so as to increment the fluid mud concentration according to the elapsed simulation time at the beginning of every timestep. However, it is difficult to see how such an alteration to the program would have any physical meaning beyond the laboratory situation as measured in the Race Track Flume. It is clear, therefore, that in order for this issue to be addressed properly in terms of fluid mud modelling, further research will have to be undertaken on the way in which concentration changes within a fluid mud layer.

7.7 Modification of the FLUIDMUDFLOW-2D Model

This section describes the various modifications made to the Wallingford FLUIDMUDFLOW-2D software in the light of the discussions in the previous section. The basic aim of all the modifications was to allow the mathematical model to represent laboratory fluid mud flow as measured by Georgiadis (1989) and in the Race Track Flume with greater accuracy, thereby allowing the basic fluid mud transport equations and explicit layered construction of the model to be properly assessed. Thus, while not all the modifications would be appropriate for a field situation to which the model might be applied in an engineering design situation, they are nevertheless justified from the point of view of verifying the FLUIDMUDFLOW-2D routines' basic transport equations and layered construction for use in such a situation.

7.7.1 Simple Modifications

In the light of the discussions in section 7.6 above, and after a number of trial runs to test various model alternative modifications, the following simple alterations were made to the Wallingford FLUIDMUDFLOW-2D modelling routines:

1. The water density ρ_w was modified to account for the concentration of mud in suspension. Following the discussion on the importance of lutoclines to the

changes in concentration above the fluid mud layer (section 6.3.3, chapter 6), the mud concentration used for this modification was taken as a constant value equal to the initial average suspended mud concentration.

2. The water friction factor f_w was taken as being equal to 0.535 times the fluid mud friction factor f_m. The value of 0.535 is the average of Harleman's (1961) laminar and turbulent values of 0.64 and 0.43 respectively. The use of an average value in this way saves resources involved in checking the flow regime and the innate error of approximately ±20% in the value of f_w was, in the light of the sensitivity analyses described in sections 7.3.5 and 7.3.6, not considered to be significant.

3. Equation 6.17a, describing hindered settling, was incorporated into the model:

$$\begin{aligned} \omega &= \omega_{s1} C^{1.291} && C \leq 4 kgm^{-3} \\ \omega &= \omega_{s3} && 4 < C < 15.3 kgm^{-3} \\ \omega &= \omega_{s4} C^{-0.450} && C \geq 15.3 kgm^{-3} \end{aligned} \qquad (6.17a)$$

Here ω_{s1}, ω_{s2} and ω_{s3} are used to indicate that allowance was made for the variation of the numerical factors in equation 6.17, chapter 6, in line with the experimental scatter as shown on figure 7.53. The value of concentration used in the equation was taken as equal to the fluid mud concentration at the point in question. Thus a condition similar to the situation observed in the laboratory, in which there was no rapid change in concentration at the fluid mud/water interface, was represented (see section 6.3.3, chapter 6).

4. Equation 6.1 was incorporated into the model so as to represent fluid mud concentration as a function only of time, as encountered in the Race Track Flume:

$$C_m = C_{m0} + 2.667 x 10^{-2} t \qquad (6.1)$$

5. Fluid mud viscosity was modelled using equation 6.32, chapter 6, which is based on Race Track Flume data:

$$\nu_m = e^{(0.1096\,\rho_m - 123.487)} \qquad (6.32)$$

This replaced equation 7.4 used in the original model.

These modifications were implemented straightforwardly and were found to operate successfully, allowing the model to converge to a solution in a stable and consistent manner. The hindered settling equation (point 3 above) does however result in a high degree of sensitivity to variations in the numerical constants used, as shown in figure 7.54. The figure indicates that if a value of ω_{s4} is to be adequately derived from settling velocity measurements at a concentration of 30kgm^{-3}, the settling velocity will have to be resolved to much finer than 0.1mms^{-1}, which is the accuracy required to set ω_{s4} to within 0.01. This is unlikely to be possible with currently available instrumentation.

7.7.2 Determination of Fluid Mud Friction Factor

Following the successful implementation of the simple alterations to the FLUIDMUDFLOW-2D software as described in the previous section, various alternative methods of determining the fluid mud friction factor f_m were investigated, as follows:

1. f_m determined from the original 'Smooth Turbulence Theory Model' from Hydraulics Research Wallingford Limited (1992) as per equation 7.3, but bearing in mind that the viscosity used in determining Reynolds number was based on equation 6.32 rather than equation 7.4 (see modification 5 in section 7.7.1 above).

2. f_m determined from a 'Couette Model' by a re-arrangement of equation 6.7, chapter 6 and using $\alpha = 0.64$ to represent laminar flow as encountered in the Race Track Flume:

$$f_m = \frac{8g(\rho_m - \rho_w)d_m S}{\rho_m(1 + \alpha)u_m^2} \qquad (7.20)$$

3. f_m determined from the 'Harleman Model' equation 6.8, chapter 6 (Harleman 1961), with Reynolds number calculated as for the original smooth turbulence theory algorithm:

$$f_m = \frac{34.688}{R} \qquad (6.8)$$

4. The 'Simple Model'; f_m not calculated at all, but specified directly and maintained at a constant value throughout the simulation.

These four alternatives were incorporated into the model and evaluated against experimental data from Georgiadis (1989) for slope 1:5, initial average concentration $30kgm^{-3}$, as shown in figure 7.55. For this test, a ω_{s4} value of 0.07 and a v_0 value of $5x10^{-4}ms^{-1}$ were used.

The best fit to the experimental data was obtained from the original model algorithm combined with the new viscosity model, as explained in point 1 above. A close second to this is the Harleman model, based on equation 6.8. The reason for the similarity in results between the Smooth Turbulence Theory Model and the Harleman Model is that Reynolds numbers in the simulation were generally less than 46, indicating laminar fluid mud flow, in which the Smooth Turbulence Theory in equation 7.3 predicts $f_m = 24/R$ and the Harleman Model predicts $f_m = 34.688/R$, giving a constant difference in the f_m values determined by the two methods of approximately 30%. The other methods of determining fm provide more widely differing values at various points in the investigation.

After the Smooth Turbulence Theory Model and the Harleman Model, the 'next best' fit to the experimental data in the situation tested is given by the Simple Model, with f_m set to a constant value of 20. Despite the scientific principles in its favour, the Couette Model produces most unsatisfactory results for the case tested, with both fluid mud velocity and thickness being vastly over-predicted, though at different times during the simulation. In fact, the Couette Model results in friction factors too high to simulate the observed relationship between fluid mud velocity and thickness.

Since the results of the Harleman Model, which match the experimental data fairly closely, and the Couette Model, the results of which do not match the experimental data at all, are closely related in theory (especially since the viscosity values used to determine Reynolds number for the Harleman model came from experimental data processed via a Couette flow analogy, as stated in section 6.6.6, chapter 6), it may be postulated that the error in the use of the Couette Model is due to the dependence of equation 7.20 on the density values ρ_m and ρ_w. In view of the limited concentration data obtained in the current investigation, it is debateable as to how quantitively accurate are the estimates of these bulk density values used in the model study.

Following this analysis, it was concluded that calculation of fluid mud friction factor should be carried out using the original smooth turbulence theory from Hydraulics Research Wallingford Limited (1992). Results of a test run for Georgiadis' (1989) data using this friction factor model and the slope, concentration and ω_{s4} and v_0 values stated above are shown in figures 7.56 and 7.57. An acceptable fit for fluid mud velocity, thickness and elevation is produced, and although no experimental data can be identified with which to compare them, the plots of the various parameters against x-distance for various elapsed times show that the simulation results are sensible throughout the model geometry. It is interesting to note that fluid mud elevation is shown to be the same at all x-positions apart from the model extremities at any given time. This follows naturally from the methods used to simulate fluid mud concentration and dewatering; its significance will be further discussed in section 7.8.2 below.

Listings of the amended versions of the author's main program, FM101.FOR, and the subroutines BEDSTRESS, INTERFACESTRESS, MUDEXCHANGE and MUDVEL are included in appendix 3, the BEDSTRESS listing including code for all the mud friction factor models tested with the unused parts commented out. It must be remembered that the model modifications and their tests described in the preceding sections are rather limited in scope. In particular, the various methods of calculating friction factor were applied only after all the simple modifications described in section 7.7.1 had been incorporated into the model routines, so the effect of the various friction factor calculations in the absence of these other modifications, or of some of them, cannot be assessed. Neither was a rigorous analysis of all the friction factor calculation methods carried out before choosing a final version for the remaining model verification runs. Great caution must therefore be taken in extending the conclusions of the study described here to situations beyond the current scope.

7.8 Verification of the Modified FLUIDMUDFLOW-2D Model

The following sections discuss the final results obtained by running the Modified FLUIDMUDFLOW-2D routines to simulate the experimental observations of Georgiadis (1989) and the current investigation using the Race Track Flume. Section 7.8.1 gives a broad overview of the model's performance in the situations to which it was applied, whilst section 7.8.2 discusses certain specific features of the model results which allow conclusions as to the merits and demerits of the model routines to be drawn.

7.8.1 General Features of the Model Results

Results from application of the modified FLUIDMUDFLOW-2D routines to the experimental arrangements of Georgiadis (1989) and the Race Track Flume are included in figures 7.58 to 7.62. These results were obtained using the values of settling constants and dewatering velocity given in table 7.13. As with the initial

verification described in section 7.5 above, a deliberate policy of not changing empirical parameters according to changes in bed slope was adopted, since no justification could be found for such adjustments.

Table 7.13: Values of Empirical Parameters Used in Modified Model Runs

Details of Experiment Simulated	ω_{s3} in Equation 6.17a	ω_{s4} in Equation 6.17a	v_0 (ms^{-1})
Georgiadis (1989), 30.0kgm^{-3}	-	0.07	$5x10^{-4}$
Georgiadis (1989), 15.6kgm^{-3}	-	0.07	$6x10^{-4}$
Georgiadis (1989), 7.0kgm^{-3}	$9.2x10^{-4}$	-	$6x10^{-4}$
Race Track Flume, 80kgm^{-3}	-	0.05	$2.25x10^{-4}$
Race Track Flume, 40kgm^{-3}	-	0.05	$2.25x10^{-4}$
Race Track Flume, 20kgm^{-3}	-	0.05	$2.25x10^{-4}$

The Race Track Flume results of figures 7.61 and 7.62 include no influence of non-zero currents in the overlying water. Fluid mud thicknesses shown on the figures have, except where stated, been processed according to equation 7.14, and fluid mud elevations are obtained from mass of mud in the settled bed by use of constant bed bulk density figures, these being 1054kgm^{-3} for Georgiadis' (1989) experiments and

1103kgm^{-3} for the Race Track Flume experiments. These are conceptual figures; the former is taken from results quoted in Ali and Georgiadis (1991) and the latter is based on the X-Ray settling column experiments carried out at the University of Oxford using Seaforth Dock Mud as used in the Race Track Flume (see section 6.4.4, chapter 6). In the range of the model results quoted, the percentage differences in fluid mud elevation caused by quite significant variations in the conceptual bed density are extremely small.

It is clear that, except in certain circumstances, the model results do not represent an acceptable fit to the experimental data, and it may be concluded that the model is not, in general, simulating observed fluid mud flow in a satisfactory manner. However, in the case of Georgiadis' (1989) experiments with initial concentrations of 30.0kgm^{-3} and 15.6kgm^{-3}, the overall pattern of fit is improved from the unmodified model, since in addition to velocity and thickness, fluid mud elevation is now simulated with reasonable accuracy. This does not, however, detract from the discouraging picture obtained when considering the results as a whole.

Figure 7.63 shows the basic response of the modified FLUIDMUDFLOW-2D routines to changes in concentration in the Race Track Flume situation compared with the observed response of fluid mud flow in the flume. As can be seen, qualitative changes in magnitude of peak velocity and in fluid mud elevation are reproduced correctly, though the timing of peak velocity and the pattern of fluid mud thickness are not.

It is fair to say that it may be possible to improve the fit between model and experimental data as shown in the figures by further very careful adjustment of the empirical parameters given in table 7.13. This is, however, an extremely time consuming process, as, for example, changes dewatering velocity cause alterations in fluid mud thickness and hence velocity, necessitating further changes in settling constant, all of which must be tested by trial and error. Neither would such adjustment be possible in a design situation, where, by definition, there would be no observed fluid mud flow data to which to fit the model results, and it would be

possible to set the various empirical parameters only according to scientific reasoning as was done for the results quoted here. It was therefore considered a waste of resources for the author to spend any further time on adjusting model parameters so as to obtain a better fit to measured data.

7.8.2 Specific Features of the Model Results

For each model run there is a limiting factor of the total amount of mud in suspension in the flume at the start of each experiment. In the case of Georgiadis' (1989) experiments, this figure was not readily available, as the water depth in the small flume was in many instances not recorded. However, in the Race Track Flume the water depth was always known, and, whilst changing the settling constant was found in some circumstances to improve the fit between modelled and measured fluid mud flow early in the simulation, it would also cause all the mud in suspension to settle out much more rapidly than was observed in the experiment, meaning that the simulation were still incorrect in at least one important respect. This problem is related to the sensitivity of modelled fluid mud flow to the constants used in the hindered settling equation 6.17a as discussed in section 7.7.1 above. It suggests that the way in which settling into the fluid mud layer is handled in the modified FLUIDMUDFLOW-2D software is not satisfactorily realistic to allow reliable simulation of the formation of fluid mud due to settling from suspension.

Figures 7.61 and 7.62, the Race Track Flume verification results, show a further worrying feature, which is that the fluid mud depth at the upstream section, section B, is heavily influenced by back-up from downstream. Thus, the fluid mud depth at section B at many points less than that at E by approximately 0.128m, which is the height difference between the two sections. This feature also influences fluid mud velocity, where negative velocities are found to occur due to back up from downstream. These results occur despite the fact that the flume was modelled for two full metres downstream of section E to allow fluid mud to flow past that section and collect at the low end of the Race Track Flume, as was the case in the experimental

situation. In the experiments, there was no evidence to suggest that the moving fluid mud layer was at all influenced by downstream conditions. The extreme thicknesses of fluid mud modelled in most of the runs carried out indicates that the vertical exchange of mass throughout the water column is not being correctly simulated. However, reduction of setting into and/or dewatering of the fluid mud layer causes not only a drop in fluid mud thickness but a corresponding drop in fluid mud velocity. This suggests that the basic relationship between fluid mud thickness and velocity, or some other factor influencing this such as bed shear stress or the density difference between the fluid mud and overlying suspension, is not being modelled satisfactorily.

As mentioned above, the Race Track Flume results shown on the figures do not include the influence of any ambient current in the water overlying the fluid mud layer. This follows from the discussions of 6.2.2, chapter 6 and 7.6.2 above. However, when such a current is included in the model, there is a marked effect on fluid mud results, as shown in figure 7.64. In preparation of this figure, paddle speed 2 was represented in the model by a mean water discharge of $0.0109m^3s^{-1}$, which was derived from fitting surface speeds observed during the fluid mud experiments to results from the computational fluid dynamics study of water flow in the Race track Flume as discussed in chapter 3. The FLUIDMUDFLOW-2D results are clearly not realistic, since as discussed in section 6.2.2, no trend linking paddle speed and fluid mud flow was observed during the experiments. It may be stated, however, that with the model as it stands, using a two-dimensional, depth-averaged approach to the movement of water and suspended mud, there is no way in which the phenomena discussed in 6.2.2 could be simulated realistically. To do this would require the complex behaviour of the mud/water suspension above the fluid mud to be simulated in three dimensions.

Figure 7.65 shows the results of the model as run for the Race Track Flume, with the critical shear stress for deposition, τ_d, set to a high value to represent the presence of laminar fluid mud flow. These are compared with results obtained with a value of $0.07Nm^{-2}$ as used by Odd and Rodger (1986). As can be seen, the effect the change

in τ_d on the results in question is insignificant, though this may be altered in the presence of significant ambient water current, which would increase the shear stress above, and thus reduce settling into, the fluid mud layer.

A further worrying trend of the model results was mentioned in section 7.7.2 above and is illustrated in figure 7.66. This shows the relationship between fluid mud elevation at sections B and E in the Race Track Flume. The model predicts fluid mud elevation to be identical at these two points, and at all other points, to be identical at any given time. This follows naturally from the dewatering model used and the fact that concentration of the fluid mud layer is unrelated to spatial location. Figure 7.66b shows experimental results corresponding to the model results of 7.66a. It can be argued that bed growth is, in this case, the same at the two locations, though as comparison of figures 6.21 and 6.24 in chapter 6 will show, this is not the overall trend of the experimental results. As discussed in section 6.2.1, chapter 6, fluid mud elevation appears in general to vary in proportion to the total depth of water column at a given location. The model results would, of course, be altered were the constant bed densities used above altered at the different locations, but use of any remotely reasonable bed density value could not alter the modelled elevations by more than about 5%, which is much less than the 30% (factor of 1.3) variation between the sections as discussed in chapter 6. It may therefore be concluded that dewatering of fluid mud is not being modelled correctly by the FLUIDMUDFLOW-2D routines.

7.9 Conclusions

Specific conclusions of the model study described in this chapter are enumerated in section 7.9.1 below. More general conclusions and recommendations for further work in the area of mathematical modelling of fluid mud transport, are included in section 7.9.2.

7.9.1 Specific Conclusions Concerning Fluid Mud Modelling using the Wallingford FLUIDMUDFLOW-2D Software

The specific conclusions arising from the model study described above may be summarised as follows:

1. Representation of fluid mud as being of a constant concentration is not appropriate to simulation of laboratory experiments such as those of Ali and Georgiadis (1991) or the experiments conducted in the Race Track Flume.

2. In order to ensure convergence and stability of the finite difference solution, timestep Δt and spacestep Δx used in the Wallingford FLUIDMUDFLOW-2D programs should be chosen so as to give the required precision of output and a ratio $r = \Delta t/\Delta x^2$ of less than 100.

3. In order to ensure consistency between the model solution and the equations represented, the model spacestep Δx should be chosen so as to keep variations in parameters at adjacent model grid locations to a minimum.

4. For the cases tested, results of FLUIDMUDFLOW-2D simulations are highly sensitive to the values of fluid mud viscosity ν_m and settling constant ω_s chosen. Fluid mud elevation is also sensitive to the value of dewatering velocity v_0 chosen.

5. When water friction factor f_w is high (ie of the order of 4000), order of magnitude changes in its value cause significant changes in modelled fluid mud flow.

6. The Wallingford FLUIDMUDFLOW-2D software is capable of modelling fluid mud with a finite thickness and a zero velocity. However, this phenomenon of stationary fluid mud has not been observed in the laboratory, where fluid mud has so far been identified due to its motion. For comparison

purposes, model results may be processed to allow for the inability to observe stationary fluid mud in the laboratory by use of equation 7.14.

7. The Wallingford FLUIDMUDFLOW-2D software as made available to the author is capable of simulating certain features of laboratory fluid mud flow under certain circumstances. However, the model routines do not produce any overall pattern of results comparable with laboratory data.

8. Critical evaluation of the model transport equations indicates them to be crucially dependent on shear stresses at the bed and at the fluid mud/water interface, and on the difference in bulk density between the fluid mud and the overlying mud/water suspension. Modelling of settling into and concentration changes within the fluid mud layer are also highly significant.

9. Various different methods of determining fluid mud friction factor f_m, such as Hydraulics Research Wallingford Limited's (1992) smooth turbulence theory and the author's Couette flow analogy, produce different results in various different situations. There is therefore considerable scope for varying the way in which f_m is calculated in the FLUIDMUDFLOW-2D programs.

10. For the laboratory situations tested, the best model results were obtained using the smooth turbulence theory method of determining fluid mud friction factor f_m. This is the method originally used by Roberts (1992).

11. The effect of laminar fluid mud flow conditions needs to be considered; in particular, traditional concepts of critical shear stress for deposition cannot apply to laminar conditions where shear stresses do not result from eddying motion with a vertical component which can resist the settling of mud flocs.

12. The FLUIDMUDFLOW-2D software as modified by the author remains highly sensitive to the numerical constants used in the hindered settling algorithm. For concentrations in the region of 30kgm^{-3}, the degree of

sensitivity appears to be greater than could be resolved by measuring settling velocity using currently available instrumentation.

13. Further research is necessary to determine the general behaviour of concentration within a fluid mud layer.

14. The FLUIDMUDFLOW-2D routines as modified by the author do not in general produce a good quantitative fit with laboratory data; however, in certain specific circumstances the fit is improved from that obtained with the unmodified version of the software.

15. It is possible to significantly change the fluid mud flow results obtained from the FLUIDMUDFLOW-2D software by altering empirical parameters such as the numerical constants in the settling velocity algorithm and the fluid mud dewatering velocity.

16. The model routines correctly simulate qualitative changes in the magnitude of peak fluid mud velocity and in fluid mud elevation with initial average mud concentration in suspension. However, corresponding qualitative changes in the time at which peak fluid mud velocity occurs, and in fluid mud thicknesses are not correctly reproduced.

17. The settling behaviour of mud in suspension above the fluid mud layer is not satisfactorily simulated, even when hindered settling is taken into account by modifying the original FLUIDMUDFLOW-2D routines.

18. Results from a simulation of fluid mud flow in the Race Track Flume indicate that observed fluid mud transport is often not simulated correctly by the FLUIDMUDFLOW-2D software; in particular, the mathematical model frequently fails to reproduce realistic relationships between fluid mud velocity and fluid mud thickness. This may be due to incorrect simulation of the

density difference between the fluid mud layer and the overlying mud/water suspension.

19. Model results show ambient current in the overlying mud/water suspension to have an effect on fluid mud flow. However, no such effect was observed in experiments carried out in the Race Track Flume.

20. At any given time, the FLUIDMUDFLOW-2D software models bed depth to be equal at every location where fluid mud is present. This does not correspond to experimental observations and indicates that the dewatering algorithm based on a single constant dewatering velocity v_0 is not satisfactory.

7.9.2 General Conclusions and Recommendations for Future Research on the Mathematical Modelling of Fluid Mud

The following passages attempt to draw out the main points from the above conclusions and to recommend possible approaches to future work on fluid mud modelling. It is important, however, to re-emphasise the limitations of the study from which the conclusions have been drawn; in particular, that the model tests described and commented on did not address the issues of erosion and entrainment of fluid mud, which clearly form an important part of the fluid mud phenomenon as a whole, and that the FLUIDMUDFLOW-2D software was conceived and written entirely for application to large scale field situations, whereas the author has tested it against relatively small scale laboratory data. The reasons for the author's approach to the problem have already been explained; however, it is important that the limitations of the study are born constantly in mind as the conclusions and recommendations arising from it are considered.

In commencing the model study described in this chapter, the author's main objective was to use laboratory data to assess the usefulness of a currently existing modelling technique as a design tool for engineers. Such an assessment of the

FLUIDMUDFLOW-2D programs had not previously been possible due to the absence of fluid mud data for comparison with model results. In commencing the study, it was known that there were obvious differences, apart from simply scale, between the laboratory and the field situation, but it still appeared that the laboratory data available was sufficient to test the basic construction and transport equations of the model, provided that the programs could be set up in such a way to allow the various process models, such as settling of mud flocs, that contribute to the overall system model, to represent the laboratory processes in a realistic manner.

It appears, however, that the author did not succeed in setting up the model in this way. In particular, as will be clear from consideration of points 12, 17 and 20 in the previous section, the vertical exchange of mass due to settling and dewatering of the fluid mud has not been effectively modelled. It may therefore be said that, whilst as indicated by point 19 in the previous section, the apparent performance of the transport equations in FLUIDMUDFLOW-2D is not reliably good, it would not be fair to make too harsh a criticism of the basic nature of the mathematical model based solely on the results discussed earlier in the chapter.

The evidence of the study, in fact, indicates the main problems with the FLUIDMUDFLOW-2D modelling approach to be the lack of three dimensional detail in the way that exchange of mud mass across the modelled layers is simulated. This may even be the cause of the apparent lack of reliability in the model's transport equations since the difference between bulk density in the fluid mud layer and in the overlying water has been shown (in section 7.6.1 above) to be a significant factor in the solution of the model momentum equations as applied to the laboratory situation. This depends crucially on the vertical density profiles in the water column, which FLUIDMUDFLOW-2D makes no attempt to model in detail. It may therefore be argued that a three dimensional simulation of the suspended mud motion above the fluid mud layer will enable the actual fluid mud transport algorithms of FLUIDMUDFLOW-2D to function in a satisfactory manner. This is basically the conclusion reached by Odd and Cooper (1986) in their original implementation of the

FLUIDMUDFLOW-2D software, and it is interesting that comparison of model results with detailed data has only served to confirm this view.

There is, of course, scope for considerable further work which will assist future attempts at fluid mud modelling. For example, point 9 in the previous section indicates that there are a number of ways in which the determination of a fluid mud friction factor may be addressed; it is possible to envisage a series of more detailed, small scale experiments designed to tackle this particular issue whilst removing other exterraneous variables. Similarly, according to point 13 above, there is a need for more study of the changes in concentration in a fluid mud layer, and indeed of the very early stages of consolidation in general. Progress in each of these issues will undoubtably shed further light on appropriate methods of modelling fluid mud transport for engineering design purposes.

As a final point, however, it must be stated that computational facilities have advanced a very great deal since 1988 when Nicholas Odd and Alan Cooper carried out their first study using the FLUIDMUDFLOW-2D routines at Hydraulics Research Wallingford Limited, and whilst an explicit layered system model, with preferably a three dimensional model of suspended mud transport above it, seemed an appropriate solution at that time, modern facilities will now enable a much more detailed approach to the fluid mud problem, as has been begun by Teisson et al (1992) and by Le Hir (1994). Here, albeit in one dimensional vertical format, attempts have been made to model mud suspensions as a two-phase fluid, with salt water as a continuous phase and mud flocs as a dispersed, solid phase. Such methods allow features such as lutoclines, and, crucially, the fluid mud/water and fluid mud settled bed interfaces to be modelled implicitly, with the whole water column treated as a single entity for computation purposes - much like it appears when viewed during a fluid mud experiment in the Race Track Flume. To this system modelling approach can be added, of course, improved process modelling such as the determination of settling velocity from physical parameters such as floc size and density, or even the direct modelling of the flocculation process itself. It is the author's belief that this type of work represents the future of fluid mud modelling, and that the time is now

ripe for the extension of such modelling approaches into two dimensional, laterally averaged or three dimensional formats. Results from such future modelling attempts could then, as an initial test, be compared with the author's data from the Race Track Flume.

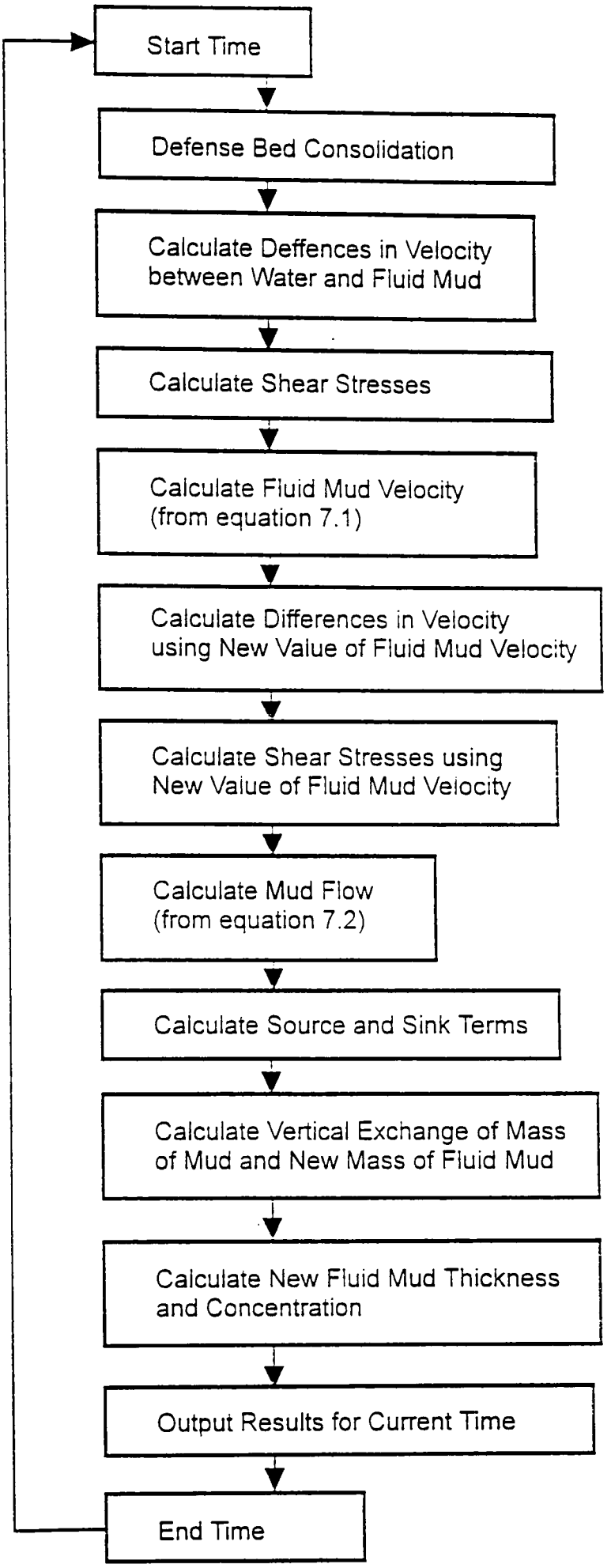

Figure 7.1: Simplified Flow Chart of the Wallingford FLUIDMUDFLOW-2D Model

i value:	1	2	3	4	5	6	7	8
j value:								
1	1	1	1	1	2	1	1	1
2	1	1	1	1	3	1	1	1
3	1	1	1	1	4	5	1	1
4	1	1	1	6	7	8	1	1
5	1	1	1	9	10	11	1	1
6	1	1	1	12	13	1	1	1
7	1	1	14	15	16	1	1	1
8	1	1	17	18	19	20	1	1
9	1	21	22	1	23	24	1	1
10	1	25	26	1	27	28	29	1
11	30	31	32	33	34	35	36	1
12	37	38	39	40	41	1	1	1
13	42	43	44	45	1	1	1	1
14	46	47	48	49	1	1	1	1

Inactive (Dry Land) Cell; k = 1

Active (Water) Cell; k > 1

karray(i,j) = k; e.g. karray(2,10) = 25

Figure 7.2: Diagram Explaining k-array as used in the Wallingford FLUIDMUDFLOW-2D Programs

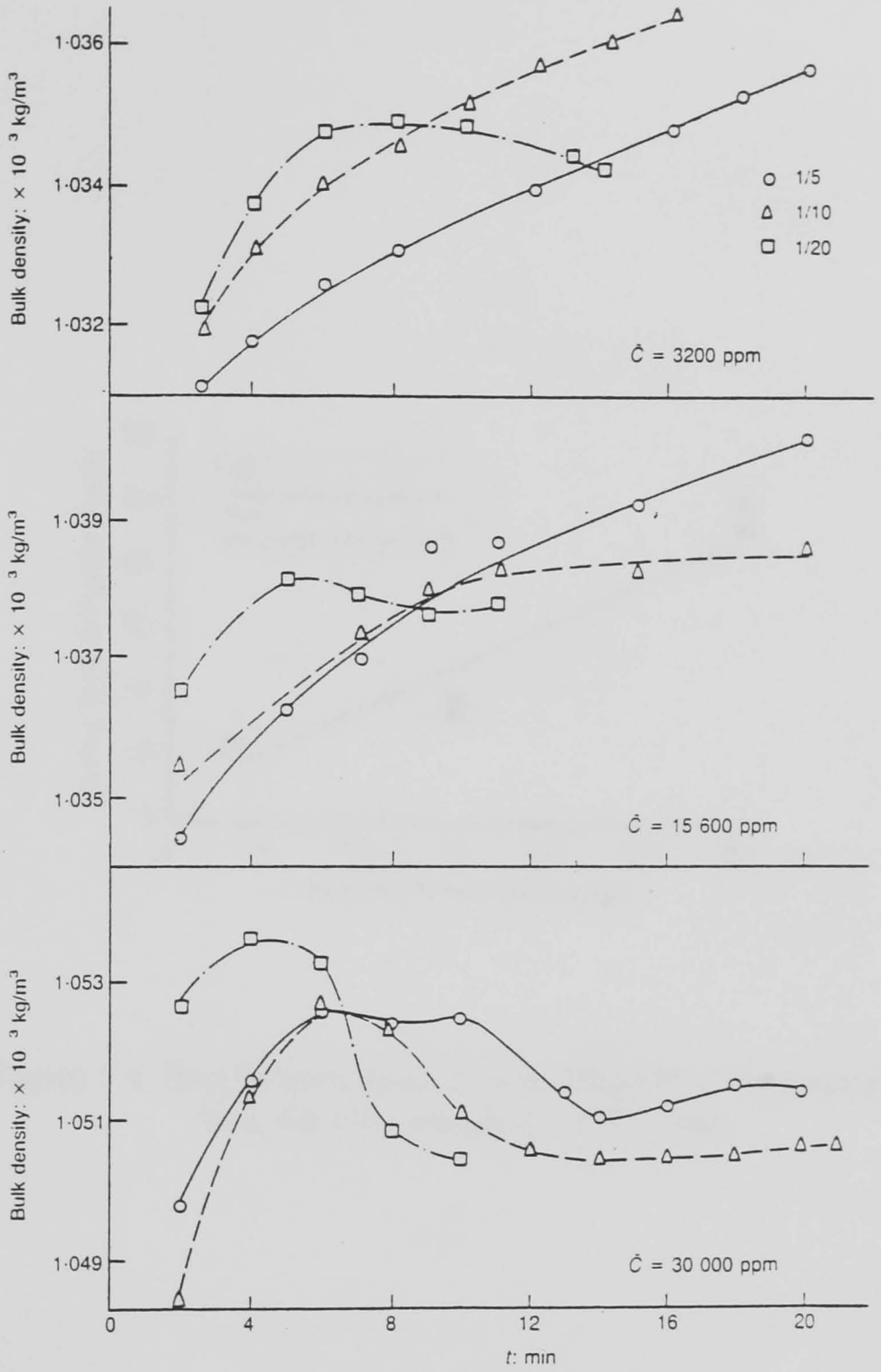

Figure 7.3: Data from Ali and Georgiadis (1991) showing Bulk Density at which Fluid Mud was First Observed

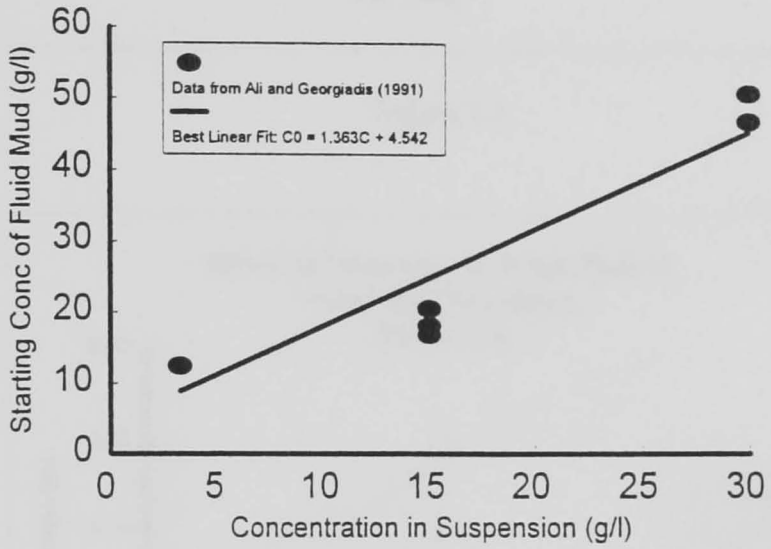

Figure 7.4: Simple Derivation of Initial Fluid Mud Concentration from Ali and Georgiadis' (1991) Data

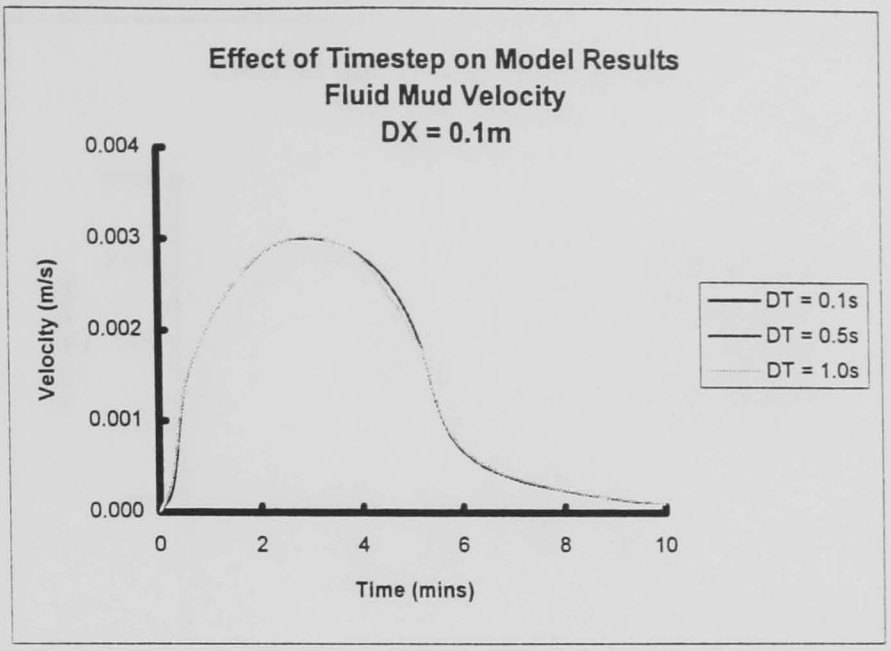

Figure 7.5

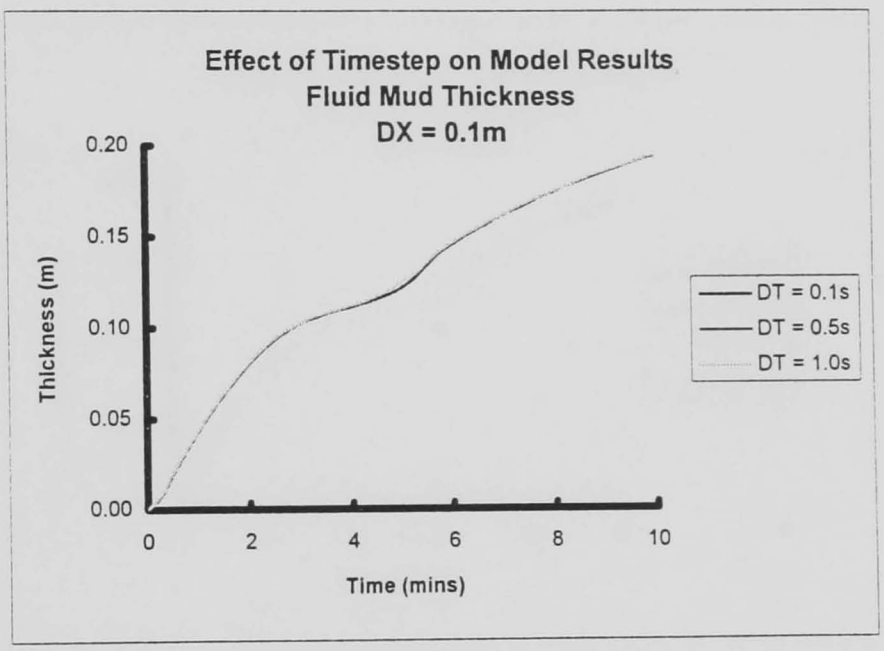

Figure 7.6

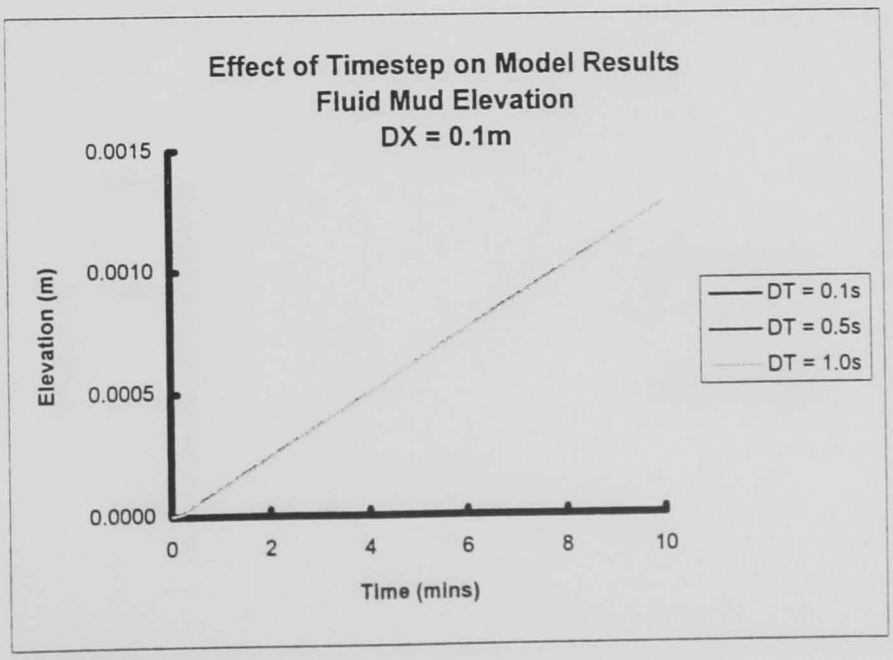

Figure 7.7

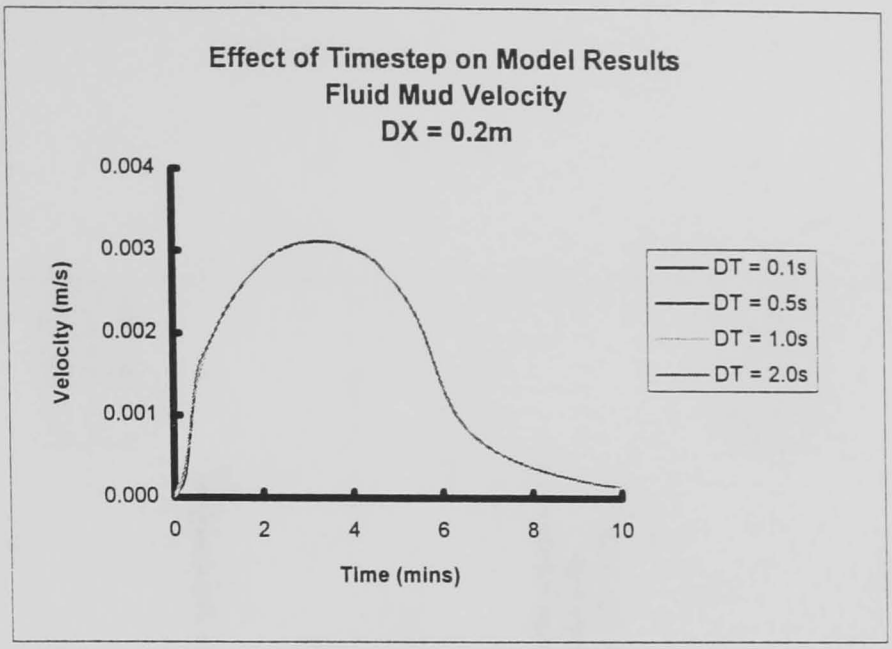

Figure 7.8

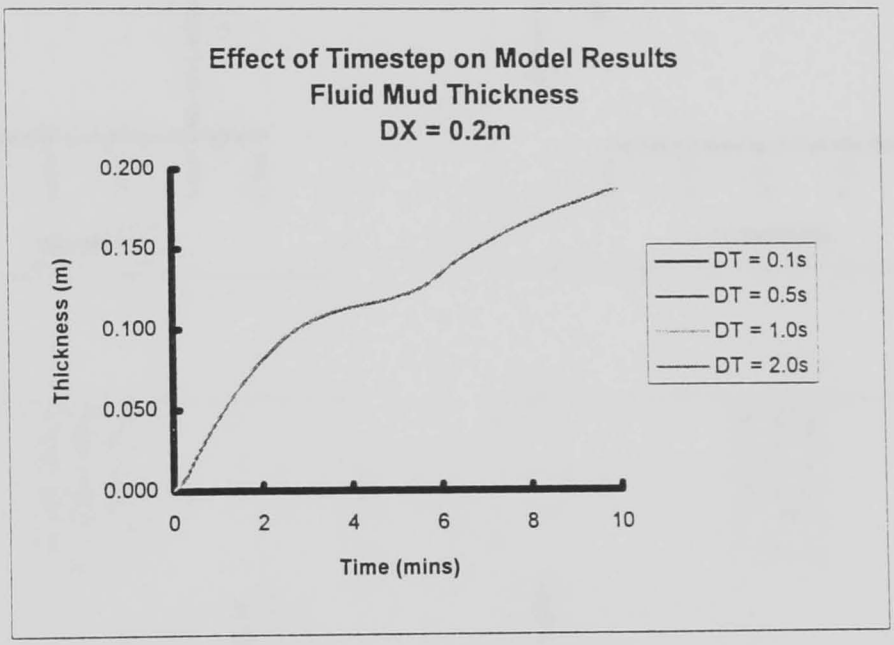

Figure 7.9

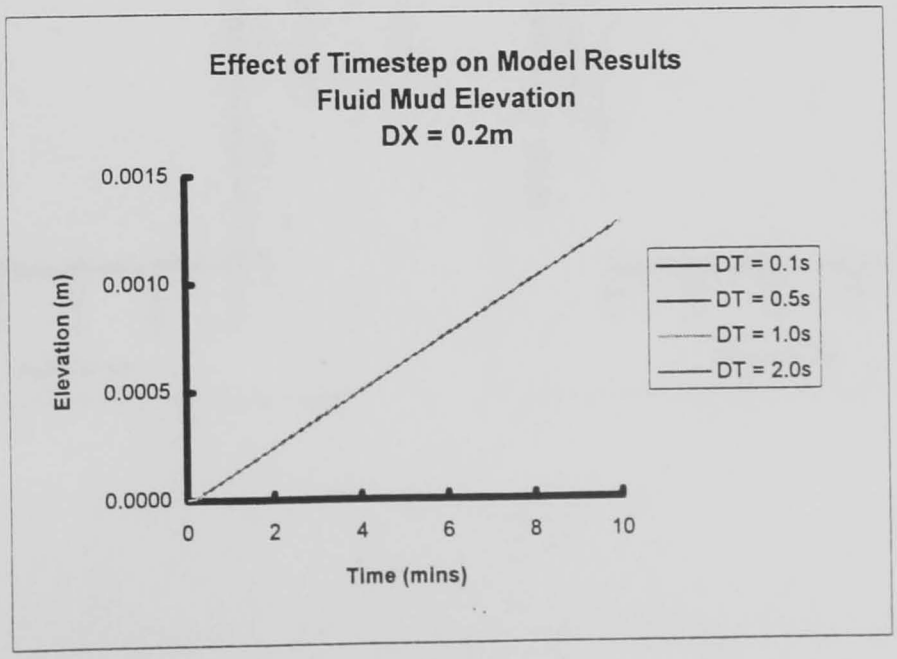

Figure 7.10

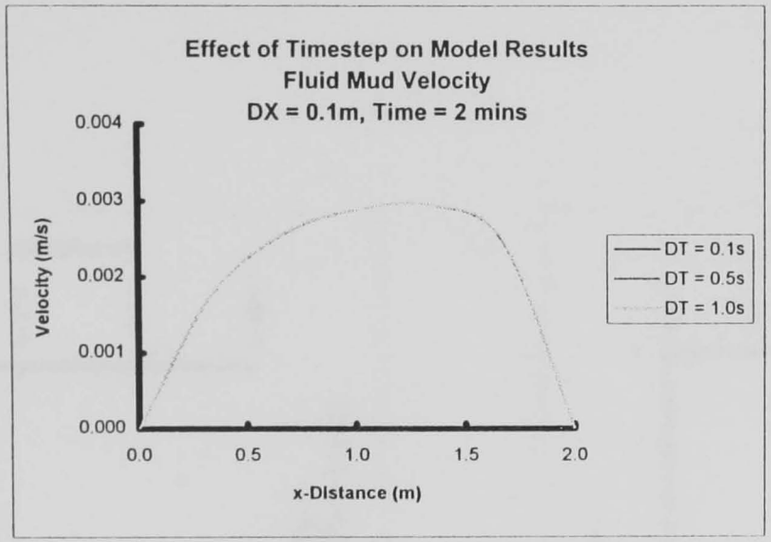

Figure 7.11

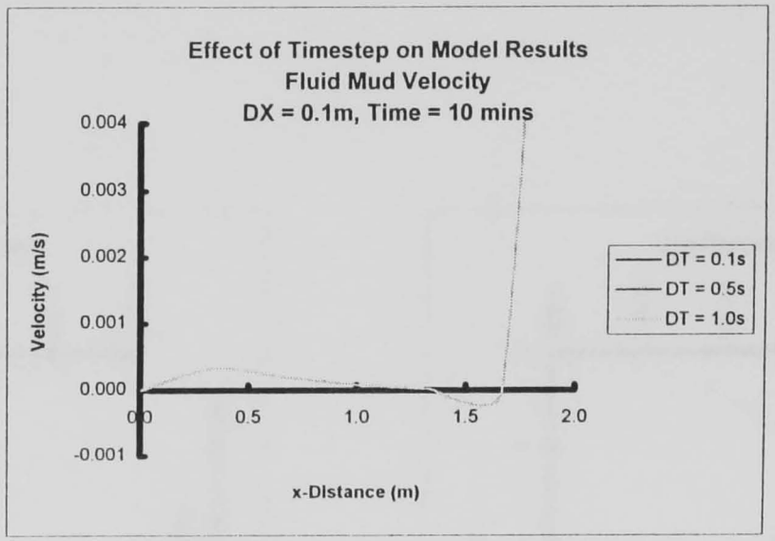

Figure 7.12

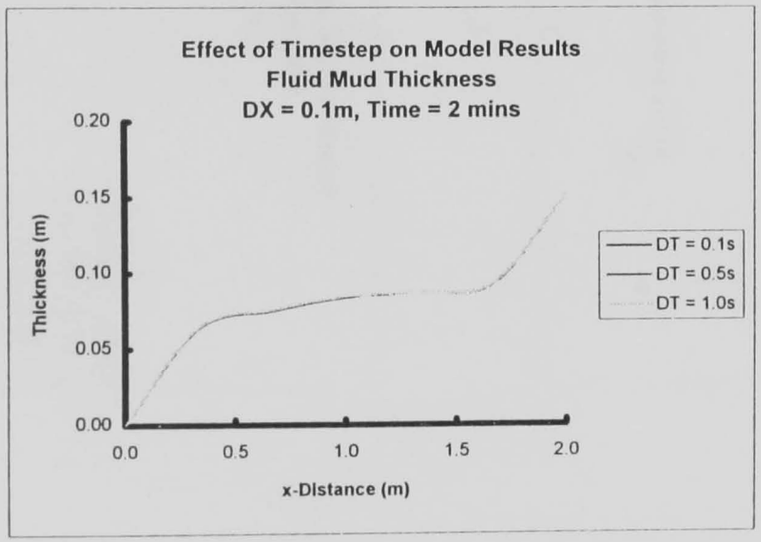

Figure 7.13

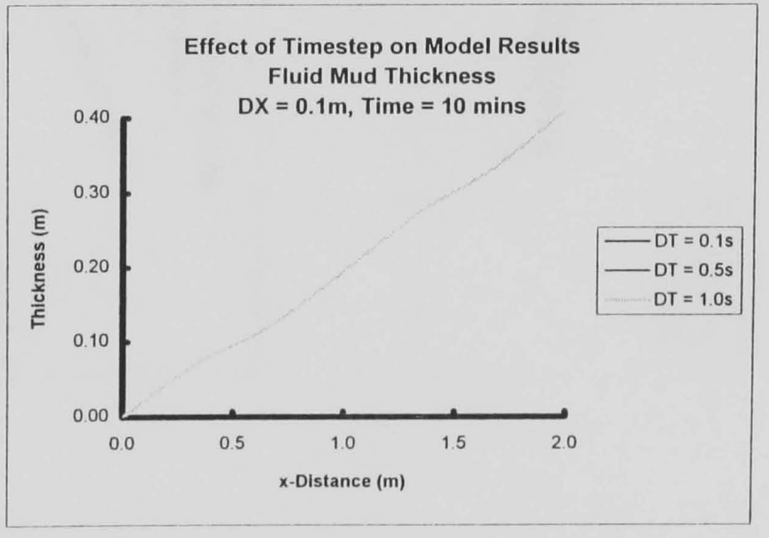

Figure 7.14

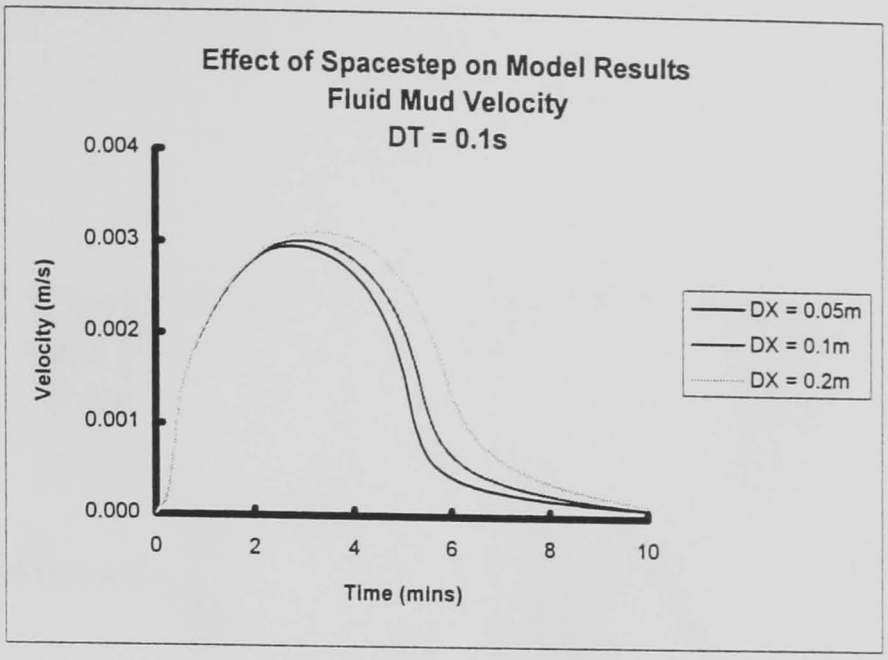

Figure 7.15

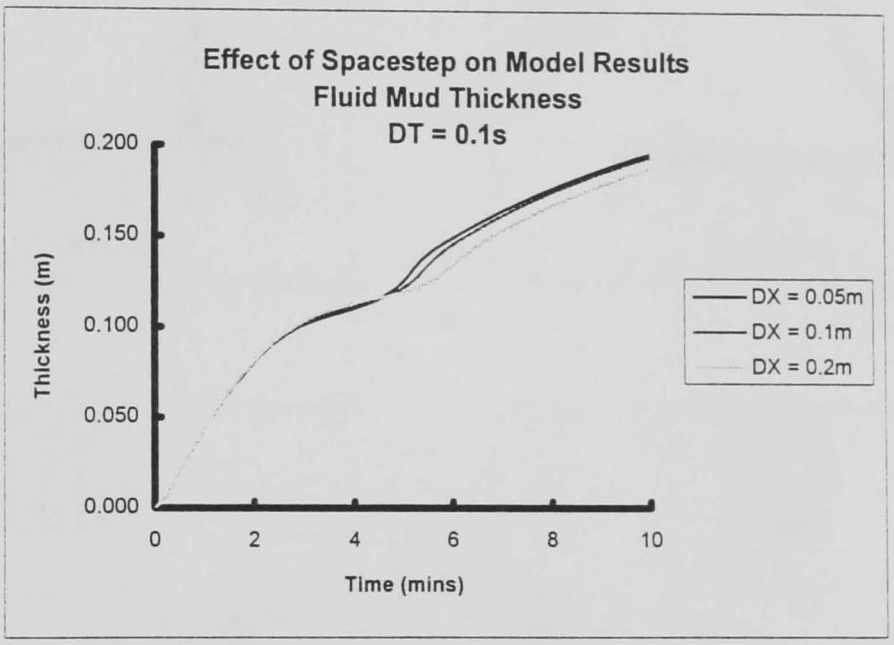

Figure 7.16

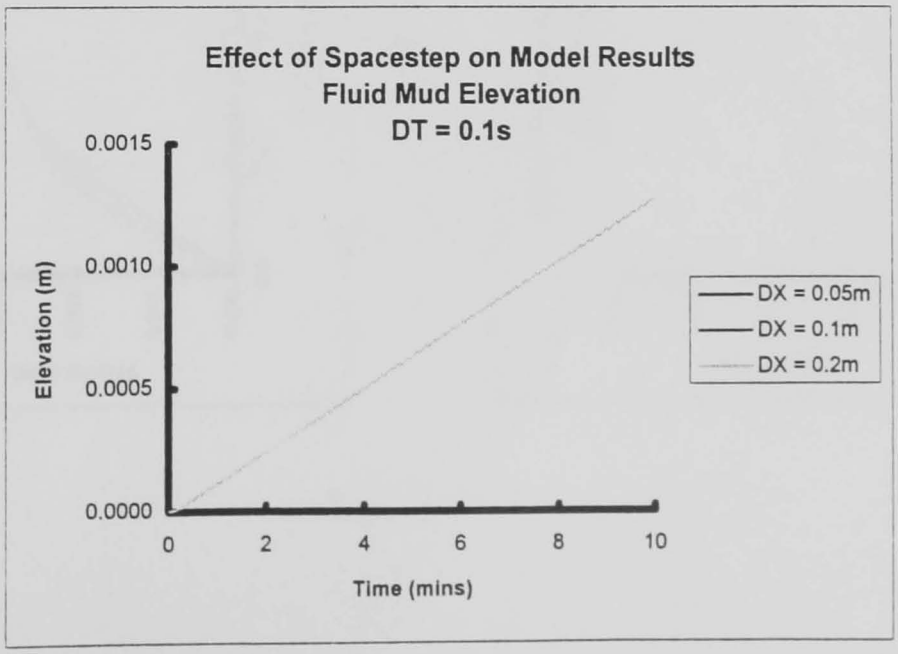

Figure 7.17

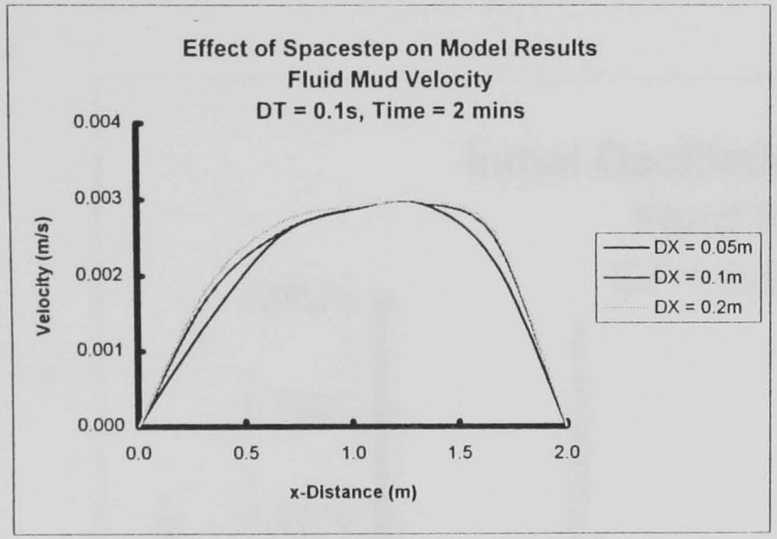

Figure 7.18

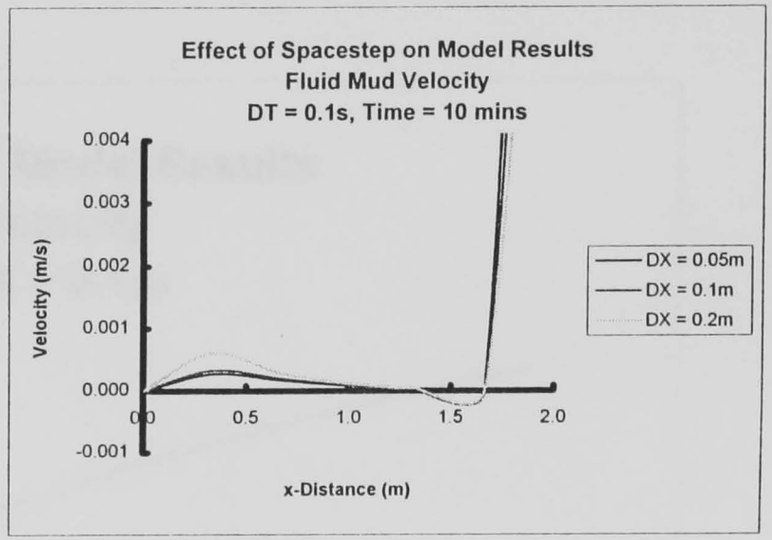

Figure 7.19

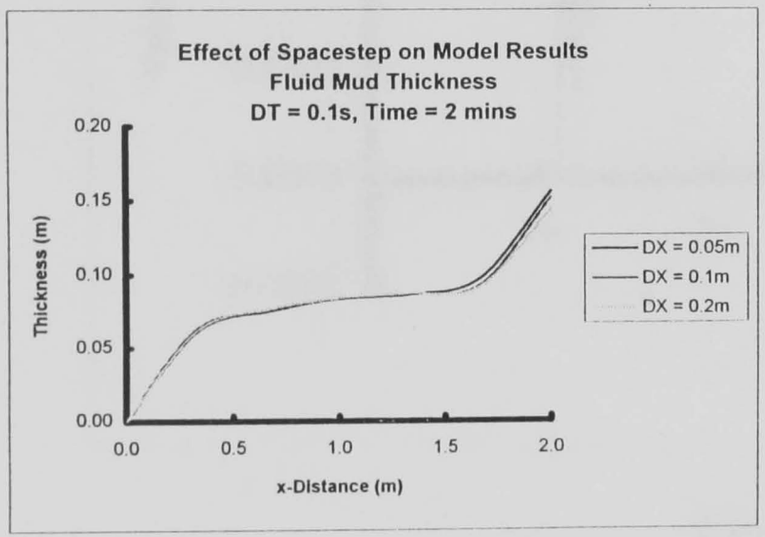

Figure 7.20

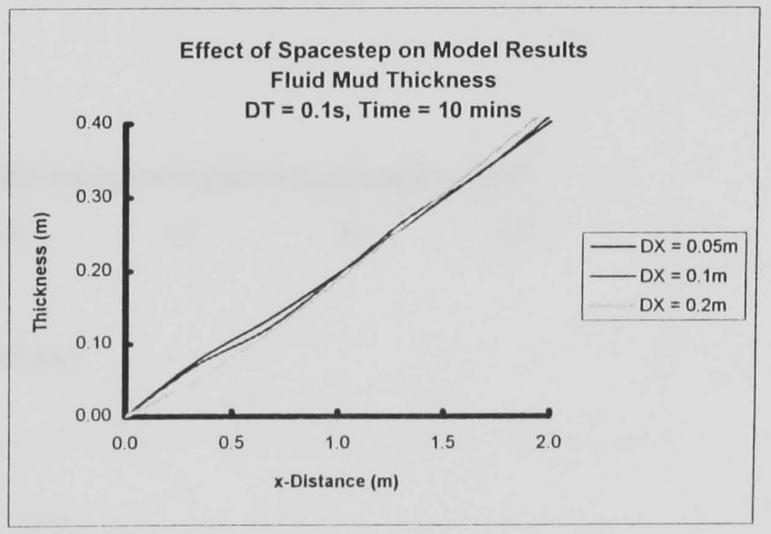

Figure 7.21

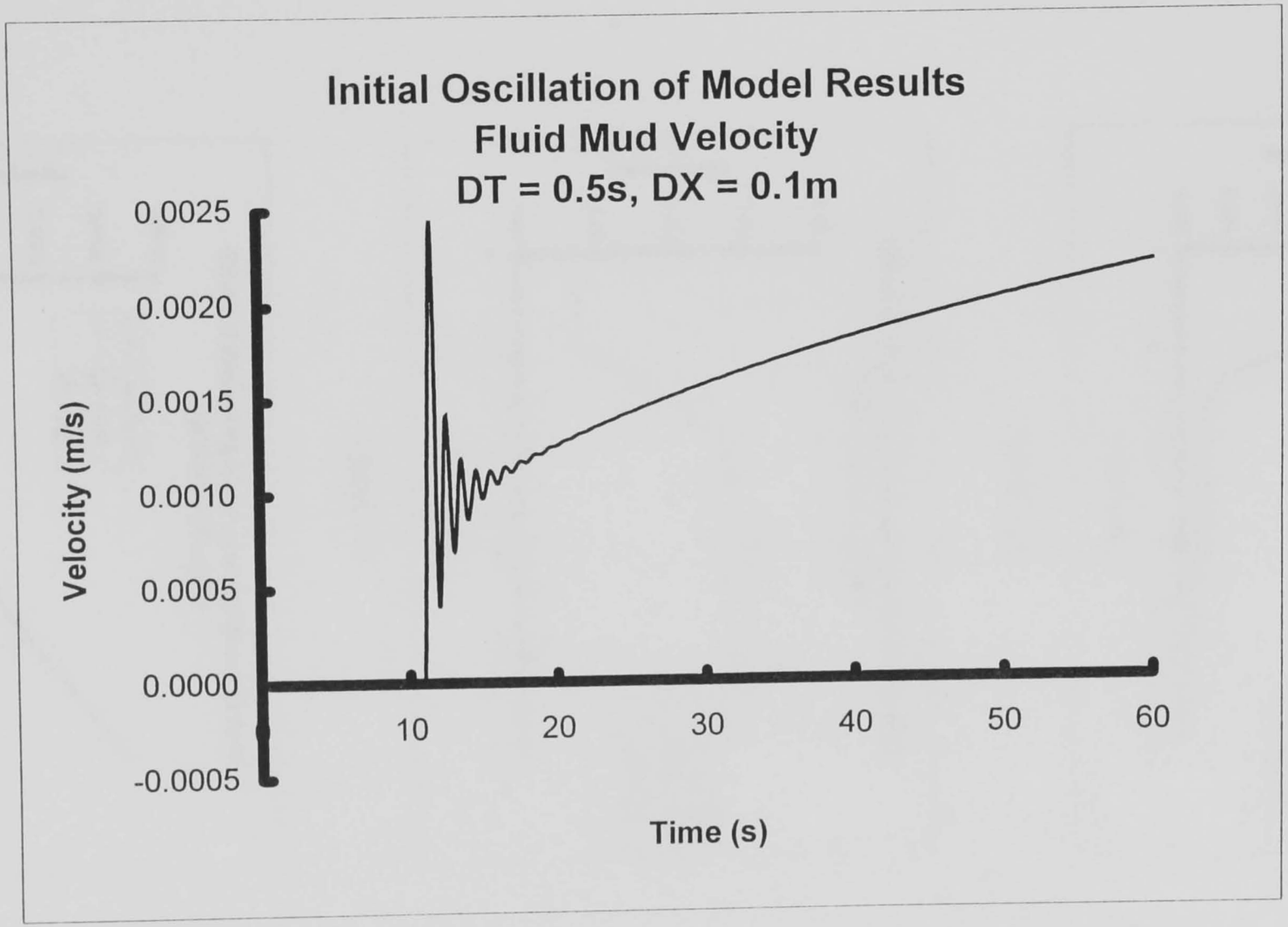
Initial Oscillation of Model Results
Fluid Mud Velocity
DT = 0.5s, DX = 0.1m
Velocity (m/s)
0.0025
0.0020
0.0015
0.0010
0.0005
0.0000
-0.0005
10
20
30
40
50
60
Time (s)

Figure 7.22

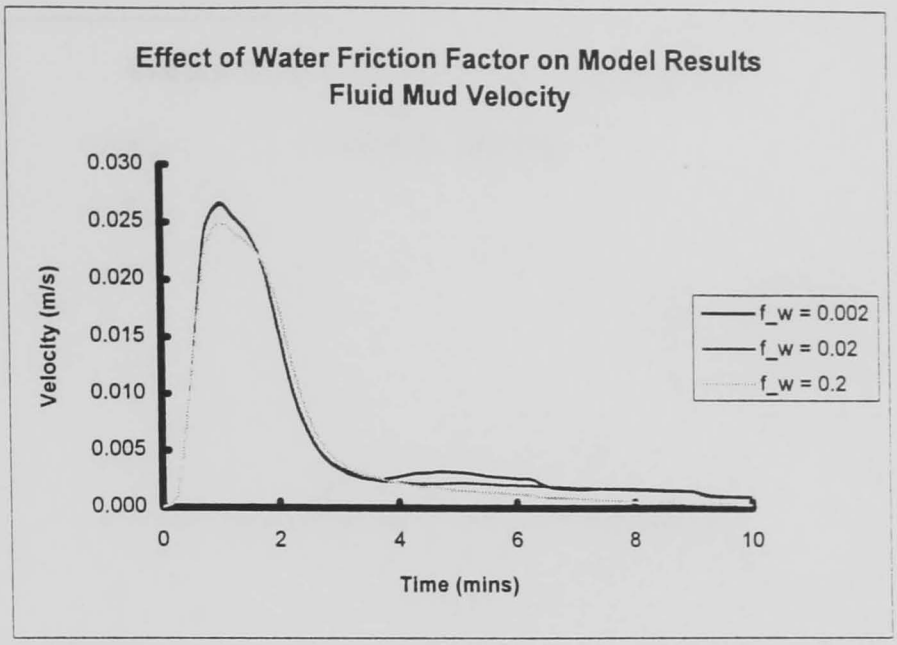

Figure 7.23

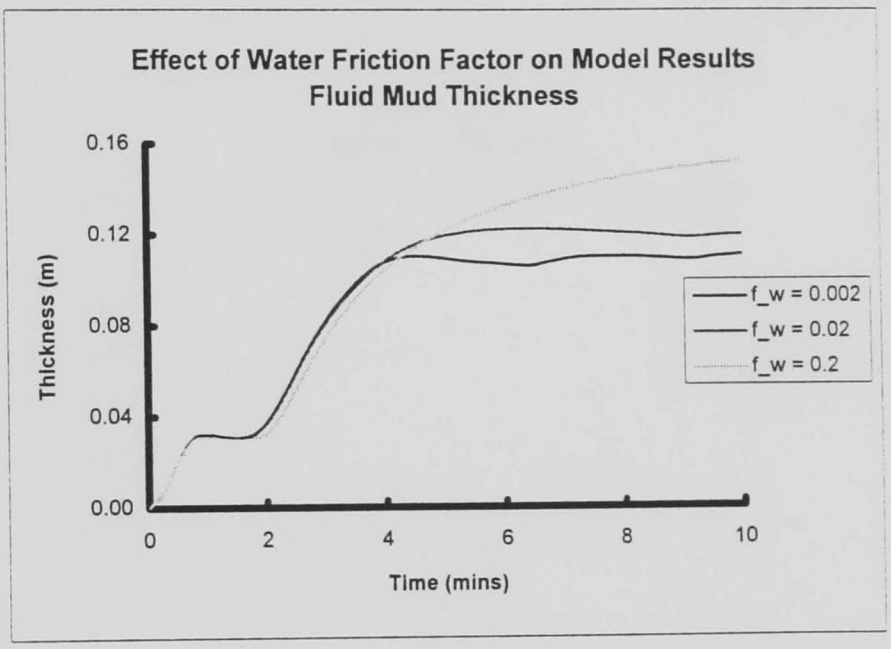

Figure 7.24

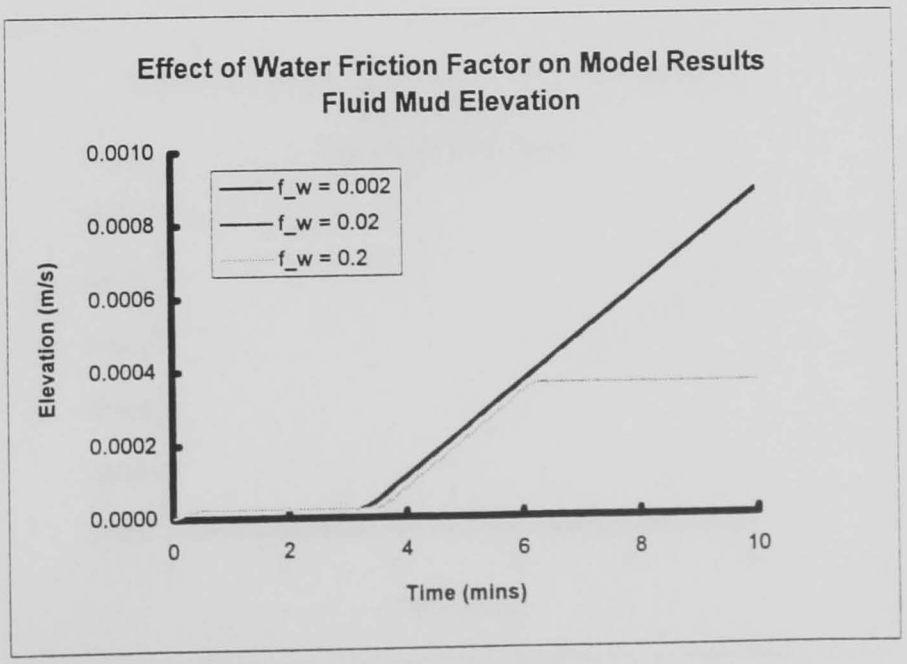

Figure 7.25

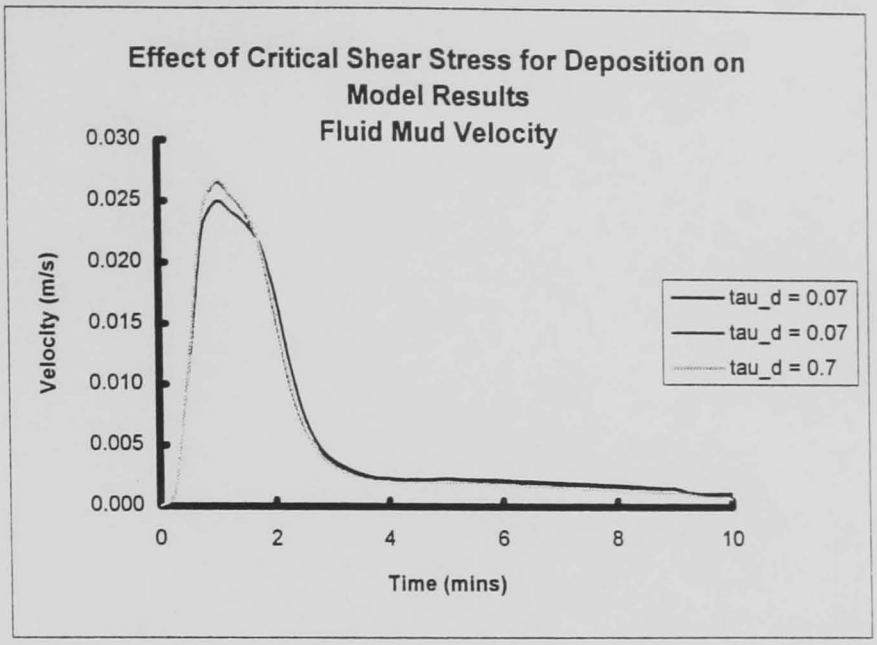

Figure 7.26

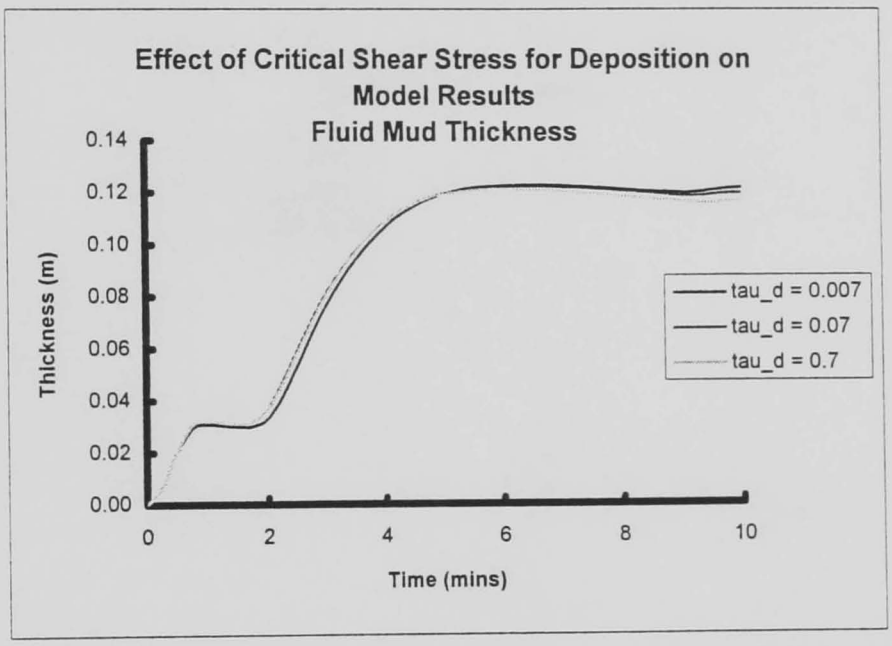

Figure 7.27

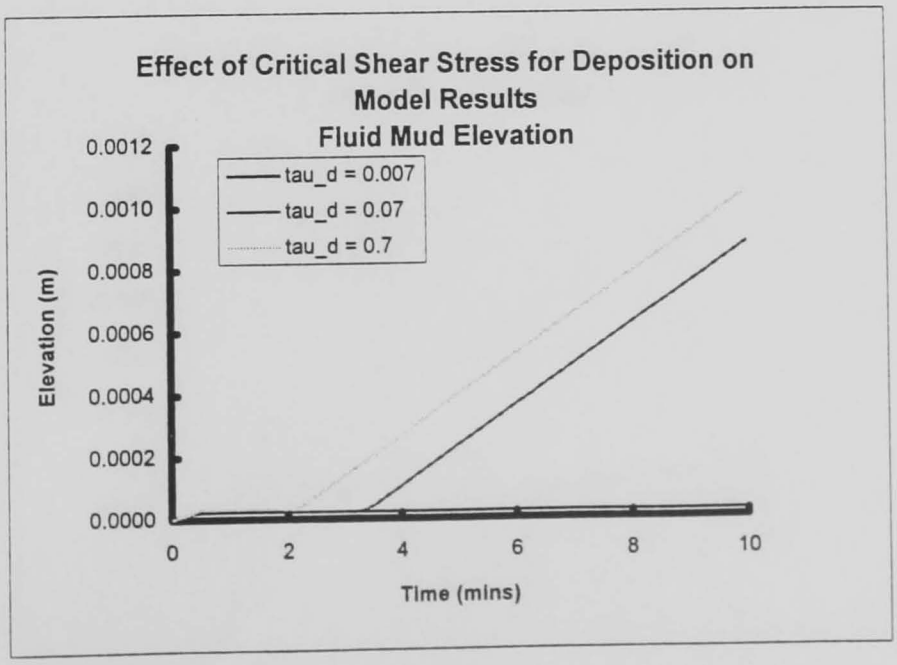

Figure 7.28

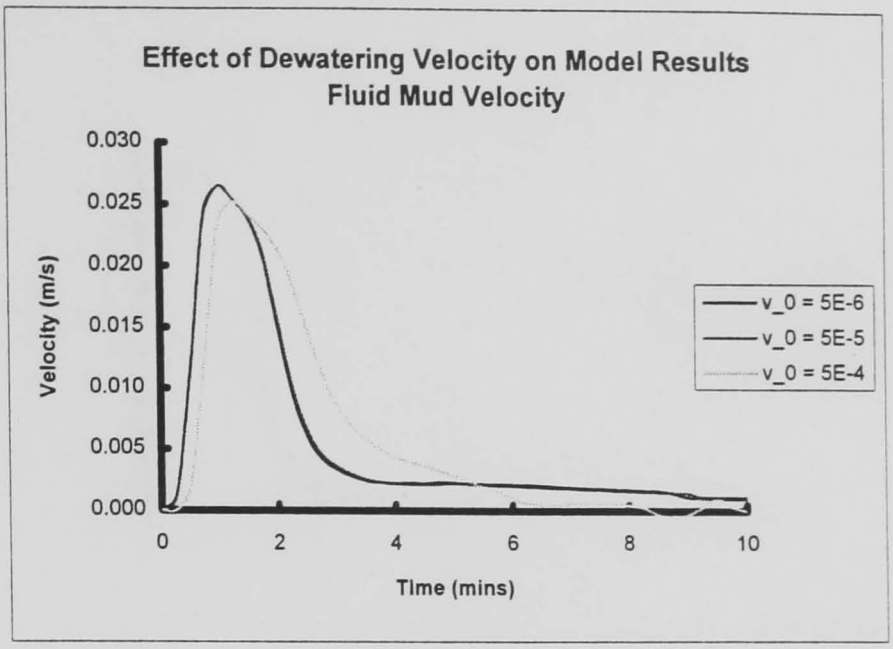

Figure 7.29

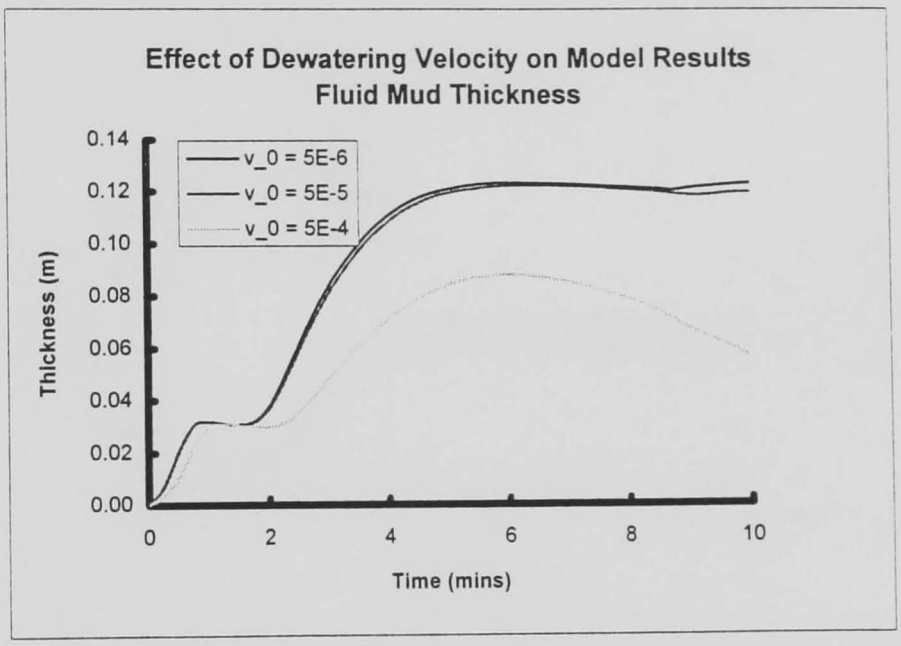

Figure 7.30

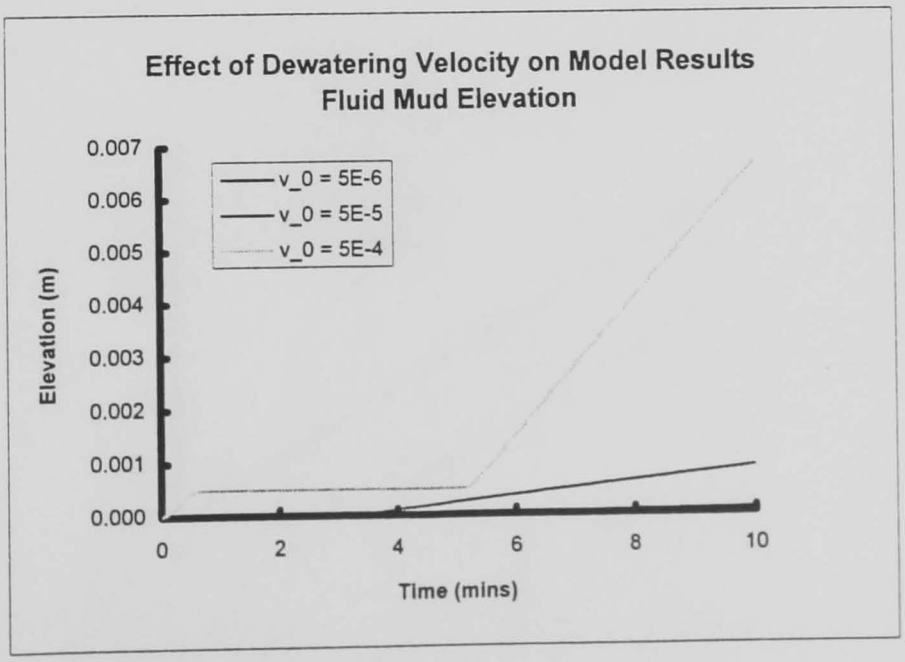

Figure 7.31

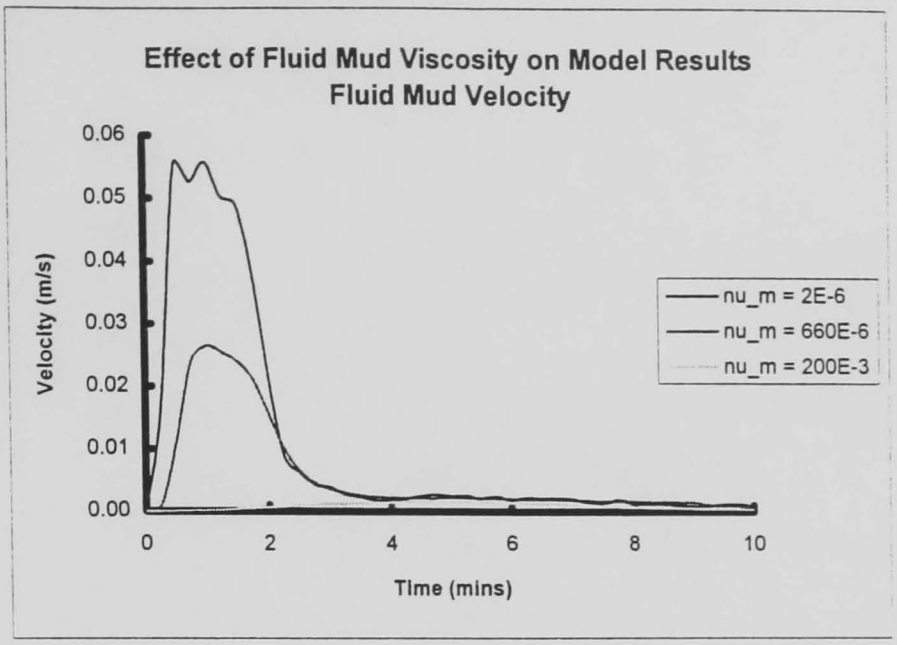

Figure 7.32

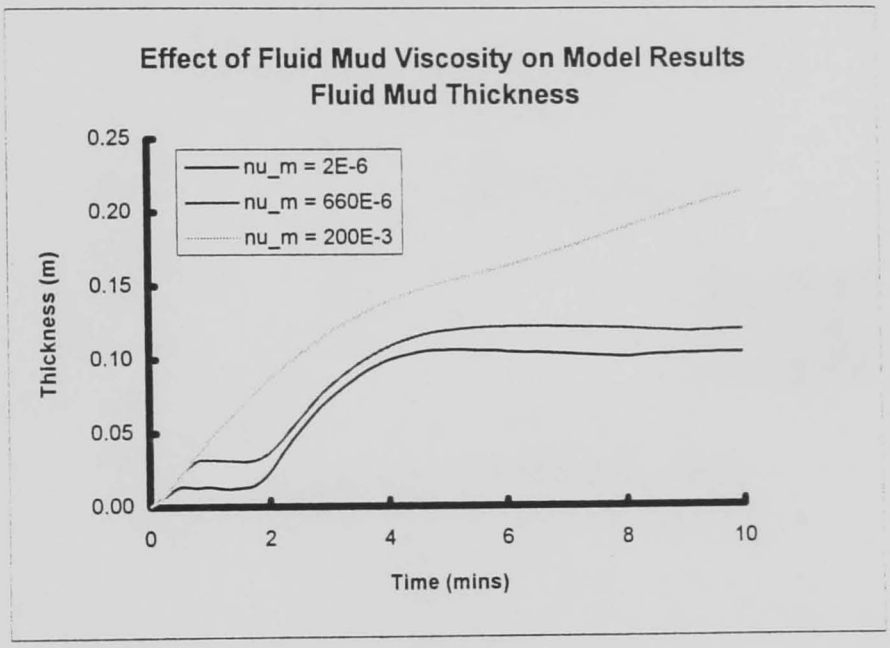

Figure 7.33

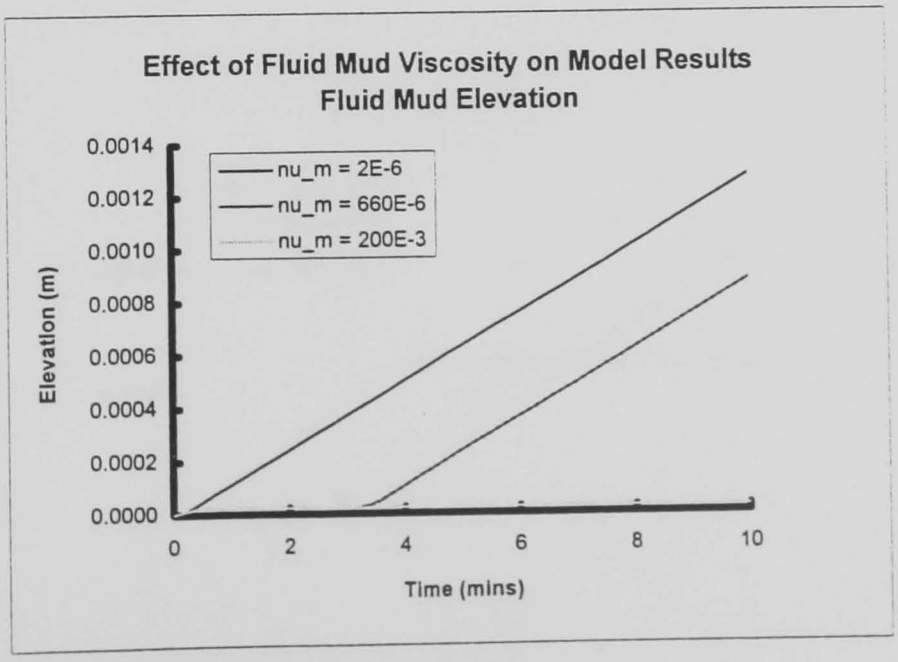

Figure 7.34

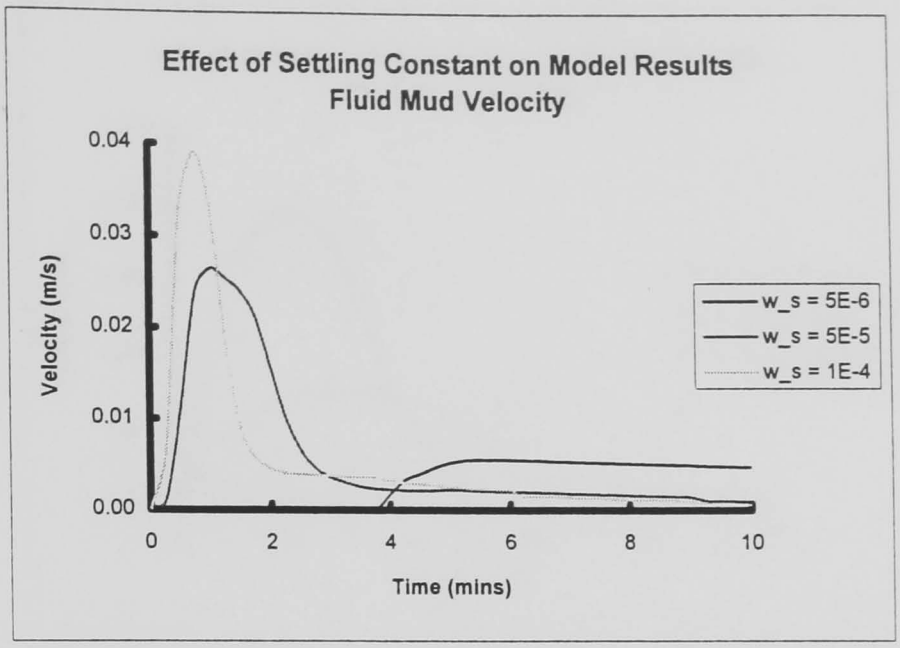

Figure 7.35

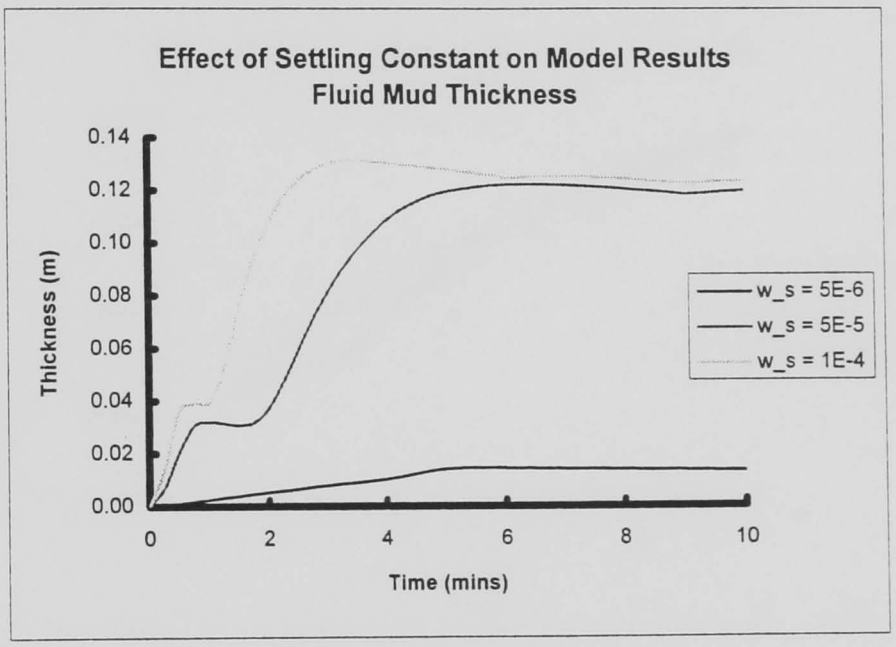

Figure 7.36

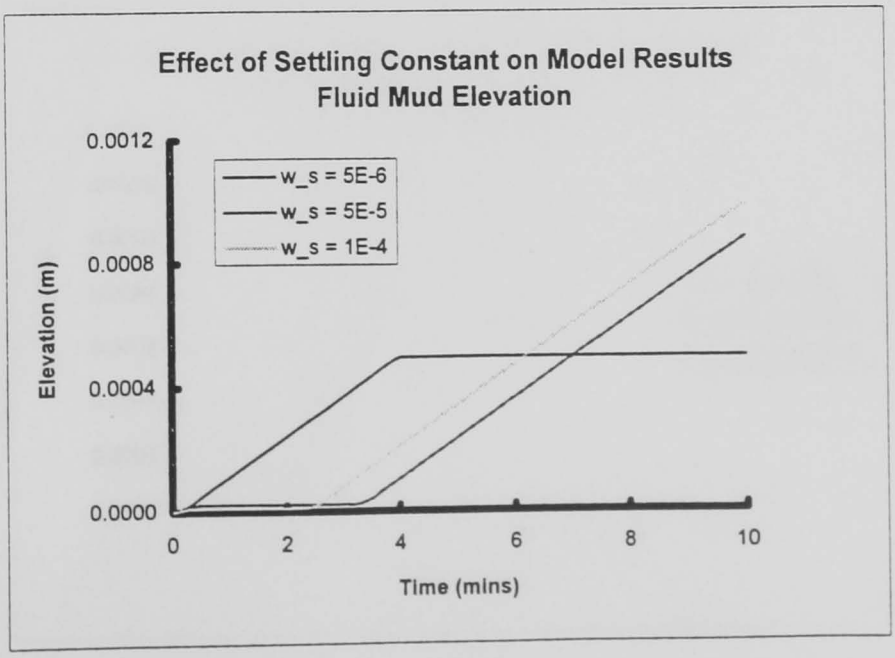

Figure 7.37

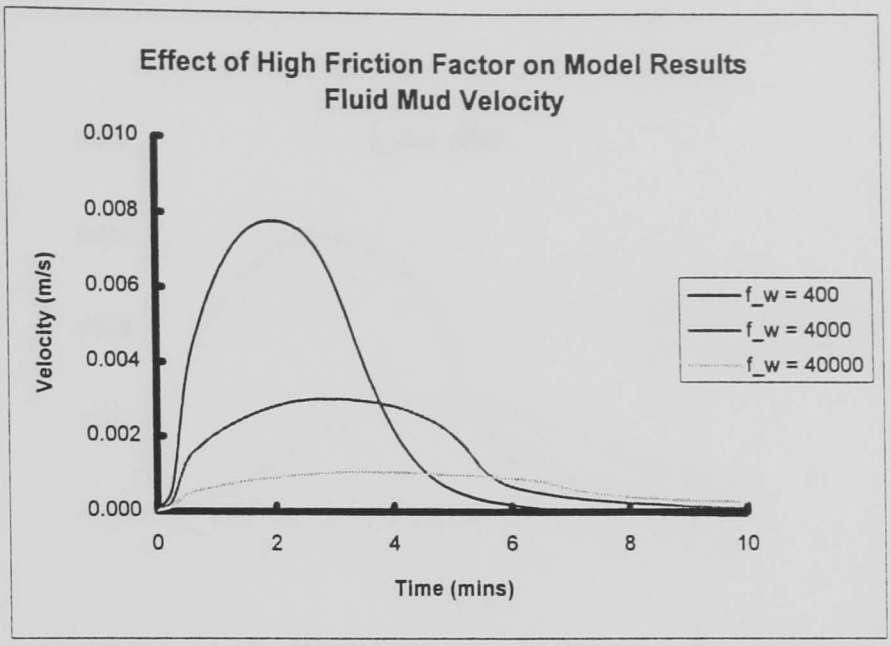

Figure 7.38

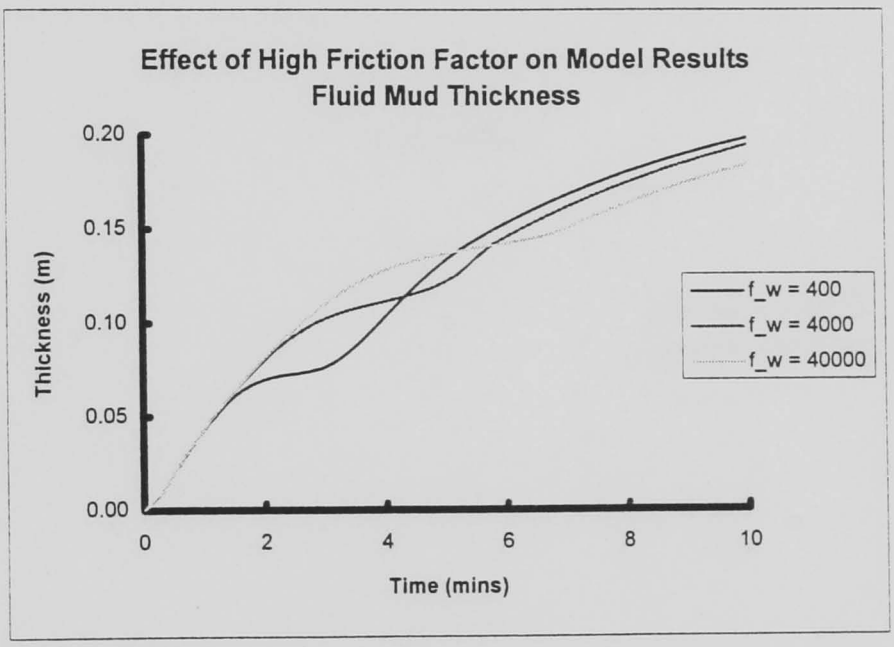

Figure 7.39

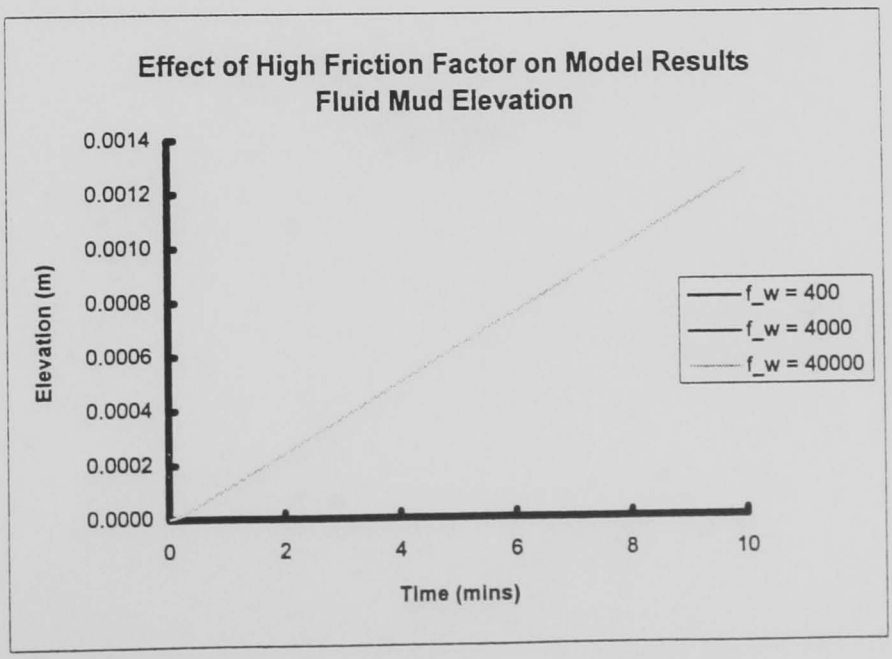

Figure 7.40

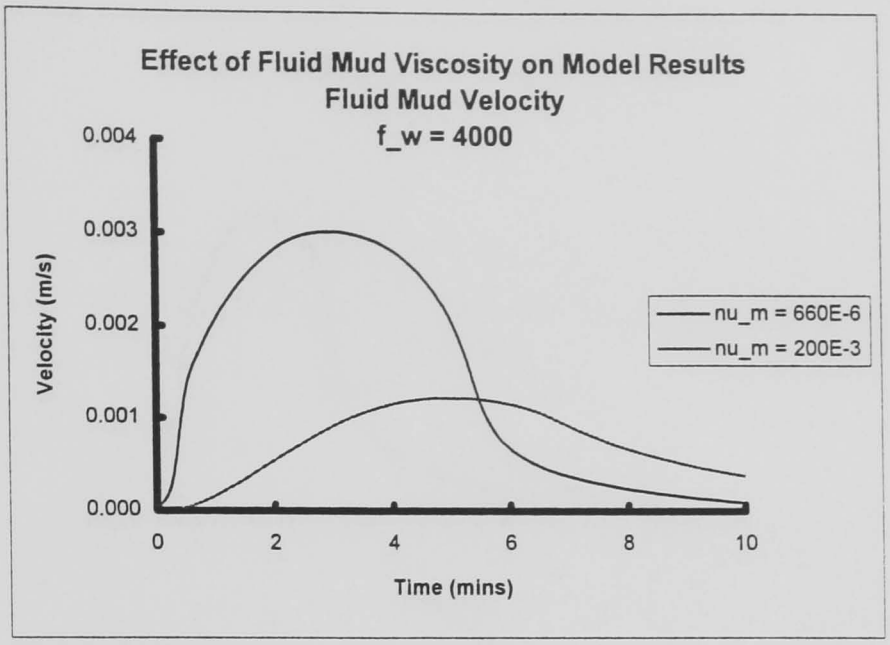

Figure 7.41

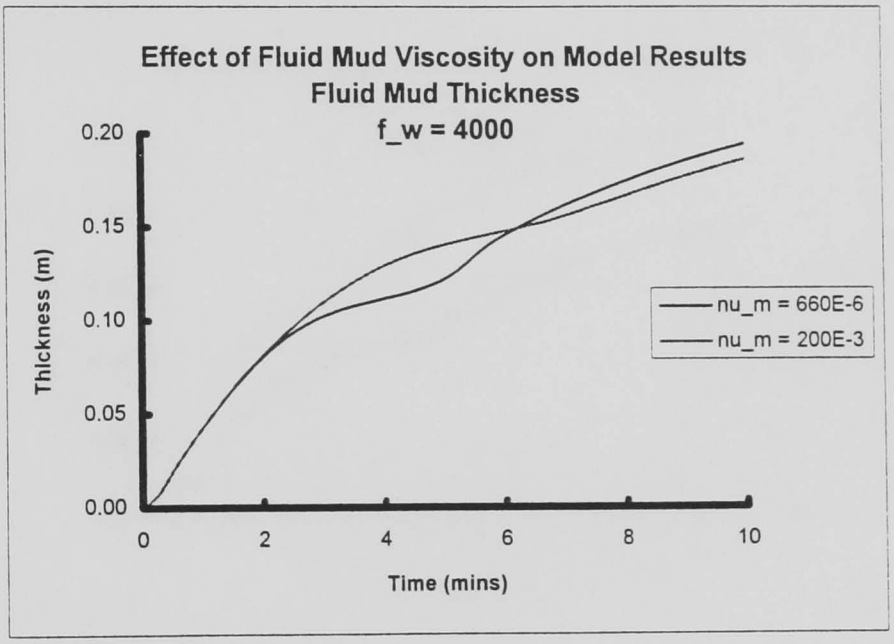

Figure 7.42

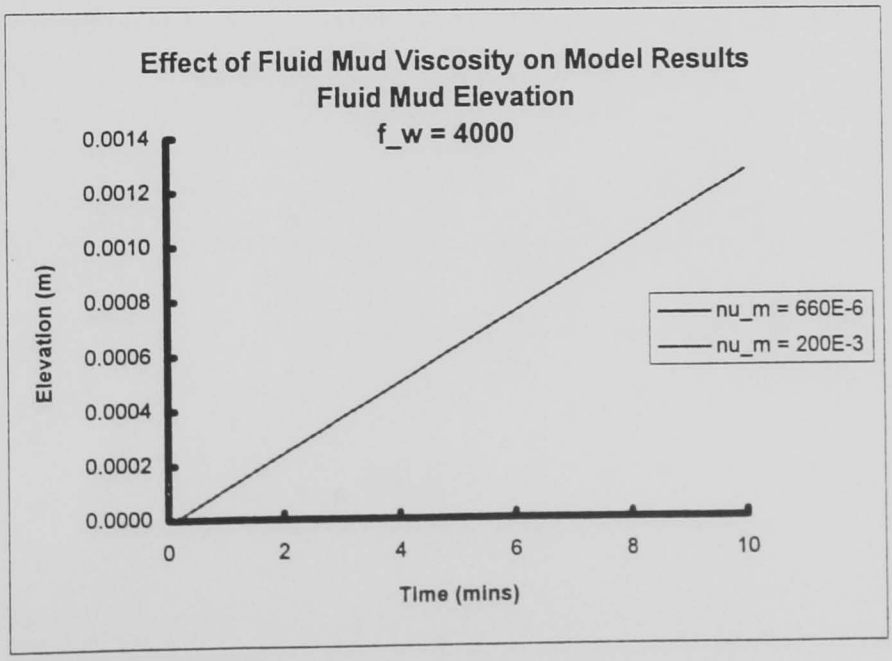

Figure 7.43

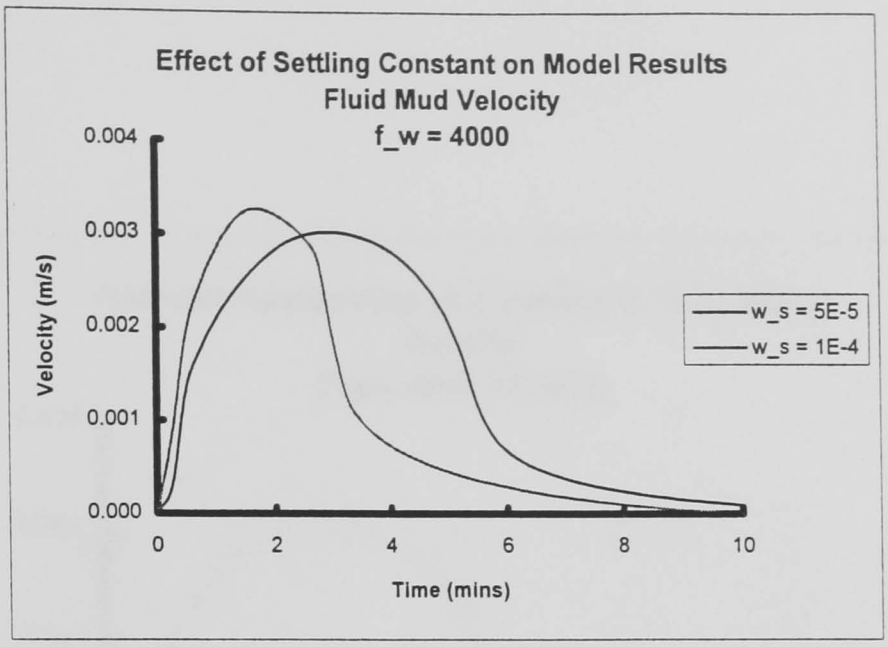

Figure 7.44

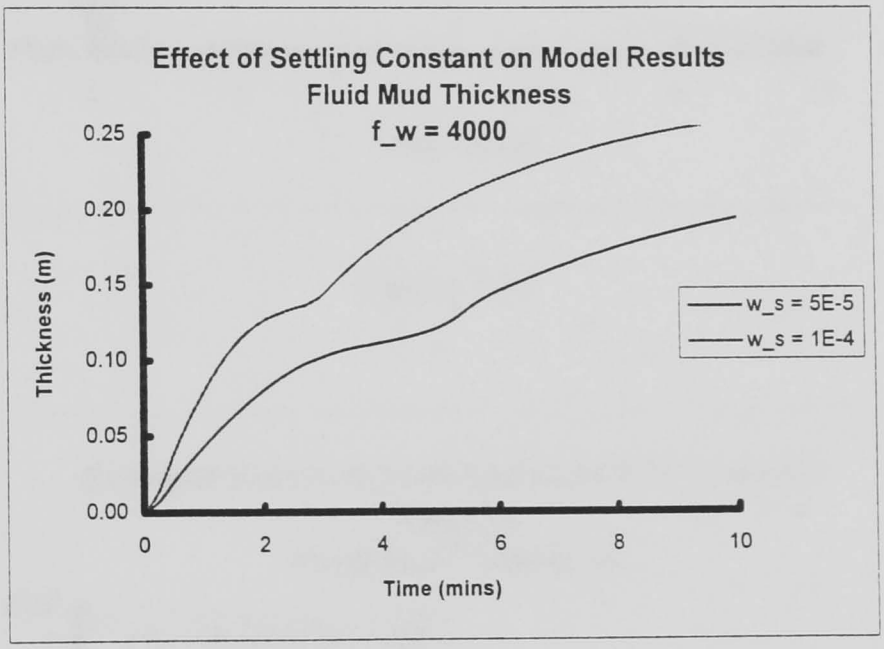

Figure 7.45

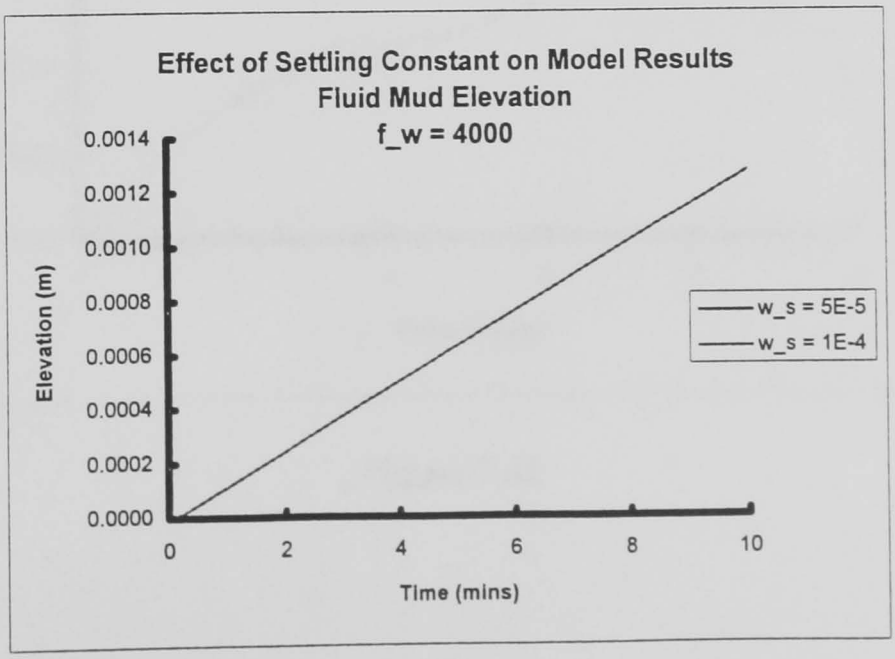

Figure 7.46

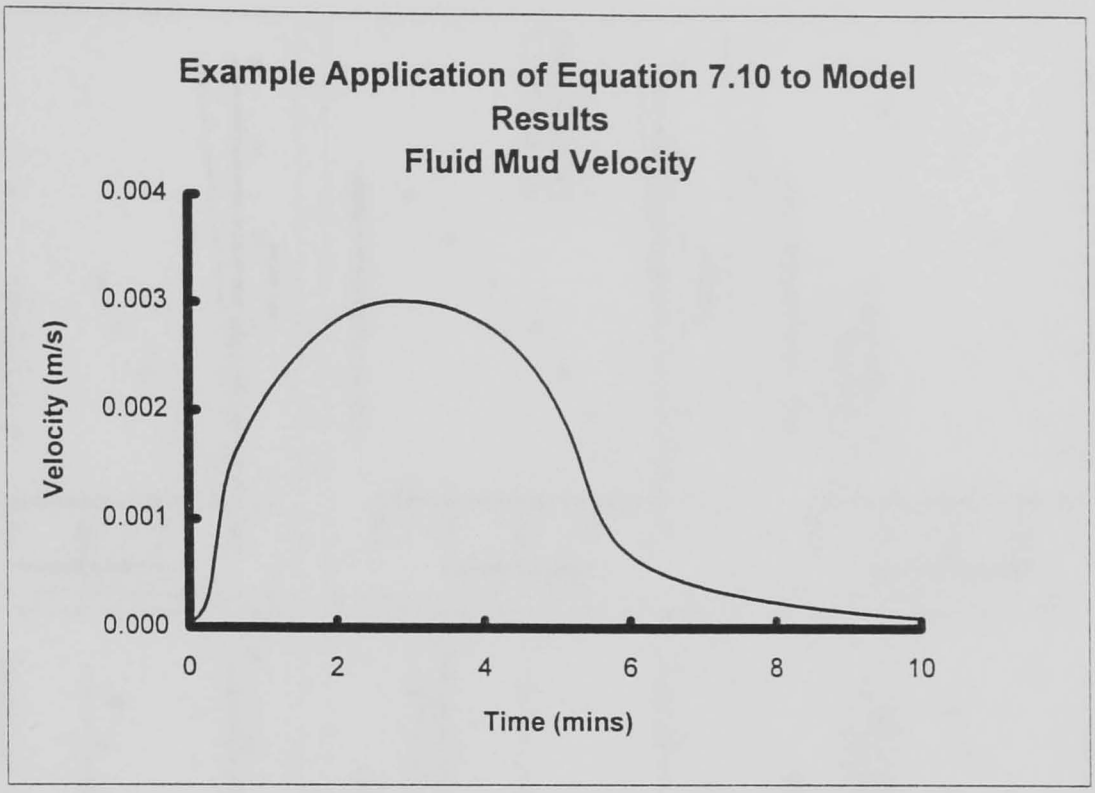

Figure 7.47

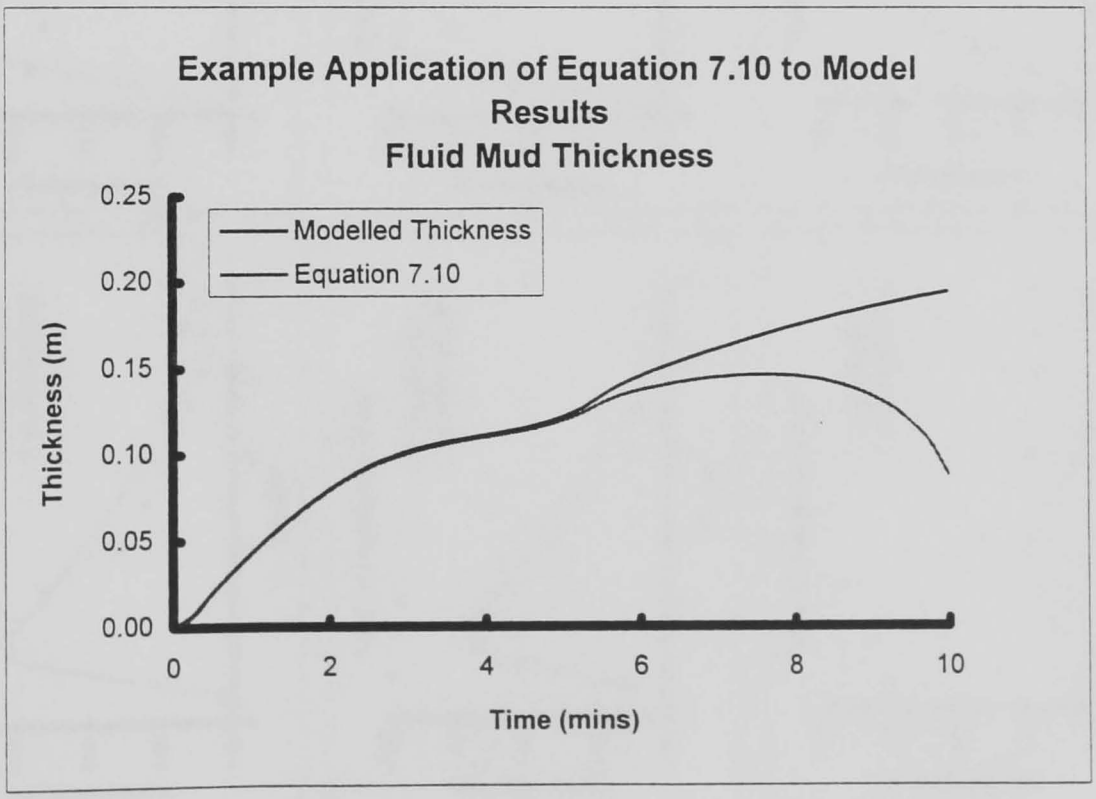

Figure 7.48

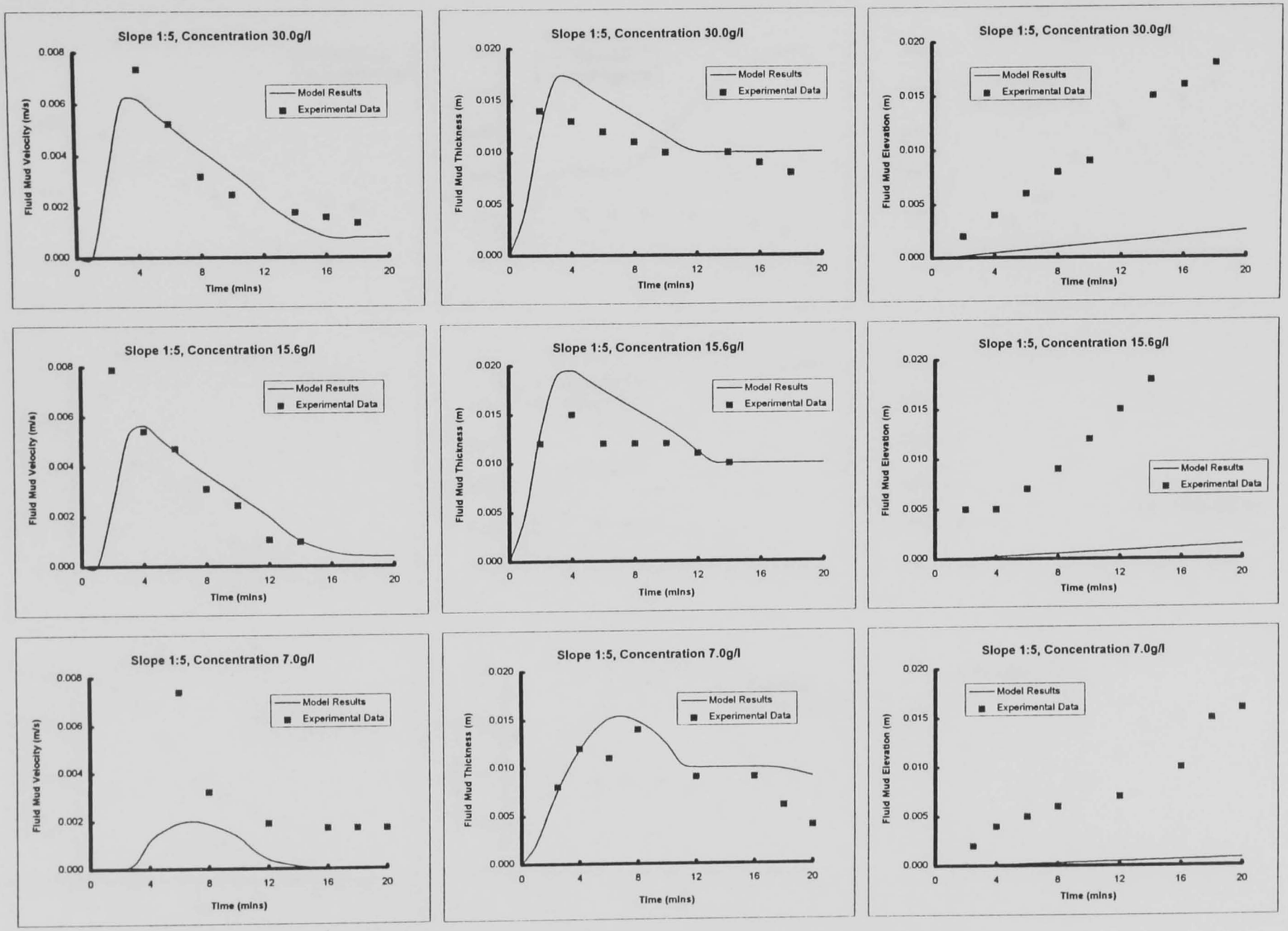

Figure 7.49: Results of Original Model Compared with Data from Ali and Georgiadis (1991), Bed Slope 1:5

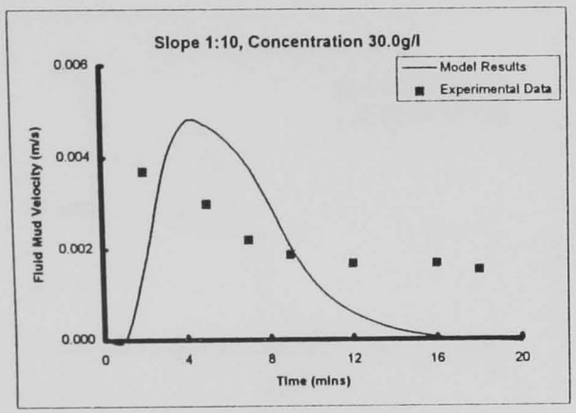

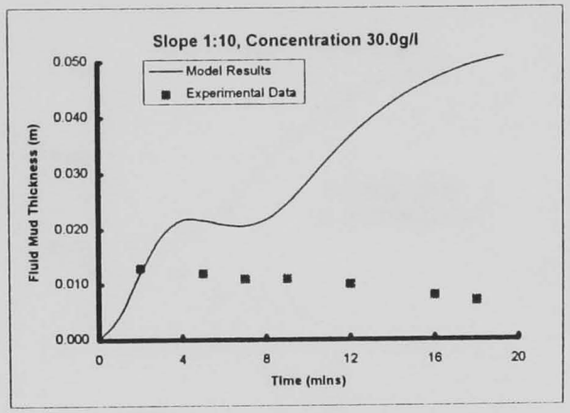

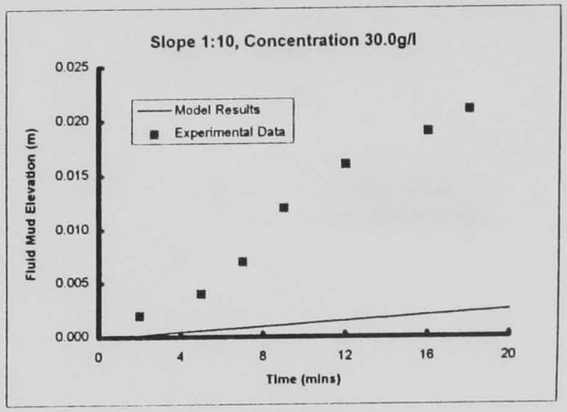

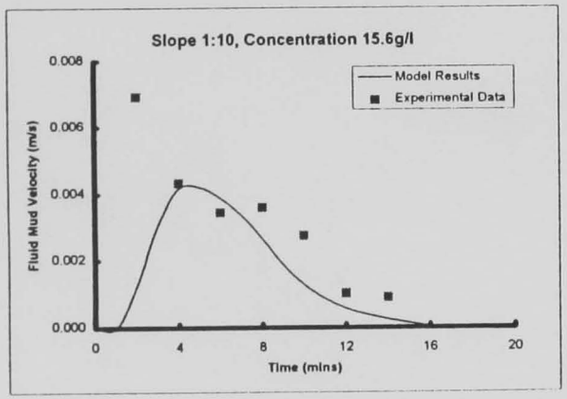

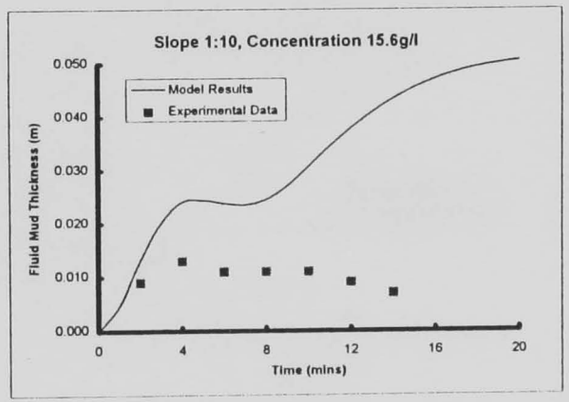

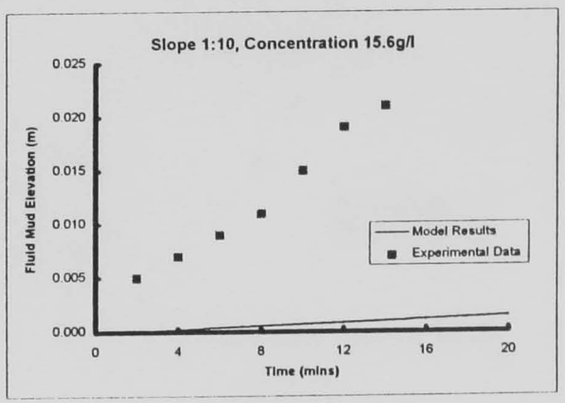

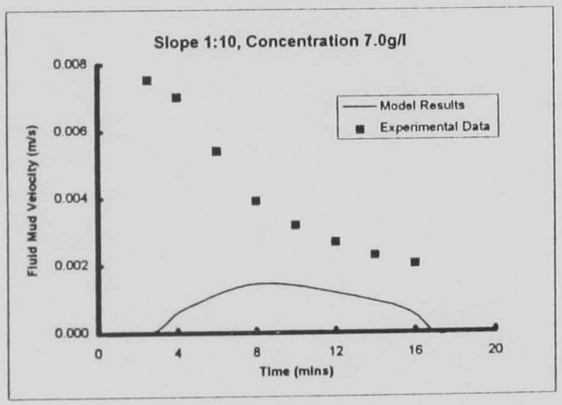

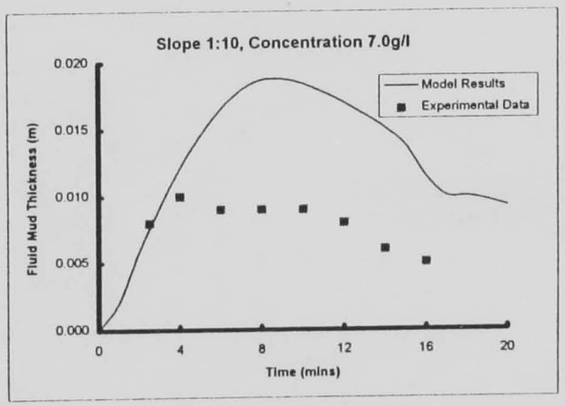

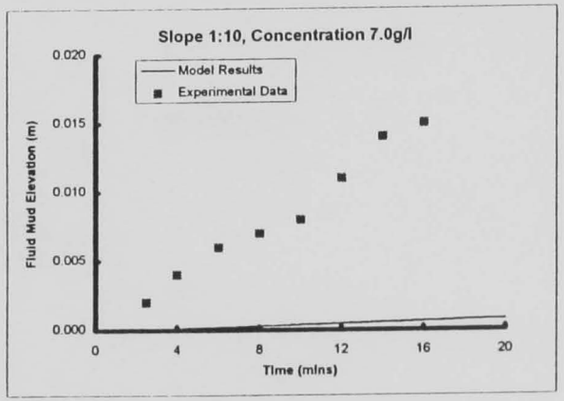

Figure 7.50: Results of Original Model Compared with Data from Ali and Georgiadis (1991); Bed Slope 1:10

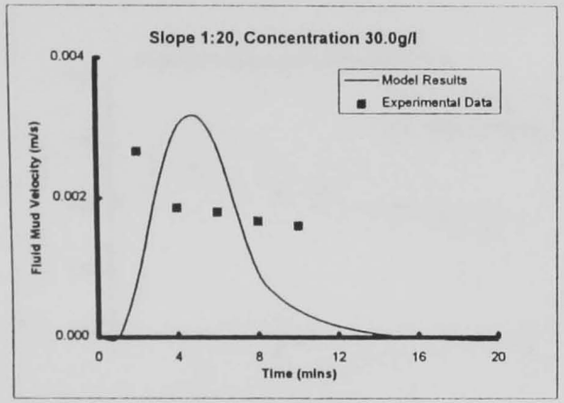

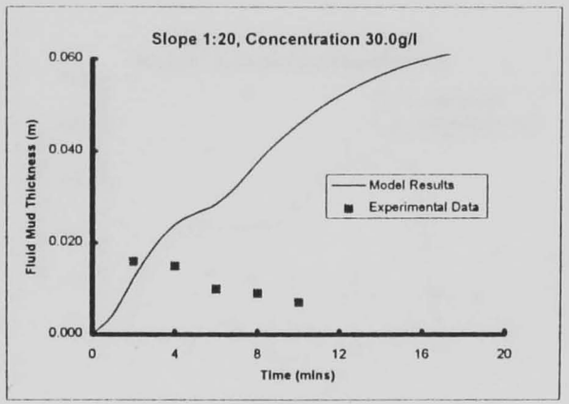

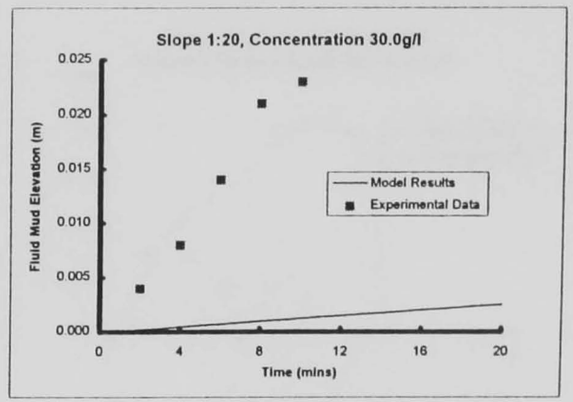

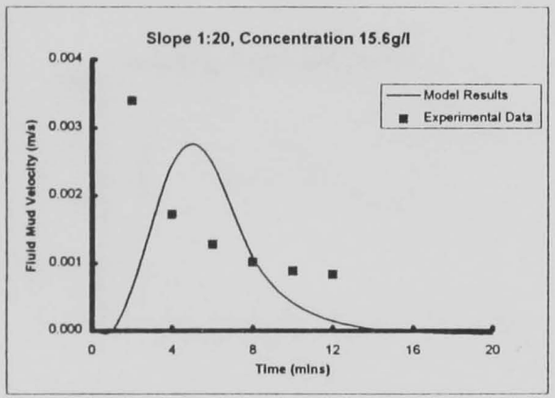

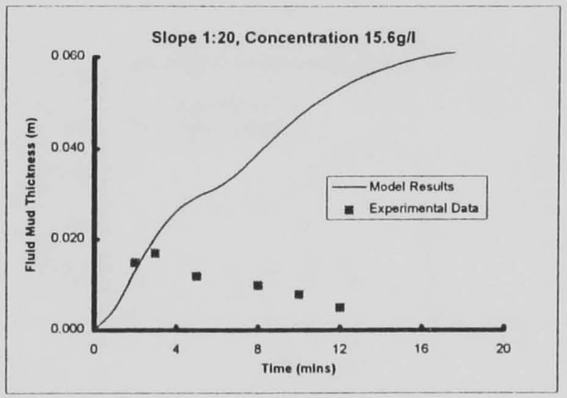

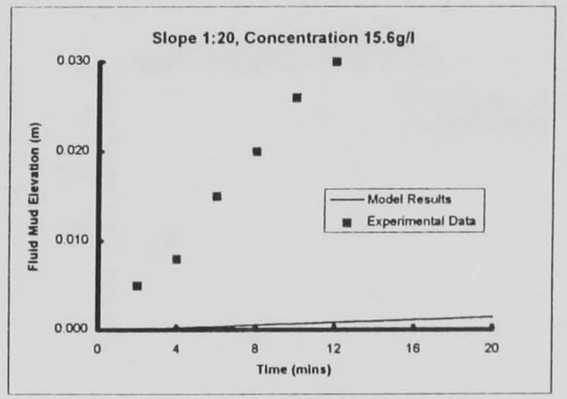

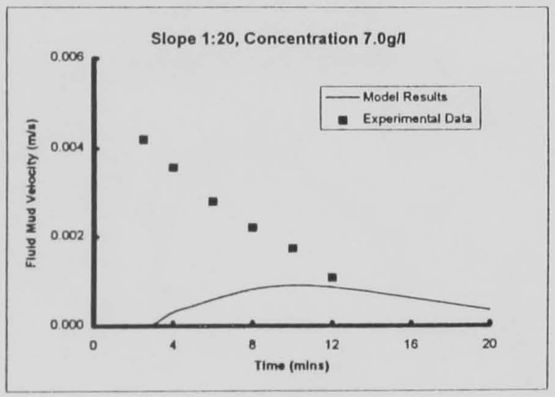

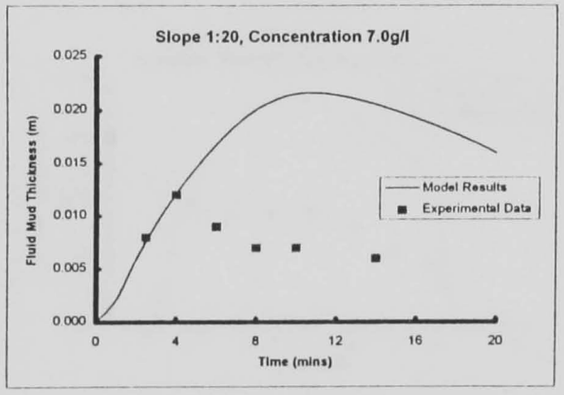

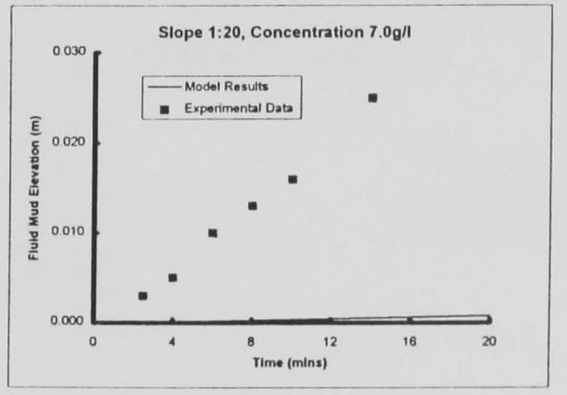

Figure 7.51: Results of Original Model Compared with Data from Ali and Georgiadis (1991), Bed Slope 1:20

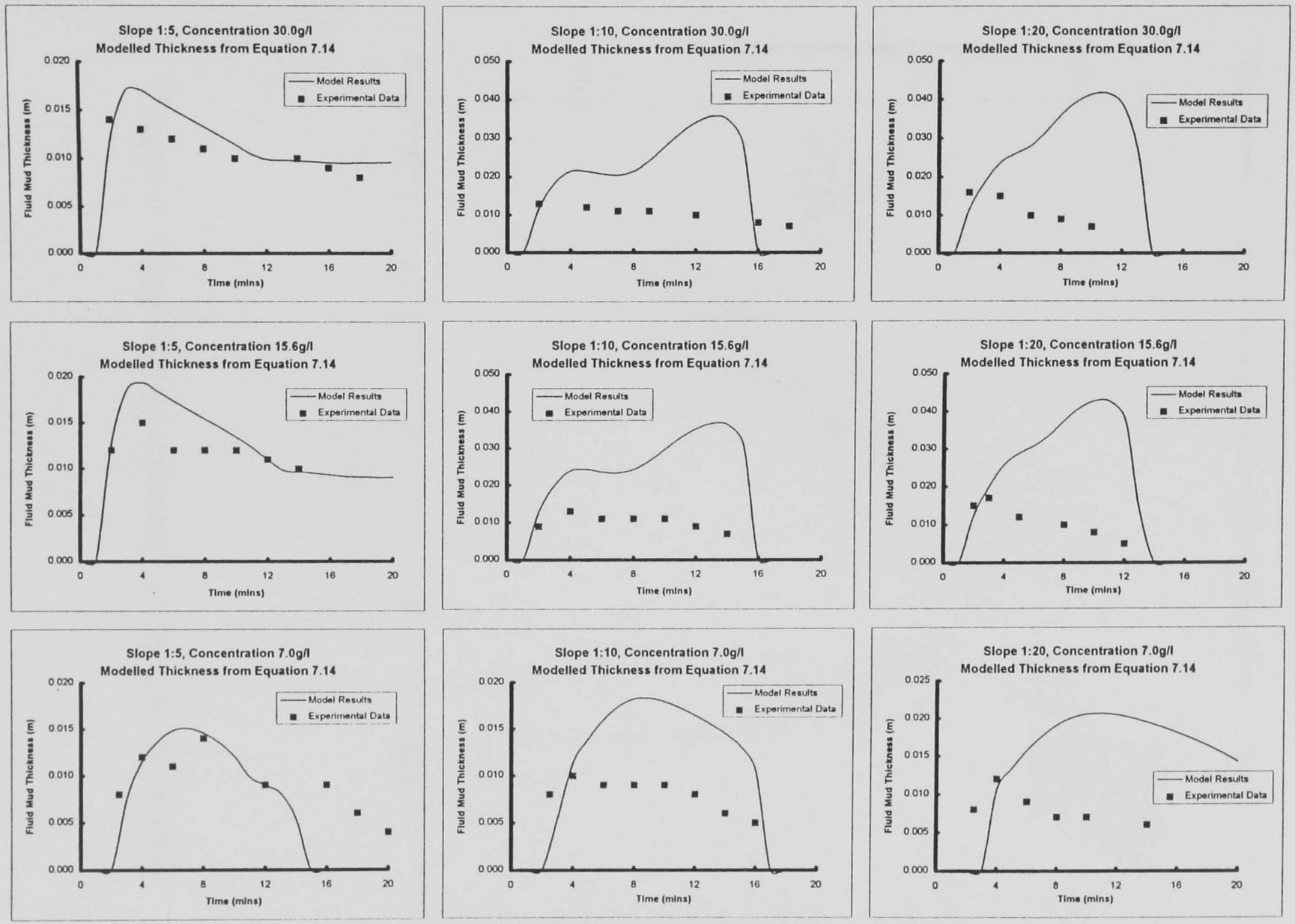

Figure 7.52: Application of Equation 7.14 to Results of Original Model

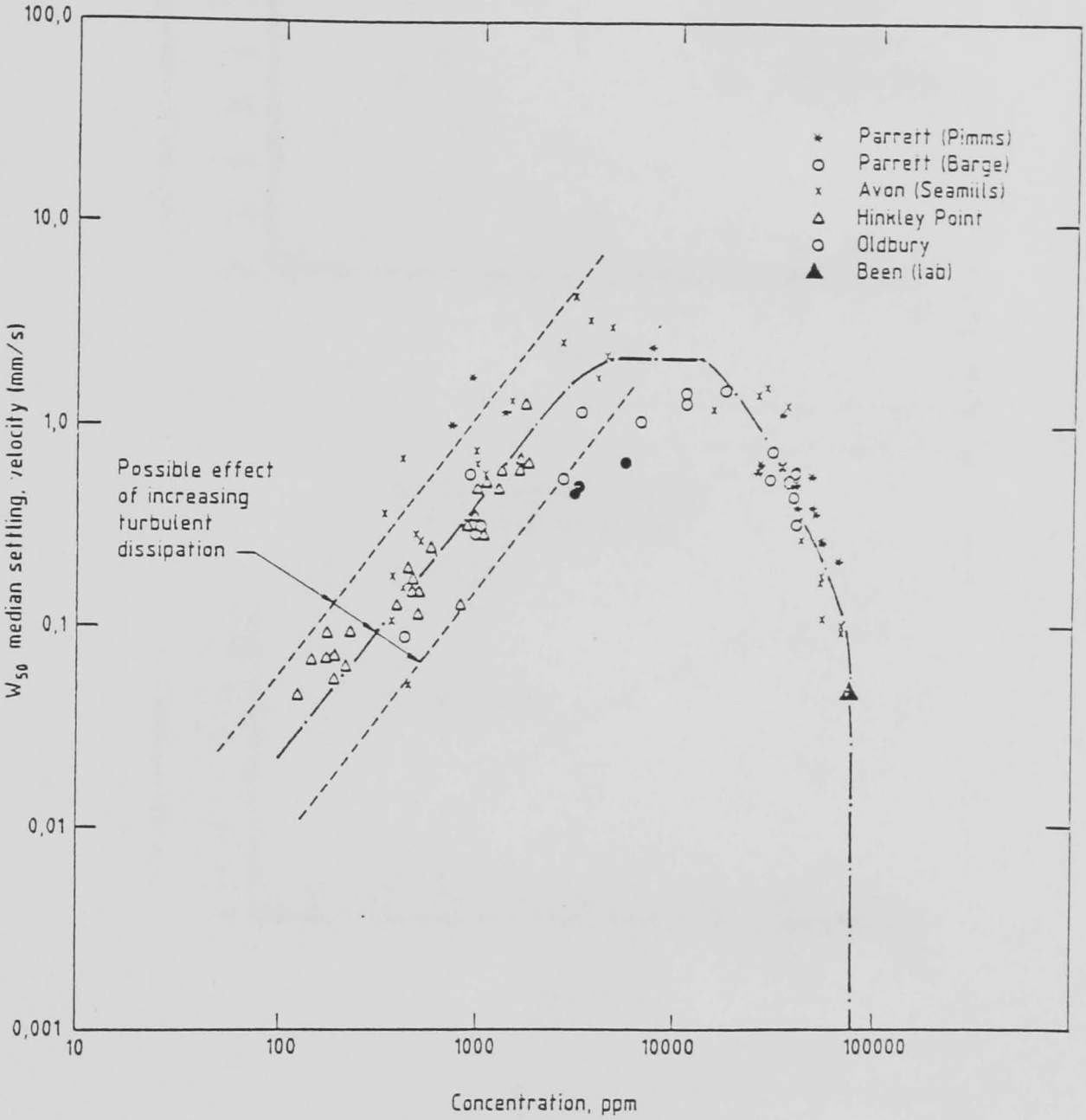

Figure 7.53: Graph Illustrating Hindered Settling (after Thorn 1981)

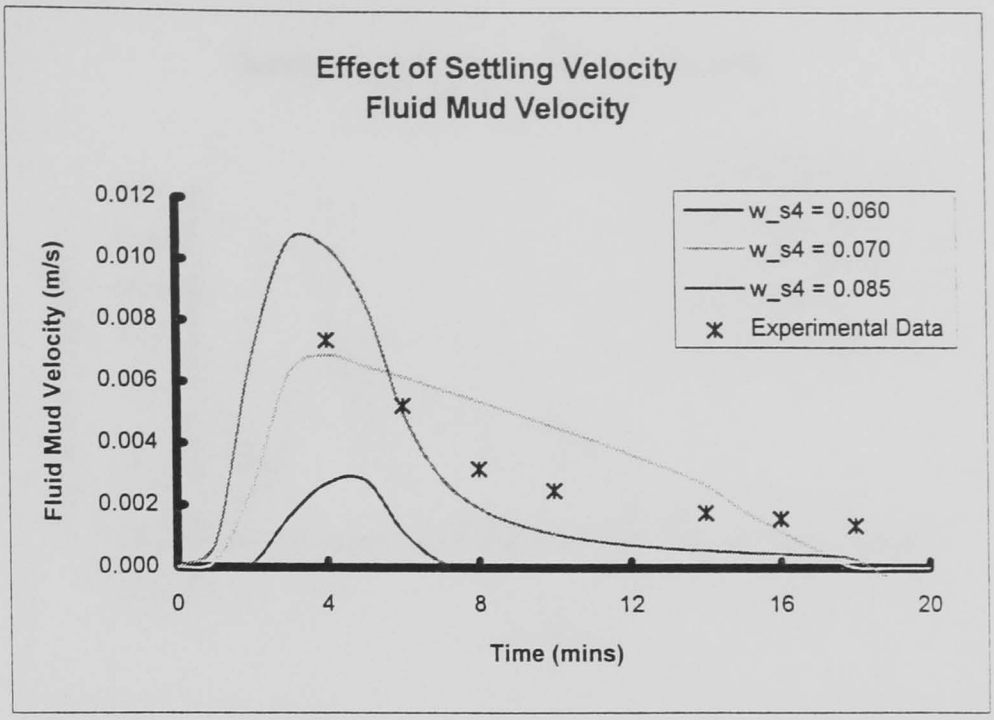

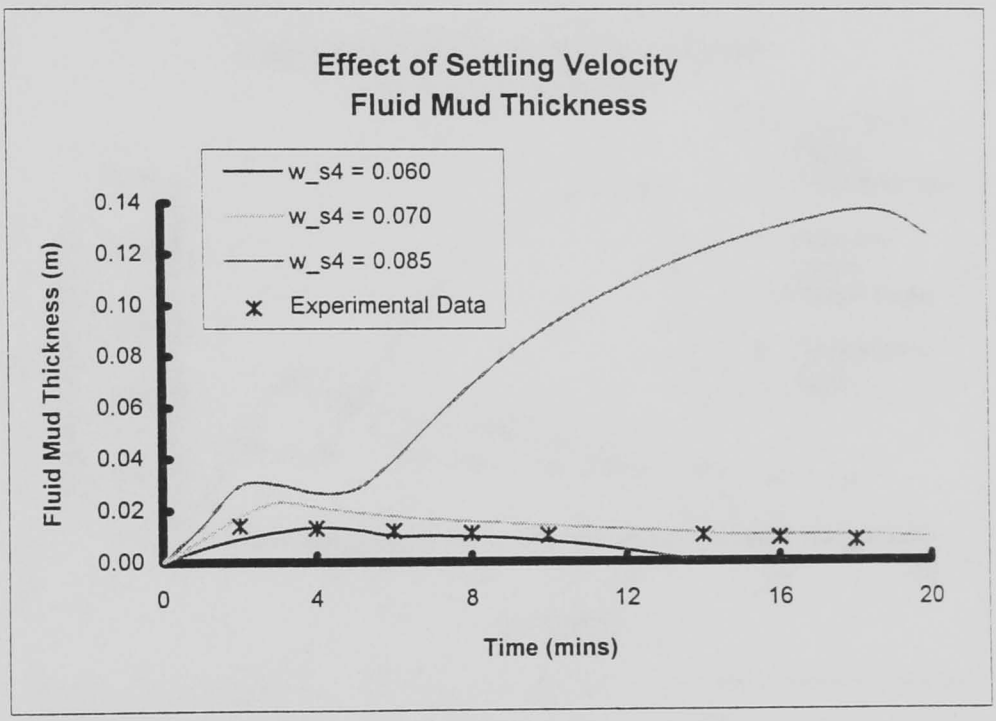

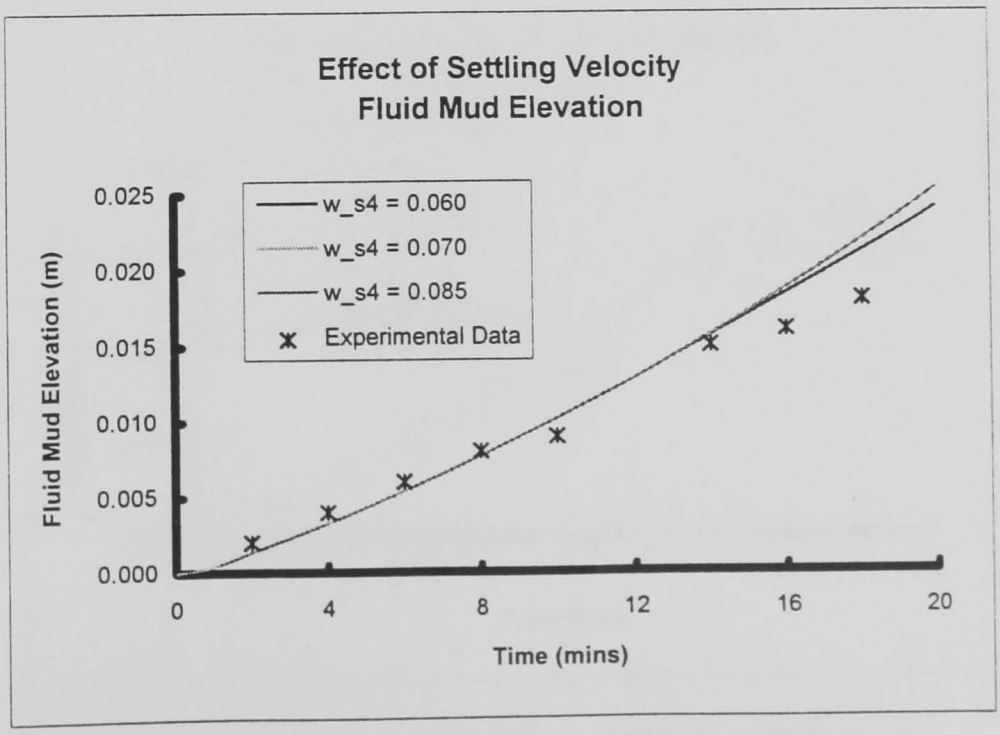

Figure 7.54: Sensitivity of Hindered Settling Algorithm to Settling Constant

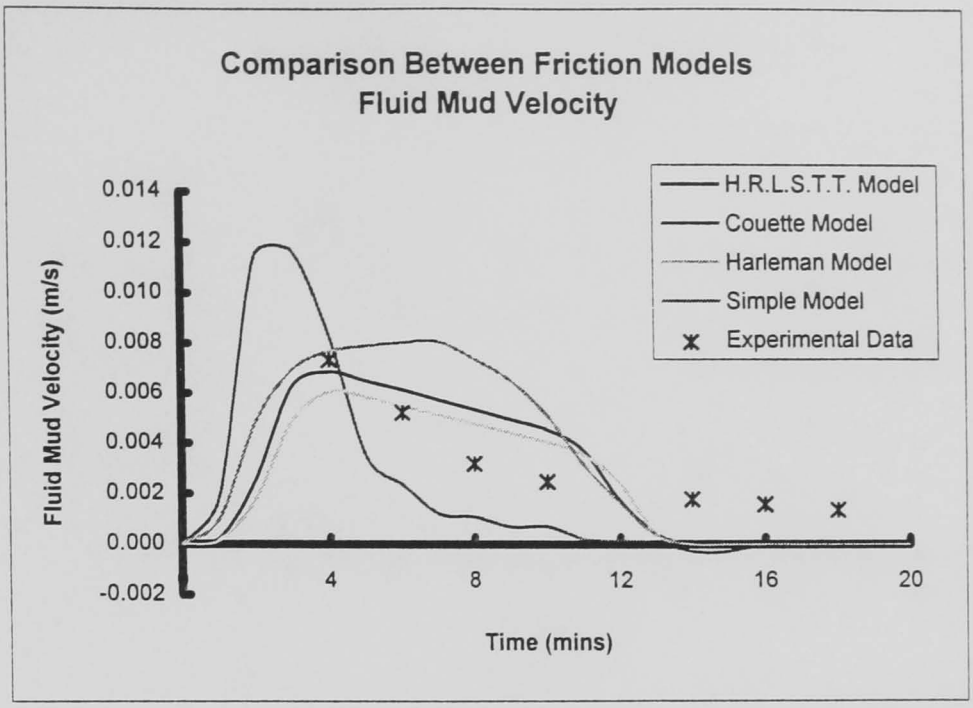

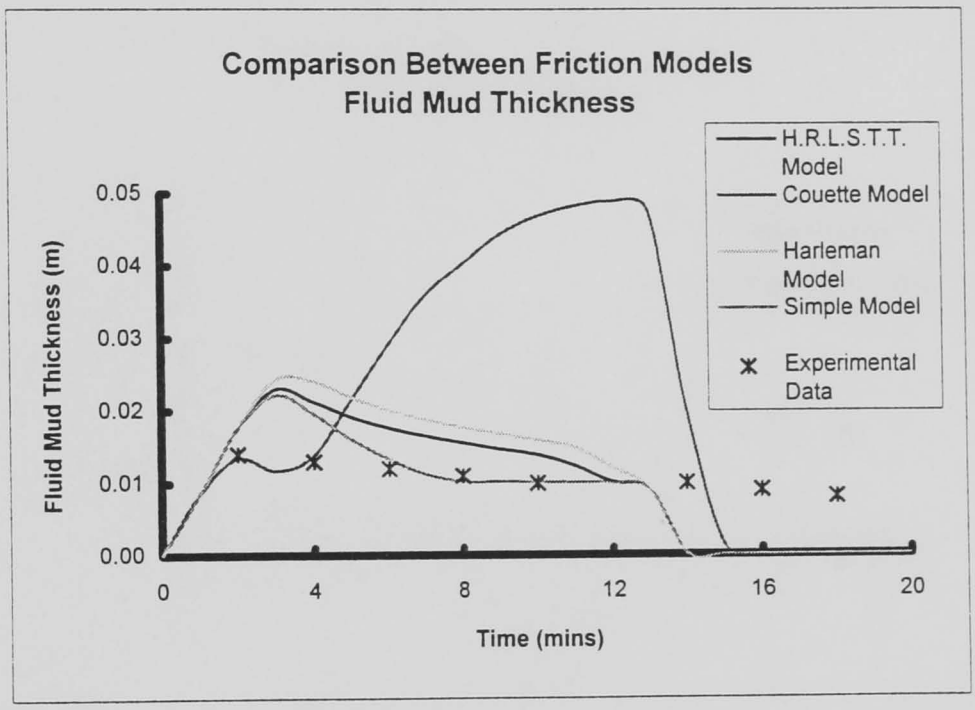

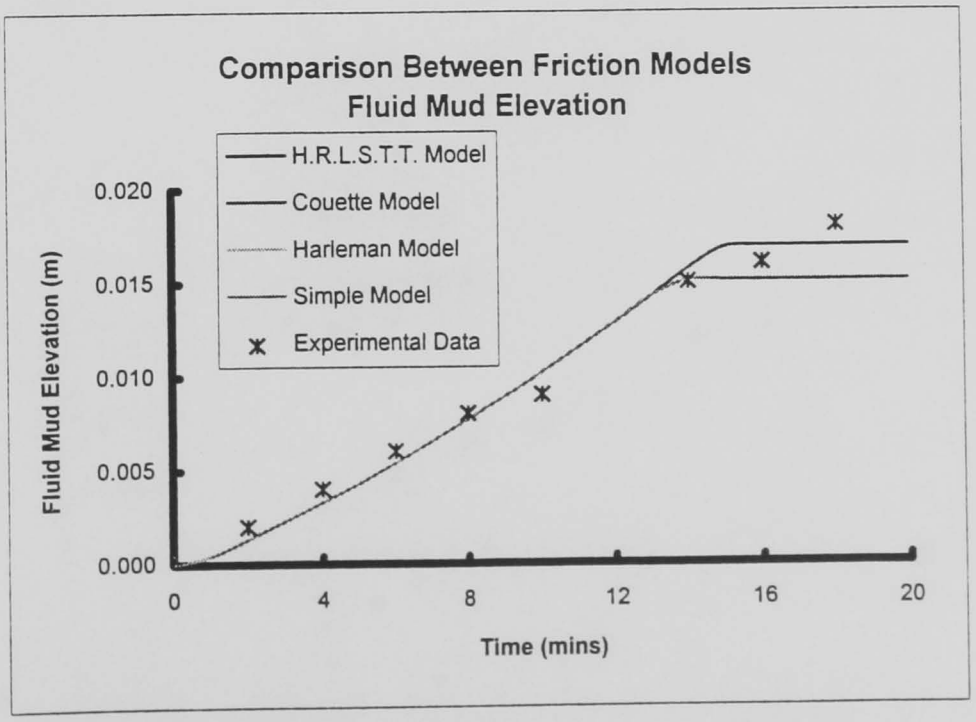

Figure 7.55: Comparison between Different Methods of Determining Fluid Mud Friction Factor

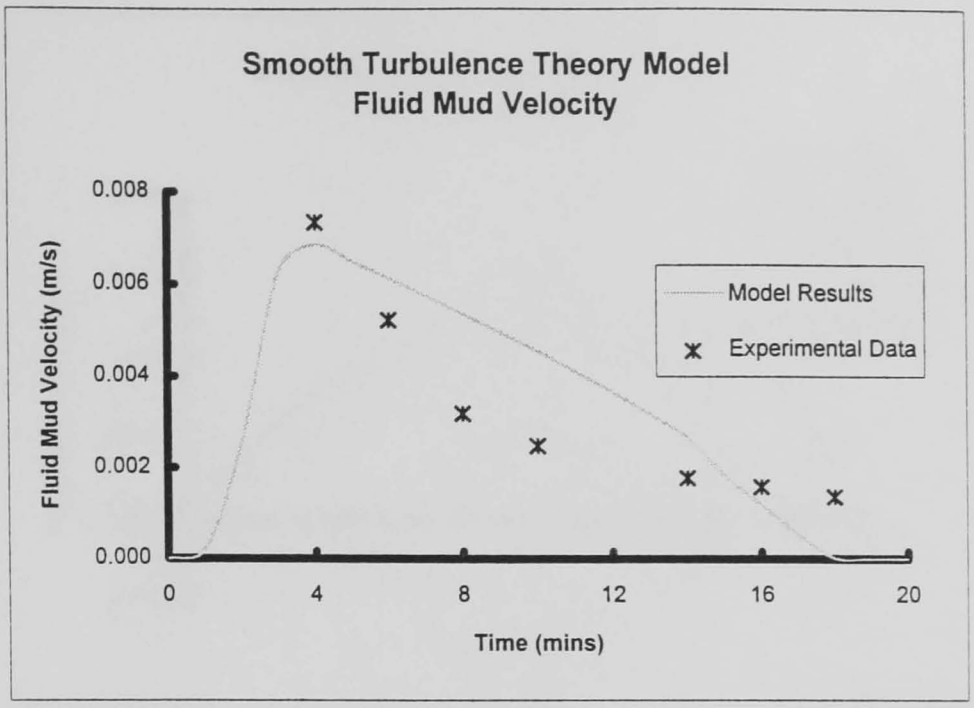

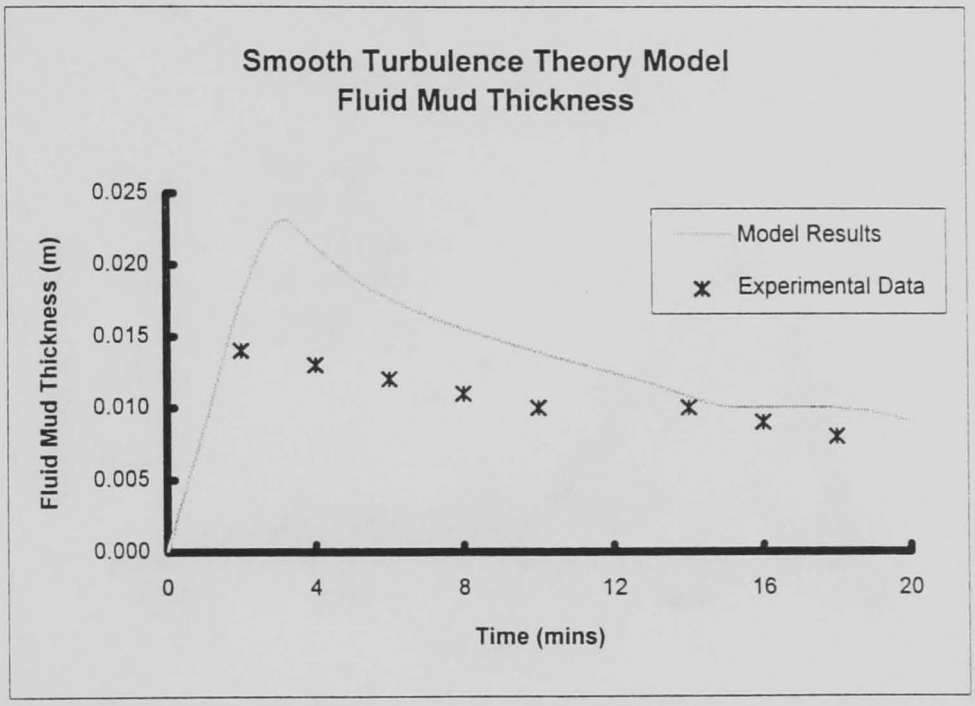

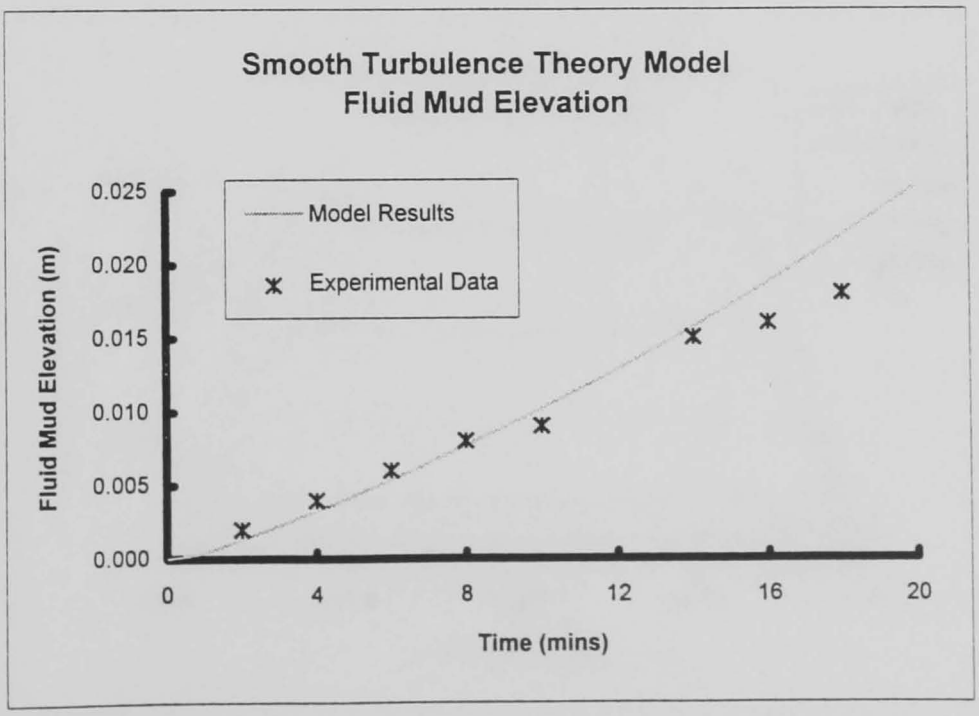

Figure 7.56: Model Results with Friction Factor Determined from Smooth Turbulence Theory

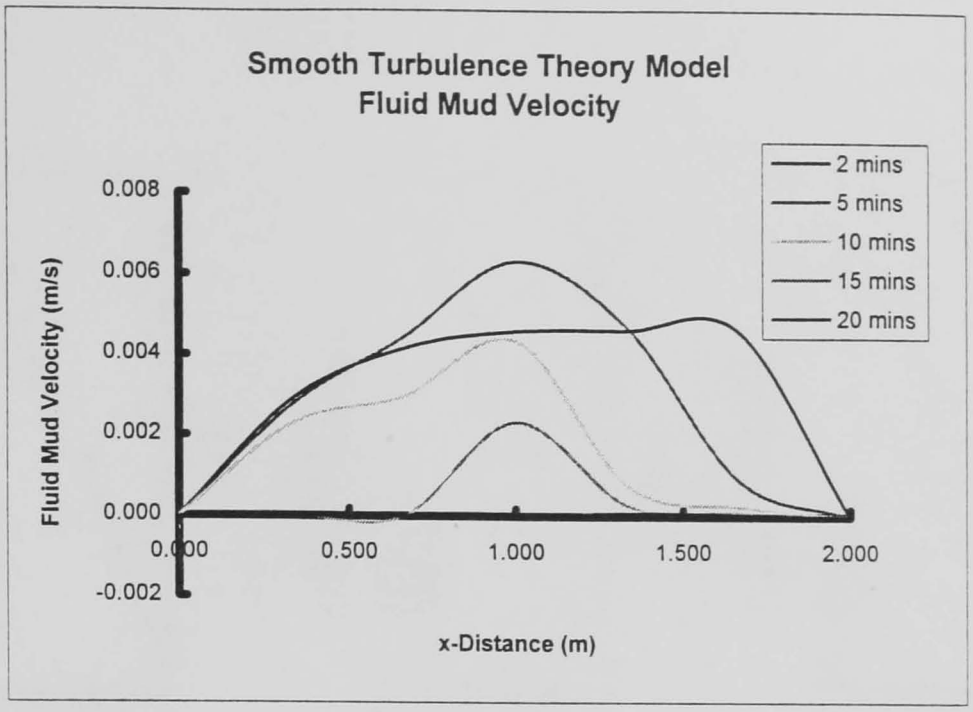

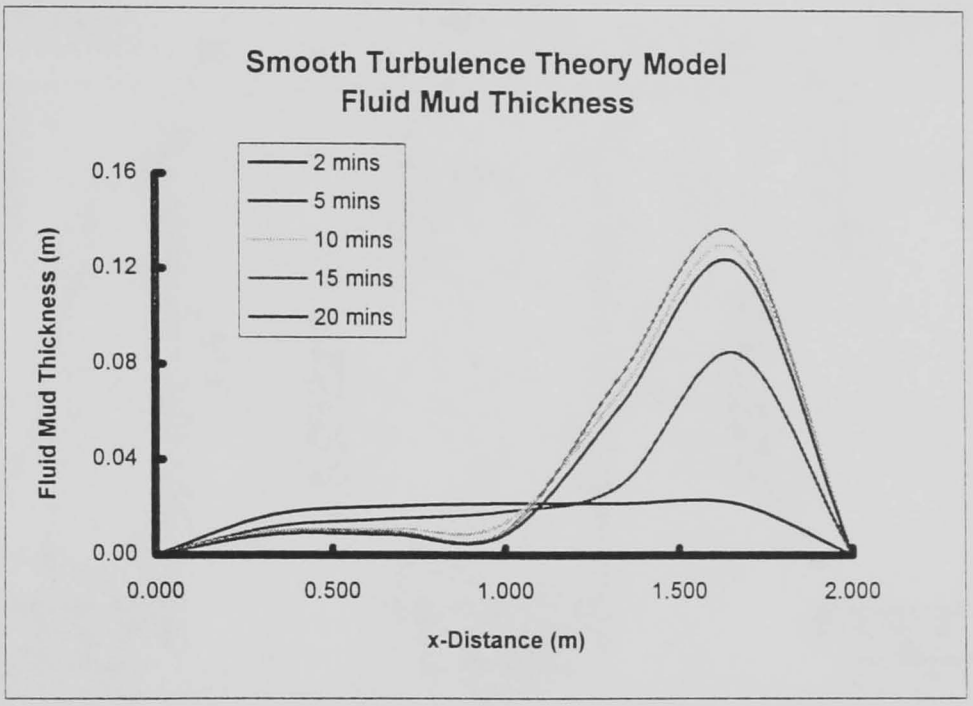

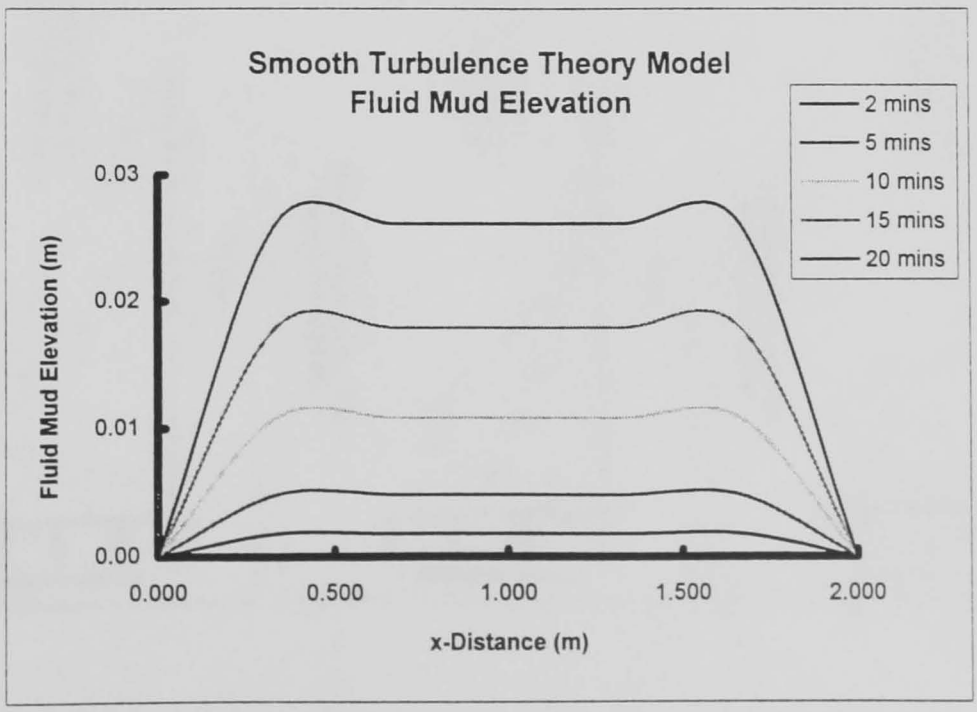

Figure 7.57: Model Results Obtained with Friction Factor Determined from the Smooth Turbulence Theory

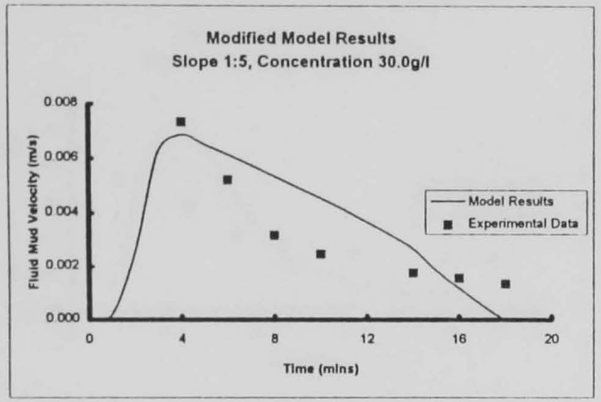

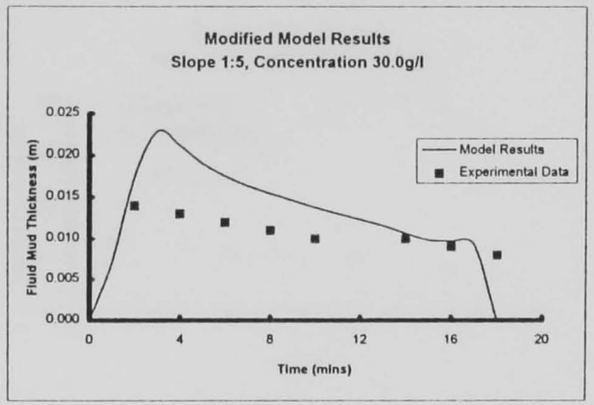

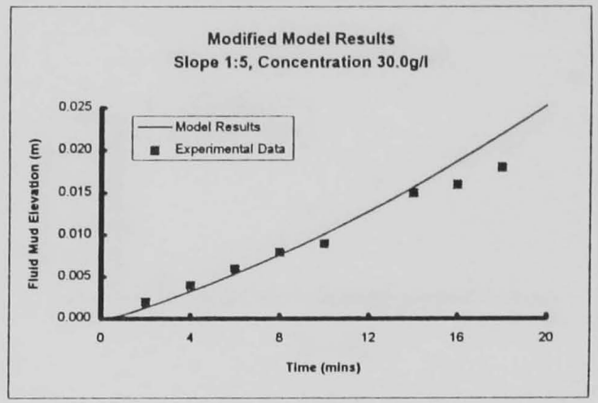

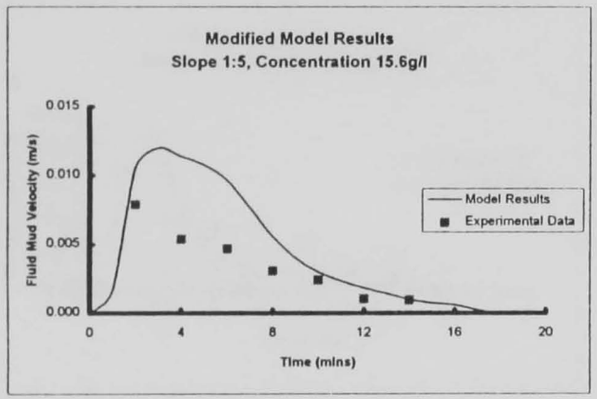

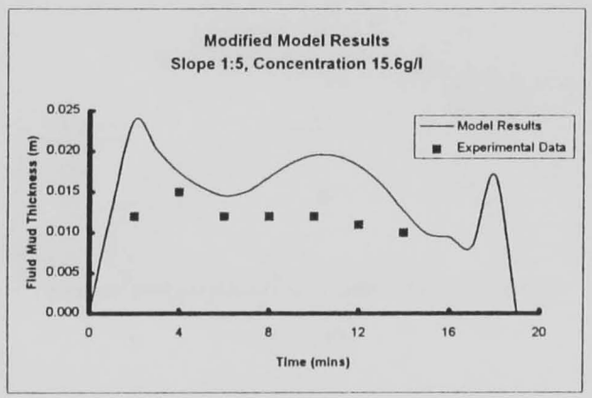

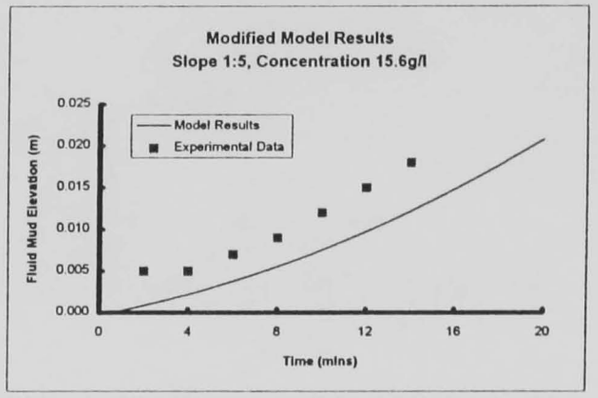

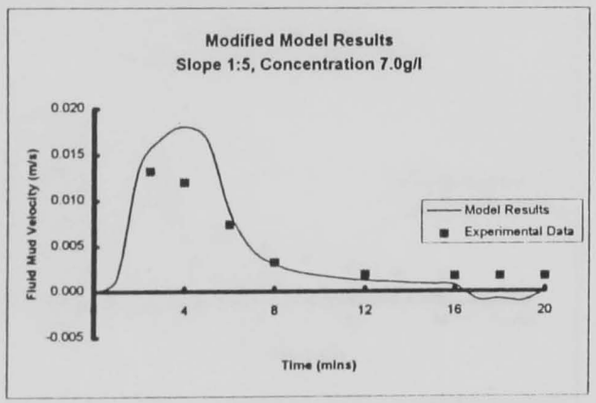

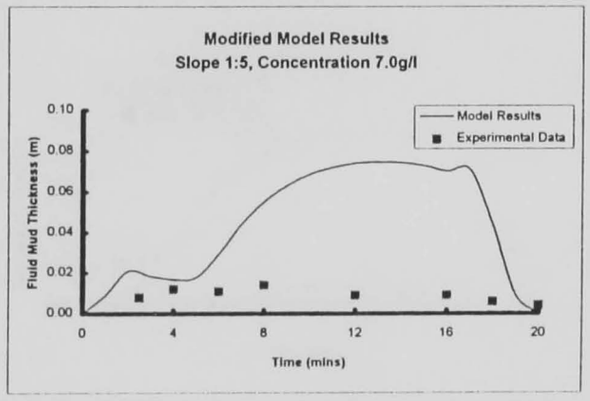

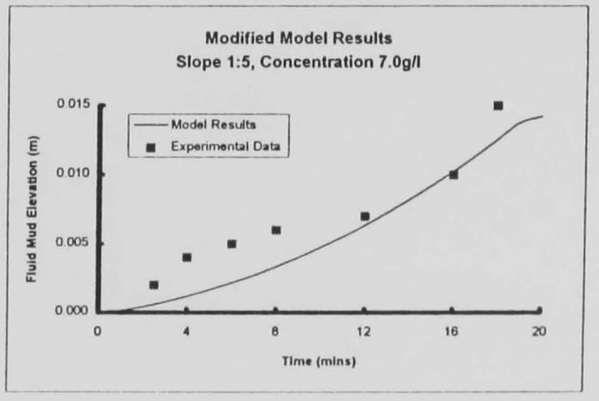

Figure 7.58: Results of Modified Model Compared with Data from Ali and Georgiadis (1991), Bed Slope 1:5

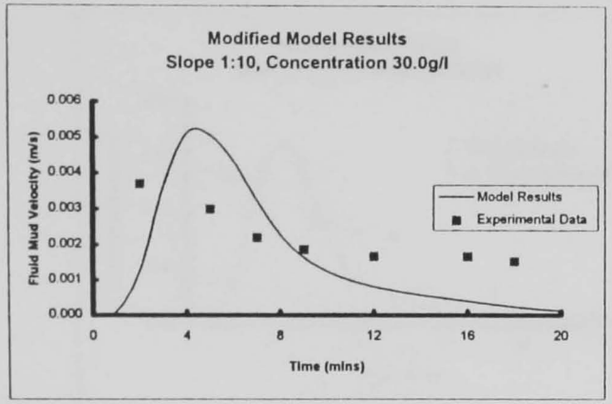

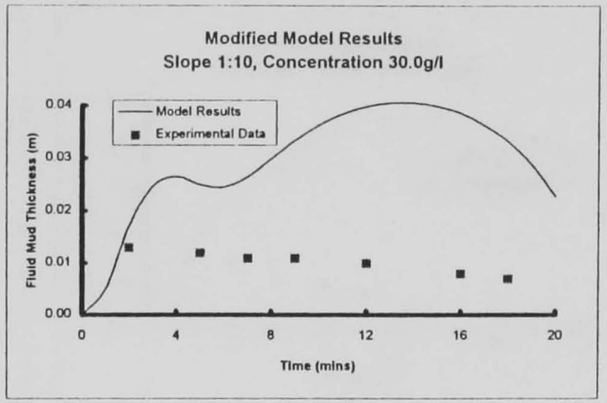

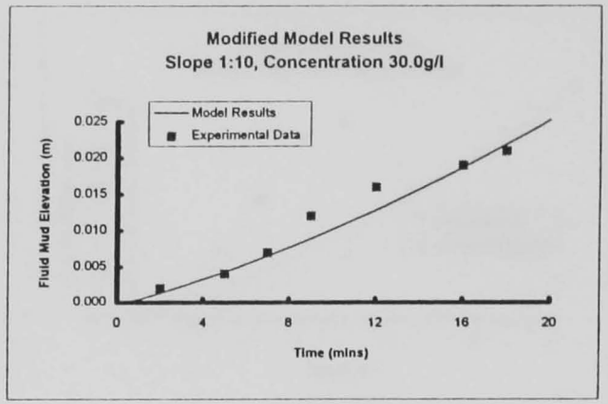

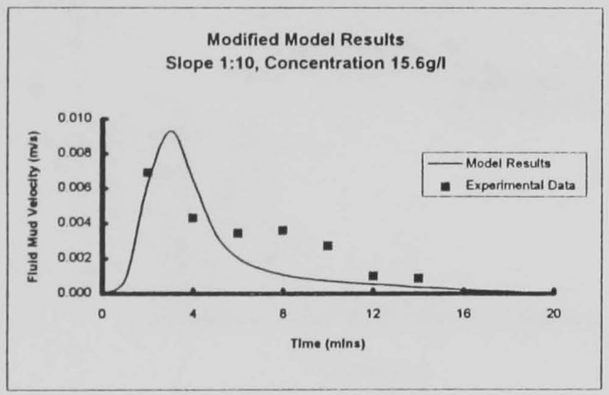

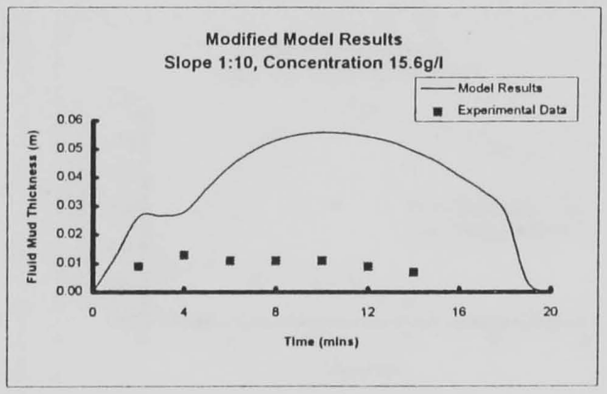

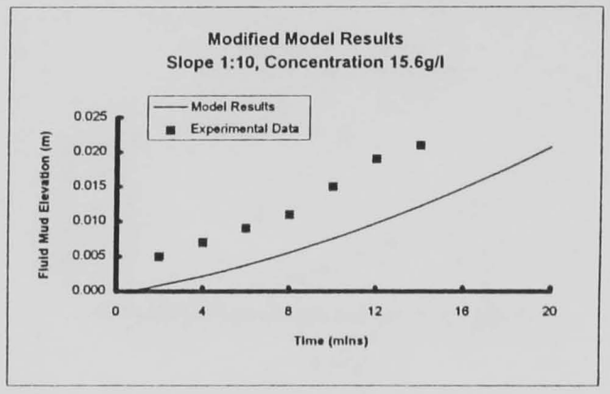

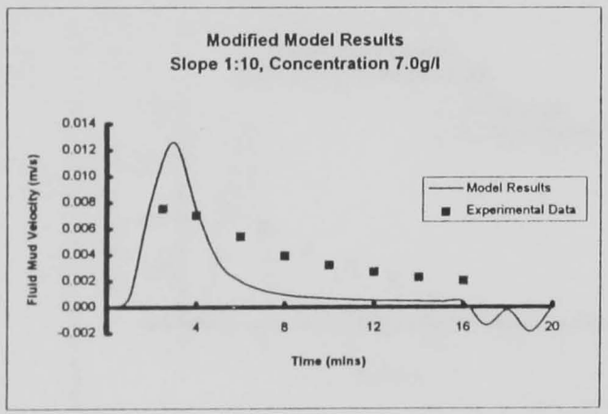

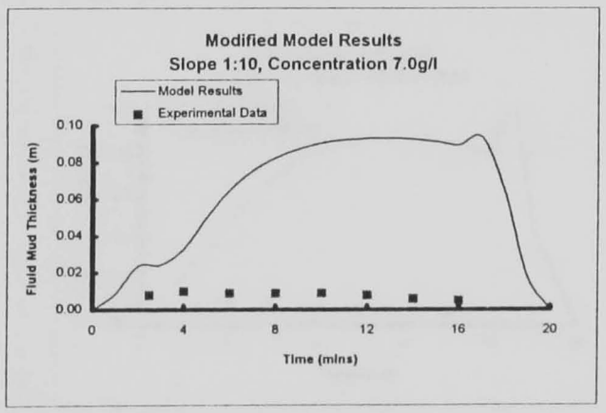

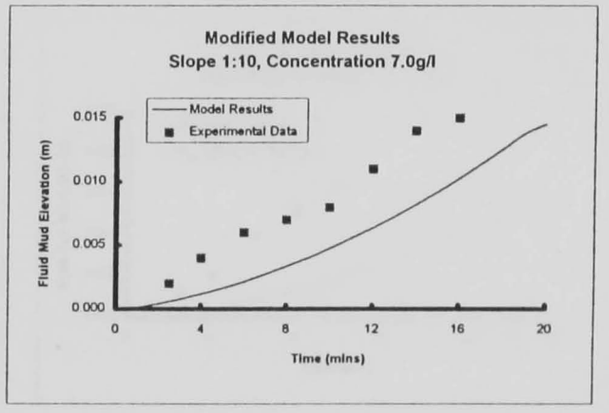

Figure 7.59: Results of Modified Model Compared with Data from Ali and Georgiadis (1991); Bed Slope 1:10

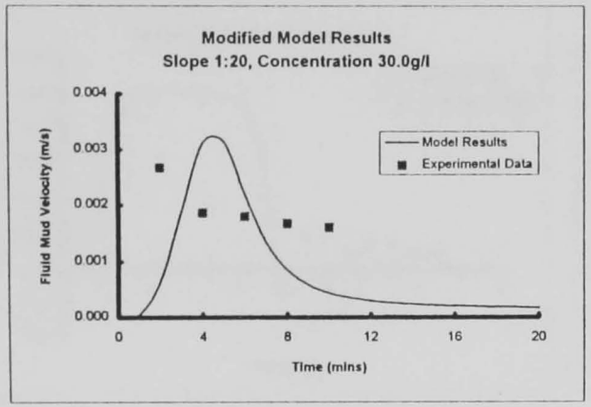

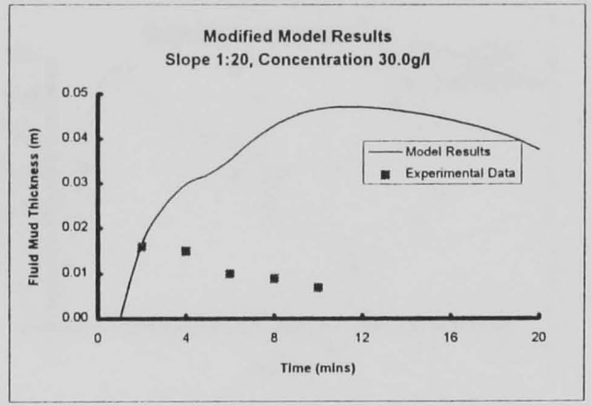

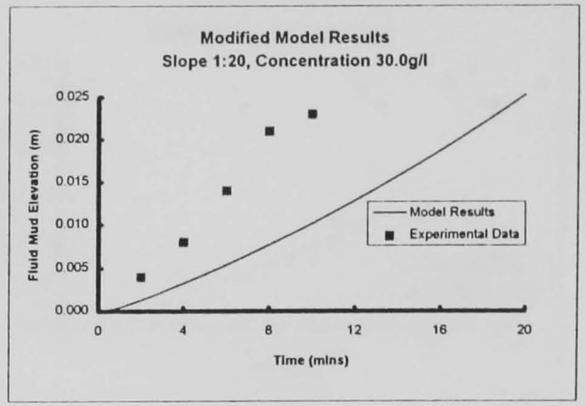

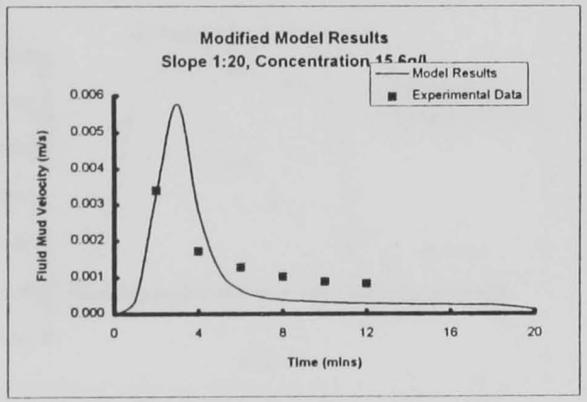

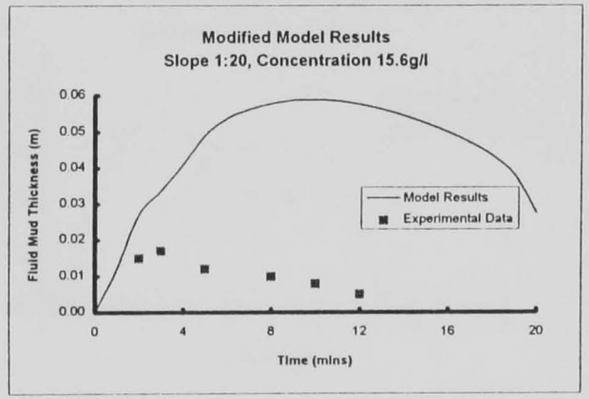

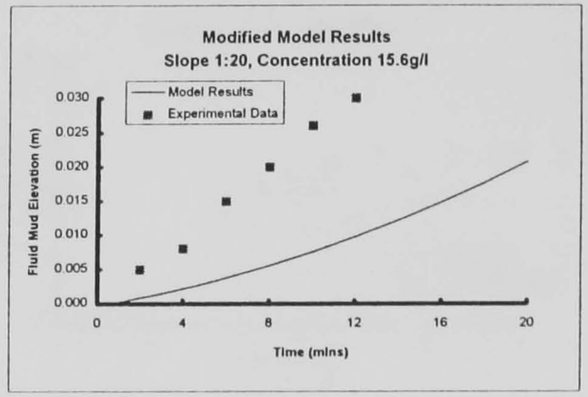

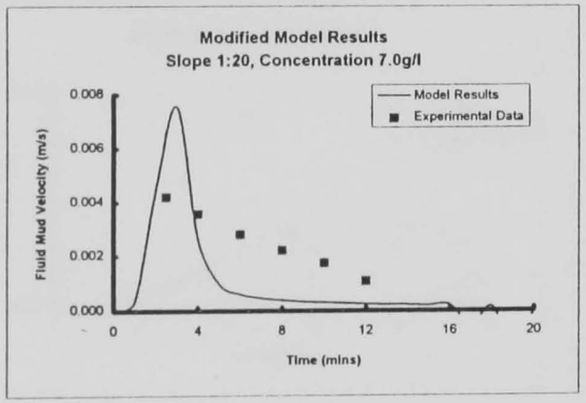

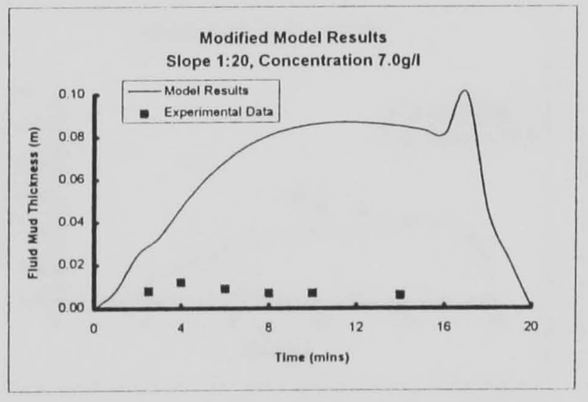

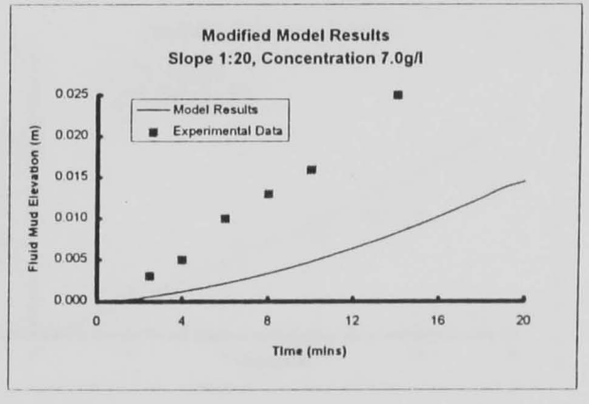

Figure 7.60: Results of Modified Model Compared with Data from Ali and Georgiadis (1991), Bed Slope 1:20

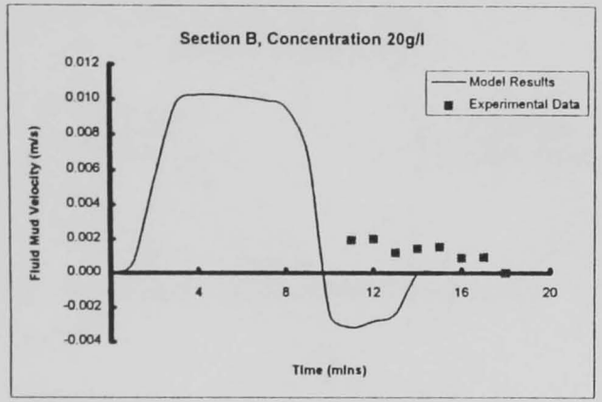

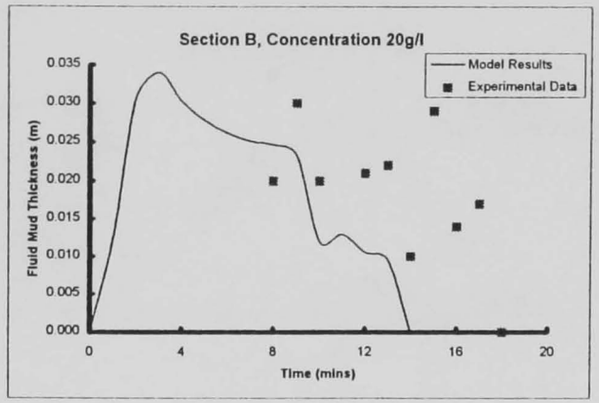

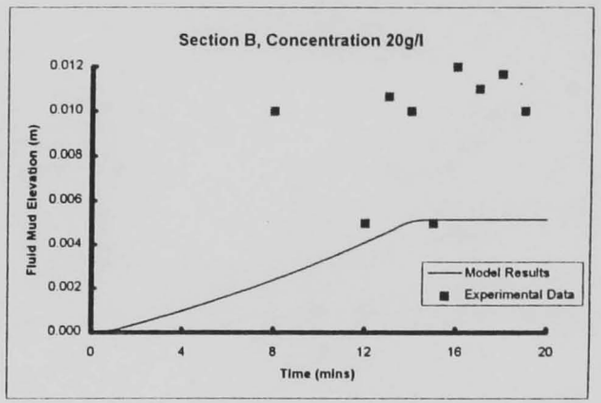

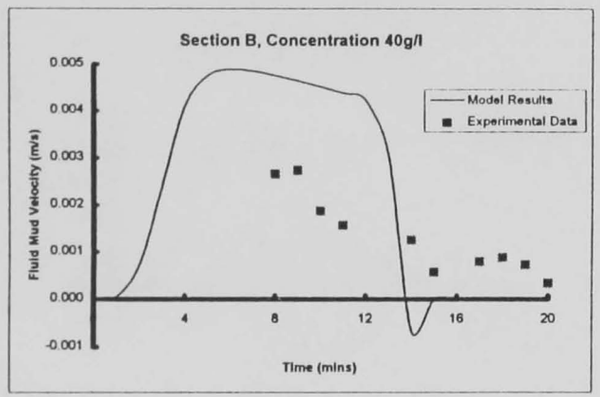

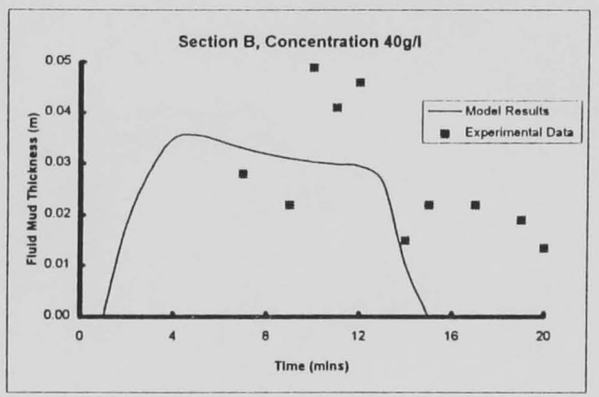

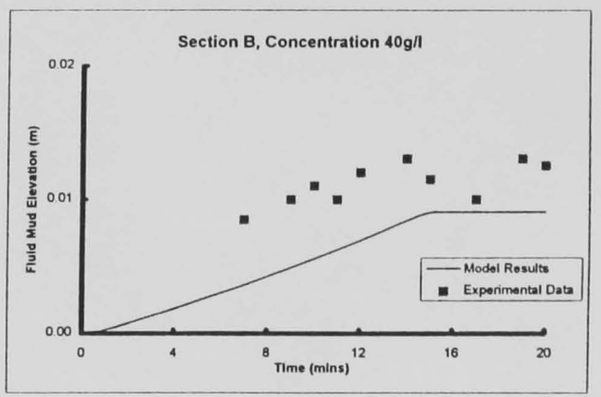

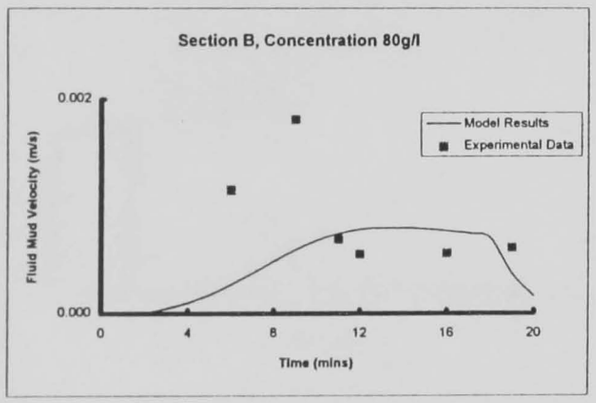

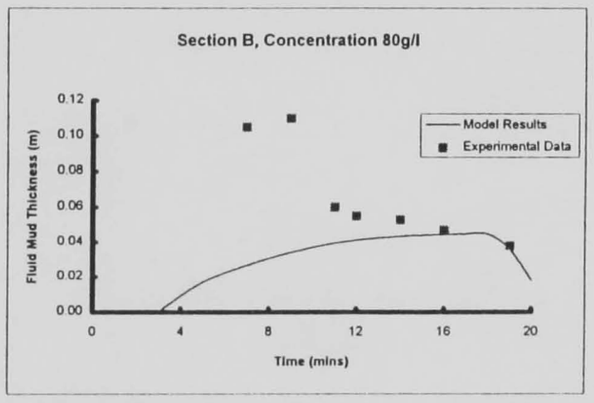

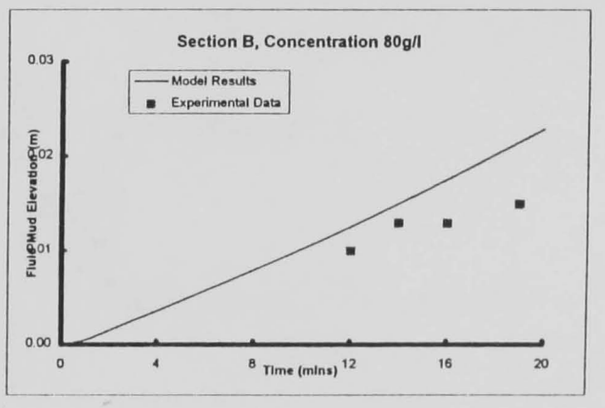

Figure 7.61: Results from Modified Model Compared with Race Track Flume Data; Section B

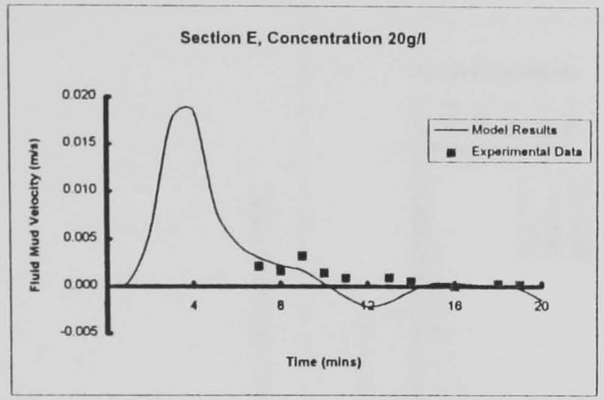

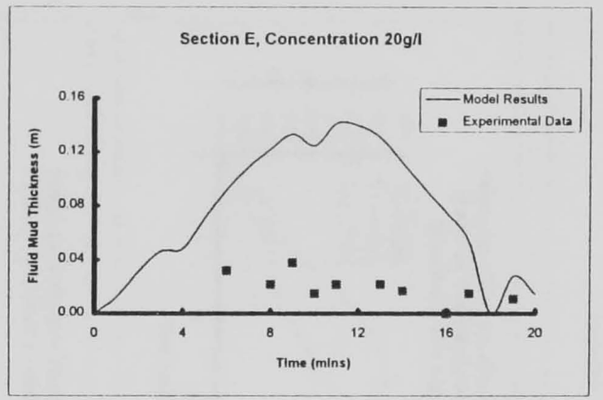

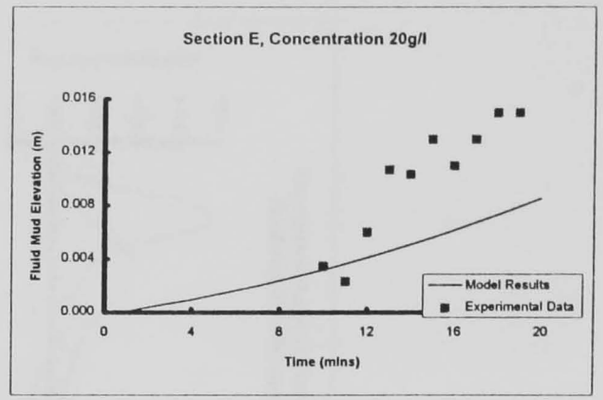

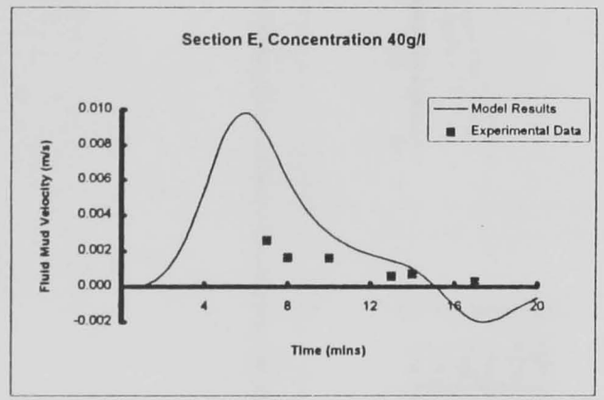

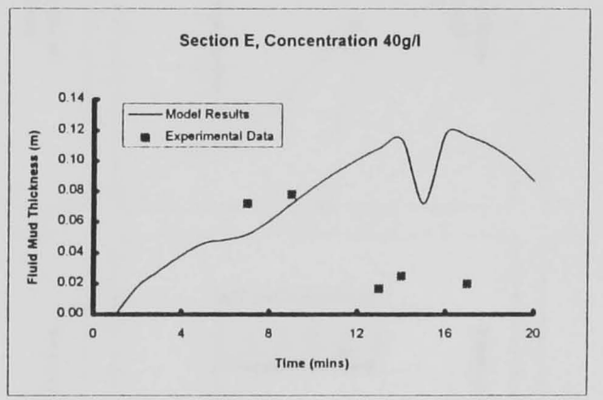

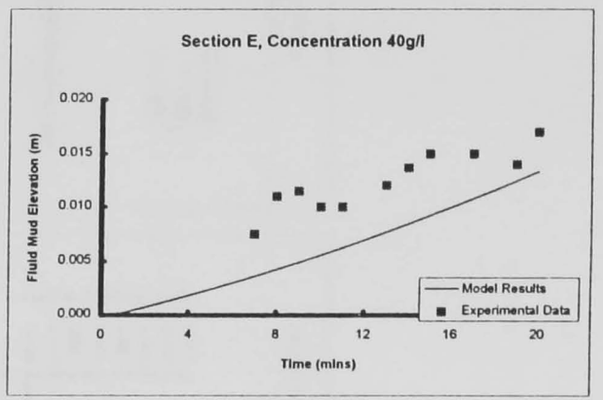

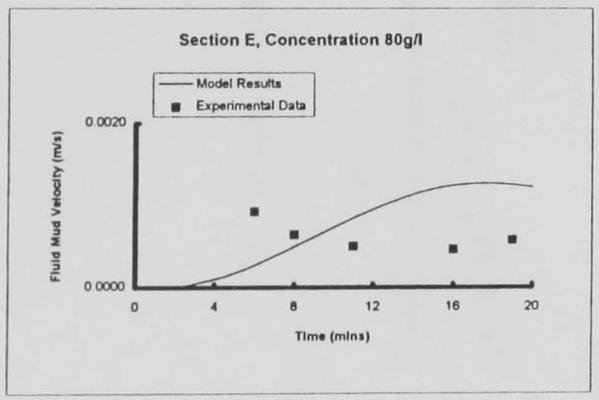

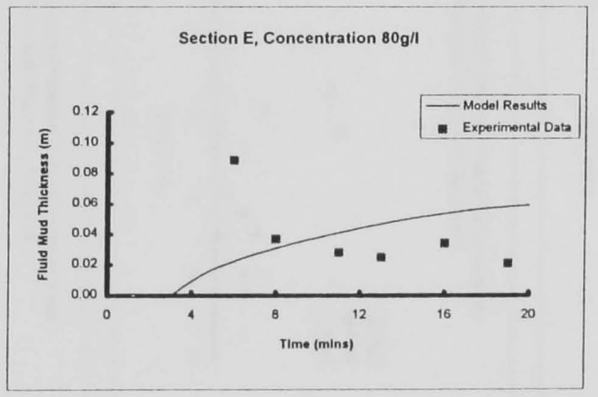

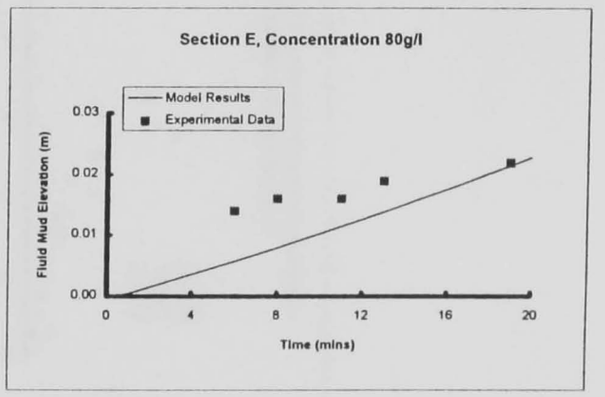

Figure 7.62: Results from Modified Model Compared with Race Track Flume Data; Section E

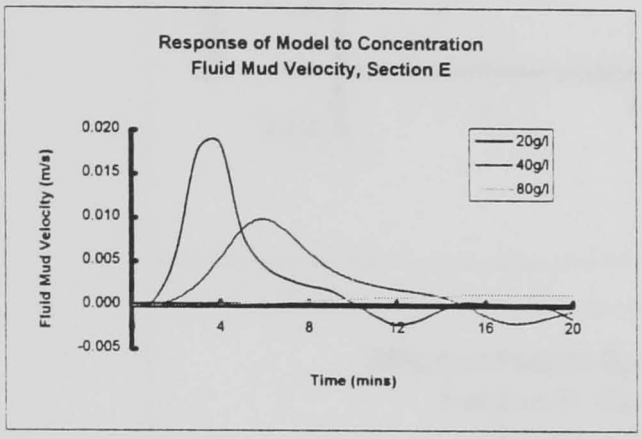

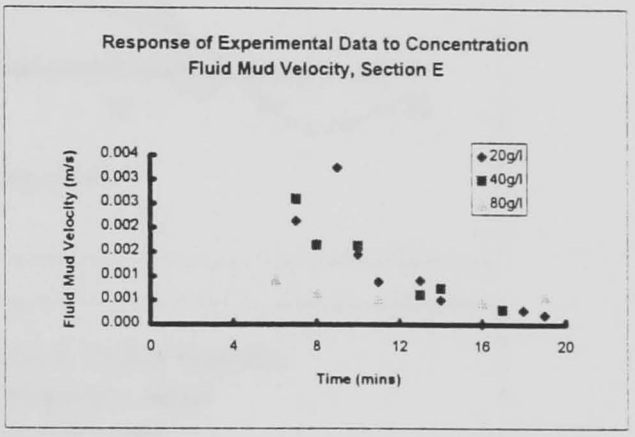

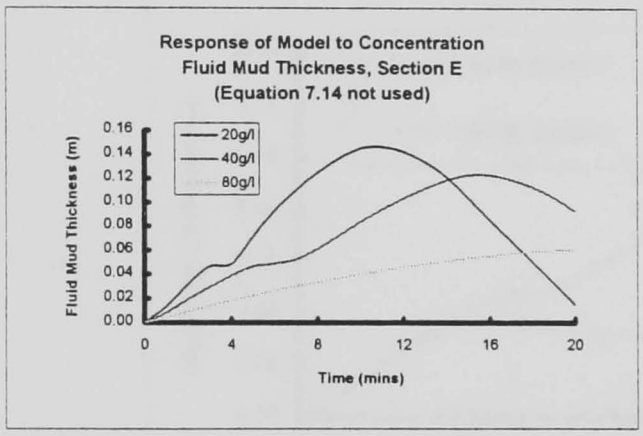

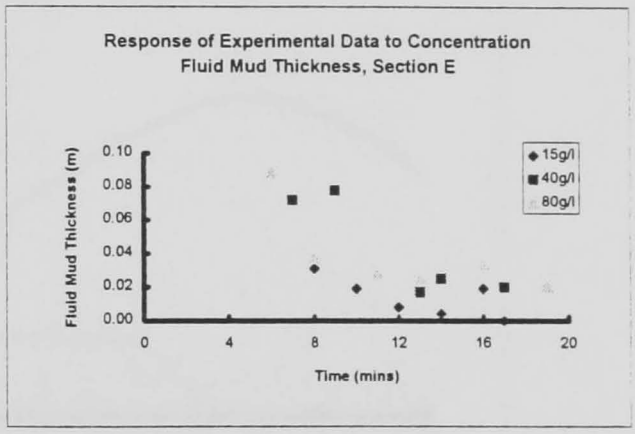

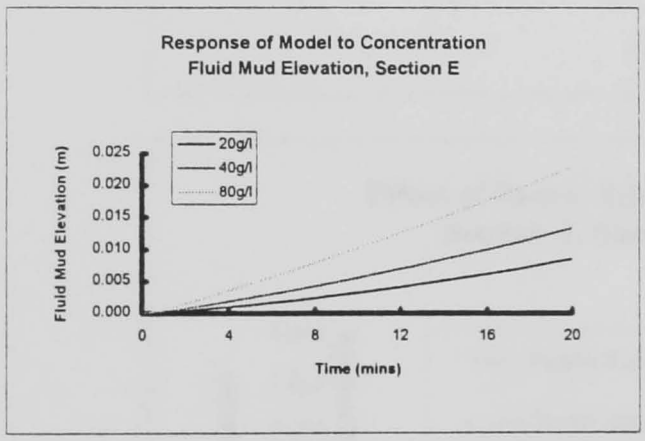

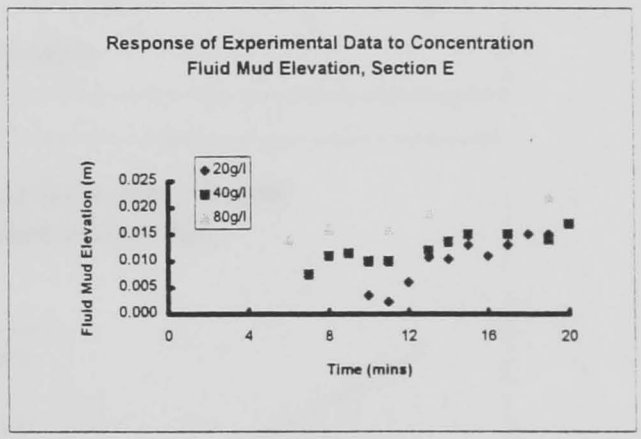

Figure 7.63: Response of Modified Model to Changes in Concentration Compared with Experimental Data

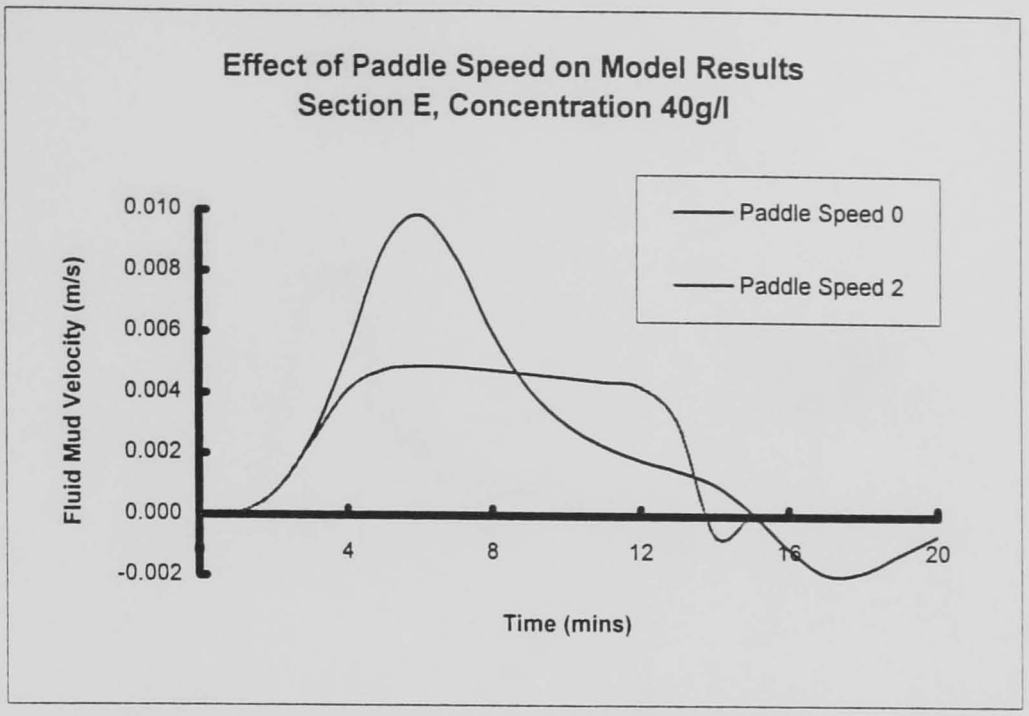

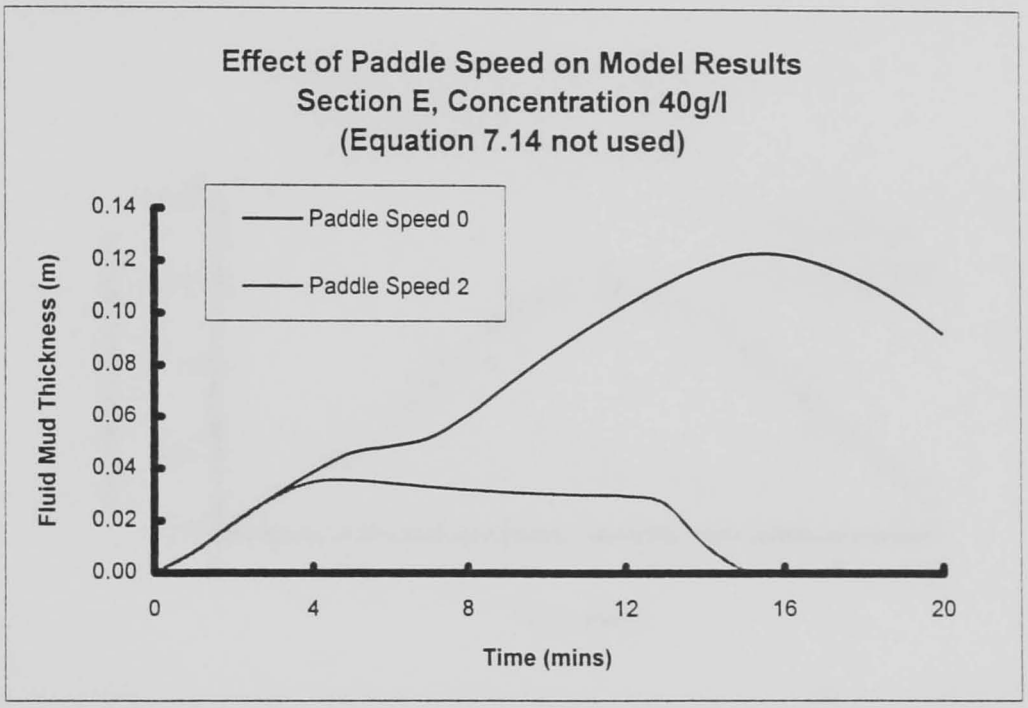

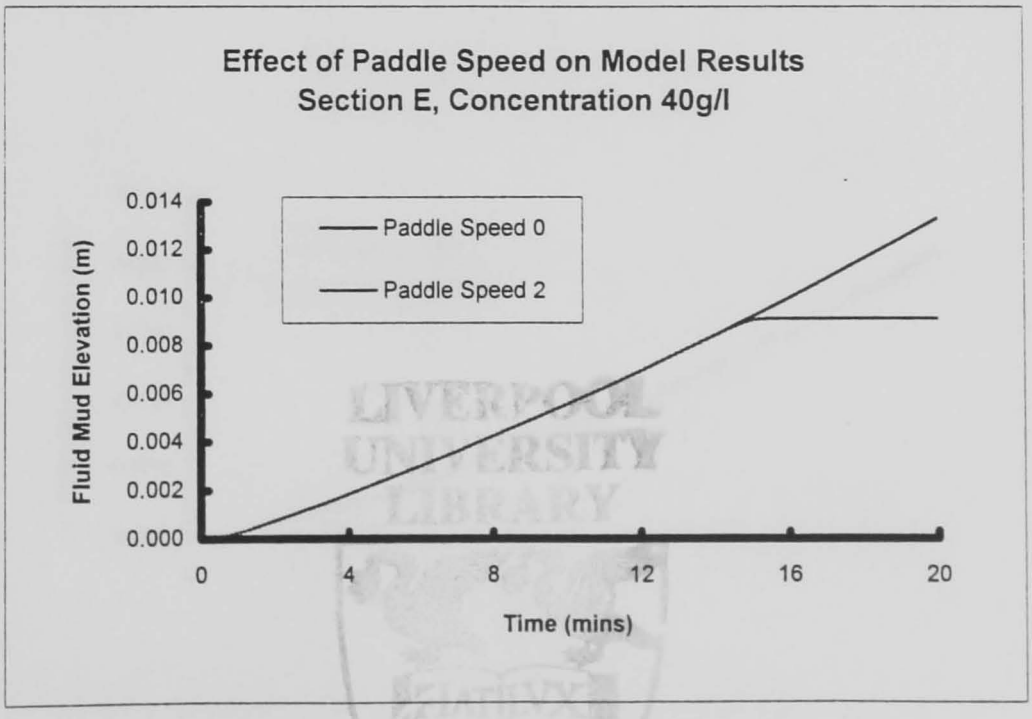

Figure 7.64: Effect of Paddle Speed on Results of Modified Model

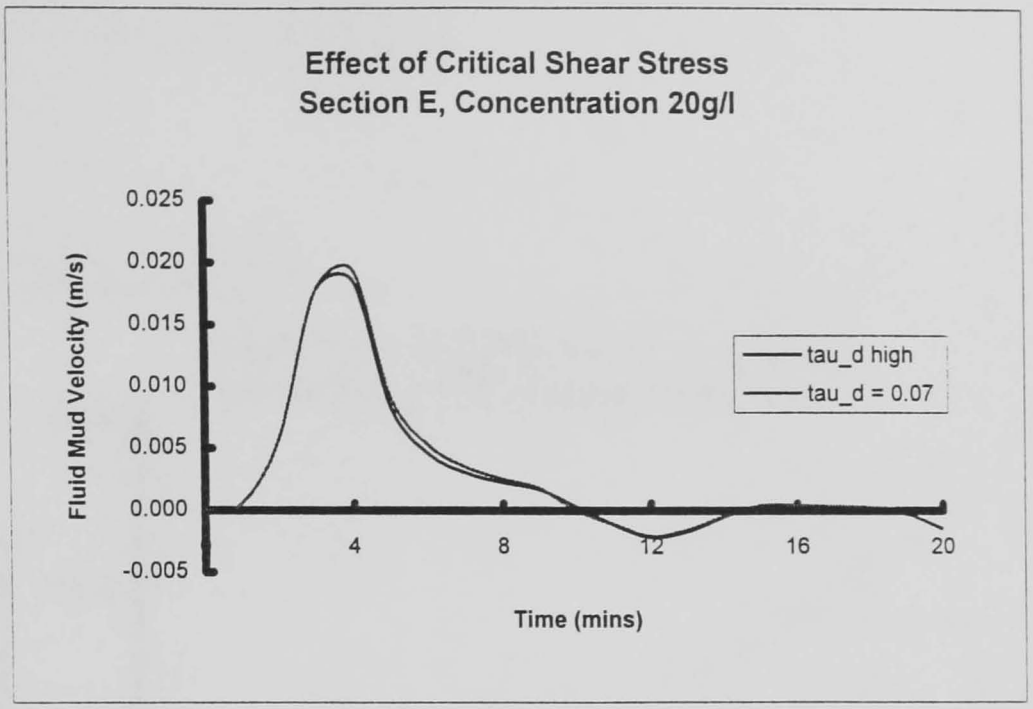

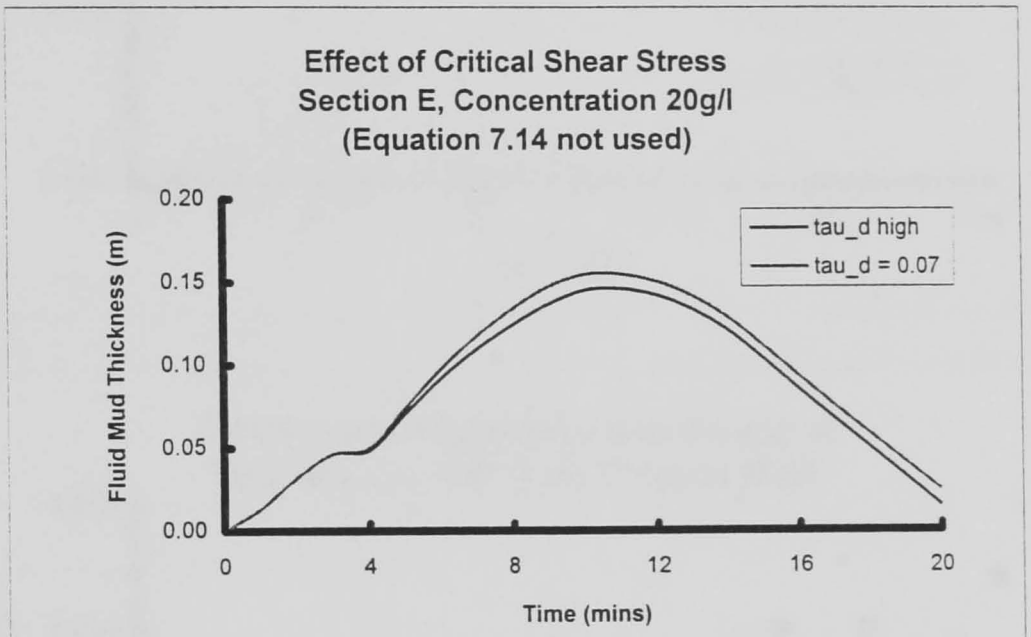

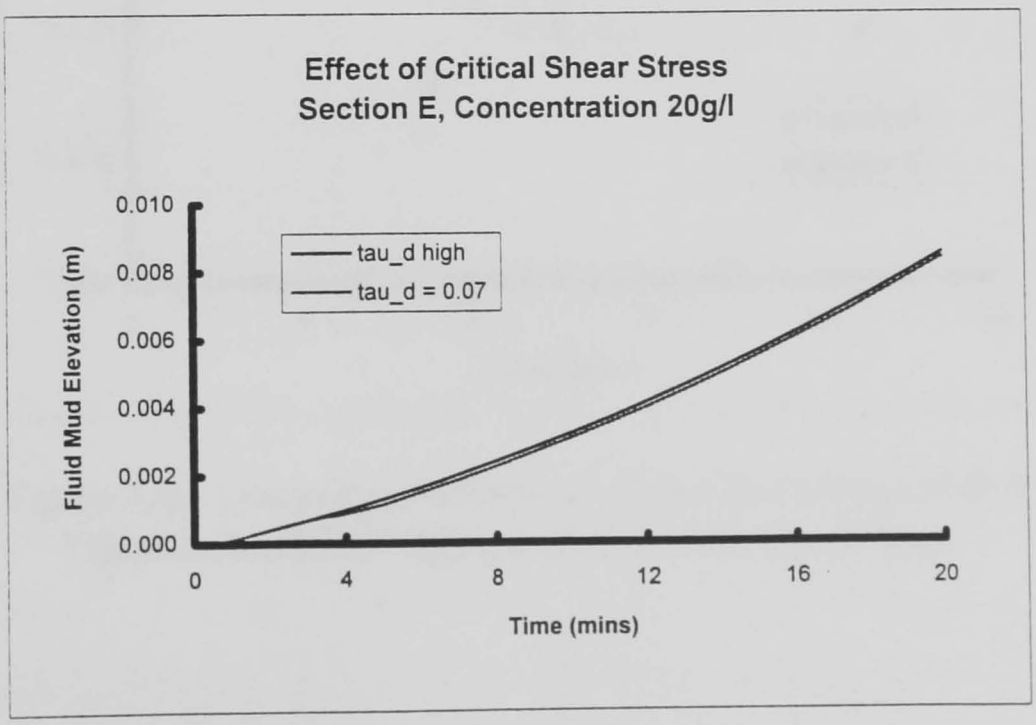

Figure 7.65: Effect of Critical Shear Stress for Deposition on Results of Modified Model

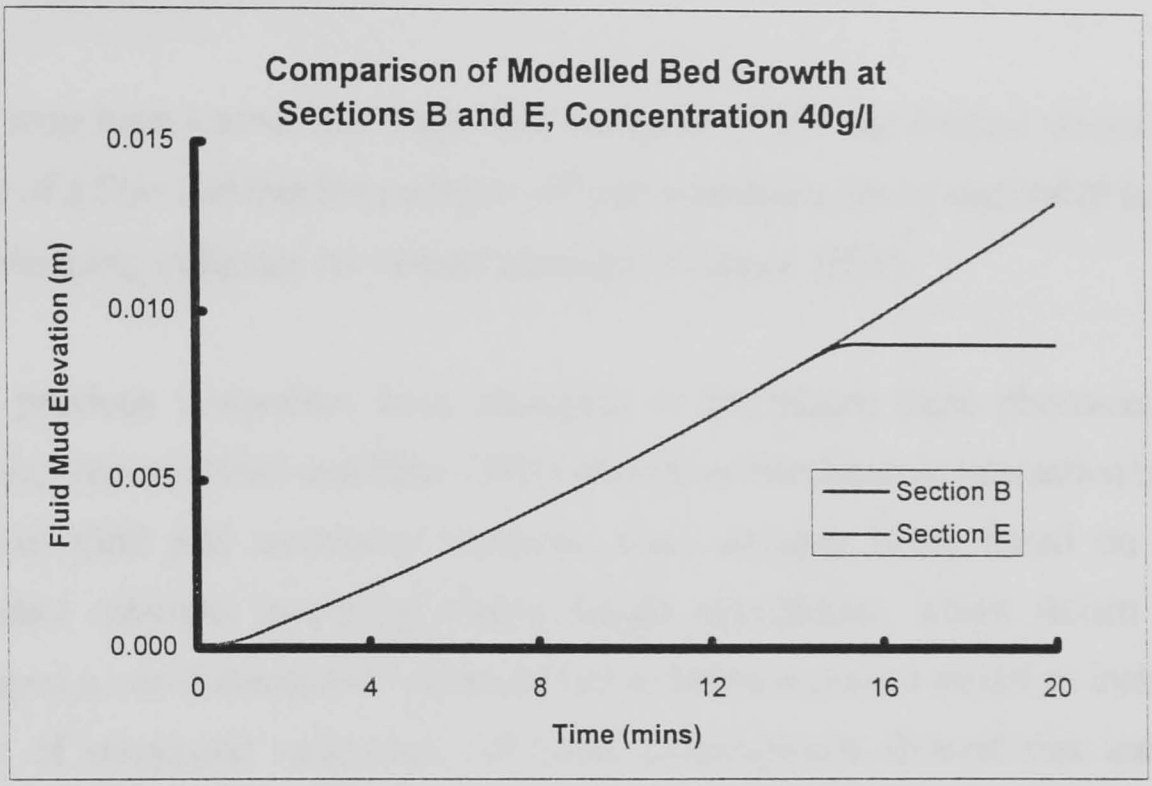

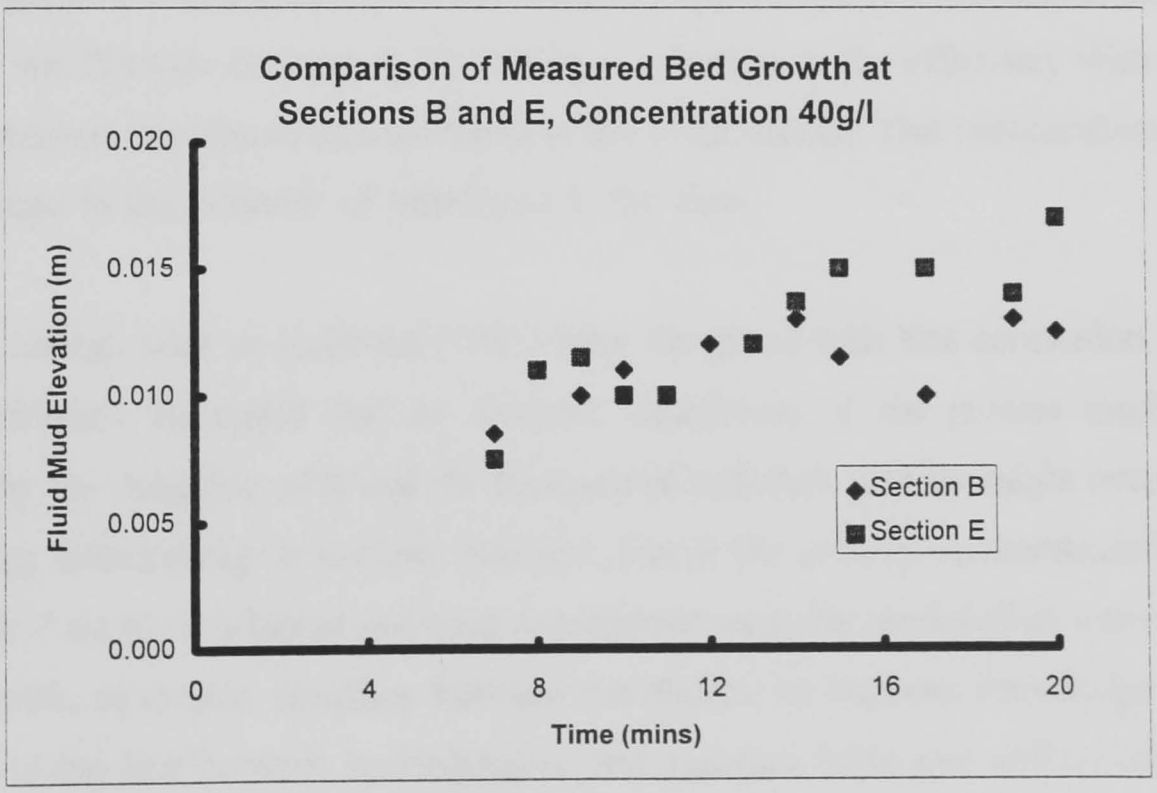

Figure 7.66: Comparison between Modelled and Measured Bed Growth; Modified Model and Race Track Flume Data

Chapter 8: The Effects of Dense Mud Suspensions on Near-Bed Velocity Distributions and Fluid Turbulence

8.1 Introductory Remarks

It has long been known that suspended sediment affects the internal dissipation of energy of a flow and that the presence of large concentrations of suspended sediment has a damping influence on vertical mixing (O'Connor 1991).

Many previous researchers have attempted to investigate these phenomena. For example, Vanoni (1946) and Hino (1963) considered the dynamic interaction between turbulent fluid and suspended sediment, their analyses being based on simple turbulence concepts involving mixing length calculations, whilst Roisin (1985) developed a one-dimensional numerical k-ε turbulence closure model to include the effects of suspended sediments. All these investigations showed that increasing concentrations of suspended sediment caused the equivalent of a decrease in the value of the von Kárman constant κ, indicating a reduction in the efficiency with which momentum is transferred through the flow due to turbulence. This was combined with a decrease in the intensity of turbulence in the flow.

Other authors such as Coleman (1981) have disagreed with this conclusion, and it may certainly be stated that no absolute description of the precise mechanism whereby the reduction of κ and the damping of turbulent activity might occur have yet been forthcoming. It is clear, however, that if the author's recommendations of chapter 7 are to be adopted and mud suspensions are to be modelled as a two-phase flow, with, of course, coupling between the phases, an accurate knowledge of the nature of the link between hydrodynamic and sediment behaviour will be essential.

The author was able, during the current investigation, to take advantage of the Toshiba SDL-01A ultrasonic pulsed-Doppler unit to obtain a series of non-intrusive measurements of near-bed velocity profiles in differing concentrations of suspended

mud in the Race Track Flume. These were used to investigate the findings of Vanoni (1946) and Hino (1963). Further, since the SDL-01A appeared to operate with a temporal resolution sufficient to resolve the turbulent fluctuations as encountered in the Race Track Flume, attempts were also made to measure turbulent fluctuations in mud suspensions directly, and to use this information to shed further light on the coupling of sediment and hydrodynamic behaviour.

This chapter discusses the results of these experiments using the Toshiba SDL-01A ultrasonic pulsed-Doppler unit, and attempts to put them in the wider context of the settling behaviour of mud such as might lead to the formation and movement of fluid mud.

8.2 Measurement of Turbulence using the Ultrasonic Doppler

A description of the Toshiba SDL-01A pulsed-Doppler unit is contained in section 4.4.3, chapter 4, whilst the implications of applying an instrument of the SDL-01A's specification to the measurement of mud flows are discussed in section 4.4.5. However, the SDL-01A, in common with all medical instruments of its type, was designed to measure relatively steady laminar blood flows, and therefore no specification was available as to the instrument's design limits in the measurement of turbulent fluctuations. The author therefore had no alternative but to evaluate the instrument's suitability for use in this context by experimental means. The results of the evaluation experiments, and the conclusions with regard to the application of the SDL-01A to measure turbulent fluctuations, are considered in the following paragraphs.

8.2.1 The Turbulent Frequencies to be Measured

As discussed in chapter 3, a series of Laser-Doppler Anemometer (LDA) results was taken at a sampling frequency of 1000Hz in clear water in the Race Track Flume. A

typical, one second duration section of LDA data is shown in figure 8.1. Fluctuations in the mean velocity, which are attributable to turbulent eddies in the flow, are clearly visible, and it is apparent that the main fluctuation corresponds to a mean frequency of approximately 5 to 7Hz (ie 5 to 7 main peaks during the one second period). This suggests that the significant turbulent features in the flow occur with a frequency very much less than the Toshiba SDL-01A's minimum pulse repetition frequency of 4000Hz, and should therefore be measurable with the instrument. A further analysis of the LDA results was carried out using a Fast Hartley Transform routine with a Hanning window (figure 8.2). This confirmed that the only significant frequencies occurring in the flow were at frequencies below 10Hz.

In the light of these observations, it was concluded that the Toshiba SDL-01A was capable of measuring flow velocity with a temporal resolution much finer than the minimum period of the significant turbulent features observed in the Race Track Flume. The SDL-01A could therefore be used, at least in theory, to obtain direct measurements of turbulent fluctuations in suspensions of mud.

There is a caveat to this analysis, which is that the use of the SDL-01A in mud suspensions depends on the turbulent frequencies in the presence of mud in the Race Track Flume being sufficiently similar to those in the clear water LDA experiments. However, it seems reasonable to assume that the presence of mud would not cause the vast increase in turbulent frequencies necessary to take them from around 10Hz at maximum to the 4000Hz lower limit of the Toshiba instrument.

8.2.2 The Turbulent Structure to be Measured and the One-Dimensional Nature of Measurements from the SDL-01A Pulsed-Doppler Unit

A typical set of results obtained from a two-component, longitudinal-vertical LDA system in turbulent flow might consist of a series of instantaneous values given by:

$$u = U + u' \qquad\qquad w = W + w' \qquad\qquad (8.1)$$

where u indicates the instantaneous longitudinal velocity, U the mean longitudinal velocity over the sampling period and u' the instantaneous longitudinal turbulent fluctuation around the mean velocity; w, W and w' are the corresponding vertical velocity components.

It is clear that, by definition [u'] = 0 and [w'] = 0, where the square brackets indicate a temporal mean over a sampling period sufficiently long to encompass many turbulent fluctuations. u' and w' cannot therefore be measured directly except as instantaneous values which shed no light on the general pattern of turbulence in the flow. However, the signals in equation 8.1 may easily be processed as follows:

$$u' = u - U \qquad\qquad w' = w - W \qquad\qquad (8.2)$$

and another instantaneous value, u'w', can then be calculated by multiplying the two signals. The value [u'w'] is then generally non-zero, and its square root is a root mean squared value that gives an indication of the magnitude of the turbulent fluctuations in the longitudinal/vertical plane of the flow over the sampling period. The value $\sqrt{[u'w']}$ has dimensions of velocity, and may be termed a 'shear velocity'.

In order to get a complete, two-dimensional picture of the turbulence in a flow, of course, it is necessary to multiply all the fluctuations from both velocity components in pairs, so as to obtain the values u'u', w'w' and u'w'. However, if the turbulence under consideration is reasonably isotropic, it follows that the magnitudes of the three shear velocities $\sqrt{[u'u']}$, $\sqrt{[w'w']}$ and $\sqrt{[u'w']}$ will be approximately the same.

As discussed in section 4.4.5, chapter 4, the Toshiba SDL-01A is limited in that its measurements are one-dimensional in the direction of the Doppler beam. In the application of the instrument to measurements in the Race Track Flume, this meant that measurements were obtained at an angle of -58.665° to the longitudinal axis of the flume. The only shear velocity which can be measured by the Toshiba instrument was therefore that given by $\sqrt{[q'q']}$, where q' represents turbulent fluctuations in the

direction of the Doppler beam. It was therefore necessary to evaluate the turbulence in the Race Track Flume to ascertain whether sufficient isotropy was present to allow the value $\sqrt{[q'q']}$ to be taken as representative of the general two-dimensional pattern of turbulence in the flume. This was done using two-component LDA readings obtained in clear water (see chapter 3), and the results are shown in figure 8.3, where values of $\sqrt{[u'u']}$ are compared with values of $\sqrt{[w'w']}$. The results show a great deal of scatter, as is to be expected from the measurement of turbulent fluctuations. They also indicate that on average, values of $\sqrt{[u'u']}$ are slightly greater than the corresponding values of $\sqrt{[w'w']}$. This is, in fact, to be expected of isotropic turbulence in which the mean velocity U is substantially greater than the mean velocity W, which was the case in the Race Track Flume (Nezu and Nakagawa 1993).

No further quantification of this analysis was attempted by the author; however, it was concluded that turbulence in the Race Track Flume is approximately isotropic in the two-dimensional longitudinal/vertical plane, and that any single value of shear velocity such as $\sqrt{[q'q']}$ in this plane should give a reasonable indication of the overall magnitude of the turbulent fluctuations in the two-dimensions considered. Of course, the caveat mentioned at the end of section 8.2.1 also applies here, in that this conclusion was obtained from experiments carried out only in clear water. As mentioned in section 4.4.1, LDA systems will not work in the presence of suspended mud, since the opaque mud particles obstruct the passage of the laser beam through the flow. However, it seems reasonable to assume that the presence of mud will not significantly affect the isotropy of turbulence in the Race Track Flume.

8.2.3 Comparison of Shear Velocity Measurements from the Toshiba SDL-01A Pulsed-Doppler Unit and a Two-Component Laser-Doppler Anemometer

After establishing that it was theoretically possible to measure some turbulent features in the Race Track Flume using the Toshiba SDL-01A, and that the features measured might give a useful indication of the overall pattern of turbulence in the flume, it was

necessary to determine whether the results produced by the SDL-01A in fact bore any resemblance to results obtained from an LDA system, which can reasonably be relied upon to measure turbulent fluctuations correctly.

In order to address this issue, an experiment was carried out to compare shear velocity measurements obtained at the same times and locations using the LDA and the SDL-01A instruments. This experiment was again carried out in clear water, since it depended on the use of the LDA system. However, other parameters such as the bed slope and water depth were set as they were for the mud experiments (see section 5.3, chapter 5). In order to compare results over a range of values, the turbulence level in the flume was varied by the simple expedient of changing the mean flow velocity.

A plot of shear velocity $\sqrt{[u'w']}$ measured with the two-dimensional LDA system against shear velocity $\sqrt{[q'q']}$ measured with the ultrasonic pulsed-Doppler unit is shown in figure 8.4. There is only limited data, and it can be seen that there is a great deal of scatter, though this is to be expected of any experiment to measure turbulence. However, the trend of the graph shows a distinct correlation between the LDA and the SDL-01A results, and a least mean squares regression analysis, evaluated assuming the error to be in the SDL-01A data, indicates that the data may be approximately represented by a straight line of slope 1.331.

Figure 8.4 was in fact plotted with the SDL-01A data as the independent variable, since it was this value that was to be measured during the mud experiments and the LDA value, regarded as a true reading, which was to be inferred from the measurements. However, since the slope of the least mean squares trend line was so close to unity and the experimental scatter was so great, it was decided to avoid any calibration procedure and to assume that the SDL-01A measurements as recorded represented a quantitative, but very approximate, value of shear velocity given by $\sqrt{[u'w']}$. Clearly, in view of the scatter on figure 8.4, it is necessary for a large number of readings to be averaged before an approximation to $\sqrt{[u'w']}$ can be assumed.

It must be emphasised that no particular value of the slope of the trend line on figure 8.4 was *a priori* expected, as the performance of the SDL-01A in measuring turbulence was not understood from the instrument specifications available. The aim of the analysis, therefore, was simply to establish whether there was any relationship at all between the two sets of readings plotted on figure 8.4. However, the presence of isotropic turbulence suggests that, if both LDA and SDL-01A are accurately and directly measuring turbulent features in the Race Track Flume, a slope of unity would be appropriate for the trend line in figure 8.4. The slope obtained of 1.331 is therefore reasonably encouraging, suggesting that the SDL-01A does directly measure useful turbulent data in clear water.

As with the discussions of the two previous sections, the conclusions of this section must simply be assumed to apply in mud suspensions. There is no way of verifying that this is the case due to the non-functionality of the LDA system in the presence of mud.

8.3 Experiments to Measure Near Bed Velocity Profiles and Turbulent Shear Velocity in the Race Track Flume

Measurements of near bed velocity and turbulent shear velocity using the Toshiba SDL-01A pulsed-Doppler unit were carried out as described in section 5.3.3, chapter 5, the measurements taking place during the period before each fluid mud run as the flume was run at paddle setting 10 to allow stirring and flocculation to take place. A total of 29 experimental runs were carried out as detailed in table 5.5, chapter 5, with near bed velocity profiles and turbulent shear velocities being recorded at either section B or section E (but not both) for all runs except number 9. The measuring section given in table 5.5 indicates where the SDL-01A probe was placed during each individual run.

Velocity profiles were obtained by placing the Toshiba instrument's measuring volume at the required location and obtaining a 10 second sample. The measuring

volume was then placed at the next location and the process repeated until the desired profile had been completed. Samples were recorded directly onto a PC equipped with a 'Global Lab' analog to digital conversion board and software (Data Translation Limited 1992). Samples were digitized at a frequency of 100Hz. The velocity samples consisted of a series of instantaneous Doppler frequency readings produced by the Toshiba SDL-01A's in-built Fast Fourrier Transform unit, and included information on both mean velocity and turbulent fluctuations (see section 4.4.3, chapter 4).

Concentration profiles were measured at the same time as near bed velocity profiles. Except for those for runs 26 to 29, nominal initial average concentration 80kgm^{-3}, these were obtained using the FOSLIM probe as described in section 4.6.2, with the samples being taken simultaneously with the velocity readings at the corresponding height and stored on the same data file on the PC. Care was taken to ensure that the FOSLIM probe did not interfere with the SDL-01A measuring volume. For runs 26 to 29, the mud concentration was too high to be measured by the FOSLIM and no satisfactory concentration profiles could be obtained.

Both velocity and concentration profiles were limited to the lower portion of the flow, typically up to 50mm from the steel base of the flume. This was because, as discussed in chapter 3, it was only in this region that a logarithmic boundary layer flow profile could be identified.

Velocity, concentration and shear velocity profiles obtained in various concentrations of suspended mud at sections B and E in the Race Track Flume are shown in tables 8.1 and 8.2. Velocity and shear velocity profiles obtained in fresh water and salt water of bulk densities 1007kgm^{-3} and 1035kgm^{-3} are shown in table 8.3, and mean values over the height 0 to 50mm for all the measured profiles are shown in table 8.4. It will be noted that the velocities recorded are in general well above the 0.055ms^{-1} lower measuring limit of the SDL-01A instrument.

Table 8.1: Near Bed Velocity and Concentration Profiles and Shear Velocity **Section B** (data is arranged in order of increasing nominal mean concentration across the page)

Height (mm)	Conc-entration (g/l)	Shear Velocity (m/s)	Mean Velocity (m/s)	Height (mm)	Conc-entration (g/l)	Shear Velocity (m/s)	Mean Velocity (m/s)	Height (mm)	Conc-entration (g/l)	Shear Velocity (m/s)	Mean Velocity (m/s)	Height (mm)	Conc-entration (g/l)	Shear Velocity (m/s)	Mean Velocity (m/s)	Height (mm)	Conc-entration (g/l)	Shear Velocity (m/s)	Mean Velocity (m/s)	Height (mm)	Conc-entratio (g/l)	Shear Velocity (m/s)	Mean Velocity (m/s)
Run 20				**Run 25**				**Run 17**				**Run 7**				**Run 2**				**Run 26 (mean concentration 80.89g/l)**			
5	8.72	0.0377	0.004	5	14.51	0.0386	0.081	5	29.28	0.0214	0.165	5	29.19	0.0273	0.172	5	35.97	0.0288	0.067	10	-	0.0229	0.031
10	8.68	0.0444	0.135	10	14.76	0.0278	0.254	10	28.79	0.0270	0.232	10	29.11	0.0361	0.232	10	35.83	0.0294	0.227	15	-	0.0252	0.131
15	8.56	0.0378	0.204	15	14.96	0.0283	0.314	15	28.47	0.0311	0.230	15	29.22	0.0349	0.232	15	38.55	0.0486	0.208	20	-	0.0364	0.192
20	8.52	0.0494	0.241	20	15.20	0.0339	0.298	20	32.22	0.0374	0.230	20	29.21	0.0348	0.276	25	37.72	0.0369	0.281	25	-	0.0479	0.236
25	8.51	0.0445	0.236	25	15.49	0.0371	0.326	25	33.39	0.0365	0.232	25	29.16	0.0429	0.253	50	37.51	0.0458	0.351	30	-	0.0446	0.255
30	8.49	0.0506	0.236	30	15.59	0.0296	0.337	37	35.21	0.0360	0.249	37	29.13	0.0382	0.282	75	38.46	0 0366	0.305	35	-	0.0420	0.270
40	8.43	0.0458	0.242	40	15.40	0.0459	0.313	50	35.29	0.0395	0.242	50	29.12	0.0336	0.261	100	38.47	0.0497	0.277	40	-	0.0449	0.244
50	8 43	0.0528	0.246	50	15.28	0.0357	0.331	62	27.54	0.0394	0.269	75	29.07	0.0405	0.257					50	-	0.0490	0.240
62	9.12	0.0504	0.251	62	15.33	0.0371	0.306	75	22.92	0.0305	0.243	100	29.04	0.0420	0.241					62	-	0.0475	0.265
75	9 48	0.0510	0.275	75	15.32	0.0364	0.267	87	22.88	0.0388	0.271									75	-	0.0480	0.279
87	8.50	0.0444	0.252	87	15.28	0.0368	0.287	100	24.36	0.0391	0.250									87	-	0.0453	0.262
100	8.37	0.0371	0.275	100	15.26	0.0333	0.299													100	-	0.0463	0.249
Run 21								**Run 18**				**Run 8**				**Run 3**				**Run 29 (mean concentration 80.89g/l)**			
5	8.47	0.0359	0.120					5	23.72	0.0250	0.107	5	33.29	0.0236	0.161	5	38.78	0.0303	0.182	5	-	0.0156	0.074
10	8 44	0.0410	0.219					10	23.52	0.0242	0.191	10	33.95	0.0257	0.200	10	38.08	0.0299	0.229	10	-	0.0245	0.136
15	8.39	0.0403	0.250					15	23.62	0.0341	0.219	15	34.90	0.0369	0.240	15	38.00	0.0318	0.288	15	-	0.0298	0.169
20	8.39	0.0459	0.272					20	23.58	0.0309	0.238	20	34.73	0.0337	0.239	20	38.36	0.0374	0.256	20	-	0.0303	0.230
25	8.48	0.0522	0.264					25	23.47	0.0397	0.232	25	34.39	0.0354	0.255	25	38.61	0.0338	0.318	25	-	0.0325	0.268
30	8.36	0.0552	0.224					37	23.49	0.0418	0.233	37	35.09	0.0367	0.250	50	38.37	0.0404	0.326	30	-	0.0376	0.272
40	8.33	0.0489	0.283					50	23.44	0.0381	0.285	50	33.76	0.0293	0.243	75	38.34	0.0353	0.294	35	-	0.0367	0.258
50	9.05	0.0444	0.257					62	23.43	0.0351	0.226	75	32.79	0.0294	0.247	100	38.38	0.0383	0.257	40	-	0.0425	0.303
62	8.21	0.0477	0.271					75	23.41	0.0398	0.232	100	34.53	0.0348	0.235					45	-	0.0403	0.293
75	8.21	0.0483	0.235					87	23.37	0.0369	0.239									50	-	0.0382	0.289
87	8.20	0.0456	0.254					100	23.39	0.0442	0.232									75	-	0.0462	0.275
100	8.24	0.0407	0.245																	100	-	0.0375	0.236
Run 19								**Run 10**								**Run 6**							
5	20.05	0.0235	0.091					5	27.44	0.0273	0.168					5	38.52	0.0057	0.092				
10	20.85	0.0267	0.194					10	28.85	0.0295	0.105					10	36.18	0.0288	0.192				
15	20.81	0.0270	0.220					15	28.75	0.0291	0.164					15	36.21	0.0311	0.245				
20	20.90	0.0347	0.283					20	28.67	0.0292	0.172					20	36.26	0.0301	0.284				
25	20.45	0.0328	0.260					25	28.50	0.0310	0.249					25	36.37	0.0362	0.287				
30	20.51	0.0354	0.239					37	28.46	0.0303	0.242					37	36.26	0.0469	0.317				
40	20.64	0.0350	0.267					50	28.52	0.0393	0.233					50	36.27	0.0430	0.300				
50	20.57	0.0361	0.289					75	28.52	0.0340	0.252					75	36.23	0.0346	0.330				
62	20.56	0.0390	0.245					100	28.50	0.0427	0.221					100	36.23	0.0430	0.280				
75	20.54	0.0379	0 240																				
87	20.57	0.0399	0.267																				
100	20.48	0.0460	0.246																				

Table 8.2: Near Bed Velocity and Concentration Profiles and Shear Velocity **Section E** (data is arranged in order of increasing nominal mean concentration across the page)

Height (mm)	Conc-entration (g/l)	Shear Velocity (m/s)	Mean Velocity (m/s)	Height (mm)	Conc-entration (g/l)	Shear Velocity (m/s)	Mean Velocity (m/s)	Height (mm)	Conc-entration (g/l)	Shear Velocity (m/s)	Mean Velocity (m/s)	Height (mm)	Conc-entration (g/l)	Shear Velocity (m/s)	Mean Velocity (m/s)	Height (mm)	Conc-entration (g/l)	Shear Velocity (m/s)	Mean Velocity (m/s)	Height (mm)	Conc-entratio (g/l)	Shear Velocity (m/s)	Mean Velocity (m/s)
Run 22				**Run 24**				**Run 14**				**Run 11**				**Run 1**				**Run 27 (mean concentration 80.89g/l)**			
5	8.27	0.0322	0.104	5	15.29	0.0447	0.146	5	23.08	0.0193	0.014	5	29.47	0.0166	0.072	5	42.19	0.0187	0.067	7	-	0.0268	0.040
10	8.25	0.0241	0.107	10	15.13	0.0262	0.125	10	22.84	0.0165	0.087	15	29.16	0.0178	0.091	10	42.24	0.0240	0.089	12	-	0.0343	0.008
15	8.24	0.0238	0.118	15	15.08	0.0220	0.151	15	22.92	0.0150	0.097	20	29.17	0.0200	0.086	15	42.37	0.0207	0.161	15	-	0.0375	0.042
20	8.17	0.0199	0.106	20	14.97	0.0277	0.186	20	22.85	0.0196	0.113	25	29.17	0.0181	0.138	25	42.75	0.0260	0.210	20	-	0.0377	0.078
25	8.21	0.0226	0.129	25	14.99	0.0246	0.203	25	22.79	0.0139	0.084	37	29.12	0.0170	0.147	50	42.30	0.0296	0.277	25	-	0.0355	0.107
30	8.21	0.0212	0.132	30	14.95	0.0300	0.183	37	22.79	0.0205	0.111	50	29.13	0.0212	0.150	100	42.25	0.0253	0.232	30	-	0.0375	0.118
40	8.21	0.0246	0.127	40	14.94	0.0308	0.205	50	22.65	0.0171	0.111	75	29.07	0.0258	0.148					35	-	0.0367	0.118
50	8.21	0.0229	0.144	50	14.92	0.0295	0.202	75	22.73	0.0201	0.163	100	29.07	0.0244	0.143					40	-	0.0355	0.137
62	8.08	0.0239	0.142	62	14.89	0.0295	0.205	100	22.67	0.0186	0.130									50	-	0.0417	0.125
75	8.06	0.0260	0.134	75	14.86	0.0260	0.212													62	-	0.0365	0.142
87	8.06	0.0271	0.150	87	14.84	0.0280	0.203													75	-	0.0397	0.144
100	8.06	0.0232	0.160	100	14.84	0.0264	0.202													87	-	0.0338	0.137
																				100	-	0.0327	0.163
Run 23								**Run 15**				**Run 12**				**Run 4**				**Run 28 (mean concentration 80.89g/l)**			
5	8.10	0.0379	0.132					5	26.29	0.0326	0.017	5	28.16	0.0246	0.014	5	41.09	0.0202	0.032	6	-	0.0205	0.001
10	8.07	0.0225	0.095					10	24.88	0.0446	0.040	10	28.19	0.0172	0.071	10	42.39	0.0221	0.135	10	-	0.0140	0.059
15	8.06	0.0296	0.056					15	24.83	0.0332	0.032	15	29.21	0.0119	0.076	15	42.76	0.0249	0.144	15	-	0.0134	0.088
20	8.05	0.0251	0.101					20	24.68	0.0180	0.098	20	28.23	0.0180	0.107	20	42.60	0.0266	0.150	20	-	0.0153	0.119
25	8.06	0.0230	0.121					25	24.72	0.0193	0.106	25	28.21	0.0149	0.103	25	42.83	0.0307	0.185	25	-	0.0182	0.134
30	8.07	0.0233	0.121					37	24.66	0.0272	0.133	37	28.22	0.0209	0.121	50	42.95	0.0304	0.178	30	-	0.0170	0.107
40	8.04	0.0250	0.139					50	24.60	0.0210	0.127	50	28.19	0.0211	0.107	75	43.04	0.0339	0.193	35	-	0.0269	0.132
50	8.05	0.0309	0.151					62	24.59	0.0223	0.118	75	28.66	0.0265	0.155	100	43.04	0.0256	0.200	40	-	0.0229	0.153
62	8.05	0.0273	0.144					75	24.55	0.0219	0.144	100	28.22	0.0243	0.143					45	-	0.0286	0.144
75	8.04	0.0309	0.157					87	24.52	0.0183	0.114									50	-	0.0202	0.164
87	8.03	0.0260	0.136					100	24.50	0.0195	0.148									75	-	0.0251	0.171
100	8.10	0.0305	0.146																	100	-	0.0212	0.188
								Run 16				**Run 13**				**Run 5**							
								5	25.66	0.0195	0.005	5	31.02	0.0188	0.030	5	38.68	0.0171	0.035				
								10	25.43	0.0167	0.045	10	31.81	0.0173	0.054	10	39.16	0.0188	0.101				
								15	25.38	0.0146	0.085	15	31.47	0.0169	0.072	15	39.31	0.0243	0.140				
								20	25.34	0.0191	0.101	20	31.45	0.0150	0.108	20	39.14	0.0250	0.136				
								25	25.28	0.0154	0.097	25	31.44	0.0201	0.109	25	39.19	0.0244	0.172				
								37	25.30	0.0235	0.110	37	31.41	0.0257	0.113	50	39.25	0.0283	0.203				
								50	25.23	0.0272	0.138	50	31.43	0.0254	0.142	75	40.09	0.0326	0.155				
								62	25.15	0.0195	0.120	75	31.42	0.0246	0.117	100	39.73	0.0283	0.193				
								75	25.37	0.0221	0.140	100	31.36	0.0225	0.141								
								87	25.15	0.0258	0.126												
								100	25.14	0.0283	0.099												

Table 8.3: Velocity and Shear Velocity Profiles Measured in Clear Water

Section B

Bulk Density:	1000g/l			1007g/l			1035g/l		
	Height Above Bed (mm)	Velocity (m/s)	Shear Velocity (m/s)	Height Above Bed (mm)	Velocity (m/s)	Shear Velocity (m/s)	Height Above Bed (mm)	Velocity (m/s)	Shear Velocity (m/s)
	5	0.173	0.0489	5	0.063	0.0357	5	0.101	0.0372
	10	0.206	0.0488	10	0.212	0.0444	10	0.138	0.0277
	15	0.213	0.0436	15	0.273	0.0381	15	0.201	0.0271
	20	0.253	0.0401	20	0.271	0.0286	20	0.225	0.0259
	25	0.266	0.0446	25	0.288	0.0343	25	0.247	0.0282
	30	0.203	0.0584	30	0.185	0.0614	30	0.182	0.0535
	35	0.138	0.0560	35	0.191	0.0644	35	0.173	0.0561
	40	0.189	0.0577	40	0.220	0.0579	40	0.203	0.0560
	50	0.298	0.0388	45	0.274	0.0446	45	0.253	0.0435
	62	0.208	0.0535	50	0.281	0.0418	50	0.270	0.0380
	75	0.245	0.0402	60	0.206	0.0556	60	0.179	0.0539
	87	0.171	0.0610	80	0.213	0.0554	70	0.197	0.0459
	100	0.254	0.0372	100	0.220	0.0425	80	0.252	0.0341
							90	0.258	0.0315
							100	0.236	0.0376

Section E

Bulk Density:	1000g/l			1007g/l			1035g/l		
	Height Above Bed (mm)	Velocity (m/s)	Shear Velocity (m/s)	Height Above Bed (mm)	Velocity (m/s)	Shear Velocity (m/s)	Height Above Bed (mm)	Velocity (m/s)	Shear Velocity (m/s)
	5	-0.010	0.0247	5	0.029	0.0372	5	0.056	0.0388
	10	0.067	0.0339	10	0.114	0.0218	10	0.045	0.0202
	16	0.118	0.0244	15	0.120	0.0266	15	0.148	0.0313
	20	0.137	0.0213	20	0.135	0.0294	20	0.136	0.0184
	25	0.154	0.0211	25	0.159	0.0270	25	0.164	0.0243
	30	0.172	0.0240	30	0.204	0.0240	30	0.156	0.0249
	35	0.155	0.0214	35	0.179	0.0250	35	0.193	0.0224
	40	0.175	0.0245	40	0.181	0.0241	40	0.176	0.0271
	50	0.203	0.0268	45	0.168	0.0264	45	0.172	0.0243
	60	0.144	0.0366	50	0.202	0.0256	50	0.210	0.0258
	70	0.163	0.0277	60	0.177	0.0301	60	0.188	0.0385
	80	0.169	0.0380	70	0.179	0.0273	70	0.191	0.0335
	90	0.169	0.0390	80	0.180	0.0229	80	0.173	0.0300
	100	0.165	0.0360	90	0.174	0.0344	90	0.205	0.0290
				100	0.135	0.0333	100	0.176	0.0339

Table 8.4: Velocity, Concentration and Shear Velocity Mean Values over Height 0-50mm

Section B

Run Number	Mean Velocity (m/s)	Mean Concen-tration (g/l)	Water Density (g/l)	Mean Bulk Density (g/l)	Mean Shear Velocity (m/s)
-	0.203	0.00	1000	1000	0.0466
-	0.212	0.00	1007	1007	0.0430
-	0.186	0.00	1035	1035	0.0375
2	0.247	37.34	1022	1043	0.0375
3	0.272	38.35	1022	1043	0.0332
6	0.248	36.61	1022	1043	0.0330
7	0.239	29.16	1023	1039	0.0345
8	0.221	34.36	1023	1042	0.0310
10	0.194	28.41	1023	1039	0.0295
17	0.219	32.41	1020	1038	0.0320
18	0.210	23.54	1020	1033	0.0336
19	0.223	20.57	1020	1031	0.0304
20	0.190	8.54	1025	1030	0.0434
21	0.228	8.47	1025	1030	0.0440
25	0.274	15.16	1019	1028	0.0338
26	0.178	80.89	1020	1066	0.0347
29	0.215	80.89	1020	1066	0.0309

Section E

Run Number	Mean Velocity (m/s)	Mean Concen-tration (g/l)	Water Density (g/l)	Mean Bulk Density (g/l)	Mean Shear Velocity (m/s)
-	0.125	0.00	1000	1000	0.0236
-	0.139	0.00	1007	1007	0.0254
-	0.135	0.00	1035	1035	0.0245
1	0.183	42.45	1022	1046	0.0239
4	0.146	42.53	1022	1046	0.0262
5	0.144	39.13	1022	1044	0.0229
11	0.113	29.21	1023	1039	0.0173
12	0.088	28.30	1023	1039	0.0177
13	0.092	31.41	1023	1040	0.0200
14	0.088	22.84	1020	1032	0.0168
15	0.086	24.95	1020	1034	0.0256
16	0.086	25.31	1020	1034	0.0190
22	0.116	8.22	1025	1030	0.0227
23	0.112	8.06	1025	1030	0.0254
24	0.170	15.03	1019	1027	0.0281
27	0.084	80.89	1020	1066	0.0332
28	0.101	80.89	1020	1066	0.0186

8.4 Variation of the von Kárman Parameter κ with Mud Concentration

Using the author's results, an attempt was made to assess the findings of Vanoni (1946) and Hino (1963) with regard to the variation of the von Kárman parameter κ with mud concentration. This analysis (ie everything in sections 8.4.1 and 8.4.2 below) was carried out by Dr. K.H.M. Ali, but the results are included here for completeness.

8.4.1 Theoretical Considerations regarding Near Bed Velocity Distributions

Using mixing length concepts (Rouse 1962, Daily and Harleman 1973), it can be seen that the velocity distribution near smooth and rough boundaries is given by:

$$\frac{u - U_{max}}{u^*} = m \log\left(\frac{z}{Z_{max}}\right) + C_1 \qquad (8.3)$$

where U is the maximum velocity at z = Z and m is the slope given by 2.303/κ. The von Kárman parameter κ is about 0.4 for clear water and the constant C_1 is about 5.5. In equation 8.3, u* represents the shear velocity $\sqrt{[u'w']}$ within the logarithmic boundary layer profile. Following von Kárman (see Webber 1971), this may be assumed to be related to the bed shear stress τ_0. Thus:

$$u* = \sqrt{[u'w']} = \sqrt{\frac{\tau_0}{\rho}} \qquad (8.4)$$

This follows from Reynolds stress concepts, as in general shear stress τ is given by:

$$\tau = \rho u'w' \qquad (8.5)$$

Rearranging equation 8.3 gives:

$$\frac{u}{U_{max}} = m_1 \log\left(\frac{z}{Z_{max}}\right) + 1 \qquad (8.6)$$

where m_1 = mu*. Clearly, evaluation of this equation depends upon a knowledge of both u* and the von Kárman parameter κ. However, in a situation in which u* can be determined experimentally, it is possible to use measured velocity data in equation 8.6 to determine a value of κ, provided of course the logarithmic law of the wall applies so that equations 8.3 and 8.6 are valid.

8.4.2 Experimental Determination of κ

The author's velocity profiles were plotted in semi-log format and reasonable straight lines were produced in most cases. The slopes of these lines represent m_1 in equation 8.6. Values of u* were obtained by plotting the measured shear velocity against height for each velocity profile and projecting the resulting line to the z = 0 axis. Figures of m_1 and u* determined in this way were then used to calculate values of κ according to the following formulation:

$$\kappa = = \frac{2.303}{m} = \frac{2.303u*}{m_1} \qquad (8.7)$$

Values of κ determined for this analysis are shown against mean suspended mud concentration in table 8.5, these figures having been averaged over sections B and E. A general trend of a reduction in κ with the increase in mud concentration is shown, qualitatively confirming the findings of Vanoni (1946) and Hino (1963) (Crapper and Ali 1994).

8.5 Variation of Shear Velocity √[u'w'] with Mud Concentration

Figure 8.5 shows the mean turbulent shear velocity over the lower 50mm of flow against the average mud concentration for measuring sections B and E in the Race

Track Flume. Since it is clear that mean velocity exerts considerable influence on the absolute level of turbulence in a flow, the values of mean shear velocity from table 8.4 have been non-dimensionalised by dividing them by the corresponding value of mean velocity, thus giving a clearer picture of the relationship between turbulence and concentration.

Table 8.5: Variation of the von Kárman Parameter with Sediment Concentration

Mean Concentration (kgm^{-3})	κ
0.0	0.47
8.4	0.37
24.0	0.30
29.7	0.32
40.8	0.25
80.9	0.10

There is considerable scatter in the results, and two values in particular seem anomalous. Nevertheless, it is possible to identify a weak trend of reduction of dimensionless shear velocity with increasing mud concentration. The trend line on the graph of figure 8.5 represents the equation:

$$\frac{\sqrt{[q'q']}}{U} = 0.191 - 0.0005C \qquad (8.8)$$

Where U represents the mean longitudinal flow velocity and C is the concentration. This formulation was determined from a least mean squares fit to the experimental

data, excluding the apparently anomalous data point corresponding to $C = 80.89 kgm^{-3}$.

This analysis takes no account of stratification effects, which have been regarded as an important mechanism whereby turbulence in a flow is damped (McDowell and O'Connor 1977). However, it will be noted from examination of the concentration profile information shown in tables 8.1 and 8.2 that no significant stratification in mud concentration was recorded during the experiments, changes in concentration between heights zero and 50mm typically being less than $1 kgm^{-3}$ ($1.78 kgm^{-3}$ bulk density). In many cases also the concentration recorded at height 50mm is greater than that at the flume bed. In view of this evidence, it may be concluded that recorded changes in mean turbulent activity between the runs are connected with the mean concentration of mud suspended during each run, rather than with the concentration gradient.

8.6 Discussion of Results with Regard to Mud Transport Modelling

From the study described in this chapter so far, and subject to the limitations of the investigation as explained in the above sections, the following conclusions may be drawn:

1. Increasing concentrations of suspended mud in the near bed region of the Race Track Flume reduce the efficiency with which momentum is transferred through a flow, resulting in a reduction of the von Kárman parameter κ.

2. The mean turbulent shear velocity in the near bed region of Race Track Flume is weakly damped by increasing concentrations of suspended mud.

These conclusions qualitatively confirm the findings of previous researchers such as Vanoni (1946), Hino (1963) and Roisin (1985). They are only new in so far as such experiments have not previously been conducted in mud suspensions as opposed to

other forms of natural or artificial sediment, and that the ultrasonic Doppler methods has not previously been used to measure turbulent features of a flow in a laboratory situation. It is interesting, however, to discuss the results obtained in order to assess their possible implications for the mathematical modelling of mud transport. Such an assessment is attempted in the following sections.

8.6.1 Equilibrium Concentrations of Mud in Suspension

One of the most intriguing features of cohesive sediment suspensions concerns the capacity of a given flow to sustain a particular concentration of sediment. This problem has been addressed in experiments designed to investigate settling behaviour under conditions of gradually reducing flow speed such as might occur prior to slack water in an estuary. Attention it therefore drawn to two papers concerning such investigations, that of Rouas et al (1994) and Burt and Game (1985). Unfortunately, so far as the author is aware, at the time of writing none of this research has been produced in a widely accessible format, though the former paper is likely to be published soon and the latter can be obtained from the library at Hydraulics Research Wallingford Limited, Wallingford, UK.

What is interesting is that both these sets of authors investigated settling of cohesive sediment in reducing flow speeds, Rouas et al using a large Race Track Flume at Grenoble, France and Burt and Game using the Hydraulics Research Wallingford Limited Carousel Flume. Rouas et al (1994) found that when the mean velocity in the flume was low enough to allow any settling at all, then sediment continued to settle out and no equilibrium concentration lower than the starting concentration was found that could be supported continuously at the flow settings used. This was the case even in experiments lasting up to five days. Burt and Game (1985) conducted a broadly similar experiment in their carousel flume, finding that at motor settings above about 215, the flow in the carousel could support mud suspensions up to at least the highest value tested of 24.28kgm^{-3} with only marginal loss due to settling. At motor settings below about 215, however, all the sediment settled out rapidly,

regardless of the starting concentration. There was thus no difference in the concentration that could be supported in equilibrium by flows corresponding to different motor settings, and no limit within the range tested to the total concentration that could be supported by motor settings above 215.

Results of Burt and Game's (1985) tests are included in figure 8.6. Whilst 215 may be regarded as is the approximate value at which rapid settling occurs for all concentrations in the figure, it will be seen that there is a variation of about 30 or so in the motor settings at which rapid settling actually begins, with the phenomenon starting at slightly higher motor settings for the higher concentrations. It will also be noted that the results of Rouas et al (1994) and Burt and Game concur with observations made during the author's fluid mud experiments in the Race Track Flume, as discussed in section 6.2.1, chapter 6.

Burt and Game (1985) explained their findings as being the result of flocculation effects: they postulated that above the flow energy level corresponding to a motor settling of about 215, there was a maximum floc size small enough to allow all the sediment to remain in suspension, with larger flocs being ripped apart by the shear stresses in the flow. Below 215, however, the energy in the flow was low enough to allow larger flocs to form, resulting in rapid settling.

The present author has no reason to doubt the plausibility of this explanation of the phenomena observed by Burt and Game (1985). However, it is interesting to approach the observed phenomena from the consideration of the possible effects of the damping of turbulent shear velocity by increasing concentrations of mud, as observed in the Race Track Flume, and such a consideration provides an alternative explanation of the observations recorded by Rouas et al, by Burt and Game, and in the Race Track Flume.

8.6.2 Theoretical Considerations with Regard to the Damping of Turbulence

It is now possible to model the interaction between turbulence and suspended mud in some detail, as has been shown by Teisson et al (1992) and Galland et al (1994). However, so far as the author is aware no such study has yet considered unsteady conditions such as occur when there is net settling of sediment to the bed, and to develop a Reynolds stress type numerical model as used by Teisson et al and Galland et al for unsteady conditions was clearly beyond the scope of the current investigation. The following treatment is therefore offered as a preliminary way of attempting to understand the possible impacts of the damping of turbulence on the settling behaviour of mud suspensions.

In an equilibrium situation, the settling under gravity of sediment suspended in a turbulent flow unidirectional in the longitudinal direction is balanced only by turbulent diffusion in the upward direction. The mean downward transport of sediment in terms of mass per unit area is given by:

$$S = \omega C \tag{8.9}$$

where S is the transport rate ($kgm^{-2}s^{-1}$), ω is the settling velocity and C is the mean concentration. The instantaneous upward mass flux due to turbulent diffusion may be evaluated as follows:

$$t = w'c \tag{8.10}$$

where w' is the instantaneous turbulent fluctuation vertical component and c is the instantaneous value of concentration. It may be seen that:

$$c = C + c' \tag{8.11}$$

where c' is the turbulent fluctuation on the mean concentration. Averaging equation 8.10 to obtain the temporal mean upward sediment transport gives:

$$T = [t] = [w'C] + [w']C + [w'c'] \tag{8.12}$$

where T is the mean upward transport ($kgm^{-2}s^{-1}$) and the square brackets, as previously, indicate a temporal mean of the quantity they enclose. By definition, [w'] = 0, so equation 8.12 may be written as:

$$T = [w'c'] \tag{8.13}$$

In equilibrium, therefore, we have:

$$T + S = [w'c'] + \omega C = 0 \tag{8.14}$$

and for non-equilibrium conditions, the net vertical sediment transport per unit area dm/dt is given by equation 8.15:

$$\frac{dm}{dt} = [w'c'] + \omega C \tag{8.15}$$

For clarity and consistency, equations 8.14 and 8.15 use the sign convention of upward is positive, and the settling velocity ω will have a negative sign. This convention is retained throughout the following analysis.

In the current investigation, ω and C have been measured, and it has been shown that the turbulence under consideration is reasonably isotropic, meaning that mean values involving a product of w' can be represented by use of the measured values of shear velocity $\sqrt{[u'w']}$ (or $\sqrt{[q'q']}$). c' could not be resolved in the Race Track Flume experiments, since the FOSLIM probe used to measure concentrations was not capable of high frequency measurements. However, for the purpose of furthering this experimental analysis, it is possible to make the simplifying assumption that

$$T = [w'c'] = \psi u^{+} C \tag{8.16}$$

where ψ is a constant and u^+ is a shorthand notation for $\sqrt{[u'w']}$.

There are three important implications of equation 8.16, none of which have been verified experimentally due to the inability of instrumentation to resolve turbulent

fluctuations in mean concentration. In the first place, equation 8.16 implies that the magnitude of the turbulent fluctuations in concentration is related to the mean value of concentration, an assumption which does not seem unreasonable. The second implication of equation 8.16 is that there is a constant phase relationship between the turbulent fluctuations in vertical velocity and in concentration, so that variations in the mean value [w'c'] between one sampling period and the next are dependent on the magnitudes of w' and c' and not on these two quantities being combined in a different way. This also does not seem unreasonable, since it is apparent that fluctuations in concentration will ultimately be driven by fluctuations in the fluid velocity. The precise nature of the phase relationship is, for the moment, unimportant: provided it remains constant from one sampling period to the next, its detail is taken account of in the selection of a value of ψ.

The final implication of equation 8.16 is that the magnitude of fluctuations in mean concentration is unrelated to the magnitude of concentrations in vertical velocity. This is not so reasonable as the other two points discussed above; indeed it seems quite possible that there would be a relationship between the magnitudes of w' and c', and that the value of u^+ in equation 8.16 should therefore be raised to a power greater than unity to allow for this. However, there would be no way at present of evaluating such a power, so any relationship between the magnitudes of w' and c' must for the moment be assumed to be negligible.

Equation 8.16 gives an expression for the upward flux of sediment that can be related to values measured in the current investigation.

Considering the damping of turbulence by increasing concentrations of mud, it is possible to re-write equation 8.8 in a more general way:

$$u^+ = U(k_\alpha + k_\beta C) \qquad (8.17)$$

where k_α and k_β are constants, k_β having a negative value. Putting equations 8.16 and 8.17 into 8.15 then gives

$$\frac{dm}{dt} = \psi U(k_\alpha + k_\beta C)C + \omega C \qquad (8.18)$$

allowing the net vertical flux of mud dm/dt ($kgm^{-2}s^{-1}$) to be evaluated in terms of the mean flow velocity, the mean concentration and the settling velocity of the mud flocs. The (downward) settling velocity may in turn be derived from the mean concentration by use of equation 6.17, chapter 6 (or 6.17a, chapter 7):

$$\begin{aligned} \omega &= 5.657x10^{-8}C^{1.291} && C \le 4kgm^{-3} \\ \omega &= 2.137x10^{-3} && 4 < C < 15.3kgm^{-3} \\ \omega &= 0.155C^{-0.450} && C \ge 15.3kgm^{-3} \end{aligned} \qquad (6.17)$$

which may be expressed more succinctly as

$$\omega = \omega_1 C^{\omega_2} \qquad (8.19)$$

where ω_1 and ω_2 are functions of concentration C. Equation 8.18 then becomes

$$\frac{dm}{dt} = \psi U(k_\alpha + k_\beta C)C + \omega_1 C^{(\omega_2 + 1)} \qquad (8.20)$$

The value of ψ in equation 8.20 may be evaluated in a conceptual way: assume an equilibrium flow, with zero net vertical sediment movement dm/dt and a mean flow velocity of $0.1ms^{-1}$. This corresponds approximately to the mean velocity at section E of the Race Track Flume with a paddle setting of 3.5 and may therefore be regarded as the lower limit for the maintenance of an equilibrium concentration in that situation. If a concentration of $30kgm^{-3}$ is assumed, equation 6.17 gives an value of $-1.498x10^{-3}ms^{-1}$. k_α and k_β may be assumed to be 0.2 and -0.002 respectively, these values corresponding approximately to a 'best fit' line drawn through the points in the concentration range 5 to $40kgm^{-3}$ on figure 8.5. Equation 8.20 can then be re-arranged to give a ψ value of 0.107. This is a reasonably small value, and corresponds to the expectations outlined above. Similar values of ψ were evaluated for various concentrations of mud within the range 5 to $40kgm^{-3}$, with the remaining values as outlined above, and the results are given in table 8.6. As can be seen from the table, the values of ψ are all fairly close.

8.6.3 Instability in Equation 8.20

Consider the region of flow as indicated in figure 8.7. The two strips of fluid L_u and L_l, of small thickness δz and unit area form part of a water column. The subscripts $_u$ and $_l$ refer to the upper and lower layers. The mean flow velocity in the x-direction is U_e and the uniformly distributed equilibrium concentration is C. If the mean velocity of flow is reduced slightly from U_e to U at time 0, then the flow is no longer able sustain concentration C in equilibrium. Settling therefore takes place, leading to local changes in the sediment concentration.

Table 8.6: Values of ψ in Equation 8.20 for U = 0.1ms^{-1}, k_α = 0.2 and k_β = -0.002

Mean Concentration (kgm^{-3})	Value of ψ
5	0.113
10	0.119
15	0.126
20	0.112
30	0.107
40	0.108

The term concentration has little meaning at point such as P, at height z between the layers L_u and L_l (figure 8.7): concentrations can only be measured or evaluated over a finite volume. The precise values of concentration to be used in evaluating equation 8.20 at a point therefore open to interpretation, and it is possible to make the following simplifying assumptions:

1. The settling term of equation 8.20 evaluated at height z will be principally dependant on the concentration immediately above z, ie in the volume δz corresponding to layer L_u in figure 8.6.

2. The upward flux term of equation 8.20 evaluated at height z will be principally dependant on the concentration immediately below z, ie in the volume δz corresponding to layer L_l in figure 8.6.

At time zero, the flux rate dm/dt evaluates exactly according to equation 8.20, since the concentration in both L_u and L_l is C. The net vertical exchange of mass over the time interval 0 to $0 + \delta t$ is then given by $dm/dt \times \delta t$. The concentration in the upper layer is then reduced, and the concentration in the lower layer increased, according to equation 8.21:

$$C_u = C - \frac{dm}{dt}\delta t$$
$$C_l = C + \frac{dm}{dt}\delta t \qquad (8.21)$$

where C_u and C_l are the concentrations in layers L_u and L_l at time δt. At time δt, then the flux rate dm/dt is given by:

$$\frac{dm}{dt} = \psi U(k_\alpha + k_\beta C_l)C_l + \omega_1 C_u^{(\omega_2 + 1)} \qquad (8.22)$$

Which is different from the dm/dt at time zero given by equation 8.20.

It will be seen that, under appropriate circumstances, dm/dt at time δt may be very much larger than dm/dt at time 0, and repeated application of the procedure may result in a positive feedback loop causing very rapid settling of all the sediment from layer L_u to L_l. This hypothesis cannot, however, be verified analytically due to the innate non-linearity of the procedures involved.

8.6.4 Numerical Model Incorporating Equation 8.20

In order to test the procedure outlined in the previous section in a more realistic manner, a simple FORTRAN program was written to model the behaviour of sediment in a water column according to equation 8.20 in a one-dimensional vertical context. A flow chart for the program is shown in figure 8.8 and a listing of the code is included in appendix 4.

This model was applied for a range of starting concentrations using a total water column height of 50mm, this being the depth over which the damping of turbulence in the Race Track Flume was studied. A vertical space step of 5mm and a timestep of 0.01 seconds were used, and a constant value of ψ of 0.114 was assumed. The effects of reducing the mean velocity were monitored, and these are discussed in the following section.

8.6.5 Results of Numerical Model and Discussion

Reduction of the mean velocity in the model from a value which supported an evenly mixed mud suspension in equilibrium to a value just below this resulted in an initial slow settling behaviour followed ultimately by a rapid final settling phase. Results for a situation in which the mean velocity was reduced from an equilibrium supporting value of $0.1ms^{-1}$ to $0.09ms^{-1}$ are included in figure 8.9. The profiles shown are the initial one, indicating an evenly mixed suspension of $30kgm^{-3}$, and those for times 100 minutes, just before the rapid settling phase, and 110 minutes, just after it. Figure 8.10 shows the calculated values of u^+ corresponding to the concentration profiles in figure 8.9. It can be seen that at time 100 minutes, just before the rapid settling phase, the turbulence in the lower part of the flow has been substantially reduced from the starting value, due to the local increase in concentration. After the rapid settling, when there is very little mud in suspension, shear velocity is increased from the initial value, though this does not result in a re-suspension of sediment due to the influence of the very dense concentrations at the base of the water column.

Table 8.7: Results of Numerical Simulation of Effects of Damping of Turbulence

Concentration

Mean Velocity (m/s):	0.09	0.09	0.09	0.085	0.085	0.085	0.085	0.085	0.085	No Damping 0.085	No Damping 0.085	No Damping 0.045	No Damping 0.045
Time (mins):	0	100	110	0	1	1.5	2	240	300	60	300	60	300
Height Above Bed (mm)													
2.5	30.00	55.76	291.23	30.00	56.99	127.35	207.10	297.94	297.94	36.98	36.98	112.83	112.83
7.5	30.00	37.44	0.67	30.00	37.49	9.21	4.65	0.00	0.00	36.80	36.80	88.01	88.01
12.5	30.00	34.07	0.90	30.00	34.16	17.64	8.50	0.01	0.00	36.48	36.48	56.02	56.02
17.5	30.00	31.57	1.05	30.00	31.72	23.97	11.21	0.01	0.00	35.91	35.91	24.64	24.64
22.5	30.00	29.40	1.17	30.00	29.64	26.01	12.68	0.01	0.01	34.89	34.89	8.30	8.30
27.5	30.00	27.34	1.26	30.00	27.58	25.11	13.05	0.01	0.01	33.12	33.12	3.18	3.18
32.5	30.00	25.25	1.32	30.00	25.31	22.83	12.56	0.02	0.01	30.12	30.12	2.09	2.09
37.5	30.00	22.99	1.37	30.00	22.63	19.72	11.49	0.02	0.01	25.34	25.34	1.74	1.74
42.5	30.00	20.47	1.40	30.00	19.48	15.86	10.12	0.02	0.01	18.51	18.51	1.61	1.61
47.5	30.00	17.58	1.42	30.00	15.00	12.29	8.64	0.02	0.01	11.78	11.78	1.55	1.55

Shear Velocity

Mean Velocity (m/s):	0.09	0.09	0.09	0.085	0.085	0.085	0.085	0.085	0.085	No Damping 0.085	No Damping 0.085	No Damping 0.045	No Damping 0.045
Time (mins):	0	100	110	0	1	1.5	2	240	300	60	300	60	300
Height Above Bed (mm)													
2.5	0.0126	0.0080	0.0000	0.0119	0.0073	0.0000	0.0000	0.0000	0.0000	0.0119	0.0119	0.0063	0.0063
7.5	0.0126	0.0113	0.0179	0.0119	0.0106	0.0154	0.0162	0.0170	0.0170	0.0119	0.0119	0.0063	0.0063
12.5	0.0126	0.0119	0.0178	0.0119	0.0112	0.0140	0.0156	0.0170	0.0170	0.0119	0.0119	0.0063	0.0063
17.5	0.0126	0.0123	0.0178	0.0119	0.0116	0.0129	0.0151	0.0170	0.0170	0.0119	0.0119	0.0063	0.0063
22.5	0.0126	0.0127	0.0178	0.0119	0.0120	0.0126	0.0148	0.0170	0.0170	0.0119	0.0119	0.0063	0.0063
27.5	0.0126	0.0131	0.0178	0.0119	0.0123	0.0127	0.0148	0.0170	0.0170	0.0119	0.0119	0.0063	0.0063
32.5	0.0126	0.0135	0.0178	0.0119	0.0127	0.0131	0.0149	0.0170	0.0170	0.0119	0.0119	0.0063	0.0063
37.5	0.0126	0.0139	0.0178	0.0119	0.0132	0.0136	0.0150	0.0170	0.0170	0.0119	0.0119	0.0063	0.0063
42.5	0.0126	0.0143	0.0177	0.0119	0.0137	0.0143	0.0153	0.0170	0.0170	0.0119	0.0119	0.0063	0.0063
47.5	0.0126	0.0148	0.0177	0.0119	0.0144	0.0149	0.0155	0.0170	0.0170	0.0119	0.0119	0.0063	0.0063

For an initial concentration of 30kgm^{-3}, reduction of the velocity below 0.09ms^{-1} resulted in immediate rapid settling of most of the suspended sediment due to reductions in the value of u^+ (figures 8.11 and 8.12). This was followed by a steady decrease in the remaining suspended mud even which continued at long simulation times. The modelling of low concentrations after the early, rapid settling does not seem particularly realistic, as concentrations high in the flow are shown to be greater than those just above the bed. However, the continued settling of low concentrations, even at long times, is clear.

The first set of concentration profiles on figure 8.13 shows the results of a control run in which k_β was set to zero and k_α adjusted to give an initial value of u^+ equivalent to that in the U = 0.085ms^{-1} run shown in figures 8.11 and 8.12. The effects of the damping of turbulence by increasing concentrations of mud were thus removed. The run shows some early settling followed by a new equilibrium at a lower suspended sediment concentration, with the data points corresponding to times 60 minutes and 300 minutes coinciding exactly. Clearly, values of u^+ remained constant throughout this run.

The rapid settling of figure 8.11 is not reproduced without the inclusion of turbulence damping effects, even when the mean velocity is reduced as low as 0.045ms^{-1}, as shown by the second set of concentration profiles on figure 8.13. Again, the data points corresponding to times 60 minutes and 300 minutes coincide exactly.

Results of the runs as shown in figures 8.9 to 8.13 are shown in tabular form in table 8.7.

Model runs were carried out for various initial average mud concentrations in order to see whether there was a velocity below which all the mud settled out rapidly due to the damping of u^+. Results of these runs are shown in table 8.8, where the mean velocities are also compared with equivalent Hydraulics Research Wallingford Limited carousel motor settings derived from data presented in Burt and Game (1985). The total range of carousel motor settings covered of 42 approximates

to the narrow range of the settings at which rapid settling first appears on figure 8.6, though clearly the absolute values of motor setting are different from the 215 quoted by Burt and Game (1985) as being the approximate value at which the phenomenon occurs.

Table 8.8: Velocities at Which Rapid Settling Occurs for Various Concentrations

Initial Average Concentration (kgm^{-3})	Highest velocity at which rapid settling occurs (ms^{-1})	HRL Carousel Motor Setting to give corresponding mean velocity
30	0.085	117
20	0.080	110
15	0.075	103
10	0.060	82
5	0.055	75

It is, of course, a natural consequence of the damping of turbulence as modelled by the author that when the concentration becomes high enough, for example close to the bed after rapid settling has taken place, the flow is unable to support turbulence at all and therefore becomes laminar. This may explain the fact that fluid mud flow observed near the bed of the Race Track Flume (see section 6.2.4, chapter 6) and by Ali and Georgiadis (1991) was entirely laminar in nature.

Clearly the analysis and the numerical modelling described in the preceding sections is far from rigorous. The model has not been quantitavely tested against experimental data; the equations used are based on a number of simplifying assumptions the

validity of which have not been tested experimentally, and the performance of the model in representing realistic behaviour of low concentrations of sediment is not good. Nevertheless, the model does give an indication that the observed phenomenon of rapid settling and the lack of equilibrium concentration conditions might in fact be the result of a positive feedback effect caused by the damping of turbulence by increasing concentrations of mud.

It will be interesting to pursue this line of research, and in particular, to develop a more rigorous model such as that of Galland et al (1994) to cope with the unsteady conditions of rapid settling and then apply this to experimental data. It is important, however, to consider the original explanation of Burt and Game (1985) regarding flocculation effects. The formation and destruction of mud flocs is closely related to fluid turbulence, and there have already been attempts to model the flocculation process itself (Krishnappan 1990), and it would be appropriate at this stage to attempt to combine such models with the detailed representation of mud/turbulence interaction.

8.7 Conclusions

The main conclusions arising from the studies described in this chapter may be summarised as follows:

1. A proper understanding of the coupling between hydrodynamic and sediment behaviour is likely to be important in future modelling of cohesive sediment transport.

2. Fluid turbulence in the Race Track Flume is reasonably isotropic, and it may therefore be assumed that an evaluation of any single root mean squared turbulent fluctuation will provide a guide to the overall pattern of turbulence in the flume.

3. It is possible to measure useful data on turbulent fluctuations using the Toshiba SDL-01A ultrasonic pulsed-Doppler instrument, though it is necessary to average a large number of samples before an approximation to a root mean squared turbulent fluctuation can be assumed.

4. The conclusions of Vanoni (1946) and Hino (1963) with regard to the reduction of the von Kárman parameter κ with increasing sediment concentrations were found to be true for mud suspensions in the Race Track Flume.

5. The root mean squared turbulent fluctuations in the Race Track Flume decrease gradually in magnitude with increasing concentration of suspended mud, indicating that fluid turbulence in the flume is weakly damped by increasing mud concentration.

6. Experiments carried out by Burt and Game (1985), by Rouas et al (1994) and by the author in the Race Track Flume all indicate that when the mean flow velocity is reduced sufficiently to allow settling to begin, there is no equilibrium concentration which can be supported by the reduced velocity and all the mud eventually settles to the bed.

7. A numerical treatment based on a number of simplifying assumptions indicates that a positive feedback situation can arise due to successive settling and damping of the turbulent mechanisms by which sediment is suspended in the flow. This can lead to rapid settling and the lack of subsequent equilibrium conditions as observed by Burt and Game (1985), by Rouas et al (1994) and by the author in the Race Track Flume.

8. For the specific conditions tested, the author's simple numerical model predicts that rapid settling for concentrations in the range 5 to 30kgm^{-3} occurs over the mean velocity range 0.055 to 0.085ms^{-1}. This corresponds closely to the range of motor settings over which rapid settling was seen to begin for

various mud concentrations in the Hydraulics Research Wallingford Limited Carousel Flume (Burt and Game 1985).

9. A natural consequence of the feedback system discussed in point 7 above is that fluid with very high concentrations of mud such as occurs at a channel bed after rapid settling has taken place is unable to sustain turbulence at all and becomes laminar. This may explain the fact that fluid mud observed close to the bed in the Race Track Flume and by Ali and Georgiadis (1991) was entirely laminar in nature.

10. Further, more detailed research is needed to study the interaction of mud suspensions and fluid turbulence in unsteady conditions. Such research should also, if possible, take account of the relationship between fluid turbulence and the mud flocculation process.

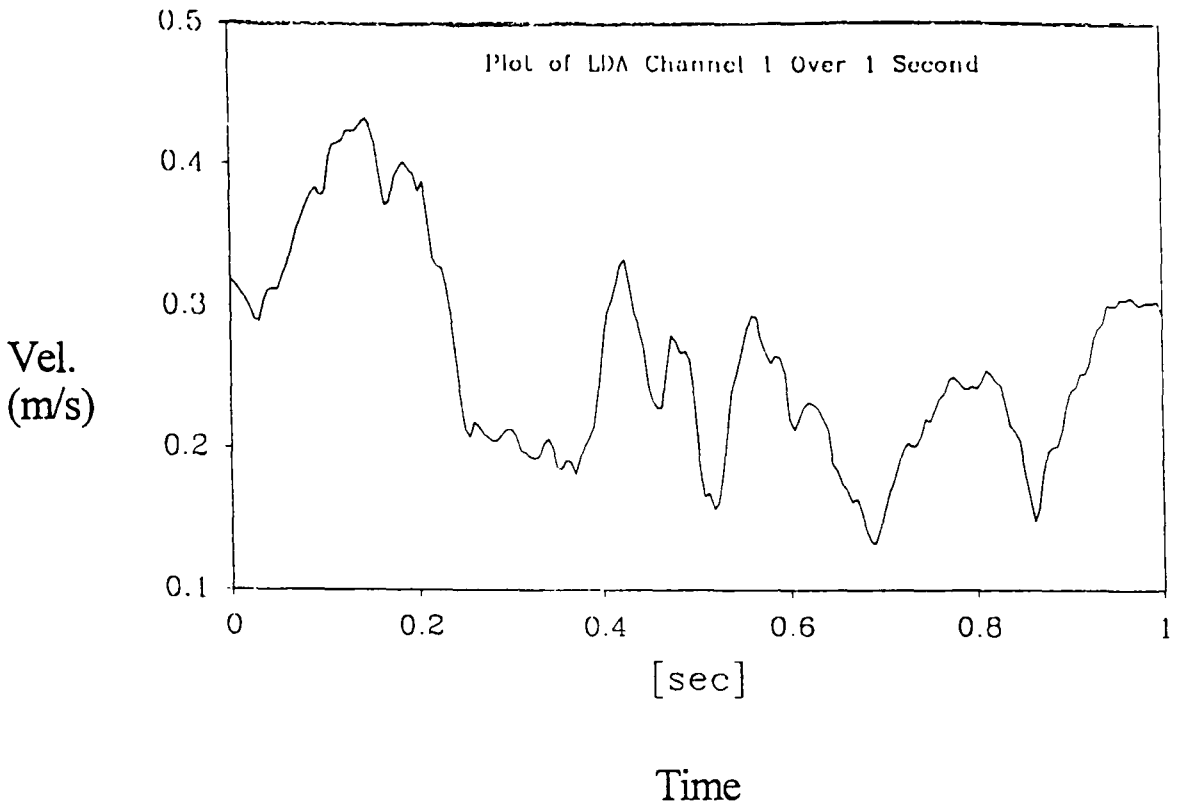

Figure 8.1: Plot of Velocity Readings from Laser-Doppler Anemometer over a 1 Second Period

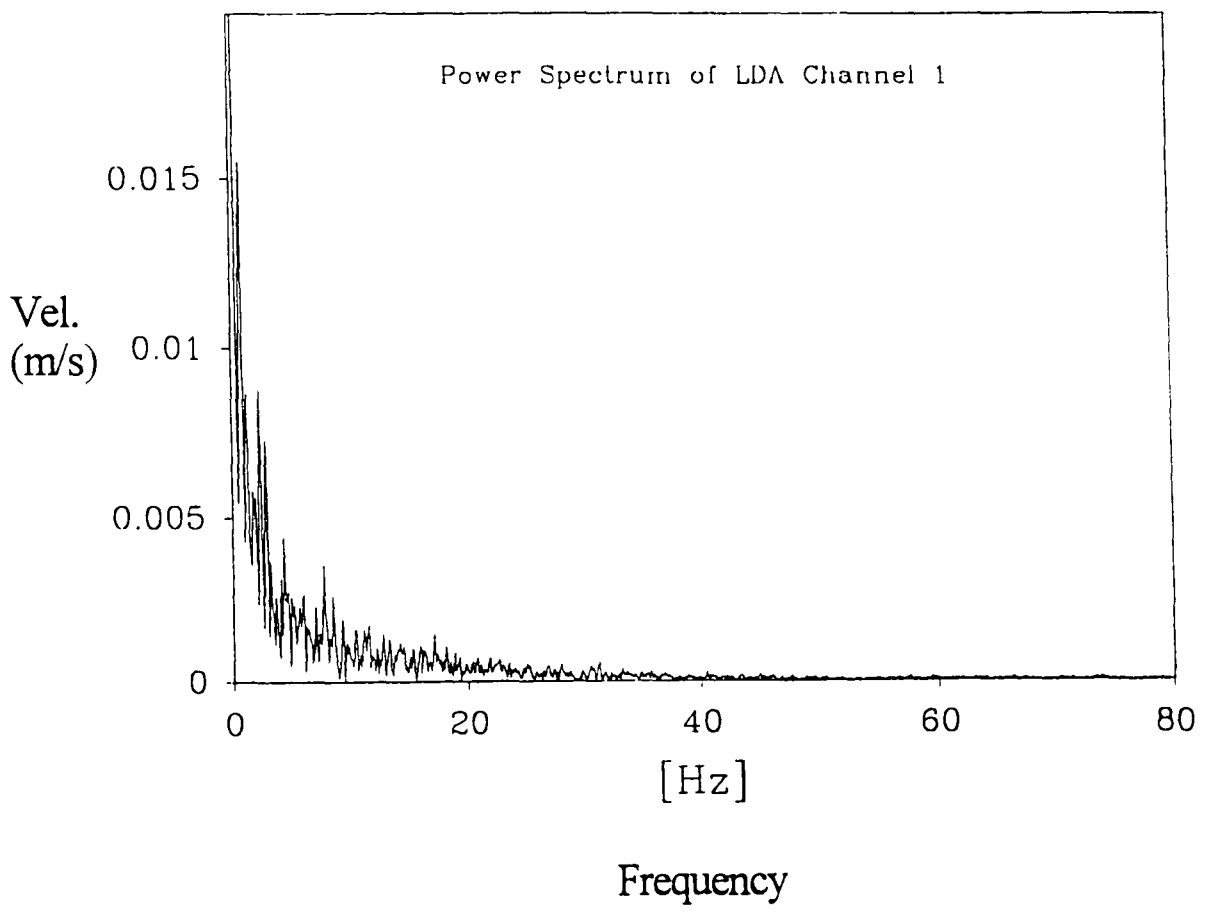

Figure 8.2: Plot of Power Spectrum of Velocity Signal from Laser-Doppler Anemometer

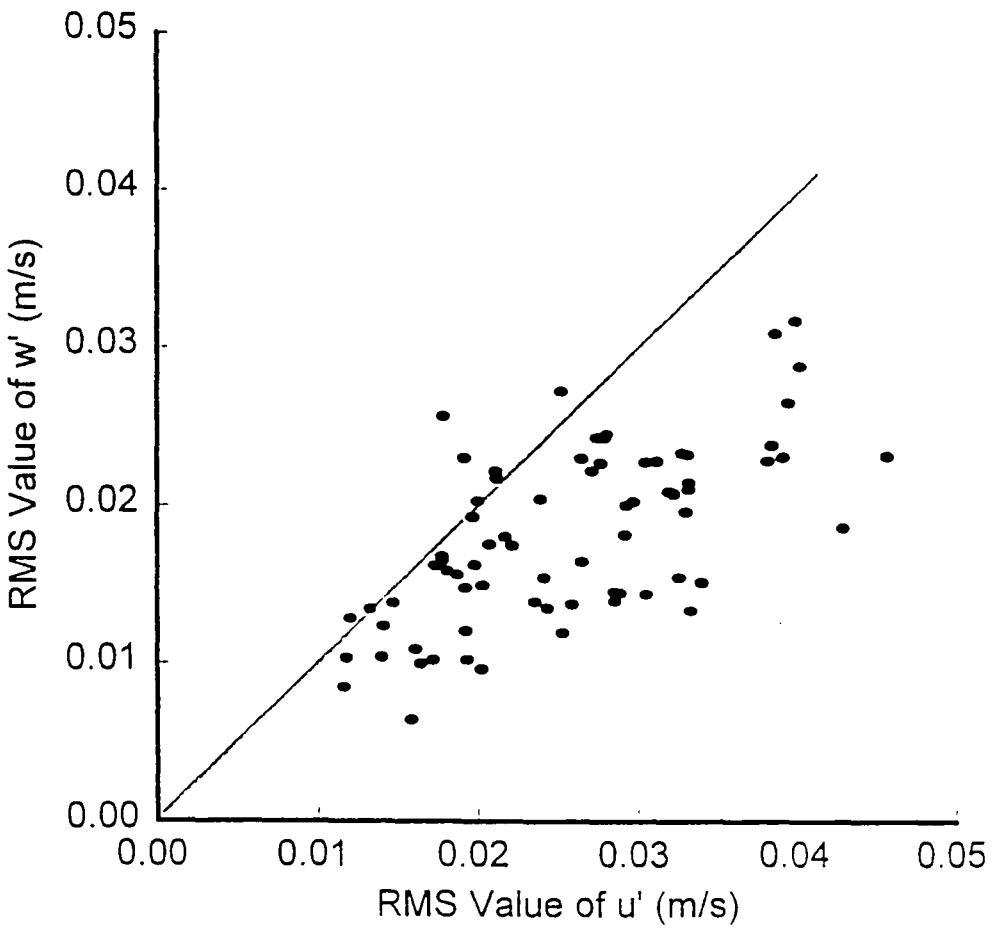

Figure 8.3: Plot of Turbulent Velocity Fluctuations in x and z Directions obtained using LDA in Clear Water

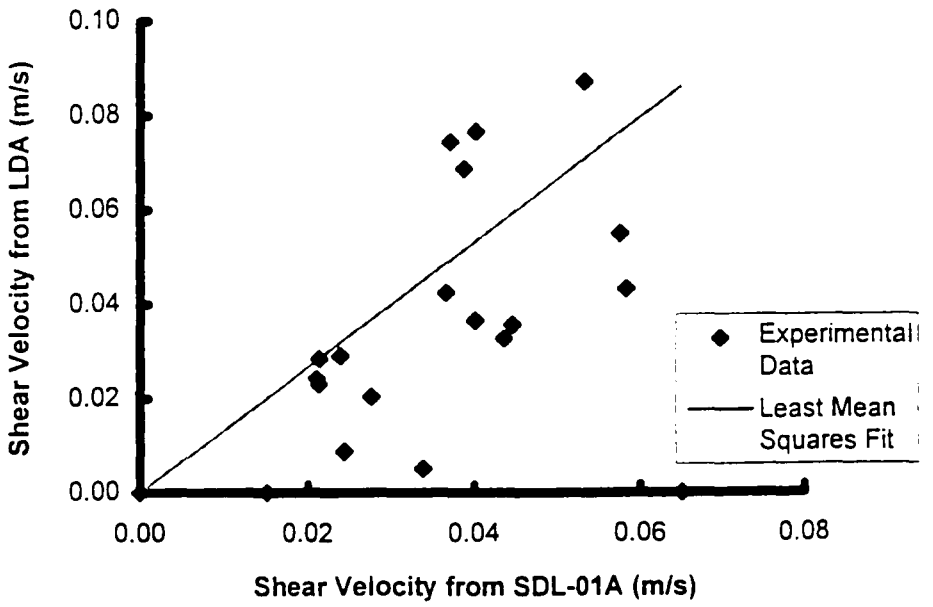

Figure 8.4: Plot of Turbulent Shear Velocity obtained from LDA against that given by SDL-01A Ultrasonic Pulsed-Doppler Unit

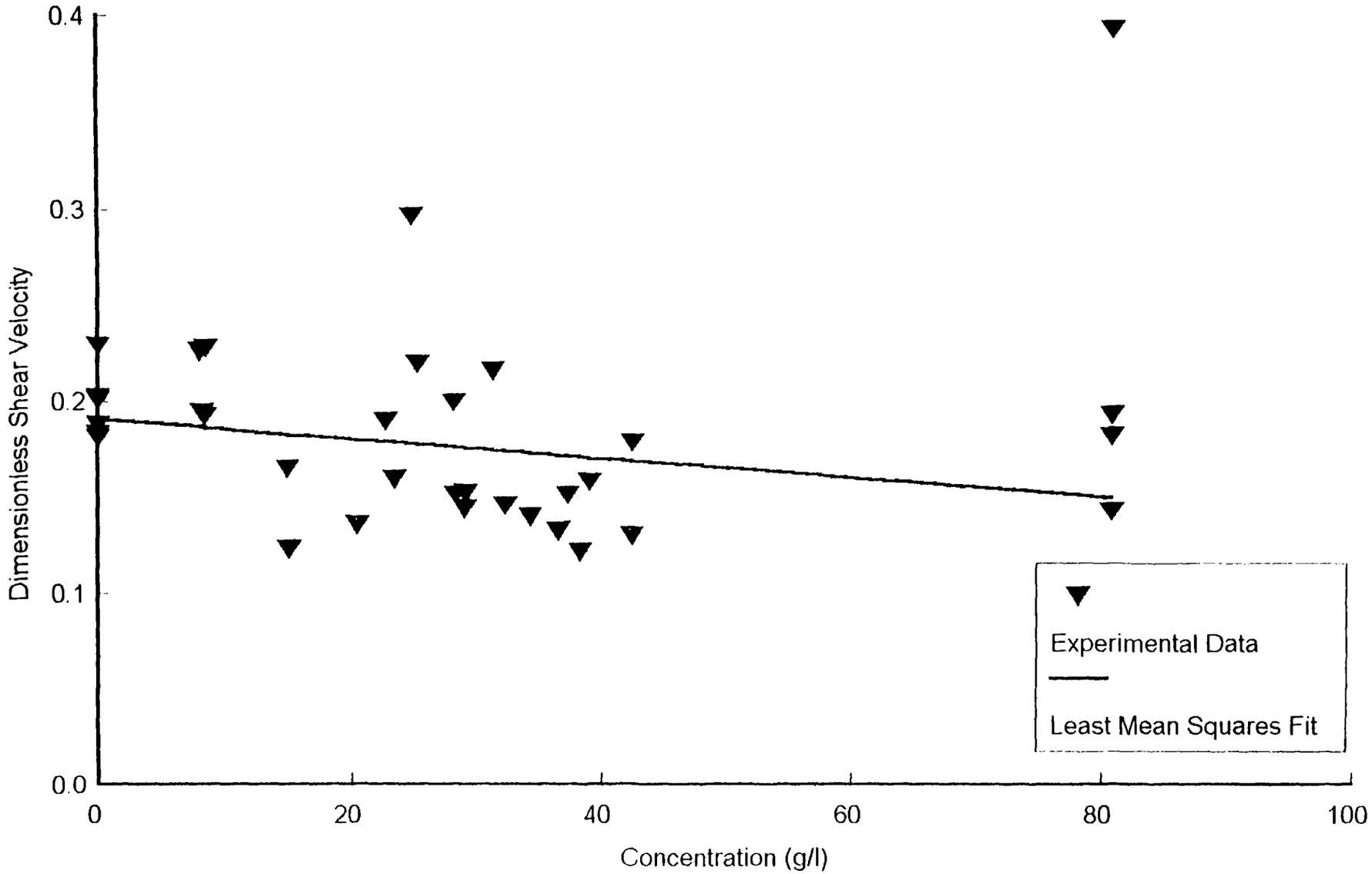

Figure 8.5: Graph of Dimensionless Shear Velocity against Mud Concentration

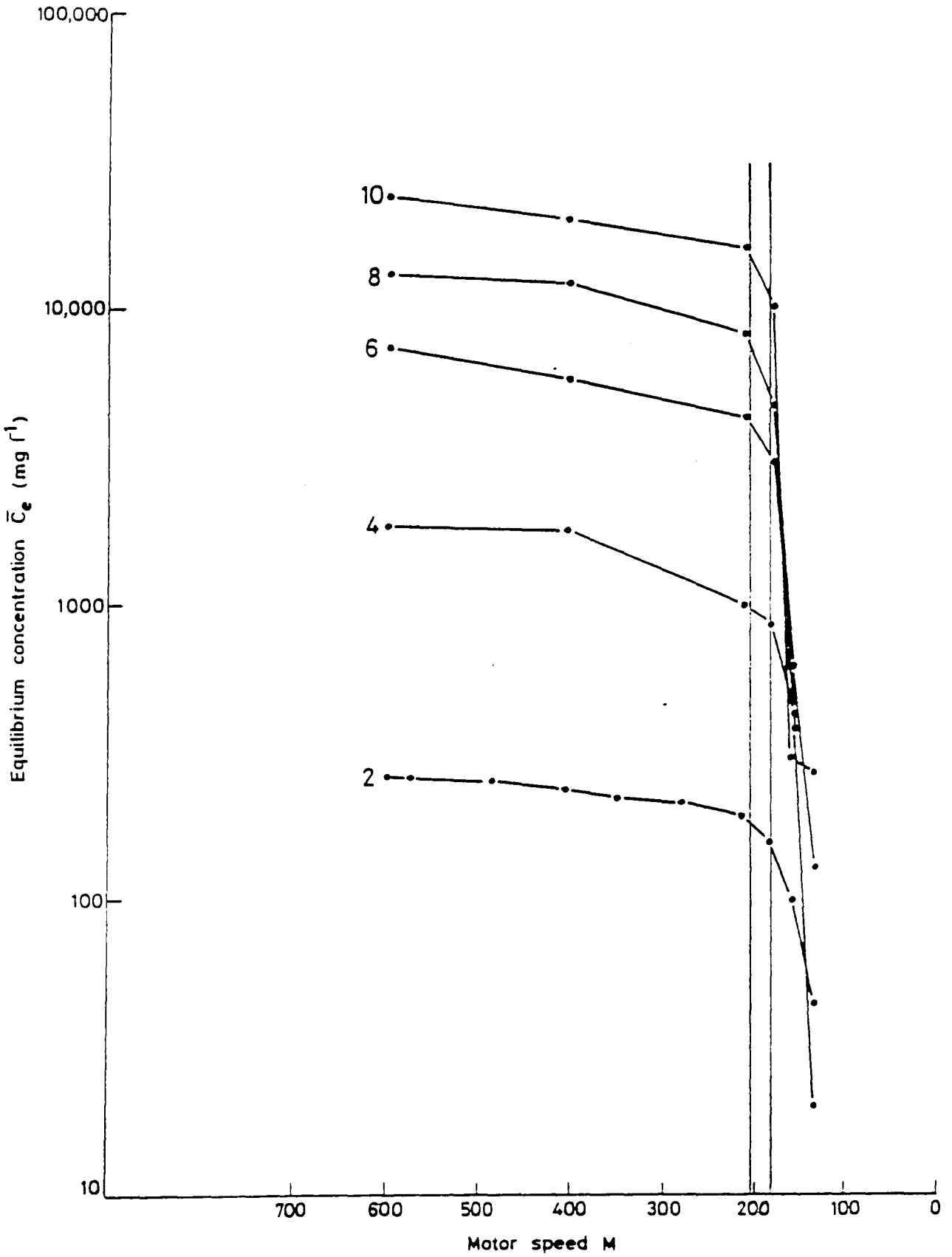

Figure 8.6: Data from Burt and Game (1985) showing Equlibrium Concentrations of Suspended Mud against Carousel Motor Speed

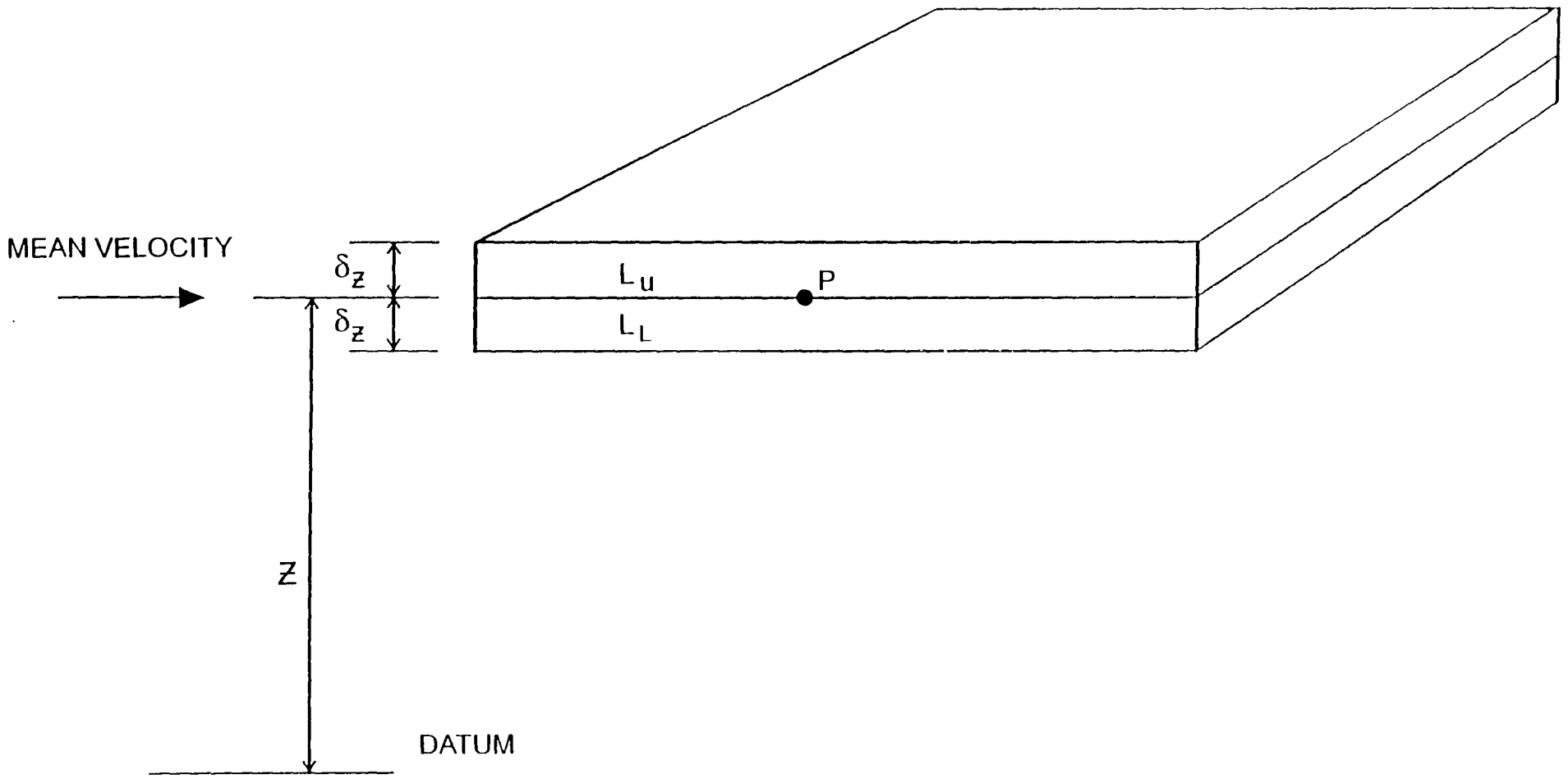

Figure 8.7: Layers of Fluid used in Consideration of Instability in Equation 8.20

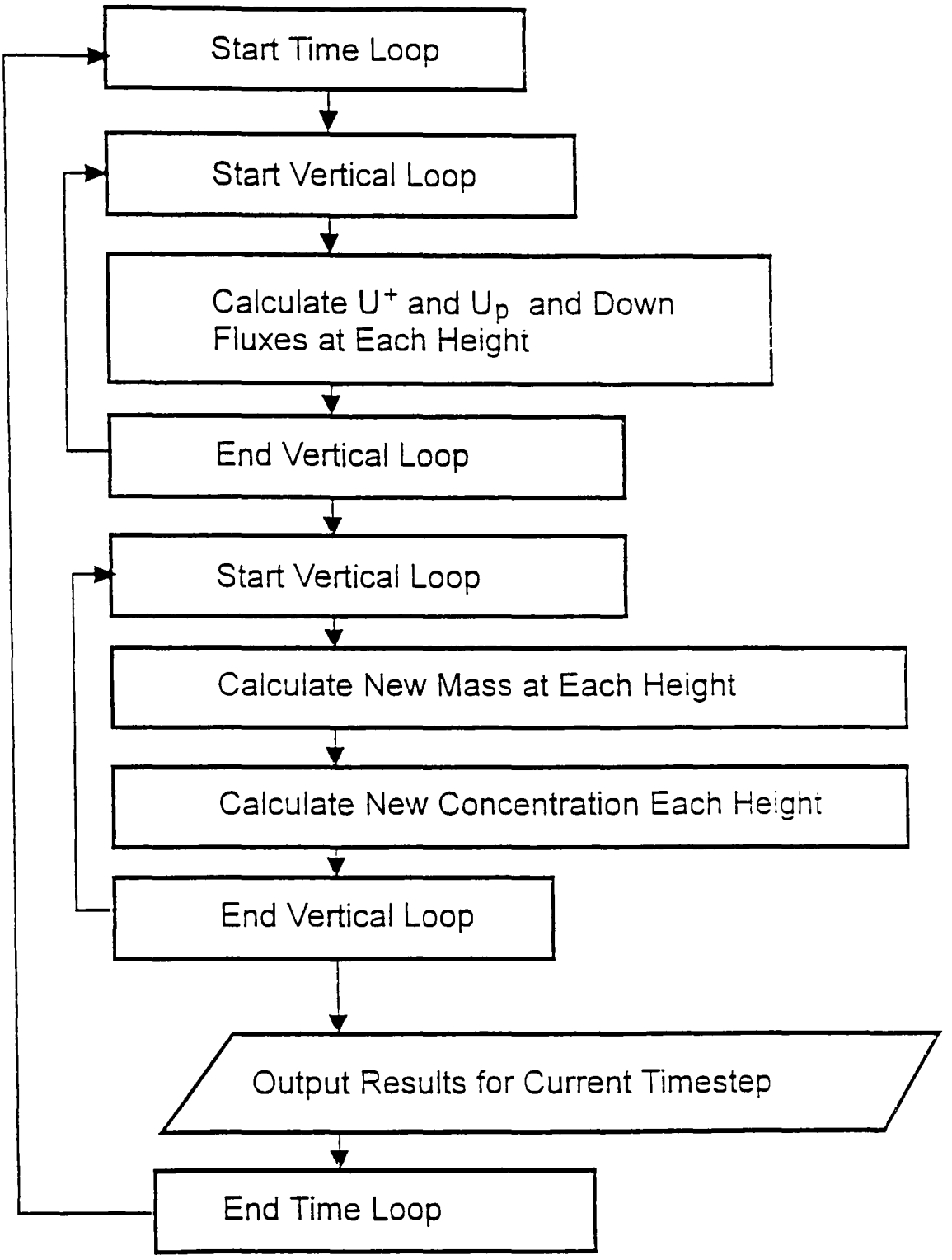

Figure 8.8: Simplified Flow Chart of Model used to Determine Effects of Damping of Turbulence

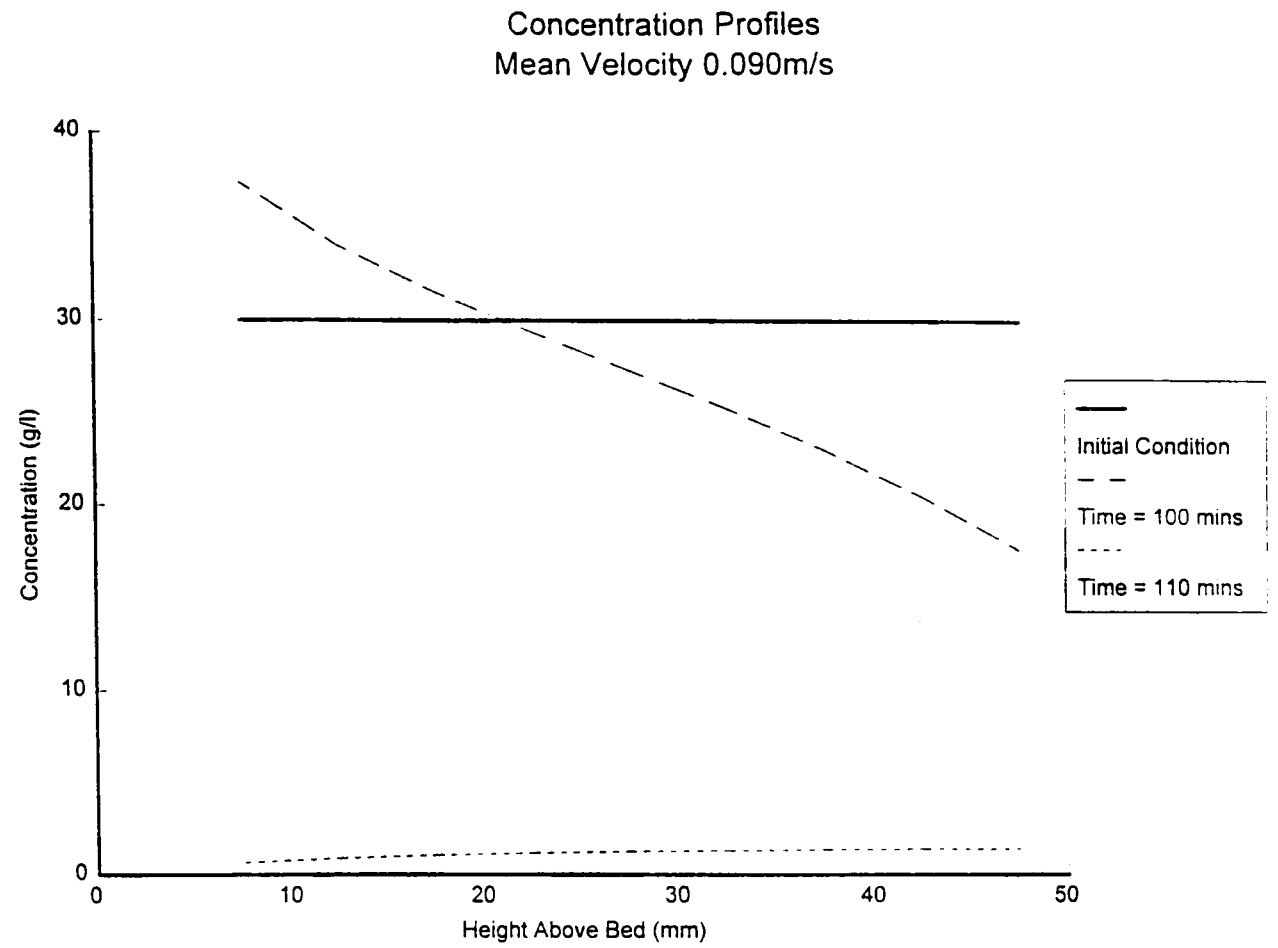

Figure 8.9: Results of Numerical Model of Turbulence Damping

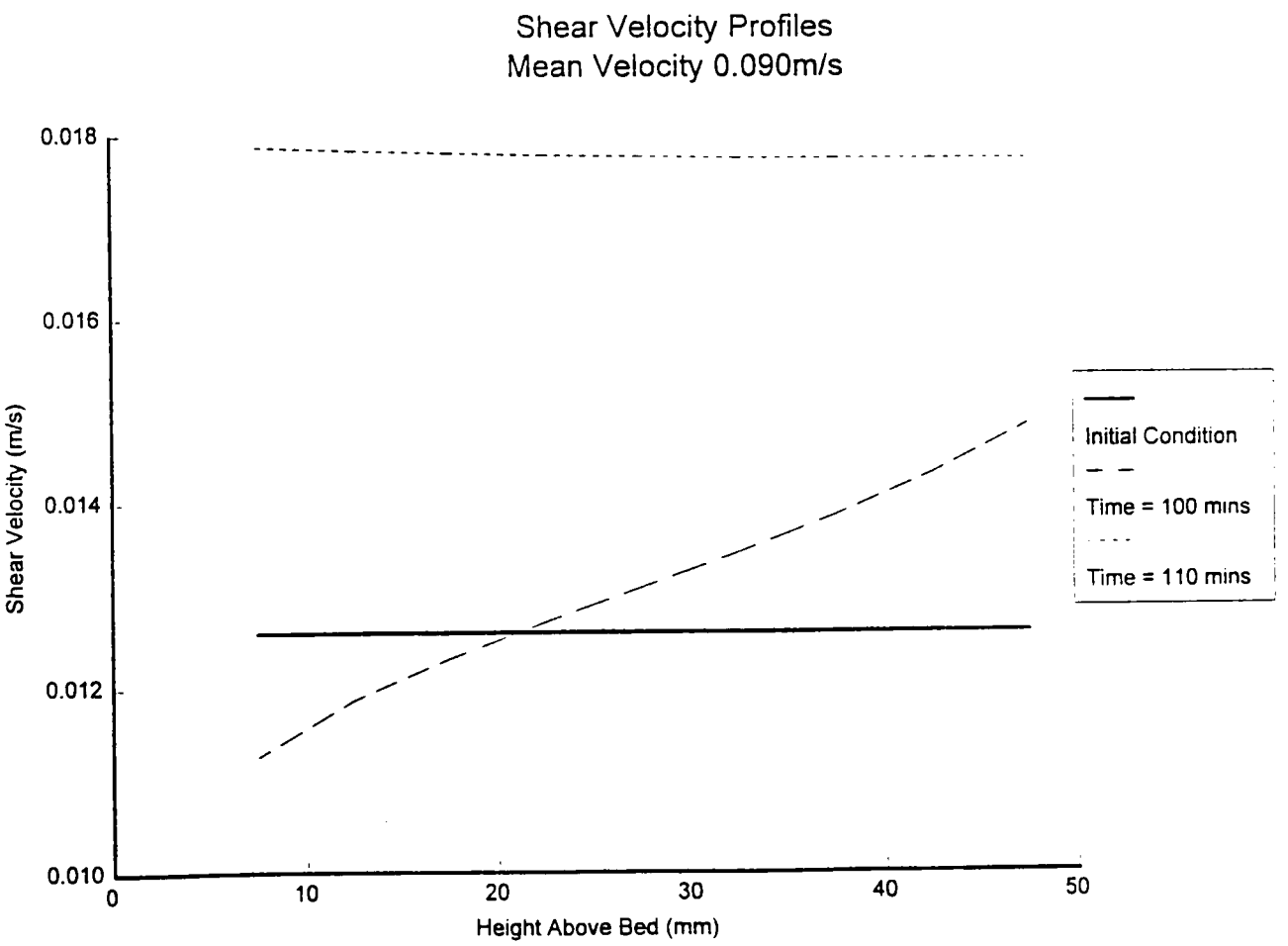

Figure 8.10: Results of Numerical Model of Turbulence Damping

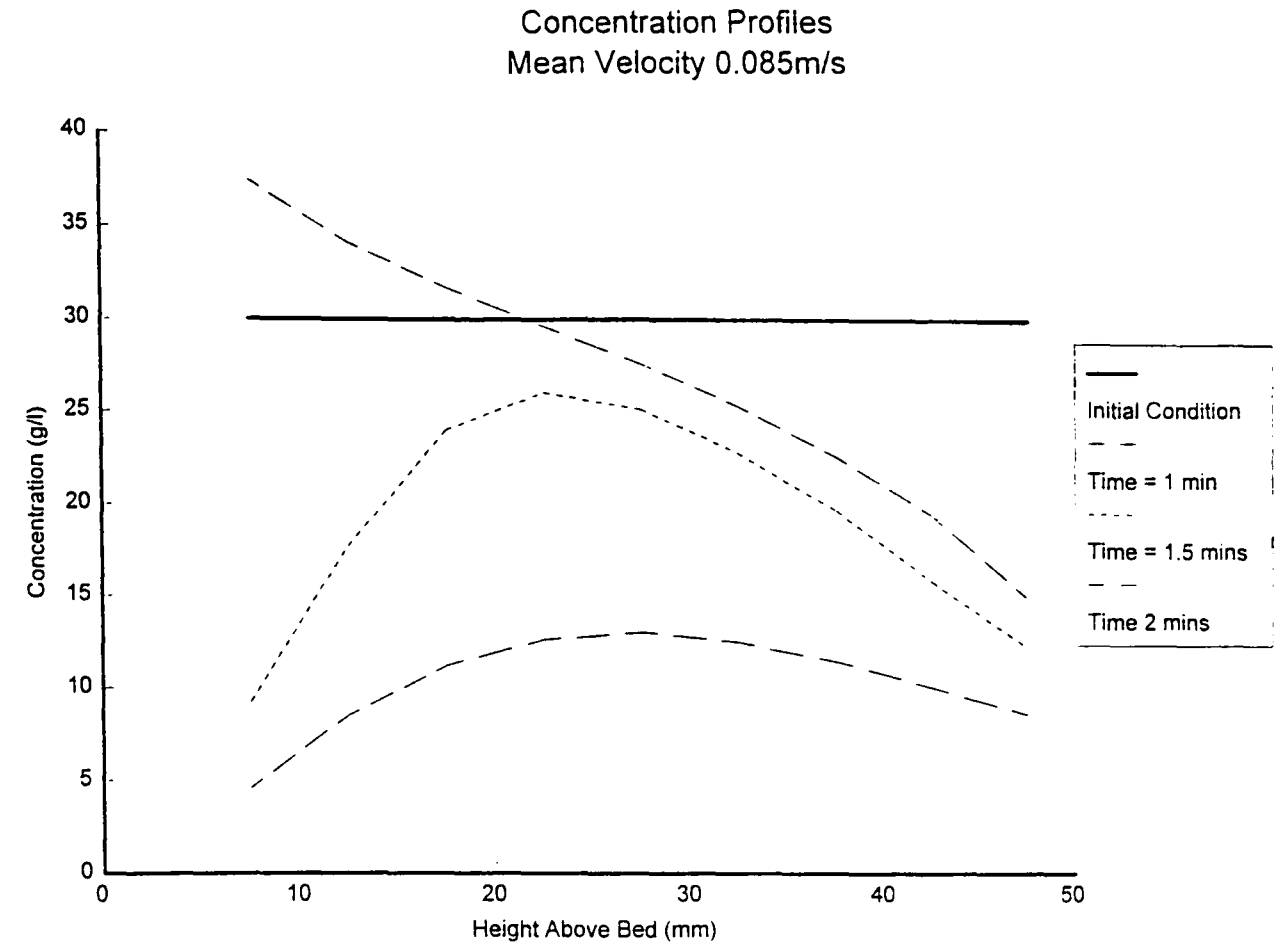

Figure 8.11: Results of Numerical Model of Turbulence Damping

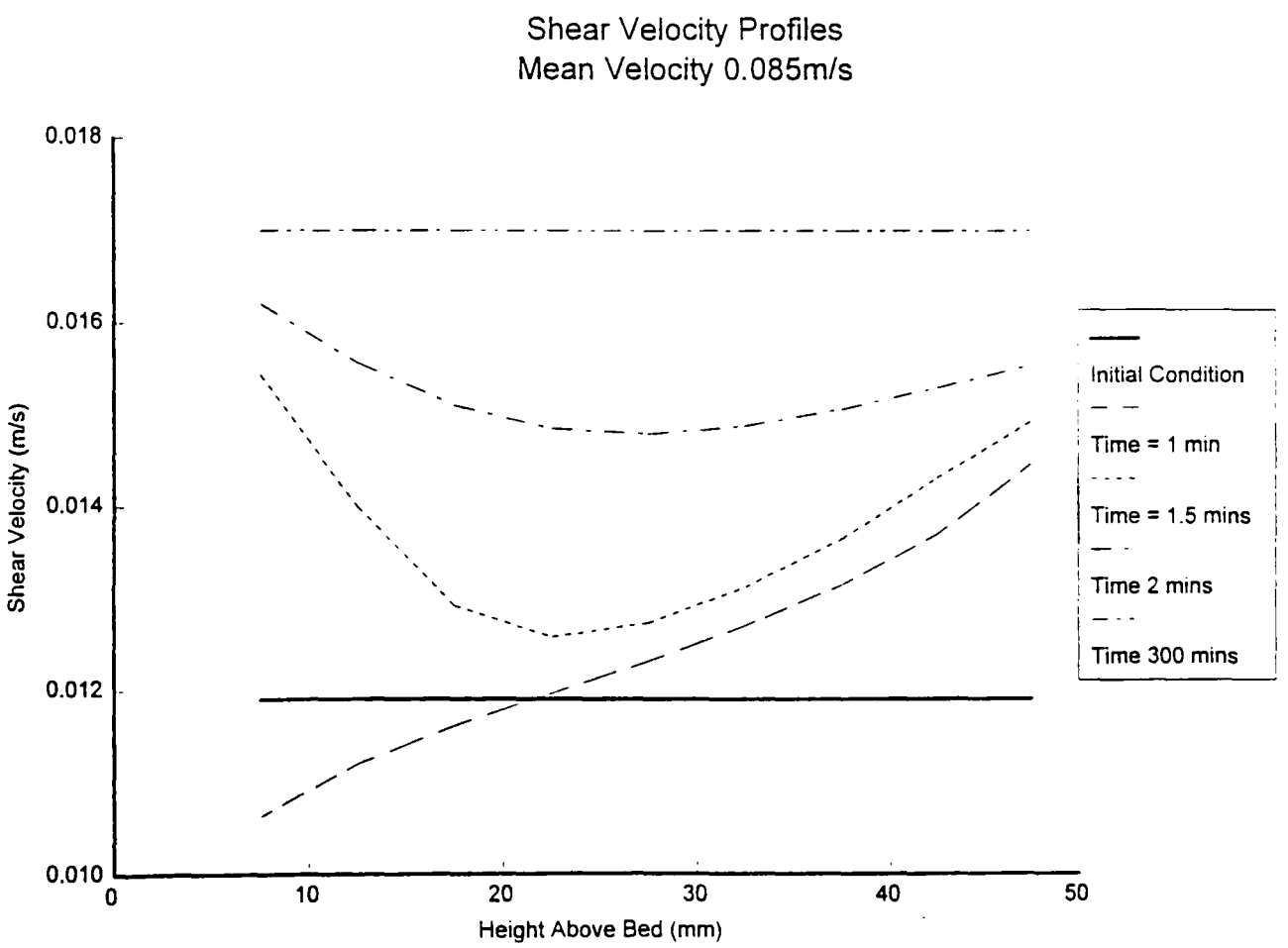

Figure 8.12: Results of Numerical Model of Turbulence Damping

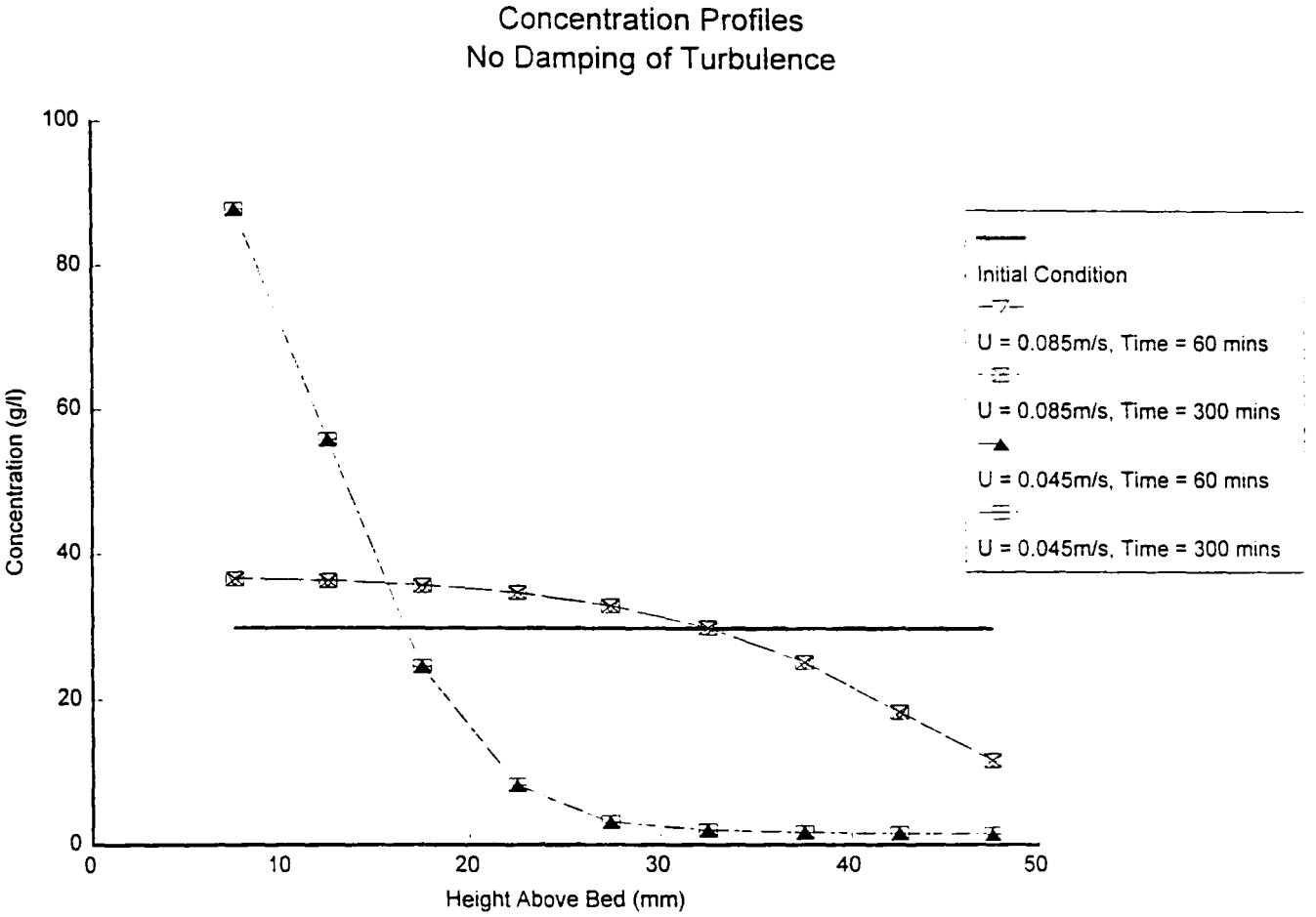

Figure 8.13: Results of Numerical Model with noDamping of Turbulence

Chapter 9: Conclusions

9.1 Introductory Remarks

The purpose of this chapter is to draw together the main conclusions of the work described in previous chapters, and to present them in the form of a *thesis* or line of argument arising from consideration of the study as a whole. Implicit in this, of course, are recommendations for further work in the field of fluid mud modelling and the study of cohesive sediments in general.

9.2 Summary Conclusions

As will be seen from consideration of the closing sections of chapters 3 to 8 above, there are many individual conclusions which may be drawn from the work described in this thesis. Some of these are new, others are merely confirmations of the work of previous researchers. The main new points arising from the author's studies may be summarised as follows:

1. The Liverpool Race Track Recirculating Flume is an extremely useful and versatile environment for the laboratory study of cohesive sediment phenomena. Its design ensures that secondary flows due to the channel curvature inherent in a recirculating flume are insignificant in its working section. This means that bed shear stresses can be determined from measurements of longitudinal flow velocity only. Further, the Race Track Flume's ability to be tilted to provide a sloping bed means that it is suitable for fluid mud experiments involving the study of the motion of dense suspensions down submarine slopes. These factors give the Race Track Flume a distinct advantage over annular, carousel-type recirculating flumes.

The Race Track Flume's principal disadvantage is the lateral variation in longitudinal flow velocities in the working section resulting from the channel curvature. However, this disadvantage is shared by all other recirculating flumes of the carousel variety. The Race Track Flume's other disadvantage, the lack of exact repeatability of experimental conditions within it, could easily be remedied by provision of an improved motor drive and paddle mechanism to control the flow in the channel.

2 A number of important factors regarding the formation and movement of fluid mud due to settling from suspension have been identified during the course of the studies described in this thesis. In particular, use of a Couette flow analogy has provided a simple means of determining friction factors, Reynolds numbers and viscosity values for a moving layer of fluid mud. Such an analogy also enables the prediction of reasonably realistic velocity profiles across a fluid mud layer. Also, vertical exchange of mass between suspension, fluid mud and settled bed has been found to be crucial in the determination of the velocity with which a dense suspension of mud is transported down a sloping bed. It has further been shown that up to mass concentrations of approximately $100kgm^{-3}$, fluid mud may be assumed to behave as a high viscosity Newtonian fluid. Above this concentration, it appears to be a dilatant or shear thickening fluid.

3. Use of laboratory fluid mud data to verify the Wallingford FLUIDMUDFLOW-2D mathematical model for the prediction of fluid mud transport has indicated that, whilst under certain circumstances, this model can accurately predict measured fluid mud flow, it may not be relied upon to do so generally. The failure of the FLUIDMUDFLOW-2D model in this respect is attributable to its inability to simulate vertical exchange of mass due to settling processes in sufficient detail.

4. Use of ultrasonic Doppler technology has resulted in successful, non-intrusive measurements of fluid velocity in suspensions of mud of concentrations up to $80kgm^{-3}$. This has not previously been achieved in a laboratory situation.

In the author's investigation, use of the ultrasonic Doppler method was limited due to the design of the particular instrument that was available. This was unable to measure velocities low enough to encompass the fluid mud flows produced in the Race Track Flume. However, other instruments working on the same principle as that used by the author are available, and would be able to measure such fluid mud flows.

In addition to determining mean flow velocities, ultrasonic Doppler technology was able to measure useful information with regard to the turbulent features in dense suspensions of mud.

5. Previous researchers have shown, and the author's experiments have confirmed, that once the flow speed has been reduced sufficiently to allow settling from a mud suspension previously in equilibrium, there is no further equilibrium suspension that can be supported by the lesser flow velocity; instead all the mud settles from suspension.

Utilising turbulence measurements obtained using ultrasonic Doppler technology, the author has shown that this lack of further equilibrium conditions may be due to a positive feedback effect resulting from the damping of turbulence in a flow by increasing concentrations of suspended mud.

9.3 Recommendations for Future Work on Fluid Mud Modelling

Following on from the summary conclusions listed in the previous sections, it is possible to make certain recommendations for future work on fluid mud modelling. These are summarised below:

1. The Liverpool Race Track Recirculating Flume should be improved by the fitting of an improved paddle motor and drive mechanism so that flow speeds can be more accurately controlled, allowing a given set of experimental conditions to be repeated exactly. The flume should also be equipped with a wave making device so as to allow experiments concerning the fluidisation of mud by waves*.

2. A position has not yet been arrived at in which the formation and transport or otherwise of fluid mud can effectively be predicted. In order for this to be achieved, further experimental work with improved instrumentation and a greater variety of test conditions will be necessary. In particular, it is important that detailed non-intrusive measurements of fluid mud velocity, corresponding velocities throughout the water column and, crucially, accurate fluid mud densities be obtained.

   Required velocities could be obtained by use of improved ultrasonic Doppler instrumentation, for instance the DOP 1000 from Signal Processing S.A. of Lausanne, Switzerland (Signal Processing 1993). This instrument can measure instantaneous velocity profiles across a water column down to values of $0.1 mms^{-1}$ and at frequencies sufficient to encompass turbulent fluctuations as encountered in the Race Track Flume. Use of such an instrument would avoid the necessity to rely on visual observations for the measurement of fluid mud flow.

---

*The author is pleased to note that at the time of writing, these recommendations are already in hand.

Measurement of fluid mud density would be considerably more difficult: ideally a nuclear transmission method should be used. However, in order to set up such a system to respond quickly enough to measure a transient phenomenon such as fluid mud, a high power X-ray of γ-ray source would be required which would lead to considerable health and safety implications (Parker 1993). It may therefore be necessary to compromise in density measurements and use an intrusive system such as a device for grabbing samples with the minimum possible disturbance to the surrounding flow. It would in the author's opinion be possible to develop such an intrusive device relatively simply.

Ideally, density measurements should be obtained down to turbulent frequencies; this would allow more detailed study of the coupling between turbulent frequencies and mud suspensions. This could not be achieved with either a nuclear system or an intrusive sampling mechanism, and thus would not be possible in very high concentrations of mud. However, the work could be carried forward using concentrations less dense than fluid mud, using a light transmission probe similar to the FOSLIM used in the current investigation, but with sufficient power to respond to local changes in concentration at rapid frequencies. As far as the author is aware, no light transmission probe of the required capabilities has yet been developed, but it is possible to envisage such a device based on currently available technology.

A new experimental programme with additional instrumentation should, of course, also extend the author's experimental programme so as to cover situations in which fluid mud is formed by erosion and by wave action as well as by settling from suspension. It should also continue to attempt to reproduce in the laboratory fluid mud flows of realistic field Reynolds numbers such as those encountered in the Parrett Estuary study carried out by Hydraulics Research Wallingford Limited (1992).

3. As discussed in chapter 7, mathematical modelling of fluid mud should be carried out in an integrated, three dimensional way, so as to simulate in detail the mass exchange processes between suspension, fluid mud and settled bed. Only in this way will the problems given by the Wallingford FLUIDMUDLFOW-2D mathematical model be avoided. In the author's opinion, a two-phase modelling approach should be used, representing the mud flocs as a dispersed, solid phase suspended in the continuous, salt water phase. Ideally, such models should be linked in with more detailed process models covering flocculation of primary mud particles and the simulation of mud/fluid turbulence interactions.

   Rather than developing extensive computer code from scratch, a more efficient procedure for this kind of modelling may be to customise a commercial computational fluid dynamics package such as the *Fluent* software used by the author for the simulation of flows in the Race Track Flume. Such packages generally provide for the use of their basic Navier-Stokes solver in custom applications, and it would make sense to concentrate research efforts on the development of specific engineering applications rather than on the writing of new basic solvers for well understood equations of motion.

4. Specific work on the formation and movement of fluid mud, on the rheological behaviour of fluid mud and on the interaction of dense suspensions of mud with fluid turbulence should continue. Attempts should be made not just to quantify these processes for predictive purposes, but to develop a detailed physical understanding of their fundamental nature.

References

It will be noticed that a number of the references cited refer to 'private conversations'. This is because during the course of the investigation the author derived a great deal of knowledge, particularly on instrumentation and experimental procedure, from conversations with other researchers or instrumentation engineers, and it would have been a misrepresentation not to give the persons who provided information in this way their due acknowledgement. The role of simple verbal communication between colleagues in the furthering of scientific research is not to be underestimated.

Alcorn A. (1991), Cohesive sediment transport in the Liverpool Race Track Flume, *Report, Civil Engineering Department, University of Liverpool*

Ali K.H.M. and Georgiadis K. (1991), Laminar motion of fluid mud, *Proceedings of the ICE, Part 2, 91, December, pp795-821*

Ali K.H.M., O'Connor B.A. and Nicholson J.M.C. (1992), Theoretical and experimental study of fluid mud, *5th International Symposium on River Sedimentation, Karlsruhe, Germany, April*

Allersma E. (1980), Mud in Estuaries and Coasts, *International Symposium on River Sedimentation, Chinese Society of Hydraulic Engineers, Beijing, China, March*

BS 1377: 1990, Methods of Testing Soils for Civil Engineering Purposes Part 2, *British Standards Institution.*

Barbier J.M. (1977), Study of the mechanism of mud movement in the Gironde, *24th International Navigation Congress, Leningrad, pp23-26*

Bata G.L. and Bogich (1953), Some observations on density currents in the laboratory and in the field, *Proc Minnesota Int Hydraulics Conv, Sept, pp387-340*

Been K. (1980), Stress-strain behaviour of a cohesive soil deposited underwater, *D.Phil. Thesis, University of Oxford*

Been K. and Sills G.C. (1980), Self weight consolidation of soft soils: an experimental and theoretical study, *Géotechnique, vol 31 No 4*

Burt T.N and Game A.C. (1985), Deposition of Fine Sediment from Flowing Water, *Report Number SR 27, Hydraulics Research Wallingford Limited*

Burt T.N., Dearnaley M.P., Ockenden M.C. and Delo E.A. (1991), Hydraulics Research Wallingford's Capabilities on Cohesive Sediment Research, *Hydraulics Research Wallingford Limited, April*

Chang H.H. (1984), Variation of flow resistence through curved channels, *ASCE Journal of Hydraulic Engineering, vol 110 no 12, pp 1772-1782*

Coleman N.L. (1981), Velocity profiles with suspended sediment, *Journal of Hydraulic Research, IAHR, vol 19, No 3*

Crapper, G. D. (1992), private conversation, *University of Liverpool*

Crapper M. and Ali K.H.M. (1994), A Laboratory Study of Cohesive Sediment Transport, *Paper No 27, Draft proceedings, 4th Nearshore and Estuarine Cohesive Sediment Workshop, Wallingford, July 11-15 (Intercoh '94)*

Curle N. and Davies H.J. (1968), Modern Fluid Dynamics, *Van Nostrand Reinhold Company Limited, London*

Daily J.W. and Harleman D.R.F. (1973), Fluid Dynamics, *Addison Wesley Publishing Co, USA, pp227-244*

Dalrymple R.A. and Liu P. L-F. (1978), Waves over soft muds: a two-layer fluid model, *Journal of Physical Oceanography, Vol. 8, pp181-195*

Dantec Electronics Limited (1983), Laser Doppler Anemometry, *Dantec Electronics Limited, Bristol*

Dantec Electronics Limited (1986), Instruction Manual, 55X Modular LDA Optics, *Dantec Electronics Limited, Bristol*

Data Translation Limited (1992), Global Lab User Manual, *Data Translation Limited, Wokingham, Berkshire*

De Vriend H.J. (1977), A mathematical model of steady flow in curved shallow channels, *Journal of Hydraulic Research, vol 15 no 1, pp 37-53*

De Wit P.J. and Kranenburg C. (1993), Liquefaction and erosion of china clay due to waves and current, *Proceedings of the 23rd International Conference on Coastal Engineering, Vol. 3, pp2937-2948*

Dearnaley M.P. (1991), Flocculation and settling of cohesive sediments, *Report No SR 272, Hydraulics Research Wallingford Limited*

Delft Hydraulics Laboratory (1991), Optical silt measuring instrument Type OSLIM, *Manual, February 1991, Delft Hydraulics, Delft, The Netherlands*

Detectronic Limited (1991), Detectronic DET 72L and 82L Installation and Operating Instructions, *Detectronic Limited, Blackburn*

Digithurst Limited (1991), Micro Eye TC Frame Grabber Board and Micro Scale TC Image Analysis System, *User Manuals, Digithurst Limited, Royston, Herts*

Einstein H.A. and Krone R.B. (1962), Experiments to determine modes of cohesive sediment transport in salt water, *Journal of Geophysical Research, vol. 67 No. 4, pp1451-1461*

Eisma D., van Leussen W. and Dyer, K.R. (1994), The in-situ determination of the settling velocities of fine-grained sediment - a review, *Paper No 2, Draft Proceedings, 4th Nearshore and Estuarine Cohesive Sediment Workshop, Wallingford, July 11-15 (Intercoh '94)*

Fischer H.B., List E.J., Koh R.Y.C., Imberger J. and Brooks N.H. (1979), *Mixing in inland and coastal waters, Academic Press*

Fluent Incorporated (1993), Fluent Version 4.2.2 User's Guide, *Fluent Incorporated, Lebanon, New Hampshire, U.S.A.*

Gade H.G. (1957), Effects of a non-rigid, impermeable bottom on plane surface waves in shallow water, *M.S. Thesis, Texas A. and M. University, College Station, Texas, U.S.A.*

Galland J-C., Laurence D. and Teisson Ch. (1994), Simulating Turbulent Vertical Exchange of Mud with a Reynolds Stress Model, *Paper No 42, Draft proceedings, 4th Nearshore and Estuarine Cohesive Sediment Workshop, Wallingford, July 11-15 (Intercoh '94)*

Georgiadis K. (1989), An experimental investigation of the movement of fluid mud down a sloping bed, *M.Sc. Thesis, Department of Civil Engineering, University of Liverpool, November*

Graham D.I., James P.W., Jones T.E.R., Davies J.M. and Delo E.A. (1992), Measurement and Prediction of Surface Shear Stress in Annular Flume, *ASCE Journal of Hydraulic Engineering, vol. 118 No. 9, September*

Hale I.P., Nicholson J.M.C., Ali K.H.M. and O'Connor B.A. (1989), The behaviour of mud suspensions as they settle onto a sloping bed: an experimental investigation, *Report, Department of Civil Engineering, The University of Liverpool*

Hardesy J. (1992), Private conversations, *Department of Geography, The University of Hull*

Hardy M.S.A.H. (1994), Private conversation, *Department of Civil and Environmental Engineering, The University of Edinburgh*

Harleman D.R.F. (Streeter V.L. ed) (1961), Stratified flow, *Handbook of fluid dynamics, McGraw-Hill, New York, chapter 26*

Henderson F.M. (1966), Open Channel Flow, *MacMillan*

Hino M. (1963), Turbulent Flow with Suspended Particles, *Proceeding of the ASCE, Journal of the Hydraulic Division, vol 89, no HY4, July, pp161-185*

How T. (1992), Private conversations, *Department of Clinical Engineering, The University of Liverpool*

Hussein A.S.A. and Smith K.V.H. (1986), Flow and Bed Deviation in Curved Open Channels, *Journal of Hydraulic Research, vol 24 no 2, pp 93-108*

Hussey M. (1985), Basic physics and technology of medical diagnostic ultrasound, *MacMillan Publishers Limited*

Hydraulics Research Station (1953), The River Thames Estuary, *Annual Report of the Director of Hydraulics Research, pp17-24*

Hydraulics Research (1975), River Avon, Bristol, Appraisal of siltation at projected barrage sites, *Report No. EX 711, October*

Hydraulics Research Wallingford Limited (1992), Fluid Mud in Estuaries, *ETSU TID 4084, Energy Technology Support Unit, U.K. Department of Energy 1992*

Ippen A.T. and Harleman D.R.F. (1952), Steady-state characteristics of sub-surface flow, *Circular No 521, US National Bureau of Standards, pp79-93*

Jarvis P. (1992), Private conversations, *Service Supervisor, Toshiba Medical Systems Limited, Crawley*, W Sussex

Jaryczewski R. (1992), Private conversations. *Service Engineer, Dantec Limited, Bristol*

Jones T.E.R. and Golden K. (1992), Rheological behaviour of River Parrett fluid mud, *Appendix 2 of Hydraulics Research Limited (1992)*

Keulegan G.H. (1944), Laminar flow at the interface of two liquids, *Circular No 32, US National Bureau of Standards, p303*

Kikkawa H., Ikeda S. and Kitagawa A. (1976), Flow and bed topography in curved open channels, *ASCE Journal of the Hydraulic Division, vol 102 no HY9, September, pp 1327-1342*

Kirby R. (1988), High Concentration Suspension (Fluid Mud) Layers in Estuaries, *in* Physical Processes in Estuaries, J. Dronkers and W. van Leussen eds., *Springer-Verlag, Berlin*

Kirby R. and Parker W.R. (1977), The physical characteristics and environmental significance of fine sediment suspensions in estuaries, *in* Studies in Geophysics, Estuaries, Geophysics and the Environment, *National Research Council, N.A.S., U.S.A., pp110-120*

Kirby R. and Parker W.R. (1983), The distribution and behaviour of fine sediment in the Severn Estuary and Inner Bristol Channel, *Canadian Journal of Fish and Aquatic Science, Vol. 40 No. 1, pp83-95*

Krishnappan B.G. (1990), Modelling of settling and flocculation of fine sediments in still water, *Canadian Journal of Civil Engineering, vol 17 no 5, pp763-770*

Krone R.B. (1963), A study of rheologic properties of esturial sediments, *Technical Bulletin No. 9, Final Report SERL, Committee on Tidal Hydraulics, U.S. Army Corps of Engineers Waterways Experimental Station, Vicksburg, Mississippi.*

Kusuda T., Watanabe R. and Yamanishi H. (1994), Mass fluxes in fluid mud layers on an inclined bed, *Paper No 39, Draft proceedings, 4th Nearshore and Estuarine Cohesive Sediment Workshop, Wallingford, July 11-15 (Intercoh '94)*

Launder B.E., Reece G.J. and Rodi W. (1975), Progress in the Development of a Reynolds Stress Turbulence Closure, *Journal of Fluid Mechanics, volume 68 part 3, April 15th, pp 537-566*

Launder B.E. and Spalding D.B. (1973), The Numerical Computation of Turbulent Flows, *Imperial College of Science and Technology, London, January, NTIS N74-12066*

Le Hir P. (1994), Fluid and sediment integrated modelling: an application to fluid mud flows in estuaries, *Paper No 40, Draft proceedings, 4th Nearshore and Estuarine Cohesive Sediment Workshop, Wallingford, July 11-15 (Intercoh '94)*

Leschziner M.A. and Rodi W. (1979), Calculation of Strongly Curved Open Channel Flow, *ASCE Journal of the Hydraulic Division, vol 105 No HY10, October, pp 1297-1314*

Littler J.D. (1992), Private conversations, *Department of Civil Engineering, The University of Liverpool*

Maa J. P-Y. and Mehta A.J. (1990), Soft mud response to water waves, *Journal of Waterway, Port, Coastal and Ocean Engineering, Vol. 116 No. 5, pp634-650*

McDowell D.M. and O'Connor B.A. (1977), Hydraulic Behaviour of Estuaries, *CivilEngineering Hydraulics Series, The MacMillan Press Limited*

Maskell J.M. (1984), A mathematical model of mud transport in a shallow estuary with a large tidal range, *Report IT 267, Hydraulics Research Wallingford Limited, March*

Mehta A.J. and Srinavas R. (1993), Observations on the Entrainment of Fluid Mud by Shear Flow, *in* Nearshore and Estuarine Cohesive Sediment Transport, Coastal and Estuarine Studies No 42, A.J. Mehta ed., *American Geophysical Union, Washington D.C., U.S.A., pp 224-246*

Mendis. M.M. (1987), Improvement of flow distribution at deep open channel bends, *MEng Thesis, University of Liverpool, December*

Migniot C. (1968), A study of the physical properties of various forms of very fine sediment and their behaviour under hydrodynamic action, *La Houille Blanche Vol 7., pp591-620 (in French)*

Møller-Jensen P. (1993), Wadden Sea Mud - Methods for Estimation of Transport, Erosion and Consolidation of Marine Cohesive Sediments, *Ph.D. Thesis, University of Ålborg, Denmark, May*

Newhouse V.L. (1980), The dependence of ultrasound Doppler bandwidth on beam geometry, *IEEE Transactions on Sonics and Ultrasonics, vol 27*

Nezu I. and Nakagawa H. (1993), Turbulence in Open Channel Flows, *IAHR Monograph Series, AA Balkema Publishers, Rotterdam, The Netherlands*

Nicholson J.M.C. and O'Connor B.A. (1986), A Cohesive Sediment Transport Model, *ASCE Journal of Hydraulic Engineering, vol 112, No 7, July, pp621-640*

O'Connor B.A. (1991), Suspended sediment transport in the coastal zone, *Proceedings of the International Symposium on the Transport of Suspended Sediments and its Mathematical Modelling, Firenze, Italy, pp17-63*

Odd N.V.M and Cooper A.J. (1988), A two-dimensional model of the movement of fluid mud in a high energy turbid estuary, *Report No SR 147, Hydraulics Research Wallingford Limited, January*

Odd N.V.M. and Owen M.W. (1972), A two-layer model of mud transport in the Thames Estuary, *Proceedings of the Institution of Civil Engineers Supplement (iv), Paper 7517S*

Odd N.V.M. and Rodger J.G. (1978), Vertical mixing in stratified tidal flows, *ASCE Journal of the Hydraulic Division, vol. HY 3, Paper 13599, March*

Odd N.V.M. and Rodger J.G. (1986), An analysis of the behaviour of fluid mud in estuaries, *Report No SR 84, Hydraulics Research Wallingford Limited*

Odgaard A.J. (1984), Flow and topography in an alluvial channel bend, *ASCE Journal of Hydraulic Engineering, vol 110 no 4, pp 521-536*

Owen M.W. (1970), Properties of a consolidating mud. *Report No. INT 83, Hydraulics Research, December*

Owen M.W. (1976), Determination of the settling velocities of cohesive muds, *Report No IT 161, Hydraulics Research Wallingford Limited*

Parker W.R. (1994), On the characterization of cohesive sediment for transport modelling - conference overview, *Paper No 1, Draft Proceedings, 4th Nearshore and Estuarine Cohesive Sediment Workshop, Wallingford, July 11-15 (Intercoh '94)*

Parker W.R. (1992), Private conversations, *Blackdown Consultants, Taunton*

Parthenaides E. (1964), A summary of the present knowledge of the behaviour of fine sediments in estuaries, *Technical Note No. 8, Department of Civil Engineering, M.I.T., U.S.A.*

Patankar S.V. (1981), Numerical Heat Transfer and Fluid Flow, *Hemisphere Publishing Company, Washington D.C., U.S.A.*

Petersen O. and Krishnappan B.G. (1994), Measurement and analysis of flow characteristics in a rotating circular flume, *Journal of Hydraulic Research, Vol. 32, No. 4*

Prandtl L. (1952), Essentials of fluid dynamics with applications to hydraulics, aeronautics, meteorology and other subjects, *Blackie and Son*

RD Instruments (1989), Acoustic Doppler current profilers principles of operation: a primer, *RDI UK Limited, Aberdeen*

Roberts W. (1992), Fluidisation of Mud by Waves Development of a mathematical model of fluid mud in the coastal zone, *Report No SR 296, Hydraulics Research Wallingford Limited*

Roisin J-P. (1985), Sediment Mixing Processes, *M.Sc. Thesis, University of Manchester*

Rosovskii I.L. (1965), Flow of water in bends of open channels, *Programme for Scientific Translation, Jerusalem, Israel*

Ross M.A. and Mehta A.J. (1989), On the mecahnics of lutoclines and fluid mud, *Journal of Coastal Research, Special Issue No 5, Summer, pp51-62*

Rosten H.I., Spalding D.B. and Tachell D.G. (1982), Phoenics - An Instruction Manual, *Concentration Heat and Momentum Limited, January*

Rouas G., Tanguy J.M., Boutin R. and Lafond L.R., (1994), An experimental contribution to the study of settlement, deposition and consolidation of cohesive sediments, *Paper No 11, Draft proceedings, 4th Nearshore and Estuarine Cohesive Sediment Workshop, Wallingford, July 11-15 (Intercoh '94)*

Rouse H. (1962), Elementary Mechanics of Fluids, *John Wiley and Sons Inc., New York, pp176-199*

Scott C.R. (1980), An introduction to soil mechanics and foundations, third edition, *Applied Science Publishers Limited*

Sensordata (1985), Minilab Model SD-12 User's Manual, *Sensordata, Norway*

Sheng Y.P. (1989), Consideration of flow in rotating annuli for sediment erosion and deposition studies, *Journal of Coastal Research, Special Issue No 5, Summer, pp 207-216*

Shimizu Y., Yamaguchi H. and Hakura T. (1990), Three dimensional computation of flow and bed deformation, *ASCE Journal of Hydraulic Engineering, vol 116 no 9, pp 1090-1108*

Shukry A. (1950), Flow around bends in open flumes, *Transactions of the ASCE, vol 115, pp 751-779, quoted in Mendis (1987)*

Signal Processing (1993), DOP1000 Operator's Manual, *Signal Processing SA, Lausanne, Switzerland*

Sills G.C. and Elder D.McG. (1994), The Transition from Sediment Suspension to Settling Bed, *Proceedings of Workshop, Estuarine Cohesive Sediment Dynamics, Lecture Notes on Coastal and Estuarine Studies, editor AJ Mehta, Springer-Verlag, Nov, Tampa, Florida, USA*

Sills G.C. and Thomas R.C. (1983), Settlement and consolidation in the laboratory of steadily deposited sediment, *Seabed Mechanics, Proceedings of the IUTAM Symposium, Newcastle*

Sills G.C. (1994), Hindered settling and consolidation in cohesive sediments, *Paper No 10, Draft proceedings, 4th Nearshore and Estuarine Cohesive Sediment Workshop, Wallingford, July 11-15 (Intercoh '94)*

Sills G.C. (1994), Private conversations, *Department of Engineering Science, The University of Oxford*

Smith G.D. (1978), Numerical solution of partial differential equations using finite difference methods, second edition, *Oxford Applied Mathematics and Computing Science Series, Clarendon Press, Oxford*

Teisson C. (1994), A Review of Cohesive Sediment Transport Models, *Paper No 36, Draft proceedings, 4th Nearshore and Estuarine Cohesive Sediment Workshop, Wallingford, July 11-15 (Intercoh '94)*

Teisson Ch., Simonin O., Galland J-C., and Laurence D. (1992), Turbulence and mud sedimentation: a Reynolds stress model and a two phase model, *Proceedings of International Conference on Coastal Engineering, Venice, Italy, October*

Thorn M.F.C. (1981), Physical Processes of siltation in tidal channels, *Hydraulic modelling applied to maritime engineering problems, Paper No 6, Institution of Civil Engineers*

Toorman E. (1994), A review of the use of the concentric cylinder viscometer for cohesive sediment suspensions, *Paper No 32, Draft proceedings, 4th Nearshore and Estuarine Cohesive Sediment Workshop, Wallingford, July 11-15 (Intercoh '94)*

Toshiba Corporation (1982, 1983), Operation manual for Pulse Doppler Unit Model SDL-01A, *No 2B760-003E*A, Japan*

Trads, S. and Andersen J.S. (1992), Investigation of fluid mud in the new Liverpool mud flume, *Report, Department of Civil Engineering, University of Liverpool.*

Vanoni V.A. (1946), Transportation of suspended sediment by water, *Transactions, ASCE, vol 111, pp67-133*

Viesmann W.J., Gary L. and Knapp J.W. (1972), Introduction to Hydrology, *Intext Educational Publishers, pp188-207*

Viscometers U.K. Limited (1990), Viscometers U.K. Limited Model ELV-8 Instrument, *Warren Spring Laboratory, Department of Trade and Industry*

WS Ocean Systems Ltd (1992), Private conversations, *Technical Support Department*

Webber N.B. (1971), Fluid mechanics for civil engineers, *Chapman and Hall*

Wellershans S. (1981), Turbidity maximum and mud shoaling in the Weser Estuary, *Arch. Hydrobiol. Vol. 92 No. 2, September, pp161-198*

Williams D.J.A. and Williams P.Rh. (1989), Rheology of concentrated cohesive sediments, *Journal of Coastal Research Special Issue No 5, Summer , pp165-174*

Wilkinson, W.L. (1960), Non-Newtonian fluids, fluid mechanics, mixing and heat transfer, *International Series of Monographs on Chemical Engineering, vol 1, Pergammon Press*

Appendix 1: Accuracy of Laser Doppler Anemometer and Minilab SD-12 Ultrasonic Probe Results

A1.1 Two Channel Laser Doppler Anemometry

The derivation of velocity readings from the Laser Doppler Anemometer (LDA) is a fairly simple process, but it does depend on a number of user controlled factors in the set up of the laser optics and on another factor over which the user has no control, this being the linearity errors in the analogue electronics of the frequency trackers.

In order to understand the effect of these errors on the final velocity reading, a brief explanation of the LDA system is required. However, for a full description of the workings of the LDA and an in depth discussion on some of the points discussed below, reference should be made to the LDA manuals (Dantec Electronics Limited 1983 and 1986)

The laser beam is split into three by the optics, one circularly polarized reference beam and two other beams, one for each channel, which are polarized with a 90° opposition. Each channel is then measured using one polarized beam and the reference beam, information from the two channels being separated in the collection optics by means of the differential polarization. If the polarization is not set up at 90° opposition, an indeterminate level of cross talk will affect both channels. It is, however, easy to check that polarization is correct by use of a piece of polarizing material to block of each laser beam in turn, so it is unlikely that errors will arise from this effect.

A1.2 Spatial Resolution

The two beams used in each channel intersect, forming a pattern of interference fringes. Particles in the flow cross these fringes, scattering light as they do so. The frequency of the scattered light corresponds to the speed of the particles as they cross the fringes, and therefore to the speed of the water flow. A phase difference between the two beams causes the fringes to move with a known velocity, enabling small and zero flow velocities to be measured.

The intersection of the laser beams forms a measuring probe of finite volume, and scattered light is generated from everywhere within this volume, though as the collection optics see this volume from one particular direction, some points of the probe volume give rise to more powerful signals than others. There is therefore a somewhat indeterminate limit to the accuracy with which the laser measurement can be located. The finite size of the probe volume (which can be different for each of the two channels) depends on the thickness of the laser beams, the angle of intersection of the two beams for the channel under consideration, the focal length of the laser optics and the wavelength of the laser light. Thus:

$$2b = \frac{d_f}{2\sin\left(\frac{\phi}{2}\right)} \qquad \text{(A1.1)}$$

and

$$2c = \frac{d_f}{\cos\left(\frac{\phi}{2}\right)} \qquad \text{(A1.2)}$$

where 2b is the probe width, 2c is the probe length, d_f is the fringe width and ϕ is the angle of intersection of the laser beams. d_f is given by:

$$d_f = \frac{4f\lambda}{\pi E d_1} \tag{A1.3}$$

where f is the focal length, λ is the wavelength of the laser light and E and d_1 are values corresponding to the beam thickness, which are obtained from the laser instrument specifications. In the present investigation, $\phi/2$ is approximately 2.3°, f is 0.6m, λ is 6.328×10^{-7}m, E is 1.9375 and d_1 is 1.1×10^{-3}m. This gives a probe width 2b of approximately 0.3mm and a probe length 2c of approximately 6mm.

It can easily be understood that this limit to the location of the measuring point will be quite significant, especially in the boundary layer measurements where the tilt of the laser beams means that the probe volume is angled downwards, causing the vertical resolution of the measuring position to be affected by the 6mm probe length.

A1.3 LDA Signal Processing

The scattered light from the measuring volume is gathered by the collection optics, which generates output signals by means of photoelectric cells. These signals are fed into a frequency shifter, which applies a known shift (20kHz in the experiments under consideration) to the LDA frequencies so that Doppler Shift frequencies due to forward and reverse flows can be separated. Each channel's shifted frequency is then fed to a frequency tracker, which tracks the most powerful frequency at any given instant and gives an analogue output corresponding to the Doppler shift frequency plus the applied shift for the given channel.

The analogue output can be related directly to the velocity in the direction in which the particular channel is oriented by a calibration factor:

$$C = \frac{\lambda}{2\sin\left(\frac{\phi}{2}\right)} \tag{A1.4}$$

so it is necessary to know the angle ϕ. In practice this is determined by projecting the laser beams onto a screen and measuring the distance between them, h and the distance from the focal point of LDA optics to the screen, L. It will be noted that the angle ϕ is calculated in air, though the measurements are in fact taken in water. However, since the value of the light wavelength λ quoted is also for air, a consideration of Snell's Law will show that no error is introduced by this approach.

The analogue voltage given out by the tracker, meanwhile, is related to the Doppler Shift frequency as follows:

$$V = \frac{(f_d - f_s)}{k} + \delta s \qquad \text{(A1.5)}$$

where f_d is the Doppler Shift frequency, f_s is the applied shift, k is a constant of proportionality and δs is an offset representing a linearity error in the analogue electronics. Clearly this formula is a simplification, because in practice δs will be a complicated function of V. This gives a formula

$$q = C(kV - f_s) \qquad \text{(A1.6)}$$

for the velocity component q in the channel direction.

Given two components, q_1 and q_2 in the two channel directions, the actual velocity vector in the two dimensional plane of measurement can be found. It will be at an angle θ to the horizontal given by:

$$\tan\theta = \frac{q_1\cos\alpha_2 - q_2\cos\alpha_1}{q_2\sin\alpha_1 - q_2\sin\alpha_1} \qquad \text{(A1.7)}$$

where α_1 and α_2 are the angles of q_1 and q_2 to the horizontal. Its magnitude Q will be given by

$$Q = \frac{q_1}{\cos(\theta - \alpha_1)} = \frac{q_2}{\cos(\theta - \alpha_2)} \qquad \text{(A1.8)}$$

and then the principal velocity components can be resolved simply. However, if α_1 and α_2 add up to 90°, equations A1.6, A1.7 and A1.8 may be simplified to:

$$\begin{aligned} u &= q_1\cos\alpha_1 + q_2\cos\alpha_2 \\ w &= q_1\sin\alpha_1 - q_2\sin\alpha_2 \end{aligned} \qquad \text{(A1.9)}$$

In practice it is very difficult to set up the laser beams at right angles, so to be absolutely accurate, the more rigorous analysis of equations A1.6, A1.7 and A1.8 is appropriate.

A1.4 Sources and Significance of Errors

Errors in the measured values of the principal velocity components u and w arise from the measurement of distances h_1 and h_2 and L_1 and L_2 used in deriving the angles ϕ_1 and ϕ_2, from the linearity error of the LDA trackers δs_1 and δs_2, and from the measurement of the angles α_1 and α_2. These errors can be built into a system of differential equations to determine the overall error in u and w that results from a given error in any of these areas (Crapper 1992):

$$\begin{aligned} \delta u = {} & \frac{\partial u}{\partial \alpha_1}\delta\alpha_1 + \frac{\partial u}{\partial \alpha_2}\delta\alpha_2 + \frac{\partial u}{\partial s_1}\delta s_1 + \frac{\partial u}{\partial s_2}\delta s_2 + \\ & \frac{\partial u}{\partial h_1}\delta h_1 + \frac{\partial u}{\partial h_2}\delta h_2 + \frac{\partial u}{\partial L_1}\delta L_1 + \frac{\partial u}{\partial L_2}\delta L_2 \end{aligned} \qquad \text{(A1.10)}$$

$$\begin{aligned} \delta w = {} & \frac{\partial w}{\partial \alpha_1}\delta\alpha_1 + \frac{\partial w}{\partial \alpha_2}\delta\alpha_2 + \frac{\partial w}{\partial s_1}\delta s_1 + \frac{\partial w}{\partial s_2}\delta s_2 + \\ & \frac{\partial w}{\partial h_1}\delta h_1 + \frac{\partial w}{\partial h_2}\delta h_2 + \frac{\partial w}{\partial L_1}\delta L_1 + \frac{\partial w}{\partial L_2}\delta L_2 \end{aligned} \qquad \text{(A1.11)}$$

where δu represents the error in u etc. and the subscripts $_1$ and $_2$ refer to the channel number.

It should be noted here that, regardless of the sign of the particular derivatives in the above equations, they must all be summed since it must be assumed that errors can be cumulative in their effect. The results δu and δw represent, however, the maximum likely error or tolerance rather than any statistical expected value or confidence limit: it may be most probable, in fact, that errors cancel out rather than accumulate.

The derivatives used in equations A1.10 and A1.11 are easily calculated as shown below. However, it should be noted that for simplicity the assumption of equation A1.9 is built into the following analysis, rather than the more complex version of equations A1.6, A1.7 and A1.8.

$$\frac{\partial u}{\partial \alpha_1} = -q_1 \sin\alpha_1 \; ; \; \frac{\partial u}{\partial \alpha_2} = -q_2 \sin\alpha_2 \qquad \text{(A1.12)}$$

$$\frac{\partial u}{\partial s_1} = \frac{\partial u}{\partial q_1}\frac{\partial q_1}{\partial V_1}\frac{\partial V_1}{\partial s_1} = C_1 k_1 \cos\alpha_1 \qquad \text{(A1.13)}$$

similarly

$$\frac{\partial u}{\partial s_2} = C_2 k_2 \cos\alpha_2 \qquad \text{(A1.14)}$$

Further,

$$\frac{\partial u}{\partial h_1} = \frac{\partial u}{\partial q_1}\frac{\partial q_1}{\partial C_1}\frac{\partial C_1}{\partial \phi_1}\frac{\partial \phi_1}{\partial h_1}$$

$$= -\cos\alpha_1(k_1V_1 - f_{s1})\frac{\lambda\cos\left(\frac{\phi_1}{2}\right)}{4\sin^2\left(\frac{\phi_1}{2}\right)}\frac{1}{L_1} \qquad \text{(A1.15)}$$

and similarly

$$\frac{\partial u}{\partial h_2} = -\cos\alpha_2(k_2V_2 - f_{s2})\frac{\lambda\cos\left(\frac{\phi_2}{2}\right)}{4\sin^2\left(\frac{\phi_2}{2}\right)}\frac{1}{L_2} \qquad \text{(A1.16)}$$

Also, by similar reasoning,

$$\frac{\partial u}{\partial L_1} = -\cos\alpha_1(k_1V_1 - f_{s1})\frac{\lambda\cos\left(\frac{\phi_1}{2}\right)}{4\sin^2\left(\frac{\phi_1}{2}\right)}\frac{1}{L_1} \qquad \text{(A1.17)}$$

and

$$\frac{\partial u}{\partial L_2} = -\cos\alpha_2(k_2V_2 - f_{s2})\frac{\lambda\cos\left(\frac{\phi_2}{2}\right)}{4\sin^2\left(\frac{\phi_2}{2}\right)}\frac{1}{L_2} \qquad \text{(A1.18)}$$

The derivatives concerning the w velocity are similarly determined:

$$\frac{\partial w}{\partial \alpha_1} = -q_1 \cos\alpha_1 \; ; \; \frac{\partial w}{\partial \alpha_2} = -q_2 \cos\alpha_2 \tag{A1.19}$$

$$\frac{\partial w}{\partial s_1} = C_1 k_1 \sin\alpha_1 \tag{A1.20}$$

$$\frac{\partial w}{\partial s_2} = -C_2 k_2 \sin\alpha_2 \tag{A1.21}$$

$$\frac{\partial w}{\partial h_1} = -\sin\alpha_1 (k_1 V_1 - f_{s1}) \frac{\lambda \cos\left(\frac{\phi_1}{2}\right)}{4\sin^2\left(\frac{\phi_1}{2}\right)} \frac{1}{L_1} \tag{A1.22}$$

$$\frac{\partial w}{\partial h_2} = \sin\alpha_2 (k_2 V_2 - f_{s2}) \frac{\lambda \cos\left(\frac{\phi_2}{2}\right)}{4\sin^2\left(\frac{\phi_2}{2}\right)} \frac{1}{L_2} \tag{A1.23}$$

$$\frac{\partial w}{\partial L_1} = -\sin\alpha_1 (k_1 V_1 - f_{s1}) \frac{\lambda \cos\left(\frac{\phi_1}{2}\right)}{4\sin^2\left(\frac{\phi_1}{2}\right)} \frac{1}{L_1} \tag{A1.24}$$

$$\frac{\partial w}{\partial L_2} = \sin\alpha_2 (k_2 V_2 - f_{s2}) \frac{\lambda \cos\left(\frac{\phi_2}{2}\right)}{4\sin^2\left(\frac{\phi_2}{2}\right)} \frac{1}{L_2} \qquad \text{(A1.25)}$$

These equations can then be used to obtain the maximum error for given values of the quantities under consideration and the likely errors in each quantity.

A1.5 Values and Errors used in the Analysis

Table A1.1 shows typical values of the quantities used in the LDA analysis under consideration. These values are used in the example error calculations detailed below.

These values of likely errors are, with the exception of δs_1 and δs_2, arrived at from experience actually measuring values in the laboratory. They represent an engineering judgement of the possible inaccuracies involved in each measurement. The values of δs were calculated from a linearity check on the frequency trackers. This was carried out using a digital signal generator accurate to 1 in 10^{-6}Hz to apply a signal of known frequency to the tracker. The output voltage was then measured using a 'Global Lab' data acquisition system (Data Translation Limited 1992), a 12 bit system with a range of 0 to 10V, and which resolves voltages to $10/2^{12}$V or 2.44mV. The results of the linearity check are given in table A1.3. It should be noted that the LDA trackers are intended to give an analogue output of between 1 and 10 volts only.

Table A1.1: Typical Values of Quantities used in LDA Measurements

Quantity	Value and Units
λ	6.328×10^{-7}m
L_1, L_2	2.667m
h_1	0.225m
h_2	0.227m
ϕ_1	0.0842rad
ϕ_2	0.0849rad
C_1	$7.51 \times 10^{-6} ms^{-1} Hz^{-1}$
C_2	$7.44 \times 10^{-6} ms^{-1} Hz^{-1}$
V_1, V_2	4.8V
k_1, k_2	10 000HzV^{-1}
f_{s1}, f_{s2}	20 000Hz
q_1	$0.210 ms^{-1}$
q_2	$0.208 ms^{-1}$
α_1	0.794rad (45.50°)
α_2	0.789rad (45.25°)

Table A1.2 shows likely values of errors in the relevant quantities.

Table A1.2: Likely Values of Errors in Quantities Used in LDA Signal Processing

Quantity	Likely Error Value and Units
δh_1, δh_2	0.004m
δL_1, δL_2	0.010m
δs_1	0.287V
δs_2	0.056V
$\delta\alpha_1$, $\delta\alpha_2$	0.0175rad (1.00°)

Linear interpolation shows the channel 1 and channel 2 errors corresponding to an expected reading of 4.8V to be 0.46V and 0.15V respectively. However, in the analysis under consideration, offsets at the 2V level (corresponding to the 20kHz applied frequency shift) were used, these being 0.173V for channel 1 and 0.094V for channel 2. Thus at 4.8V, the net errors were, for channel 1, 0.46 - 0.173 = 0.287V and for channel 2, 0.15 - 0.094 = 0.056V.

Table A1.3: Results of Linearity Check on LDA Trackers

Frequency of Applied Signal (kHz)	Expected Output Voltage	Actual Output Voltage Channel 1	Actual Output Voltage Channel 2
5	1.0	0.791	0.610
10	1.0	1.081	1.003
20	2.0	2.189	2.015
30	3.0	3.289	3.059
40	4.0	4.392	4.153
50	5.0	5.473	5.149
60	6.0	6.596	6.238
70	7.0	7.617	7.175
80	8.0	8.640	8.174
90	9.0	9.692	9.175
100	10.0	9.997	9.997
110	10.0	9.997	9.997

Inserting the values shown in tables 1 and 2 into equations 10 and 11 gives the following results for the maximum likely error in u and w:

$$\begin{aligned}\delta u &= 2.62\times10^{-3} + 2.58\times10^{-3} \\ &+ 0.0151 + 2.94\times10^{-3} \\ &+ 2.63\times10^{-3} \\ &+ 2.60\times10^{-3} \\ &+ 9.85\times10^{-6} \\ &+ 9.74\times10^{-6} \\ &= 0.028 ms^{-1}\end{aligned} \qquad \text{(A1.26)}$$

and

$$\begin{aligned}\delta w &= 2.58\times10^{-3} + 2{,}56\times10^{-2} \\ &+ 0.0154 + 2.96\times10^{-3} \\ &+ 2.67\times10^{-3} \\ &+ 2.62\times10^{-3} \\ &+ 5.63\times10^{-4} \\ &+ 5.57\times10^{-4} \\ &= 0.030 ms^{-1}\end{aligned} \qquad \text{(A1.27)}$$

The value of $0.028ms^{-1}$ represents about 10% of a typical value of u velocity, though the value of $0.030ms^{-1}$ represents at least 200% of a typical w velocity. This is, therefore, highly significant. However, it should be noted that these values are, as mentioned, maximum likely errors, not statistical confidence limits, and there is nothing in the above analysis to suggest that all, or indeed any, of the LDA results were subject to that degree of inaccuracy. In practice it is much more likely that some errors will cancel each other out rather than accumulate to a total inaccuracy. It will, however, be noted that by far the most significant proportion of the errors δu and δw is given by the third component in equations 10 and 11, the linearity error in channel 1, over which the user has effectively no control. It is therefore logical to assume that time taken making the other errors quoted in table 2 even smaller will probably be wasted.

A1.6 The Minilab SD-12 Ultrasonic Velocity Meter

A Minilab SD-12 three channel ultrasonic velocity meter was used to obtain velocity information at the rear of the race track flume, where it was not possible to use the LDA system. This probe measures the time taken for an ultrasonic pulse to be transmitted between its prongs, and determines the average velocity of the flow

between the prongs from this. It gives both a direct digital readout and an analogue signal for each channel.

Table A1.4: Results for Calibration of Minilab SD-12 Ultrasonic Probe against the Laser-Doppler Anemometer

	u Velocity (ms^{-1})		w Velocity (ms^{-1})	
Paddle Setting	LDA Results	SD-12 Results	LDA Results	SD-12 Results
5.0	0.190	0.184	0.004	-0.012
5.0	0.216	0.208	0.007	-0.006
5.0	0.177	0.171	0.004	-0.009
7.5	0.268	0.271	0.009	0.007
7.5	0.276	0.277	0.009	0.006
7.5	0.292	0.292	0.007	-0.013
10.0	0.328	0.329	0.003	-0.018
10.0	0.355	0.368	0.004	-0.017
10.0	0.350	0.362	0.004	-0.015

The SD-12 velocity meter was calibrated against the LDA system by arranging the LDA beams to intersect at the mid point between the ultrasonic probe's prongs. Velocity values were then collected simultaneously for each instrument and compared. Readings were collected on the 'Global Lab' data acquisition system mentioned above, using the ultrasonic probe's analogue output. The results are shown in table A1.4 below.As can be seen, the two sets of results for the relatively large u

velocity are very close, though there is discrepancy in both magnitude and direction for the smaller w velocity. However, in view of the above discussion on the LDA system, it is perhaps doubtful as to how much reliance may be placed on low velocity readings from either the LDA or the ultrasonic probe.

A1.7 Conclusions

The following conclusions may be drawn from the above analyses:

1. The maximum error likely to occur in a typical u velocity measured with the LDA system is about 10%

2. The corresponding maximum error in a typical w velocity could be so large as to make the reading entirely unreliable.

3. The most significant errors in the LDA system are due to non linearity in the analogue output of the frequency trackers and are therefore beyond the user's control.

4. In view of point 3 above, excessive care and accuracy in setting up and measuring other quantities involved in LDA signal processing will be wasteful.

5 The Minilab SD-12 ultrasonic velocity meter is as accurate as the LDA for values obtained for u velocity, and probably just as inaccurate for low flows such as were obtained for w velocity.

Appendix 2: Quadrature Phase Detection with Frequency Domain Processing

This appendix describes the method used by the Toshiba SDL-01A pulsed-Doppler velocimeter and other such instruments to distinguish the forward and reverse velocity components in a fluctuating flow.

Frequencies are of course non-directional numbers and a Doppler shift frequency can arise from either forward or reverse fluid motion. The reflected signal received at the monitor therefore takes the form:

$$S(t) = A_0 \cos(\omega_0 t + \phi_0) + A_f \cos(\omega_0 t + \omega_f t + \phi_f) + A_r \cos(\omega_0 t - \omega_r t + \phi_r) \qquad \text{(A2.1)}$$

where A, ω and ϕ refer to the amplitude, angular frequency and phase of each signal and the subscripts $_{0,f}$ and $_r$ refer to the carrier, forward and reverse signals (Hussey 1985).

Various methods are available to separate the frequencies due to forward and reverse motion, one of the most widely used systems being quadrature phase detection with frequency domain processing (Hussey 1985). When the reflected signal is received at the monitor, it is demodulated, the original emission frequency being removed leaving only the Doppler sidebands. The reference signal for the demodulation is taken directly from the pulsed-Doppler system's master oscillator, and in order to generate the quadrature signal, the demodulation is carried out both directly with the master oscillator and also with a signal derived from the master oscillator but shifted by 90°. The direct signal D(t) is derived by multiplying equation A2.1 by $\cos(\omega_0 t)$:

$$
\begin{aligned}
D(t) &= \frac{1}{2}A_0[\cos(\phi_0) + \cos(2\omega_0 t + \phi_0)] \\
&+ \frac{1}{2}A_f[\cos(\omega_f t + \phi_f) + \cos(2\omega_0 t + \omega_f t + \phi_f)] \\
&+ \frac{1}{2}A_r[\cos(\omega_r t - \phi_r) + \cos(2\omega_0 t + \omega_r t + \phi_r)]
\end{aligned}
\tag{A2.2}
$$

Filtering out the DC component and terms of the order $2\omega_0$ then leads to:

$$
D(t)' = \frac{1}{2}A_f\cos(\omega_f t + \phi_f) + \frac{1}{2}A_r\cos(\omega_r t - \phi_r) \tag{A2.3}
$$

Multiplying the signal given in equation A2.1 by $\sin(\omega_0 t)$ leads similarly to a filtered quadrature signal Q(t)', given by:

$$
Q(t)' = -\frac{1}{2}A_f\sin(\omega_f t + \phi_f) + \frac{1}{2}A_r\sin(\omega_r t - \phi_r) \tag{A2.4}
$$

or

$$
\begin{aligned}
Q(t)' &= \frac{1}{2}A_f\cos\left(\omega_f t + \phi_f + \frac{\pi}{2}\right) \\
&+ \frac{1}{2}A_r\cos\left(\omega_r t - \phi_r - \frac{\pi}{2}\right)
\end{aligned}
\tag{A2.5}
$$

Both the direct and quadrature signals are then mixed with quadrature signals from a pilot oscillator, a process which results in the forward and reverse flow components being separated on either side of the pilot frequency ω_p. Multiplying equation A2.3 by $A_p\cos(\omega_p t)$ where A_p and ω_p are the amplitude and frequency of the signal from the pilot oscillator gives:

$$
\begin{aligned}
S1(t) &= \frac{1}{2}A_p[a_f\cos(\omega_f t + \phi_f)\cos(\omega_p t) \\
&+ A_r\cos(\omega_r t - \phi_r)\cos(\omega_p t)]
\end{aligned}
\tag{A2.6}
$$

which can be expanded to give:

$$
\begin{aligned}
S1(t) &= \frac{1}{4}A_p\Big\{A_f[\cos(\omega_p t - \omega_f t - \phi_f) \\
&+ \cos(\omega_p t + \omega_f t + \phi_f)] + A_r[\cos(\omega_p t - \omega_r t + \phi_r) \\
&+ \cos(\omega_p t + \omega_r t - \phi_r)]\Big\}
\end{aligned}
\tag{A2.7}
$$

Multiplying equation A2.4 by $A_p\sin(\omega_p t)$ results in:

$$
\begin{aligned}
S2(t) &= \frac{1}{4}A_p\Big\{A_f[-\cos(\omega_p t - \omega_f t - \phi_f) \\
&+ \cos(\omega_p t + \omega_f t + \phi_f)] + A_r[\cos(\omega_p t - \omega_r t + \phi_r) \\
&- \cos(\omega_p t + \omega_r t - \phi_r)]\Big\}
\end{aligned}
\tag{A2.8}
$$

Finally, adding equations A2.7 and A2.8 gives:

$$
\begin{aligned}
S3(t) &= S1(t) + S2(t) \\
&= \frac{A_p}{2}\Big\{A_f\cos[(\omega_p + \omega_f)t + \phi_f] \\
&+ A_r\cos[(\omega_p - \omega_r)t + \phi_r)]\Big\}
\end{aligned}
\tag{A2.9}
$$

enabling ω_f and ω_r to be easily distinguished in relation to the known ω_p.

Appendix 3: Program Listings for the Wallingford FLUIDMUDFLOW-2D Software

A3.1 FLUIDMUDFLOW-2D SUBROUTINES AS FIRST IMPLEMENTED BY THE AUTHOR

In the following listings, lowercase type is used to indicate code received from Hydraulics Research Wallingford Limited. The author's alterations made so as to implement the FLUIDMUDFOW-2D software for the current investigation are shown in UPPERCASE.

Comments written in lowercase are from Hydraulics Research and do not necessarily apply to the author's implementation of the routines.

For details of the function of each subroutine, see table 7.1, chapter 7.

A3.1.1 SUBROUTINE BEDSUM

```
c*************************************************************
      SUBROUTINE BEDSUM(bed,bedl,nbedlayers,kmax)
c*************************************************************
c
c   This routine adds up the mud in each of the bed layers to
c    give  a total deposit for each cell (kg/m*m)
c
c    Arguments
c    =========
c
c    bed                 total deposits
c    bedl                deposits in each layer
c    nbedlayers          number of bed layers
c    kmax                number of active cells
c
c
c-------------------------------------------------------------

      real bed(kmax),bedl(kmax*nbedlayers)

      do 100,k=1,kmax
        total = 0.0
        do 200,l=1,nbedlayers
          total = total + bedl(((l-1)*kmax)+k)
 200    continue
        bed(k) = total
 100  continue

      return

      end
```

A3.1.2 SUBROUTINE CONCENTRATION

```
c*******************************************************************
      SUBROUTINE CONCENTRATION(c,d,fx,fy,
     1                         flagz,karray,m,n,mn,kmax)
c*******************************************************************
c
c This subroutine calculates the change in concentration of
c suspended mud at each active cell, due to the net water flux
c into the cell and the exchange of mud between suspension,
c the fluid mud layer and the bed.
c
c
c   Arguments
c   =========
c  c          suspended mud concentration
c  d          water depth
c  fx,fy      water flux (kg/m*m)
c  flagz      usual
c  karray     as usual
c  m          no. of cells in each row
c  n          no. of cells in each column
c  mn         m*n
c  kmax       no. of active cells
c
c-------------------------------------------------------------------
      real c(kmax),d(kmax),fx(kmax),fy(kmax)
      integer  karray(mn)
      integer flagz(kmax)
c
c
      do 100, kij = 1, mn
c  find location of current cell
        k = karray(kij)
c  if cell is inactive  or no water then skip it
        if ((k .le. 1) .or. (d(k).le.0.0))goto 100
        if (flagz(k).eq.1) then
c
c
c  find location of neighbours to N, W
          kn = karray(kij-m)
          kw = karray(kij-1)
c  change in concentration due to net flux  - note that effect
c  of mud exchange between layers is dealt with in subroutine mudexchange
c  Note that mudexchange leaves us with conc at NEW depth
          c(k) = c(k) + (fx(kw) - fx(k) + fy(k)
     1                -fy(kn))/d(k)
c
        endif
100   continue
c
      return
c
      end
c
c-------------------------------------------------------------------
```

A3.1.3 SUBROUTINE CONSOLIDATION

```
c**********************************************************************
      SUBROUTINE CONCENTRATION(c,d,fx,fy,
     1                         flagz,karray,m,n,mn,kmax)
c**********************************************************************
c
c This subroutine calculates the change in concentration of
c suspended mud at each active cell, due to the net water flux
c into the cell and the exchange of mud between suspension,
c the fluid mud layer and the bed.
c
c
c   Arguments
c   =========
c  c          suspended mud concentration
c  d          water depth
c  fx,fy      water flux (kg/m*m)
c  flagz      usual
c  karray     as usual
c  m          no. of cells in each row
c  n          no. of cells in each column
c  mn         m*n
c  kmax       no. of active cells
c
c----------------------------------------------------------------------
      real c(kmax),d(kmax),fx(kmax),fy(kmax)
      integer  karray(mn)
      integer flagz(kmax)
c
c
      do 100, kij = 1, mn
c  find location of current cell
         k = karray(kij)
c  if cell is inactive  or no water then skip it
        if ((k .le. 1) .or. (d(k).le.0.0))goto 100
        if (flagz(k).eq.1) then
c
c
c  find location of neighbours to N, W
          kn = karray(kij-m)
          kw = karray(kij-1)
c  change in concentration due to net flux  - note that effect
c  of mud exchange between layers is dealt with in subroutine mudexchange
c  Note that mudexchange leaves us with conc at NEW depth
          c(k) = c(k) + (fx(kw) - fx(k) + fy(k)
     1                -fy(kn))/d(k)
c
        endif
100   continue
c
      return
c
      end
c
c----------------------------------------------------------------------
```

A3.1.4 SUBROUTINE BEDSTRESS

```
c*************************************************************
      subroutine bedstress(taubed,tbed,um,vm,dm,flagmud,flagz,flagu,
     1           flagv,viscmud,cmud,c0,rhow,karray,m,n,mn,kmax,mudon)
c*************************************************************
c
c
c This subroutine calculates the shear stress at the bed. If no
c mud is present, the shear stress induced by the water is
c calculated  in the subroutine 'interfacestress';
c if fluid mud is present, it is assumed to be a turbulent
c boundary layer with a viscous sub-layer. A fluid mud Reynolds
c number is evaluated to ascertain if the whole mud layer is
c non-turbulent -- i.e if the thickness of the viscous sub-layer
c is equal to the full mud layer thickness.
c
c
c   Arguments
c   =========
c   taubed      bed stress at each active cell
c   tbed        bed stress/modulus of velocity
c   um,vm       fluid mud velocity
c   dm          fluid mud depth
c   flagmud     =1 if fluid mud present
c   flagz       usual
c   flagu
c   flagv
c   viscmud     kinematic viscosity of fluid mud
c   cmud        concentration of fluid mud
c   rhow        density of water
c   karray
c   m
c   n
c   mn
c   kmax        no. of active cells
c   mudon       fluid mud switch
c
c
c
c
c-------------------------------------------------------------
c
      real      taubed(kmax),um(kmax),vm(kmax),dm(kmax),tbed(kmax)
      real cmud(kmax)
      logical  mudon
      integer flagmud(kmax)
      integer  flagz(kmax),flagu(kmax),flagv(kmax),karray(mn)
c
      if (.not.mudon) return
c  viscosity of water
      viscw = 1e-6
      gamma = (alog(viscmud/viscw))/c0
      rcrit1 = 46.0
      rcrit2 = 1200
      dmin = 0.01
      do 100, kij=1,mn
        k = karray(kij)
        if (k.le.1) goto 100
        kn = karray(kij-m)
        kw = karray(kij-1)
        if ((flagmud(k).eq.1).and.(flagz(k).gt.0)) then
c
          if (dm(k).lt.dmin) then
            taubed(k) = 0.0
            tbed(k) = 0
            goto 100
```

```
          endif
          rhom = rhow + 0.62*cmud(k)
          viscm = viscw*exp(gamma*cmud(k))
          if ((flagmud(kw).le.0).or.(flagu(kw).le.0)) then
            uu = um(k)
            if (flagu(k).le.0) uu= 0
          else if (flagu(k).le.0) then
            uu = um(kw)
          else
            uu = 0.5*(um(k)+um(kw))
          endif
          if ((flagmud(kn).le.0).or.(flagv(kn).le.0)) then
            vv = vm(k)
            if (flagv(k).le.0) vv= 0
          else if (flagv(k).le.0) then
            vv = vm(kn)
          else
            vv = 0.5*(vm(k) + vm(kn))
          endif
c
          vel = sqrt(uu*uu + vv*vv)
c
c
          rmud = vel*dm(k)/viscm
c         write (2,*) rmud
          if (rmud .lt. rcrit1) then
c
c   calculate stress due to viscous sub-layer
c
            tt = 3*rhom*viscm/dm(k)
            tbed(k) = tt
            taubed(k) = vel*tt
          else if (rmud .lt. rcrit2) then
            rlog = (alog10(rmud))**(-0.88)
            ff = 188250*((0.01*(10**rlog))**4.74)
            tt = rhom*ff*vel
            tbed(k) = tt
            taubed(k) = tt*vel
          else
            rlog = (alog10(rmud))**(-1.23)
            ff = 57.5*((0.05*(10**rlog))**4)
            tt = rhom*ff*vel
            tbed(k) = tt
            taubed(k) = tt*vel
          endif
        else
c   no mud present or flagz.le.0:
          taubed(k) = 0
          tbed(k) = 0
        endif
c       write (2,*) ff
100   continue
c
      return
c
      end
c
```

A3.1.5 SUBROUTINE INTERFACESTRESS

```
c*****************************************************************
      SUBROUTINE INTERFACESTRESS(delu,delv,d,flagmud,flagz,flagu,
     1          flagv,taui,ti,ffm, ffb, cmud, rhow, karray,m,n,mn,kmax)
c*****************************************************************
c
c
c  subroutine to calculate x and y components of interface
c  stress between fluid mud layer and overlying water or
c  between water and bed if no fluid mud present
c
c      Arguments
c      =========
c  delu, delv   x,y cpts of velocity difference between water
c               and fluid mud-- see subroutine "vdiff"
c  d       water depth
c  flagmud =1 if fluid mud present
c  flagz   usual
c  flagu
c  flagv
c  taui    stress at interface
c  ti      stress/modulus of velocity difference
c  ffm     friction factor for mud-water interface stress
c  ffb     friction factor for water-bed interface stress
c  rhow    density of water
c  cmud    concentration of fluid mud
c    Note that density of fluid mud, rhom = rhow + 0.62*cmud
c  karray  usual
c  m       no. of cells in each row
c  n       no. of cells in each column
c  mn      m*n
c  kmax    no. of active cells
c
c
c
c-----------------------------------------------------------------
c
c
      real delu(kmax), delv(kmax), d(kmax),cmud(kmax)
      real taui(kmax),ti(kmax)
      integer flagmud(kmax)
      integer flagz(kmax),karray(mn),flagu(kmax),flagv(kmax)
c
c
c   loop through all active cells
c
      do 100, kij = 1, mn
        k = karray(kij)
        if (k.le.1) goto 100
      if ((flagz(k).gt.0).and.(d(k).gt.0)) then
        kn = karray(kij-m)
        kw = karray(kij-1)
c
c    if fluid mud present, calculate mud-water interface stress,
c      if not, calculate water-bed stress
c      If no mud present then delu,delv are just water velocity
c
      du = 0.5*(delu(k)+delu(kw))
      if (flagu(k).ne.1) du = delu(kw)
      if (flagu(kw).ne.1) du = delu(k)
      dv = 0.5*(delv(k)+delv(kn))
      if (flagv(k).ne.1) dv = delv(kn)
      if (flagv(kn).ne.1) dv = delv(k)
      velsq = du*du + dv*dv
      rhom = rhow + 0.62*cmud(k)
      if (flagmud(k).eq.1) then
```

```
        tt = ffm*rhom/8
      else
        tt = ffb*rhow/8
      endif
      taui(k) = tt*velsq
      ti(k) = tt*sqrt(velsq)
      else
c flagz.le.0:
        taui(k)=0
        ti(k) = 0
      endif
c
100   continue
c
c
      return
c
      end
```

A3.1.6 SUBROUTINE MUDDEPTH

```
c*******************************************************************
      SUBROUTINE MUDDEPTH(dm,fmx,fmy,d,bed,cmud,c,c0,beta,flagz,
     1                    karray,m,n,mn,kmax,mudon)
c*******************************************************************
c
c
c This routine calculates the change in depth of the fluid mud layer
c at each active cell due to the net flow of mud into the cell
c and the exchange of mud between the bed, the fluid mud and the
c overlying water, assuming that the fluid mud has a constant
c concentration, c0.
c
c
c
c     Arguments
c     =========
c  dm             mud depth
c  fmx,fmy        mud flux through E,S faces of each cell
c  cmud           concentration of fluid mud
c  c0             max conc of fluid mud
c  c              suspended mud concentration
c  beta           concentration factor
c  flagz          usual
c  karray         as usual
c  m              no. of cells in each row
c  n              no. of cells in each column
c  mn             m*n
c  kmax           no. of active cells
c  mudon          fluid mud switch
c
c
c-------------------------------------------------------------------
c
      real dm(kmax),fmx(kmax),fmy(kmax),bed(kmax),d(kmax),cmud(kmax)
      real c(kmax)
      integer karray(mn)
      integer flagz(kmax)
      logical mudon
c
      if (.not.mudon) return
      do 100, kij = 1,mn
c find location of current cell
        k = karray(kij)
c if cell is inactive then skip it
        if (k.NE.1) then
c
c find location of neighbours to N, W
          kn = karray(kij-m)
          kw = karray(kij-1)
c change in mud depth due to mud flux: (note fluxes in kg/m*m)
          olddm = dm(k)
c note:totalmud is mass of mud per unit area
          TNEWMUD=(fmx(kw) - fmx(k) + fmy(k) - fmy(kn))
          totalmud = (dm(k)*cmud(k)) + (fmx(kw) -
     1       fmx(k) + fmy(k) - fmy(kn))
          if (totalmud .le.0) then
            dm(k) = 0
            cmud(k) = 0
          else IF (TNEWMUD.GT.0) THEN
            DNEWMUD=TNEWMUD/C0
            dm(k) = DM(K)+DNEWMUD
            cmud(k) = TOTALMUD/DM(K)
          ELSE
            IF (CMUD(K).LE.0) CMUD(K)=C0
            DM(K)=TOTALMUD/CMUD(K)
```

```
          endif
          if ((d(k).le.0.001).and.(dm(k).gt.0)) then
            bed(k) = bed(k) + dm(k)*cmud(k)
            dm(k) = 0
            CMUD(K)=0.0
          endif
        ELSE
          DM(K)=0.0
          CMUD(K)=0.0
        endif
c note convention that fluxes are positive to the  east and to the north,
c but i and j increase to the east and south respectively.
c
c change in mud depth due to mud exchange between layers is already
c done in subroutine mudexchange
c
100   continue
c
      return
c
      end
c
c-----------------------------------------------------------------------
```

A3.1.7 SUBROUTINE MUDEXCHANGE

```
c**********************************************************************
      SUBROUTINE MUDEXCHANGE(BED,bedl,c,d,oldd,dm,delu,delv,um,vm,cmud,
     1                       taubed,taui,flagz,flagu,flagv,flagmud,
     2                       rhom,rhow,taud,taudm,taue,tauem,dt,c0,v0,
     3                       beta,wset,wsmin,srate,erate,karray,m,n,mn,
     4                       kmax,ilayer,nbedlayers,mudon)
c**********************************************************************
c
c
c   This routine calculates the exchange of mud between three layers:
c              bed
c              fluid mud
c              suspended mud,
c   by means of seven processes:
c              erosion of bed by water
c              erosion of bed by fluid mud
c              settling of suspended mud onto fluid mud
c              settling of suspended mud onto bed
c              entrainment of fluid mud by water
c              erosion of fluid mud by water
c              dewatering of fluid mud.
c   Having calculated the mass of mud per square metre transferred
c   by these processes, the change in the bed deposit (kg/m*m), the
c   suspended mud concentration (kg/m*m*m) and the fluid mud depth (m)
c   are calculated. The fluid mud is assumed to have a constant
c   concentration, c0.
c
c
c      Arguments
c      =========
c  bed              mud deposits on bed (kg/m*m)
c  c                suspended mud concentration (kg/m*m*m)
c  d                water depth (m)
c  oldd             water depth at previous sub-timestep
c  dm               fluid mud depth (m)
c  delu,delv        water velocity - fluid mud velocity (m/s)
c  cmud             fluid mud concentration
c  taubed           stress on bed DUE TO FLUID MUD only (kg/m*s*s)
c  taui             stress on fluid mud or bed due to water ( " )
c  flagz            usual flag, = 1 if active cell
c  flagu
c  flagv
c  flagmud          =1 if fluid mud depth > 0
c  rhom,rhow        density of fluid mud, water
c  taud             critical stress for deposition  onto bed
c  taudm            critical stress for deposition onto fluid mud
c  taue             critical stress for erosion of bed - one value
c                     for each layer
c  tauem            critical stress for erosion of fluid mud layer
c                       by overlying water
c  dt               sub timestep duration
c  c0               max concentration of fluid mud (kg/m*m*m)
c  v0               dewatering velocity (m/s)
c  beta             concentration factor
c  wset             coefficient for settling velocity(m*m*m*m/kg*s)
c  wsmin            minimum settling velocity (m/s)
c  srate            settling rate
c  karray           usual
c  m                no. of cells in each row
c  n                no. of cells in each column
c  mn               m*n
c  kmax             number of active cells
c  nbedlayers       number of layers of bed deposits
c  mudon            fluid mud switch - if .false. then no fluid mud allowed
c
```

```
c-------------------------------------------------------------------
c  set constants
      parameter(g    = 9.81)
      parameter(dmin = 0.01)
      parameter(tiny = 1E-8)
c
      integer flagz(kmax),flagu(kmax),flagv(kmax),karray(mn)
      integer ilayer(kmax)
      logical mudon
      integer flagmud(kmax)
      real delu(kmax),delv(kmax),dm(kmax),um(kmax),vm(kmax)
      real taubed(kmax),taui(kmax),c(kmax),d(kmax)
      real oldd(kmax),bedl(kmax*nbedlayers)
      real cmud(kmax)
      real taue(nbedlayers)
      REAL BED(KMAX),MASSK,MASSKNEW,TOTMASS,TOTMASSN
c
c
c     delrho = rhom-rhow
c     write(*,*) 'posn| dew  | entr  | eroA  | eroB  | setA  | setB  |
c    1taui  | tbed  | delu  | delv  |  um   |  vm   |   d   |   dm |
c    2wblt  | cmud  | bed'
c
c     k1 = karray((m*37)+13)
c     k2 = karray((m*18)+76)
c     k3 = karray((m*7)+87)
c     k4 = karray((m*73)+5)
c     k5 = karray((m*44)+30)
c     k6 = karray((m*34)+50)
c     k7 = karray((m*83)+32)
c     k8 = karray((m*52)+40)
c     k9 = karray((m*69)+33)

      TOTMASS=0.0
      TOTMASSN=0.0
      do 100, kij=1,mn
        k = karray(kij)
c  initialise exchange variables
        flmud2bed  = 0.0
        bed2flmud  = 0.0
        flmud2susp = 0.0
        susp2flmud = 0.0
        bed2susp   = 0.0
        susp2bed   = 0.0
c
c temporary variables to cut down on array look-ups
        tb = taubed(k)
        ti = taui(k)
        cc = c(k)
        cm = cmud(k)
        ddm = dm(k)
        layer = ilayer(k)
        kk = (layer-1)*kmax + k
        if ((flagmud(k).eq.1).and.(mudon)) then
C
        if ((flagz(k) .eq. 1).and.(d(k).gt.0)) then
c
c  fluid mud present
c  *****************
c
c-------------------------------------------------------
c   erosion by fluid mud
c-------------------------------------------------------
c  Note: layer = 0 means that there are no mud deposits
          if (layer.ne.0)  then
           IF (tB.gt.taue(layer)) THEN
             bd = bedl(kk)
```

```
              bed2flmud = dt*erate*(tb-taue(layer))
c check there's enough mud on bed
              if (bed2flmud.gt.bd) bed2flmud=bd
            endif
          ENDIF
c
c-------------------------------------------------
c   dewatering
c-------------------------------------------------
            if (tb .lt. taud) then
              flmud2bed = v0*cm*dt
            endif
c-------------------------------------------------
c   entrainment
c-------------------------------------------------
c  Only allow entrainment or erosion if fluid mud is more concentrated
c  than overlying water
            if (cm.gt.cc) then
              kn = karray(kij-m)
              kw = karray(kij-1)
              du = 0.5*(delu(k)+delu(kw))
              if (flagu(k).ne.1) du = delu(kw)
              if (flagu(kw).ne.1) du = delu(k)
c note if both flagu entries are .ne.1 then get du = 0.
              dv = 0.5*(delv(k)+delv(kn))
              if (flagv(k).ne.1) dv = delv(kn)
              if (flagv(kn).ne.1) dv = delv(k)
              dmud = ddm
              diffsq = du*du + dv*dv
              if (dmud .lt. dmin) dmud = dmin
              if (diffsq .gt. tiny) then
                delrho = 0.62*cm
                rich = delrho*g*dmud/diffsq
                if (rich .lt. 10.0) then
c  entrainment velocity
                  ve = 0.1*sqrt(diffsq)/((1+63*rich*rich)**0.75)
                  flmud2susp = dt*ve*cm
                endif
              endif
c if entrainment is less than erosion of fluid mud, assume that
c erosion takes place instead:
              erosion = dt*erate*(ti-tauem)
              if (erosion .lt. 0) erosion = 0.0
              if (erosion .gt. flmud2susp) flmud2susp = erosion
c
c check there's enough fluid mud for both dewatering and entrainment
c  (or erosion)
              totalmud = flmud2bed + flmud2susp
              available = ddm*cm
              if (totalmud .gt. available) then
                flmud2bed = flmud2bed*available/totalmud
                flmud2susp = flmud2susp*available/totalmud
              endif
c
            endif
c-------------------------------------------------
c   settling onto fluid mud
c-------------------------------------------------
            if (ti.lt.taudm) then
              ws = cc*wset
              if (ws .lt. wsmin) ws = wsmin
              susp2flmud = srate*cc*ws*(taudm-ti)
C             SUSP2FLMUD = SRATE*CC*WS
c  check there's enough mud in suspension
              if (susp2flmud.gt.(cc*d(k))) susp2flmud=cc*d(k)
            endif
c
```

```
          endif
c
          else
c
c no fluid mud present
c ********************
c
c-------------------------------------------------------
c   erosion by water
c-------------------------------------------------------
           if (layer.ne.0)  then
            IF (ti.gt.taue(layer)) THEN
             bd = bedl(kk)
               bed2susp = dt*erate*(ti-taue(layer))
c  check there's enough mud on the bed
               if (bed2susp.gt.bd) bed2susp = bd
            ENDIF
           endif
c
c-------------------------------------------------------
c   settling
c-------------------------------------------------------
           if (ti .lt. taud) then
             ws = cc*wset
             if (ws .lt. wsmin) ws = wsmin
             settling = srate*cc*ws*(taud-ti)
C            SETTLING = SRATE*CC*WS
             totalsusp = cc*d(k)
c  check that there's enough mud in suspension
             if (settling .gt. totalsusp) settling = totalsusp
c  if it settles quickly, some will form fluid mud
             if ((settling .gt. (v0*c0*dt)).and.(mudon)) then
               susp2bed = v0*c0*dt
               susp2flmud = settling - susp2bed
             else
               susp2bed = settling
             endif
c
           endif
c
c-------------------------------------------------------
         endif
c
c
c now calculate changes in depth, concentration, bed deposits
c
C CALCULATE ORIGINAL MASS OF MUD AT LOCATION K

      MASSK=BED(K)+(C(K)*D(K))+(DM(K)*CMUD(K))

c  deposition onto top layer (ie layer 1):
         bedl(k) = bedl(k) + susp2bed + flmud2bed
c  erosion from erosion layer  -- if layer = 0, no mud to erode
         if (layer .ne. 0) then
           bedl(kk) = bedl(kk) - bed2flmud - bed2susp
         endif
c  reset erosion layer pointer:
         ilayer(k) = 0
         do 750,i=nbedlayers,1,-1
           kk = (i-1)*kmax + k
           if (bedl(kk).gt.0) ilayer(k) = i
 750     continue
         c(k) = (oldd(k)*cc + flmud2susp + bed2susp -
     1              susp2flmud - susp2bed)/d(k)
         totalmud = ddm*cm +susp2flmud+bed2flmud-flmud2susp-
     1               flmud2bed
         olddm = ddm
```

```
          if (totalmud.le.0) then
            dm(k) = 0
            cmud(k) = 0
          else
            dm(k) = totalmud/c0
            cmud(k) = c0
          endif

C CALCULATE NEW MASS OF MUD AT LOCATION K

      MASSKNEW=BED(K)+(C(K)*D(K))+(DM(K)*CMUD(K))
      TOTMASS=TOTMASS+MASSK
      TOTMASSN=TOTMASSN+MASSKNEW


c
100   continue
C      WRITE (2,9999) TOTMASS,TOTMASSN,(TOTMASSN-TOTMASS)
c
C9999  format(1X,11HMUDEXCHANGE,3(3X,f7.2))
      return
c
      END
```

A3.1.8 SUBROUTINE MUDFLUX

```
c*****************************************************************
      SUBROUTINE MUDFLUX(fmx,fmy,dm,um,vm,cmud,flagmud,
     1                   flagu,flagv,karray,m,n,mn,DTBYDX,kmax,mudon)
c*****************************************************************
c
c    This subroutine calculates the flux of fluid mud through
c    the south and east edges of each active cell in the system
c     using the depth of mud in the upstream cell
c
c    Arguments
c    =========
c  fmx           x-cpt of fluid mud flux (in kg/m*m)
c  fmy           y-cpt "    "    "   "
c  dm            depth of fluid mud layer
c  um,vm         velocity of fluid mud
c  cmud            fluid mud concentration (kg/m*m*m)
c  flagmud       =1 if mud present
c  flagu         as usual
c  flagv         as usual
c  karray        as usual
c  m             no. of cells in each row
c  n             no. of cells in each column
c  mn            m*n
c  dtbydx      timestep/grid spacing. Note that grid spacing is
c                 the same in both x and y directions
c  kmax          no. of active cells in system
c  mudon         fluid mud switch
c
c---------------------------------------------------------------
c
      real fmx(kmax),fmy(kmax),dm(kmax),um(kmax),vm(kmax),cmud(kmax)
      integer karray(mn)
      logical mudon
      integer flagu(kmax),flagv(kmax),flagmud(kmax)
c
      if (.not.mudon) return
      do 100, kij = 1, mn
c  find location of current cell
        k = karray(kij)
c  if cell is inactive then skip it
        if (k .le. 1) goto 100
c find location of neighbours to E,S
        ke = karray(kij+1)
        ks = karray(kij+m)
c  temporary variables
        dd = dm(k)
        dds = dm(ks)
        dde = dm(ke)
        uu = um(k)
        vv = vm(k)
c  calculate x-cpt of mud flux (+ve east)
        if (flagu(k) .ne. 0) then
c note: if flagz(k).eq.0 then flagmud(k)=0 so don't
c need to test explicitly for flagz.
          if ((uu.gt.0).and.(flagmud(k).eq.1.AND.KE.GT.1)) then
            fmx(k) = dtbydx*uu*dd*cmud(k)
C            fmx(k) = dt*uu*cmud(k)
          else if ((uu.lt.0).and.(flagmud(ke).eq.1.AND.KE.GT.1)) then
            fmx(k) = dtbydx*uu*dde*cmud(ke)
C            fmx(k) = dt*uu*cmud(ke)
          else
            fmx(k) = 0
          endif
        else
c  flagu .le. 0
```

```
          fmx(k) = 0
        endif
c calculate y-cpt of mud flux (+ve north)
        if (flagv(k).ne.0) then
c see note above about flagz
          if ((vv.gt.0).and.(flagmud(ks).eq.1.AND.KS.GT.1)) then
            fmy(k) = dtbydx*vv*dds*cmud(ks)
C            fmy(k) = dt*vv*cmud(ks)
          else if ((vv.lt.0).and.(flagmud(k).eq.1.AND.KS.GT.1)) then
            fmy(k) = dtbydx*vv*dd*cmud(k)
C            fmy(k) = dt*vv*cmud(k)
          else
            fmy(k) = 0
          endif
        else
c  flagv .le. 0
          fmy(k)=0
        endif
100   continue
c
      return
c
      end
```

A3.1.9 SUBROUTINE MUDVEL

```
c*********************************************************************
      SUBROUTINE MUDVEL(um,vm,u,v,dm,d,oldd,h,hu,hv,flagu,
     1                  flagv,tbed,ti,dtbydx,dt,cmud,rhow,
     2                  omega,karray,m,n,mn,kmax,mudon)
c*********************************************************************
c
c
c  This subroutine calculates the velocity of fluid mud at each active
c  cell. If no fluid mud is present, the velocity is set to zero.
c    Note that um is +ve to the east, vm is +ve to the north,
c  i increases to the east, j increases to the south.
c
c     Arguments
c     =========
c  um,vm        fluid mud velocity
c  delu,delv    difference in velocity between mud and water
c  u,v          water velocity
c  dm           depth of fluid mud layer
c  d            depth of water (above bed, rather than above fluid mud)
c  oldd         depth at previous sub-timestep (velocities are calculated
c                  at half time-steps)
c  h            max depth of bed (+ve below datum)
c  hu,hv        depth of bed at u, v edges of cell
c  flagu,flagv, as usual
c  tbed      bed stress/mud velocity modulus
c  taui         mud-water interface stress/velocity difference modulus
c  dtbydx       timestep divided by grid spacing
c  dt           timestep
c  cmud         fluid mud concentration
c  rhow         water density
c  omega        Coriolis coefficient
c  karray       as usual
c  m            no. of cells in each row
c  n            no. of cells in each column
c  mn           m*n
c  kmax         no. of active cells
c  mudon        fluid mud switch
c
c
c--------------------------------------------------------------------
c
      real um(kmax),vm(kmax),dm(kmax),d(kmax),h(kmax)
      real oldd(kmax),hu(kmax),hv(kmax)
      real tbed(kmax),ti(kmax),cmud(kmax)
      real u(kmax),v(kmax)
      integer karray(mn)
      logical mudon
      integer flagu(kmax),flagv(kmax)
c
      if (.not.mudon) return
c accel. due to gravity
      g = 9.81
      tiny = 1E-8
c  minimum fluid mud depth:
      dmin = 0.01
c
      do 100, kij = 1, mn
c location of current cell
        k = karray(kij)
c if cell is inactive then skip it
        if (k .le. 1) goto 100
        ks = karray(kij+m)
        ke = karray(kij+1)
c--------------------------------------------------------------------
c  Calculate u velocity
```

```
        dd = d(k)
        de = d(ke)
        if ((flagu(k).eq.0).or.(dd.le.dmin).or.(de.le.dmin)) then
          um(k) = 0
        else
          dmm = dm(k)
          dme = dm(ke)
          hh = h(k)
          he = h(ke)
          uu = um(k)
          vv = vm(k)
          dep = 0.25*(dd+de+oldd(k)+oldd(ke)) -
     1          0.5*(hh+he) + hu(k)
          if (dep.le.dmin) then
c  ...                 water too shallow to flow
            um(k) = 0
          else
            if ((dmm.le.dmin).and.(dme.le.dmin)) then
c  ...                 mud too shallow to go anywhere
              um(k) = 0
            elseif ((dmm.gt.dmin).and.(dme.gt.dmin))then
c   ...                                 Mud in both cells
              tti = 0.5*(ti(k) + ti(ke))
              ttb = 0.5*(tbed(k)+tbed(ke))
              drhom = 0.62*cmud(k)
              drhome = 0.62*cmud(ke)
              avdrhomu = 0.5*(drhom+drhome)
              ddu = 2*dt/((dmm*(rhow+drhom)) + (dme*(rhow+drhome)))
              gdu = g/(rhow+avdrhomu)
              eta = dd-hh
              etae = de-he
              etam = dmm - hh
              etame = dme - he
              diffu = rhow*(etae - eta) + avdrhomu*(etame - etam) +
     1             0.25*(dmm+dme)*(drhome-drhom)
              um(k) = (uu - gdu*dtbydx*diffu  +
     1             omega*vv*dt + ddu*tti*u(k))/(1.0 + ddu*(ttb+tti))
c
            elseif ((dmm.gt.dmin).and.(dme.le.dmin))then
c  ...                                 Mud in current cell but none to east
              tti = ti(k)
              ttb = tbed(k)
              drhom = 0.62*cmud(k)
              ddu = dt/(dmm*(rhow+drhom))
              gdu = g/(rhow+drhom)
              eta = dd-hh
              etae = de - he
              etam = dmm - hh
c   NB dme = 0
              etame = - he
              diffu = rhow*(etae-eta)+drhom*(etame-etam) -
     1                0.5*dmm*drhom
              um(k) = (uu - gdu*dtbydx*diffu  +
     1             omega*vv*dt + ddu*tti*u(k))/(1.0 + ddu*(ttb+tti))
c  ...                                  Don't allow mud to flow westward
              if (um(k).lt.0.0) um(k) = 0.0
c
            elseif ((dmm.le.dmin).and.(dme.gt.dmin))then
c  ...                                  No mud in current cell but mud to east
              tti = ti(ke)
              ttb = tbed(ke)
              drhome = 0.62*cmud(ke)
              ddu = dt/(dme*(rhow+drhome))
              gdu = g/(rhow+drhome)
              eta = dd - hh
              etae = de - he
c  NB dmm = 0
```

```
              etam = - hh
              etame = dme - he
              diffu = rhow*(etae-eta)+drhomE*(etame-etam) +
     1                 0.5*dme*drhome
              um(k) = (uu - gdu*dtbydx*diffu  +
     1            omega*vv*dt + ddu*tti*u(k))/(1.0 + ddu*(ttb+tti))
c  ...                                    Don't allow mud to flow west
              if (um(k).gt.0.0) um(k) = 0.0
            endif
c
          endif
c
        endif
c end of u velocity section
c-----------------------------------------------------------------------
c  Calculate v velocity
        dd = d(k)
        ds = d(ks)
        if ((flagv(k).eq.0).or.(dd.le.dmin).or.(ds.le.dmin)) then
          vm(k) = 0
        else
          dmm = dm(k)
          dms = dm(ks)
          hh = h(k)
          hs = h(ks)
          uu = um(k)
          vv = vm(k)
          dep = 0.25*(dd+ds+oldd(k)+oldd(ks)) -
     1          0.5*(hh+hs) + hv(k)
          if (dep.le.dmin) then
c  ...                 water too shallow to flow
            vm(k) = 0
          else
            if ((dmm.le.dmin).and.(dms.le.dmin))then
c   ...                                 No mud in either cell
              vm(k) = 0
c
            elseif ((dmm.gt.dmin).and.(dms.gt.dmin))then
c   ...                                  Mud in both cells
              tti = 0.5*(ti(k) + ti(ks))
              ttb = 0.5*(tbed(k)+tbed(ks))
              drhom = 0.62*cmud(k)
              drhoms = 0.62*cmud(ks)
              avdrhomv = 0.5*(drhom+drhoms)
              ddv = 2*dt/((dmm*(rhow+drhom)) + (dms*(rhow+drhoms)))
              gdv = g/(rhow+avdrhomv)
              eta = dd-hh
              etas = ds-hs
              etam = dmm - hh
              etams = dms - hs
              diffv = rhow*(eta - etas) + avdrhomv*(etam - etams) +
     1                0.25*(dmm+dms)*(drhom-drhoms)
              vm(k) = (vv -gdv*dtbydx*diffv -
     1            omega*uu*dt + ddv*tti*v(k))/(1.0 + ddv*(ttb+tti))
c
            elseif ((dmm.gt.dmin).and.(dms.le.dmin))then
c  ...                               Mud in current cell but none to south
              tti = ti(k)
              ttb = tbed(k)
              drhom = 0.62*cmud(k)
              ddv = dt/(dmm*(rhow+drhom))
              gdv = g/(rhow+drhom)
              eta = dd-hh
              etas = ds - hs
              etam = dmm - hh
c   NB dms = 0
              etams = - hs
```

```
                diffv = rhow*(eta - etas) + drhom*(etam - etams) +
     1               0.5*dmm*drhom
                vm(k) = (vv -gdv*dtbydx*diffv -
     1              omega*uu*dt + ddv*tti*v(k))/(1.0 + ddv*(ttb+tti))
c  .. Don't allow mud to flow north
                if (vm(k).gt.0.0) vm(k) = 0.0
c
              elseif ((dmm.le.dmin).and.(dms.gt.dmin))then
c  ...                                  No mud in current cell but mud to south
                tti = ti(ks)
                ttb = tbed(ks)
                drhoms = 0.62*cmud(ks)
                ddv = dt/(dms*(rhow+drhoms))
                gdv = g/(rhow+drhoms)
                eta = dd - hh
                etas = ds - hs
c  NB dmm = 0
                etam = - hh
                etams = dms - hs
                diffv = rhow*(eta - etas) + drhomS*(etam - etams) -
     1               0.5*dms*drhoms
                vm(k) = (vv -gdv*dtbydx*diffv -
     1              omega*uu*dt + ddv*tti*v(k))/(1.0 + ddv*(ttb+tti))
c  ...  Don't allow mud to flow south
                if (vm(k).lt.0.0) vm(k) = 0.0
              endif
c
            endif
c
          endif
c end of v velocity section
c-----------------------------------------------------------------------
c  ...                      end of loop over kij
 100  continue
c
      return
c
      end
c
c-----------------------------------------------------------------------
```

A3.1.10 SUBROUTINE SETFLAGMUD

```
c*****************************************************************
      SUBROUTINE SETFLAGMUD(flagmud,dm,kmax,mudon)
c*****************************************************************
c
c
c   Arguments
c   =========
c   flagmud   integer array-- 1 if fluid mud present, 0 if not
c   dm        depth of fluid mud
c   kmax      number of active cells
c   mudon     fluid mud switch
c
c-----------------------------------------------------------------
c
c
      logical mudon
      integer flagmud(kmax)
      real dm(kmax)
      tiny = 1E-6
c
      if (.not.mudon) return
      do 100,k=2,kmax
        if (dm(k).gt.tiny) then
          flagmud(k) = 1
        else
          flagmud(k) = 0
        endif
100   continue
c
      return
c
      end
```

A3.1.11 SUBROUTINE VDIFF

```
c*******************************************************************
      SUBROUTINE VDIFF(delu,delv,u,v,um,vm,flagmud,kmax)
c*******************************************************************
c
c
c     This subroutine calculates the difference in velocity between the
c     fluid mud and the overlying water. If no mud is present, the
c     fluid mud velocity is zero and the difference becomes simply
c     the velocity of the water.
c
c     Note: if flagu<1    or flagv<1   then corresponding
c     velocities u,um or v,vm are zero so delu or delv is zero.
c
c     Arguments
c     =========
c  delu,delv      x,y cpts of velocity difference
c  u,v             "   "   of water velocity
c  um,vm           "   "   of fluid mud velocity
c  flagmud        =1 if mud present
c  kmax           no. of active cells present
c  mudon          fluid mud switch
c-------------------------------------------------------------------
c
      real delu(kmax),delv(kmax),u(kmax),v(kmax)
      real um(kmax),vm(kmax)
      integer flagmud(kmax)
c
      do 100,k=2,kmax
        if  (flagmud(k).eq.1) then
          delu(k) = u(k) - um(k)
          delv(k) = v(k) - vm(k)
        else
          delu(k) = u(k)
          delv(k) = v(k)
        endif
100   continue
c
      return
c
      end
```

A3.2 NEW MAIN PROGRAM TO RUN HYDRAULICS RESEARCH WALLINGFORD'S FLUIDMUDFLOW-2D SUBROUTINES

```
C     MAIN PROGRAM TO RUN WALLINGFORD FLUIDMUDFLOW-2D SUBROUTINES
C     COPYRIGHT M.CRAPPER AND HR WALLINGFORD LTD 1993
C
C     THIS IS THE VERSION USED FOR INITIAL SET UP AND TESTING
C
C     DECLARE ARRAYS AND VARIABLES ETC
C
      REAL BED(1000),BEDL(5000),C(1000),CMUD(1000),D(1000),DELU(1000),
     1DELV(1000),DM(1000),DMUD(1000),FLUXX(1000),FLUXY(1000),FMX(1000),
     2FMY(1000),HMAX(1000),HU(1000),HV(1000),ILAYER(1000),MASS1(1000),
     3TAU(1000),TAUE(5),TAUI(1000),TBED(1000),TI(1000),UMUD(1000),
     4UVEL(1000),VMUD(1000),VVEL(1000),YIELD(10)
C
      REAL FMMASS1(1000),SMMASS1(1000),FMMASS,SMMASS,BED1,MINS,
     1SIMTIME,MINSOUT,WSET
C
      INTEGER FLAGMUD(1000), FLAGU(1000),FLAGV(1000),FLAGZ(1000),
     1KARRAY(1000)
C
      REAL BETA,C0,CONRATE,CSTART,DT,ERODM,FCON,FMUD,MASS,OLDMASS,
     1OMEGA,RHOW,SRATE,TAUD,TAUDM,TAUEM,TBYDS,VISCMUD,WSMIN
C
      INTEGER K, KMAX, M, MN, N, NBEDLAYERS, NITSUBS, NOUTS
C
      INTEGER*4 ITSUB,NSUB
C
      LOGICAL MUDON
C
C     ***************************************************************
C
C     OPEN OUTPUT FILES AND DEFINE MAJOR VARIABLES
C
      OPEN (UNIT=5,FILE='TEST_OP.PRN')          SOME NOTES ON VARIABLES
C     OPEN (UNIT=6,FILE='<FILENAME>.PRN')       AND THEIR MEANING
C
C     NOTE UNIT 6 RESERVED FOR EXTRA OUTPUT NOT NORMALLY USED
C
      DT=0.001                                  timestep in secs
      DX=0.1                                    spacestep in m
      MINSOUT=0.25                              output interval in mins
      SIMTIME=10                                simulation time in mins
      M=22                                      cells in x-direction
      N=3                                       cells in y-direction
      KOUT=IFIX((M*1.5)+0.5)                    kout = output location in
C                                               terms of k-array
C     ***************************************************************
C
C     DEFINE REMAINING VARIABLES
C
      BEDTOT=0                                  totaliser for bed mass
      BETA=1.0                                  ratio of near bed conc
C     C0=75.0                                   FM concentration (kg/m3)
      CONRATE=0.00003                           bed consolid rate (/s)
      CMTOT=0                                   totaliser for FM conc
      CSTART=30.00                              initial avge conc (kg/m3)
      DMTOT=0                                   totaliser for FM thickness
      ERODM=0.00643                             me in equation 5.9
      FW=0.08                                   friction factor for water
      FLAG1=0                                   flag use in o/p routines
      MASS=0.0                                  totaliser for mud mass
      MUDON= .TRUE.                             flag indicates FM
      NBEDLAYERS=5                              no of bed layers
      OLDMASS=0.0                               totaliser for mud mass
      Q=0.0                                     x water discharge(m3/s)
```

```
      RHOW=1025.00                                  density of water (kg/m3)
      TAUD=10000                                    crit shears for deposition
      TAUDM=10000                                   (set to high value to
C     TAUD=0.08                                      ensure deposition)
C     TAUDM=0.08
      TAUE(1)=10000                                 ditto for erosion
      TAUE(2)=10000                                 (all in N/m2)
      TAUE(3)=10000
      TAUE(4)=10000
      TAUE(5)=10000
C     TAUEM=2.1
C     TAUE(1)=2.2
C     TAUE(2)=2.35
C     TAUE(3)=2.62
C     TAUE(4)=2.8
C     TAUE(5)=3.0
C     TAUEM=2.1
      UMTOT=0.0                                     totaliser for FM u-vel
      V0=0.00005                                    dewatering velocity in m/s
      VISCMUD=660E-6                                FM kin visc at Cm=C0 (m2/s)
      VMTOT=0.0                                     totaliser for FM v-vel
      WSET=5E-5                                     omega_s in eq 5.7
      WSMIN=0.00004                                 omega_min in eq 5.7 (m/s)
      YIELD(1)=0.38                                 yield strength of bed
      YIELD(2)=2.78                                 layers (kg/m2)
      YIELD(3)=10.53
      YIELD(4)=85
      YIELD(5)=100000
C
C     SET UP OTHER VARIABLES DEPENDENT SOLELY ON THOSE ABOVE
C
      AREA=DX**2                                    area of cell
      BEDENS=1054                                   arbitrary bed density
      C0=(1.363*CSTART)+4.542                       new C0 algorithm
      CONRATE=CONRATE*DT                            this is from HRL
      FCON=FW                                       from HRL
      FMUD=FW                                       from HRL
      DTBYDX=DT/DX
      NOUTS=IFIX((MINSOUT*60/DT)+0.5)               no of timesteps to o/p
C     NOUTS=1
C     USE LINE ABOVE FOR O/P EVERY TIMESTEP
      NSUB=IFIX((SIMTIME*60/DT)+0.5)                no of timesteps in run
C     NSUB=600000
C     USE LINE ABOVE WHEN TOO MANY TIMESTEPS FOR IFIX FUNCTION
      SRATE=BETA*DT/TAUD                            from HRL's settling model
      TBYDS=DT/DX                                   this is from HRL
C
C     DEFINE GRID USING K-ARRAY SYSTEM
C
      MN=M*N
      KMAX=MN
C
C     READ IN KARRAY VALUES
C     THIS ROUTINE VALID FOR TEST RUNS ONLY - CHECK IT LATER - 13/2/94
C
      K=0
      DO NCOUNT=1,(KMAX/M)
            DO MCOUNT=1,(KMAX/N)
                  K=K+1
                  IF (K.GT.KMAX) STOP 1
                  IF (NCOUNT.eq.1.OR.NCOUNT.eq.N) THEN
                        KARRAY(K)=1
                        FLAGZ(K)=0
                        FLAGU(K)=0
                        FLAGV(K)=0
                        C(K)=0
                  ELSE
```

```
                        KARRAY(K)=K
                        FLAGZ(K)=1
                        C(K)=CSTART
                        FLAGU(K)=1
                        FLAGV(K)=1
                        END IF
C
C     SET UP DATUM AND DEPTH FOR SLOPE
C
                  HMAX(K)=0.4+((MCOUNT-0.5)*DX/5)
                  HU(K)=0.4+(MCOUNT*DX/5)
                  HV(K)=0.4+((MCOUNT-0.5)*DX/5)
                  D(K)=0.4+((MCOUNT-0.5)*DX/5)
                  DM(K)=D(K)
            END DO
      END DO
C
C     DEFINE INITIAL CONDITIONS EXCEPT FOR C(K) DEFINED ABOVE
C
      DO K=1,KMAX
            BED(K)=0
            MASS1(K)=0
            UMUD(K)=0.0
            VMUD(K)=0.0
            DMUD(K)=0.0
            CMUD(K)=0.0
            UVEL(K)=q/d(k)
            VVEL(K)=0.0
            FLUXX(K)=0.0
            FLUXY(K)=0.0
      END DO
C
C     CALCULATE AND WRITE OUT INITIAL CONDITION
C
      MINS=0
      MASS=0.0
      FMMASS=0.0
      SMMASS=0.0
      BED1=0.0
      DO K=1,KMAX
            BED(K)=0.0
      END DO
      CALL BEDSUM(BED(1),BEDL(1),NBEDLAYERS,KMAX)
      DO K=1,KMAX
            FMMASS1(K)=CMUD(K)*DMUD(K)*AREA
            SMMASS1(K)=C(K)*D(K)*AREA
            FMMASS=FMMASS+FMMASS1(K)
            SMMASS=SMMASS+SMMASS1(K)
            BED1=BED1+(BED(K)*AREA)
            MASS=MASS+FMMASS1(K)+SMMASS1(K)+(BED(K)*AREA)
      END DO
      OLDMASS=MASS
      WRITE (2,9991)
      WRITE (2,9996)
      WRITE (2,9995)
      WRITE (2,9994)
      WRITE (2,9993)
      WRITE (2,9992)
      WRITE (2,9999) MINS,OLDMASS,MASS,FMMASS,SMMASS,BED1
      BILLY=0.0
C     BILLY IS DUMMY VARIABLE TO GIVE CORRECT INITIAL VALUE IN O/P
      WRITE (5,9998) MINS,DMUD(kout),UMUD(kout),
     1               CMUD(KOUT),BILLY
C
C     START TIME LOOP
C
```

set up water depths water depth 0.4m at u/s end of flume

```
      NITSUBS=0                                          these counters define
      NITSUBS2=IFIX((NITSUBS+0.5)/2)                     o/p and averaging
      NLINES=0                                           parameters
      DO ITSUB=1,NSUB
C
            MINS=ITSUB*DT/60
C
C     CHECK TOTAL MASS OF MUD IN SYSTEM
C
            OLDMASS=MASS
            MASS=0.0
            FMMASS=0.0
            SMMASS=0.0
            BED1=0.0
            DO K=1,KMAX
                  BED(K)=0.0
            END DO
            CALL BEDSUM(BED(1),BEDL(1),NBEDLAYERS,KMAX)
            DO K=1,KMAX
                  FMMASS1(K)=CMUD(K)*DMUD(K)*AREA
                  SMMASS1(K)=C(K)*D(K)*AREA
                  FMMASS=FMMASS+FMMASS1(K)
                  SMMASS=SMMASS+SMMASS1(K)
                  BED1=BED1+(BED(K)*AREA)
                  MASS=MASS+FMMASS1(K)+SMMASS1(K)+(BED(K)*AREA)
            END DO
C
C     LINES WHICH FOLLOW ARE MAIN CALLS TO HRL ROUTINES
C     WRITTEN IN LOWERCASE TEXT FOR CLARITY
C
            call consolidation(bedl(1),yield(1),ilayer(1),KMAX,
     1                         nbedlayers,conrate)
C
            call setflagmud(flagmud(1),dmud(1),KMAX,mudon)
C
            call vdiff(delu(1),delv(1),uvel(1),vvel(1),umud(1),vmud(1),
     1                 flagmud(1),KMAX)
C
            call bedstress(tau(1),tbed(1),umud(1),vmud(1),dmud(1),
     1                     flagmud(1),flagz(1),flagu(1),flagv(1),
     2                     viscmud,cmud(1),c0,rhow,KARRAY(1),m,n,mn,
     3                     KMAX,mudon)
C
            call interfacestress(delu(1),delv(1),d(1),flagmud(1),
     1                           flagz(1),flagu(1),flagv(1),taui(1),
     2                           ti(1),fmud,fcon,cmud(1),rhow,
     3                           KARRAY(1),m,n,mn,KMAX)
C
            call mudvel(umud(1),vmud(1),uvel(1),vvel(1),dmud(1),d(1),
     1                  dm(1),hmax(1),hu(1),hv(1),flagu(1),flagv(1),
     2                  tbed(1),ti(1),tbyds,dt,cmud(1),rhow,omega,
     3                  KARRAY(1),m,n,mn,KMAX,mudon)
C
            call vdiff(delu(1),delv(1),uvel(1),vvel(1),umud(1),vmud(1),
     1                 flagmud(1),KMAX)
C
            call bedstress(tau(1),tbed(1),umud(1),vmud(1),dmud(1),
     1                     flagmud(1),flagz(1),flagu(1),flagv(1),
     2                     viscmud,cmud(1),c0,rhow,KARRAY(1),m,n,mn,
     3                     KMAX,mudon)
C
            call interfacestress(delu(1),delv(1),d(1),flagmud(1),
     1                           flagz(1),flagu(1),flagv(1),taui(1),
     2                           ti(1),fmud,fcon,cmud(1),rhow,
     3                           KARRAY(1),m,n,mn,KMAX)
C
            call mudflux(fmx(1),fmy(1),dmud(1),umud(1),vmud(1),cmud(1),
```

```
     1                    flagmud(1),flagu(1),flagv(1),KARRAY(1),m,
     2                    n,mn,DTBYDX,KMAX,mudon)
C
           call mudexchange(BED(1),bedl(1),c(1),d(1),dm(1),dmud(1),
     1                      delu(1),delv(1),umud(1),vmud(1),cmud(1),
     2                      tau(1),taui(1),flagz(1),flagu(1),flagv(1),
     3                      flagmud(1),rhom,rhow,taud,taudm,taue,tauem,
     4                      dt,c0,v0,beta,wset,wsmin,srate,
     5                      erodm,KARRAY(1),m,n,mn,KMAX,ilayer(1),
     6                      nbedlayers,mudon)
C
           call muddepth(dmud(1),fmx(1),fmy(1),d(1),bed(1),cmud(1),
     1                   c,c0,beta,flagz(1),KARRAY(1),m,n,mn,KMAX,
     2                   mudon)
C
           call concentration(c(1),d(1),fluxx(1),fluxy(1),flagz(1),
     1                        KARRAY(1),m,n,mn,KMAX)
C
C     OUTPUT RESULTS AVERAGING VELOCITIES OVER TIME INTERVAL
C     BETWEEN OUTPUTS
C     EXTRA OUTPUT NOT NORMALLY USED
C
C          WRITE (6,9990) MINS
C          WRITE (6,9989) UMUD(23),UMUD(27),UMUD(32),UMUD(33),
C    1                    UMUD(36),UMUD(38),UMUD(40),UMUD(41)
C          WRITE (6,9988) DMUD(23),DMUD(27),DMUD(32),DMUD(33),
C    1                    DMUD(36),DMUD(38),DMUD(40),DMUD(41)
C          WRITE (6,9987) (BED(23)/BEDENS),(BED(27)/BEDENS),
C    2                    (BED(32)/BEDENS),(BED(33)/BEDENS),
C    2                    (BED(36)/BEDENS),(BED(38)/BEDENS),
C    3                    (BED(40)/BEDENS),(BED(41)/BEDENS)
C          WRITE (6,9991)
C
C     THESE LINES TOTAL UP VELOCITIES ETC FOR AVERAGING OVER O/P STEP
C
           NITSUBS2=NITSUBS2+1
           NITSUBS=NITSUBS+1
           UMTOT=UMTOT+(UMUD(KOUT)*DT)
           VMTOT=VMTOT+(VMUD(KOUT)*DT)
           DMTOT=DMTOT+(DMUD(KOUT)*DT)
           CMTOT=CMTOT+(CMUD(KOUT)*DT)
           BEDTOT=BEDTOT+((BED(KOUT)/BEDENS)*DT)
C
C     THESE LINES WRITE OUTPUT ON SCREEN FOR CHECKING DURING RUN
C
           IF (NITSUBS.EQ.NOUTS) THEN
                 WRITE (2,9999) MINS,OLDMASS,MASS,FMMASS,SMMASS,BED1
                 NLINES=NLINES+1
                 IF (NLINES.GT.16) THEN
                       WRITE (2,9991)
                       WRITE (2,9996)
                       WRITE (2,9995)
                       WRITE (2,9994)
                       WRITE (2,9993)
                       WRITE (2,9992)
                       NLINES=0
                 END IF
                 MINSOUT=MINS
                 FLAG1=1
                 NITSUBS=0
           END IF
C
C     THESE LINES AVERAGE VALUES OVER O/P STEP AND WRITE O/P
C     TO FILE
C
           IF (FLAG1.GE.1.0) THEN
                 IF (NITSUBS2.EQ.NOUTS) THEN
```

```
                        UOUT=UMTOT/(NITSUBS2*DT)
                        VOUT=VMTOT/(NITSUBS2*DT)
                        DOUT=DMTOT/(NITSUBS2*DT)
                        COUT=CMTOT/(NITSUBS2*DT)
                        BEDOUT=BEDTOT/(NITSUBS2*DT)
                        WRITE (5,9998) MINSOUT,DOUT,UOUT,COUT,BEDOUT
                        UMTOT=0
                        VMTOT=0
                        DMTOT=0
                        CMTOT=0
                        BEDTOT=0
                        NITSUBS2=0
                    END IF
                END IF
            END DO
C
9999  FORMAT(1X,F6.2,5(3X,F7.2))
9998  FORMAT(1X,F7.3,4(3X,F10.6))
9996  FORMAT(1X,6H TIME ,3X,7HMASS AT,3X,7HMASS AT,3X,7HFM MASS,
     1       3X,7HSM MASS,3X,7H  BED  )
9995  FORMAT(1X,6H MINS ,3X,7H LAST  ,3X,7H THIS  ,3X,7H KG/M2 ,
     1       3X,7H KG/M2 ,3X,7H MASS  )
9994  FORMAT(1X,6H      ,3X,7HTIME ST,3X,7HTIME ST,3X,7H      ,
     1       3X,7H       ,3X,7H KG/M2 )
9993  FORMAT(1X,6H      ,3X,7H KG/M2 ,3X,7H KG/M2 )
9992  FORMAT(1X,56(1H-))
9991  FORMAT(1X)
C9990  FORMAT(1X,F7.3)
C9989  FORMAT(1X,8F9.6)
C9988  FORMAT(1X,8F9.6)
C9987  FORMAT(1X,8F9.6)


      END
```

A3.3 VERSIONS OF SUBROUTINES INCLUDING AUTHOR'S MODIFICATIONS TO THE FLUIDMUDFLOW-2D MODEL

As previously, original Hydraulics Research code is written in lowercase, whilst the author's code is written in UPPERCASE.

A3.3.1 SUBROUTINE BEDSTRESS

This listing incorporates code for all the friction factor models tested. The code for the author's Couette, Harleman and Simple Models is shown commented out.

```
c*************************************************************
      subroutine bedstress(taubed,tbed,um,vm,dm,flagmud,flagz,flagu,
     1           flagv,viscmud,cmud,c0,rhow,karray,m,n,mn,kmax,mudon,
     2           SLOPE,FM,CSTART,C)
c*************************************************************
c
c
c This subroutine calculates the shear stress at the bed. If no
c mud is present, the shear stress induced by the water is
c calculated  in the subroutine 'interfacestress';
c if fluid mud is present, it is assumed to be a turbulent
c boundary layer with a viscous sub-layer. A fluid mud Reynolds
c number is evaluated to ascertain if the whole mud layer is
c non-turbulent -- i.e if the thickness of the viscous sub-layer
c is equal to the full mud layer thickness.
c
c
c   Arguments
c   =========
c   taubed      bed stress at each active cell
c   tbed        bed stress/modulus of velocity
c   um,vm       fluid mud velocity
c   dm          fluid mud depth
c   flagmud     =1 if fluid mud present
c   flagz       usual
c   flagu
c   flagv
c   viscmud     kinematic viscosity of fluid mud
c   cmud        concentration of fluid mud
c   rhow        density of water
c   karray
c   m
c   n
c   mn
c   kmax        no. of active cells
c   mudon       fluid mud switch
c   SLOPE   CONSTANT SLOPE
c   FM MUD FRICTION FACTOR
c
c
c-------------------------------------------------------------
c
      real      taubed(kmax),um(kmax),vm(kmax),dm(kmax),tbed(kmax)
      real cmud(kmax),SLOPE,FM,CSTART,C(KMAX),HARLK
      logical  mudon
      integer flagmud(kmax)
      integer  flagz(kmax),flagu(kmax),flagv(kmax),karray(mn)
c
      if (.not.mudon) return
c  viscosity of water
      viscw = 1e-6
C     gamma = (alog(viscmud/viscw))/c0
      rcrit1 = 46.0
      rcrit2 = 1200
```

```
      dmin = 0.01
      do 100, kij=1,mn
        k = karray(kij)
        if (k.le.1) goto 100
        kn = karray(kij-m)
        kw = karray(kij-1)
        if ((flagmud(k).eq.1).and.(flagz(k).gt.0)) then
          IF (C(K).GT.0) THEN
            CST=CSTART
          ELSE
            CST=0
          ENDIF
C         CST=C(K)
c
          if (dm(k).lt.dmin) then
            taubed(k) = 0.0
            tbed(k) = 0
            goto 100
          endif
C         rhom = rhow + 0.62*cmud(k)
          RHOM = RHOW +0.561*CMUD(K)
C         viscm = viscw*exp(gamma*cmud(k))
          VISCM = EXP((0.1096*RHOM)-123.487)
          IF (VISCM.LT.VISCW) THEN
            VISCM=VISCW
          ENDIF
          if ((flagmud(kw).le.0).or.(flagu(kw).le.0)) then
            uu = um(k)
            if (flagu(k).le.0) uu= 0
          else if (flagu(k).le.0) then
            uu = um(kw)
          else
            uu = 0.5*(um(k)+um(kw))
          endif
          if ((flagmud(kn).le.0).or.(flagv(kn).le.0)) then
            vv = vm(k)
            if (flagv(k).le.0) vv= 0
          else if (flagv(k).le.0) then
            vv = vm(kn)
          else
            vv = 0.5*(vm(k) + vm(kn))
          endif
c
          vel = sqrt(uu*uu + vv*vv)
c
c
          rmud = vel*dm(k)/viscm
c         write (2,*) rmud
          if (rmud .lt. rcrit1) then
c
c   calculate stress due to viscous sub-layer
c
            tt = 3*rhom*viscm/dm(k)
            tbed(k) = tt
            taubed(k) = vel*tt
            IF (RMUD.LE.(1E-8)) THEN
              FF=0
            ELSE
             FF=24/RMUD
            ENDIF
          else if (rmud .lt. rcrit2) then
            rlog = (alog10(rmud))**(-0.88)
            ff = 188250*((0.01*(10**rlog))**4.74)
            tt = rhom*ff*vel
            tbed(k) = tt
            taubed(k) = tt*vel
          else
```

```
            rlog = (alog10(rmud))**(-1.23)
            ff = 57.5*((0.05*(10**rlog))**4)
            tt = rhom*ff*vel
            tbed(k) = tt
            taubed(k) = tt*vel
          endif
          FM=FF
C
C     COUETTE FLOW ROUTINE TO DETERMINE FM BASED ON RTF DATA
C     ONLY WORKS FOR LAMINAR FLOW AND CONSTANT BED SLOPE
C     SLOPE IS EASY TO CHANGE. FOR TURBULENCE, CHANGE 1.64 TO 1.43
C
C           IF (ABS(VEL).LT.0.00001) THEN
C                 TT=0
C           ELSE
C                 TOP = 8*9.81*(RHOM-((0.561*CST)+RHOW))*DM(K)*SLOPE
C                 BOTTOM = (VEL**2)*RHOM*1.64
C                 FM=TOP/BOTTOM
C                 TT=RHOM*FM*VEL/8
C           ENDIF
C           TBED(K)=TT
C           TAUBED(K)=TT*VEL
C
C     NEW BED STRESS MODEL BASED ON HARLEMAN, F=K/R
C     REALLY ONLY VALID FOR LAMINAR FLOW
C
C           HARLK=34.688
C           IF (RMUD.LE.(1E-8)) THEN
C                 FF=0
C           ELSE
C                 FF=HARLK/RMUD
C           ENDIF
C           TT=RHOM*FF*VEL/8
C           TBED(K)=TT
C           TAUBED(K)=TT*VEL
C           FM=FF
C           WRITE (2,*) FM
C     EVEN SIMPLER VERSION WITH FIXED FM VALUE FROM MAIN PROG.
C
C           TT=RHOM*FM*VEL/8
C           TBED(K)=TT
C           TAUBED(K)=TT*VEL
C
      else
c   no mud present or flagz.le.0:
          taubed(k) = 0
          tbed(k) = 0
        endif
c       write (2,*) ff
100   continue
c
      return
c
      end
c
```

A3.3.2 SUBROUTINE INTERFACESTRESS

```
c*******************************************************************
      SUBROUTINE INTERFACESTRESS(delu,delv,d,flagmud,flagz,flagu,
     1          flagv,taui,ti,ffm, ffb, cmud, rhow, karray,m,n,mn,kmax,
     2          FM,CSTART,C)
c*******************************************************************
c
c
c  subroutine to calculate x and y components of interface
c  stress between fluid mud layer and overlying water or
c  between water and bed if no fluid mud present
c
c      Arguments
c      =========
c  delu, delv   x,y cpts of velocity difference between water
c               and fluid mud-- see subroutine "vdiff"
c  d       water depth
c  flagmud =1 if fluid mud present
c  flagz   usual
c  flagu
c  flagv
c  taui    stress at interface
c  ti      stress/modulus of velocity difference
c  ffm     friction factor for mud-water interface stress
c  ffb     friction factor for water-bed interface stress
c  rhow    density of water
c  cmud    concentration of fluid mud
c    Note that density of fluid mud, rhom = rhow + 0.62*cmud
c  karray  usual
c  m       no. of cells in each row
c  n       no. of cells in each column
c  mn      m*n
c  kmax    no. of active cells
c
c
c
c----------------------------------------------------------------------
c
c
      real delu(kmax), delv(kmax), d(kmax),cmud(kmax)
      real taui(kmax),ti(kmax),FM,CSTART,C(KMAX)
      integer flagmud(kmax)
      integer flagz(kmax),karray(mn),flagu(kmax),flagv(kmax)
C
      FFM=FM
      FFB=FM
c
c
c   loop through all active cells
c
      do 100, kij = 1, mn
        k = karray(kij)
        if (k.le.1) goto 100
      if ((flagz(k).gt.0).and.(d(k).gt.0)) then
        kn = karray(kij-m)
        kw = karray(kij-1)
        IF (C(K).GT.0) THEN
         CST = CSTART
        ELSE
         CST =0
        ENDIF
C       CST=C(K)
c
c    if fluid mud present, calculate mud-water interface stress,
c      if not, calculate water-bed stress
c      If no mud present then delu,delv are just water velocity
```

```
c
      du = 0.5*(delu(k)+delu(kw))
      if (flagu(k).ne.1) du = delu(kw)
      if (flagu(kw).ne.1) du = delu(k)
      dv = 0.5*(delv(k)+delv(kn))
      if (flagv(k).ne.1) dv = delv(kn)
      if (flagv(kn).ne.1) dv = delv(k)
      velsq = du*du + dv*dv
C     rhom = rhow + 0.62*cmud(k)
      RHOM = RHOW + 0.561*CMUD(K)
      if (flagmud(k).eq.1) then
C       tt = ffm*rhom/8
        TT = 0.535*FFM*RHOM/8
C     0.535 IN ABOVE LINE IS AVERAGE OF 0.64 AND 0.43 TO REPRESENT
C     COMPROMISE BETWEEN LAMINAR AND TURBULENT CONDITIONS
      else
        tt = ffb*(rhow+(0.561*CST))/8
      endif
      taui(k) = tt*velsq
      ti(k) = tt*sqrt(velsq)
      else
c flagz.le.0:
        taui(k)=0
        ti(k) = 0
      endif
c
100   continue
c
c
      return
c
      end
```

A3.3.3 SUBROUTINE MUDEXCHANGE

```
c*************************************************************************
      SUBROUTINE MUDEXCHANGE(BED,bedl,c,d,oldd,dm,delu,delv,um,vm,cmud,
     1                       taubed,taui,flagz,flagu,flagv,flagmud,
     2                       rhom,rhow,taud,taudm,taue,tauem,dt,c0,v0,
     3                       beta,wset,wsmin,srate,erate,karray,m,n,mn,
     4                       kmax,ilayer,nbedlayers,mudon,CSTART)
c*************************************************************************
c
c
c   This routine calculates the exchange of mud between three layers:
c             bed
c             fluid mud
c             suspended mud,
c   by means of seven processes:
c             erosion of bed by water
c             erosion of bed by fluid mud
c             settling of suspended mud onto fluid mud
c             settling of suspended mud onto bed
c             entrainment of fluid mud by water
c             erosion of fluid mud by water
c             dewatering of fluid mud.
c   Having calculated the mass of mud per square metre transferred
c   by these processes, the change in the bed deposit (kg/m*m), the
c   suspended mud concentration (kg/m*m*m) and the fluid mud depth (m)
c   are calculated. The fluid mud is assumed to have a constant
c   concentration, c0.
c
c
c      Arguments
c      =========
c  bed              mud deposits on bed (kg/m*m)
c  c                suspended mud concentration (kg/m*m*m)
c  d                water depth (m)
c  oldd             water depth at previous sub-timestep
c  dm               fluid mud depth (m)
c  delu,delv        water velocity - fluid mud velocity (m/s)
c  cmud             fluid mud concentration
c  taubed           stress on bed DUE TO FLUID MUD only (kg/m*s*s)
c  taui             stress on fluid mud or bed due to water ( " )
c  flagz            usual flag, = 1 if active cell
c  flagu
c  flagv
c  flagmud          =1 if fluid mud depth > 0
c  rhom,rhow        density of fluid mud, water
c  taud             critical stress for deposition  onto bed
c  taudm            critical stress for deposition onto fluid mud
c  taue             critical stress for erosion of bed - one value
c                     for each layer
c  tauem            critical stress for erosion of fluid mud layer
c                       by overlying water
c  dt               sub timestep duration
c  c0               max concentration of fluid mud (kg/m*m*m)
c  v0               dewatering velocity (m/s)
c  beta             concentration factor
c  wset             coefficient for settling velocity(m*m*m*m/kg*s)
c  wsmin            minimum settling velocity (m/s)
c  srate            settling rate
c  karray           usual
c  m                no. of cells in each row
c  n                no. of cells in each column
c  mn               m*n
c  kmax             number of active cells
c  nbedlayers       number of layers of bed deposits
c  mudon            fluid mud switch - if .false. then no fluid mud allowed
c
```

```
c-----------------------------------------------------------------
c  set constants
      parameter(g    = 9.81)
      parameter(dmin = 0.01)
      parameter(tiny = 1E-8)
c
      integer flagz(kmax),flagu(kmax),flagv(kmax),karray(mn)
      integer ilayer(kmax)
      logical mudon
      integer flagmud(kmax)
      real delu(kmax),delv(kmax),dm(kmax),um(kmax),vm(kmax)
      real taubed(kmax),taui(kmax),c(kmax),d(kmax)
      real oldd(kmax),bedl(kmax*nbedlayers)
      real cmud(kmax)
      real taue(nbedlayers)
      REAL BED(KMAX),MASSK,MASSKNEW,TOTMASS,TOTMASSN,WSET(5)
      REAL CSTART
c
c
c     delrho = rhom-rhow
c     write(*,*) 'posn| dew  | entr  | eroA  | eroB  | setA  | setB  |
c    1taui  | tbed  | delu  | delv  |  um   |  vm   |   d   |   dm |
c    2wblt  | cmud  | bed'
c
c     k1 = karray((m*37)+13)
c     k2 = karray((m*18)+76)
c     k3 = karray((m*7)+87)
c     k4 = karray((m*73)+5)
c     k5 = karray((m*44)+30)
c     k6 = karray((m*34)+50)
c     k7 = karray((m*83)+32)
c     k8 = karray((m*52)+40)
c     k9 = karray((m*69)+33)

      TOTMASS=0.0
      TOTMASSN=0.0
      do 100, kij=1,mn
        k = karray(kij)
c  initialise exchange variables
        flmud2bed  = 0.0
        bed2flmud  = 0.0
        flmud2susp = 0.0
        susp2flmud = 0.0
        bed2susp   = 0.0
        susp2bed   = 0.0
c
c temporary variables to cut down on array look-ups
        tb = taubed(k)
        ti = taui(k)
        IF (C(K).GT.0) THEN
             CST=CSTART
        ELSE
             CST=0
        ENDIF
C       CST=C(K)
C       cc = c(k)
        CC=CMUD(K)
        cm = cmud(k)
        ddm = dm(k)
        layer = ilayer(k)
        kk = (layer-1)*kmax + k
        if ((flagz(k) .eq. 1).and.(d(k).gt.0)) then
C
        if ((flagmud(k).eq.1).and.(mudon)) then
c
c  fluid mud present
c  ******************
```

```
c
c-----------------------------------------------------
c   erosion by fluid mud
c-----------------------------------------------------
c  Note: layer = 0 means that there are no mud deposits
           if (layer.ne.0)  then
            IF (tB.gt.taue(layer)) THEN
              bd = bedl(kk)
              bed2flmud = dt*erate*(tb-taue(layer))
c check there's enough mud on bed
              if (bed2flmud.gt.bd) bed2flmud=bd
            endif
           ENDIF
c
c-----------------------------------------------------
c   dewatering
c-----------------------------------------------------
            if (tb .lt. taud) then
              flmud2bed = v0*cm*dt
            endif
c-----------------------------------------------------
c   entrainment
c-----------------------------------------------------
c  Only allow entrainment or erosion if fluid mud is more concentrated
c  than overlying water
            if (cm.gt.c(K)) then
              kn = karray(kij-m)
              kw = karray(kij-1)
              du = 0.5*(delu(k)+delu(kw))
              if (flagu(k).ne.1) du = delu(kw)
              if (flagu(kw).ne.1) du = delu(k)
c note if both flagu entries are .ne.1 then get du = 0.
              dv = 0.5*(delv(k)+delv(kn))
              if (flagv(k).ne.1) dv = delv(kn)
              if (flagv(kn).ne.1) dv = delv(k)
              dmud = ddm
              diffsq = du*du + dv*dv
              if (dmud .lt. dmin) dmud = dmin
              if (diffsq .gt. tiny) then
C               delrho = 0.62*cm
                DELRHO = 0.561*(CM-CST)
                rich = delrho*g*dmud/diffsq
                if (rich .lt. 10.0) then
c  entrainment velocity
                  ve = 0.1*sqrt(diffsq)/((1+63*rich*rich)**0.75)
                  flmud2susp = dt*ve*cm
                endif
              endif
c if entrainment is less than erosion of fluid mud, assume that
c erosion takes place instead:
              erosion = dt*erate*(ti-tauem)
              if (erosion .lt. 0) erosion = 0.0
              if (erosion .gt. flmud2susp) flmud2susp = erosion
c
c check there's enough fluid mud for both dewatering and entrainment
c  (or erosion)
              totalmud = flmud2bed + flmud2susp
              available = ddm*cm
              if (totalmud .gt. available) then
                flmud2bed = flmud2bed*available/totalmud
                flmud2susp = flmud2susp*available/totalmud
              endif
c
            endif
c-----------------------------------------------------
c   settling onto fluid mud
c-----------------------------------------------------
```

```
            if (ti.lt.taudm) then
C             ws = cc*wset
              IF (CC.LT.4) THEN
                  WS=WSET(1)*((CC*1000)**WSET(2))
              ELSE IF (CC.LT.15.3) THEN
                  WS=WSET(3)
              ELSE
                  WS=WSET(4)*((CC*1000)**(WSET(5)))
              END IF
              if (ws .lt. wsmin) ws = wsmin
C             susp2flmud = srate*cc*ws*(taudm-ti)
              SUSP2FLMUD = SRATE*CC*WS*(TAUDM-TI)
c  check there's enough mud in suspension
              if (susp2flmud.gt.(c(K)*d(k))) susp2flmud=c(K)*d(k)
            endif
c
c
          else
c
c no fluid mud present
c ********************
c
c-------------------------------------------------------
c   erosion by water
c-------------------------------------------------------
           if (layer.ne.0)  then
            IF (ti.gt.taue(layer)) THEN
             bd = bedl(kk)
               bed2susp = dt*erate*(ti-taue(layer))
c  check there's enough mud on the bed
              if (bed2susp.gt.bd) bed2susp = bd
            ENDIF
           endif
c
c-------------------------------------------------------
c   settling
c-------------------------------------------------------
           if (ti .lt. taud) then
C             ws = cc*wset
              IF (CC.LT.4) THEN
                  WS=WSET(1)*(CC*WSET(2))
              ELSE IF (CC.LT.15.3) THEN
                  WS=WSET(3)
              ELSE
                  WS=WSET(4)*(CC**(WSET(5)))
              END IF
              if (ws .lt. wsmin) ws = wsmin
C             settling = srate*cc*ws*(taudm-ti)
              SETTLING = SRATE*CC*WS*(TAUDM-TI)
              totalsusp = c(K)*d(k)
c  check that there's enough mud in suspension
             if (settling .gt. totalsusp) settling = totalsusp
c  if it settles quickly, some will form fluid mud
             if ((settling .gt. (v0*c0*dt)).and.(mudon)) then
               susp2bed = v0*c0*dt
               susp2flmud = settling - susp2bed
             else
               susp2bed = settling
             endif
c
           endif
c
c-------------------------------------------------------
         endif
c
c
c now calculate changes in depth, concentration, bed deposits
```

```
c
C CALCULATE ORIGINAL MASS OF MUD AT LOCATION K

      MASSK=BED(K)+(C(K)*D(K))+(DM(K)*CMUD(K))

c  deposition onto top layer (ie layer 1):
         bedl(k) = bedl(k) + susp2bed + flmud2bed
c  erosion from erosion layer  -- if layer = 0, no mud to erode
         if (layer .ne. 0) then
           bedl(kk) = bedl(kk) - bed2flmud - bed2susp
         endif
c  reset erosion layer pointer:
         ilayer(k) = 0
         do 750,i=nbedlayers,1,-1
           kk = (i-1)*kmax + k
           if (bedl(kk).gt.0) ilayer(k) = i
 750     continue
         c(k) = (oldd(k)*C(K) + flmud2susp + bed2susp -
     1               susp2flmud - susp2bed)/d(k)
C        CMASS(K)=CMASS(K) + flmud2susp + bed2susp -
C    1               susp2flmud - susp2bed
C        IF (CMASS(K).LE.0) THEN
C           C(K) = 0.0
C        ENDIF
         totalmud = ddm*cm +susp2flmud+bed2flmud-flmud2susp-
     1                flmud2bed
         olddm = ddm

         if (totalmud.le.0) then
           dm(k) = 0
           cmud(k) = 0
         else
           dm(k) = totalmud/c0
           cmud(k) = c0
         endif

C CALCULATE NEW MASS OF MUD AT LOCATION K

      MASSKNEW=BED(K)+(C(K)*D(K))+(DM(K)*CMUD(K))
      TOTMASS=TOTMASS+MASSK
      TOTMASSN=TOTMASSN+MASSKNEW

          endif

c
100   continue
C      WRITE (2,9999) TOTMASS,TOTMASSN,(TOTMASSN-TOTMASS)
c
C9999  format(1X,11HMUDEXCHANGE,3(3X,f7.2))
      return
c
      END
```

A3.3.4 SUBROUTINE MUDVEL

```
c**********************************************************************
      SUBROUTINE MUDVEL(um,vm,u,v,dm,d,oldd,h,hu,hv,flagu,
     1                  flagv,tbed,ti,dtbydx,dt,cmud,rhow,
     2                  omega,karray,m,n,mn,kmax,mudon,CSTART,C)
c**********************************************************************
c
c
c  This subroutine calculates the velocity of fluid mud at each active
c  cell. If no fluid mud is present, the velocity is set to zero.
c    Note that um is +ve to the east, vm is +ve to the north,
c  i increases to the east, j increases to the south.
c
c     Arguments
c     =========
c  um,vm         fluid mud velocity
c  delu,delv     difference in velocity between mud and water
c  u,v           water velocity
c  dm            depth of fluid mud layer
c  d             depth of water (above bed, rather than above fluid mud)
c  oldd          depth at previous sub-timestep (velocities are calculated
c                   at half time-steps)
c  h             max depth of bed (+ve below datum)
c  hu,hv         depth of bed at u, v edges of cell
c  flagu,flagv, as usual
c  tbed       bed stress/mud velocity modulus
c  taui          mud-water interface stress/velocity difference modulus
c  dtbydx        timestep divided by grid spacing
c  dt            timestep
c  cmud          fluid mud concentration
c  rhow          water density
c  omega         Coriolis coefficient
c  karray        as usual
c  m             no. of cells in each row
c  n             no. of cells in each column
c  mn            m*n
c  kmax          no. of active cells
c  mudon         fluid mud switch
c
c
c----------------------------------------------------------------------
c
      real um(kmax),vm(kmax),dm(kmax),d(kmax),h(kmax)
      real oldd(kmax),hu(kmax),hv(kmax)
      real tbed(kmax),ti(kmax),cmud(kmax)
      real u(kmax),v(kmax),CSTART,C(KMAX),RHOW1
      integer karray(mn)
      logical mudon
      integer flagu(kmax),flagv(kmax)
c
      if (.not.mudon) return
c accel. due to gravity
      g = 9.81
      tiny = 1E-8
c  minimum fluid mud depth:
      dmin = 0.01
c
      do 100, kij = 1, mn
c location of current cell
        k = karray(kij)
c if cell is inactive then skip it
        if (k .le. 1) goto 100
        ks = karray(kij+m)
        ke = karray(kij+1)
        IF (C(K).GT.0) THEN
         CST=CSTART
```

```
        ELSE
         CST=0
        ENDIF
C       CST = C(K)
C     RHOW1 REPRESENTS WATER CONC INC SUSP MUD
C     RHOW JUST REPRESENTS WATER DENSITY NOT INC ANY MUD
        RHOW1 = RHOW+(0.561*CST)
c-----------------------------------------------------------------------
c  Calculate u velocity
        dd = d(k)
        de = d(ke)
        if ((flagu(k).eq.0).or.(dd.le.dmin).or.(de.le.dmin)) then
          um(k) = 0
        else
          dmm = dm(k)
          dme = dm(ke)
          hh = h(k)
          he = h(ke)
          uu = um(k)
          vv = vm(k)
          dep = 0.25*(dd+de+oldd(k)+oldd(ke)) -
     1          0.5*(hh+he) + hu(k)
          if (dep.le.dmin) then
c  ...                 water too shallow to flow
            um(k) = 0
          else
            if ((dmm.le.dmin).and.(dme.le.dmin)) then
c  ...                mud too shallow to go anywhere
              um(k) = 0
            elseif ((dmm.gt.dmin).and.(dme.gt.dmin))then
c   ...                                 Mud in both cells
              tti = 0.5*(ti(k) + ti(ke))
              ttb = 0.5*(tbed(k)+tbed(ke))
              drhom = 0.561*(cmud(k)-CST)
              drhome = 0.561*(cmud(ke)-CST)
              avdrhomu = 0.5*(drhom+drhome)
              ddu = 2*dt/((dmm*(rhow+drhom)) + (dme*(rhow+drhome)))
              gdu = g/(rhow+avdrhomu)
              eta = dd-hh
              etae = de-he
              etam = dmm - hh
              etame = dme - he
              diffu = RHOW1*(etae - eta) + avdrhomu*(etame - etam) +
     1             0.25*(dmm+dme)*(drhome-drhom)
              um(k) = (uu - gdu*dtbydx*diffu  +
     1            omega*vv*dt + ddu*tti*u(k))/(1.0 + ddu*(ttb+tti))
c
            elseif ((dmm.gt.dmin).and.(dme.le.dmin))then
c  ...                                 Mud in current cell but none to east
              tti = ti(k)
              ttb = tbed(k)
              drhom = 0.561*(cmud(k)-CST)
              ddu = dt/(dmm*(rhow+drhom))
              gdu = g/(rhow+drhom)
              eta = dd-hh
              etae = de - he
              etam = dmm - hh
c   NB dme = 0
              etame = - he
              diffu = RHOW1*(etae-eta)+drhom*(etame-etam) -
     1                0.5*dmm*drhom
              um(k) = (uu - gdu*dtbydx*diffu  +
     1            omega*vv*dt + ddu*tti*u(k))/(1.0 + ddu*(ttb+tti))
c  ...                                 Don't allow mud to flow westward
              if (um(k).lt.0.0) um(k) = 0.0
c
            elseif ((dmm.le.dmin).and.(dme.gt.dmin))then
```

```
c  ...                                  No mud in current cell but mud to east
               tti = ti(ke)
               ttb = tbed(ke)
               drhome = 0.561*(cmud(ke)-CST)
               ddu = dt/(dme*(rhow+drhome))
               gdu = g/(rhow+drhome)
               eta = dd - hh
               etae = de - he
c  NB dmm = 0
               etam = - hh
               etame = dme - he
               diffu = RHOW1*(etae-eta)+drhomE*(etame-etam) +
     1                   0.5*dme*drhome
               um(k) = (uu - gdu*dtbydx*diffu  +
     1             omega*vv*dt + ddu*tti*u(k))/(1.0 + ddu*(ttb+tti))
c  ...                                     Don't allow mud to flow west
               if (um(k).gt.0.0) um(k) = 0.0
             endif
c
           endif
c
         endif
c end of u velocity section
c-----------------------------------------------------------------------
c  Calculate v velocity
         dd = d(k)
         ds = d(ks)
         if ((flagv(k).eq.0).or.(dd.le.dmin).or.(ds.le.dmin)) then
           vm(k) = 0
         else
           dmm = dm(k)
           dms = dm(ks)
           hh = h(k)
           hs = h(ks)
           uu = um(k)
           vv = vm(k)
           dep = 0.25*(dd+ds+oldd(k)+oldd(ks)) -
     1           0.5*(hh+hs) + hv(k)
           if (dep.le.dmin) then
c  ...                 water too shallow to flow
             vm(k) = 0
           else
             if ((dmm.le.dmin).and.(dms.le.dmin))then
c  ...                                  No mud in either cell
               vm(k) = 0
c
             elseif ((dmm.gt.dmin).and.(dms.gt.dmin))then
c  ...                                  Mud in both cells
               tti = 0.5*(ti(k) + ti(ks))
               ttb = 0.5*(tbed(k)+tbed(ks))
               drhom = 0.561*(cmud(k)-CST)
               drhoms = 0.561*(cmud(ks)-CST)
               avdrhomv = 0.5*(drhom+drhoms)
               ddv = 2*dt/((dmm*(rhow+drhom)) + (dms*(rhow+drhoms)))
               gdv = g/(rhow+avdrhomv)
               eta = dd-hh
               etas = ds-hs
               etam = dmm - hh
               etams = dms - hs
               diffv = RHOW1*(eta - etas) + avdrhomv*(etam - etams) +
     1                 0.25*(dmm+dms)*(drhom-drhoms)
               vm(k) = (vv -gdv*dtbydx*diffv -
     1             omega*uu*dt + ddv*tti*v(k))/(1.0 + ddv*(ttb+tti))
c
             elseif ((dmm.gt.dmin).and.(dms.le.dmin))then
c  ...                                 Mud in current cell but none to south
               tti = ti(k)
```

```
              ttb = tbed(k)
              drhom = 0.561*(cmud(k)-CST)
              ddv = dt/(dmm*(rhow+drhom))
              gdv = g/(rhow+drhom)
              eta = dd-hh
              etas = ds - hs
              etam = dmm - hh
c   NB dms = 0
              etams = - hs
              diffv = RHOW1*(eta - etas) + drhom*(etam - etams) +
     1              0.5*dmm*drhom
              vm(k) = (vv -gdv*dtbydx*diffv -
     1             omega*uu*dt + ddv*tti*v(k))/(1.0 + ddv*(ttb+tti))
c  .. Don't allow mud to flow north
              if (vm(k).gt.0.0) vm(k) = 0.0
c
            elseif ((dmm.le.dmin).and.(dms.gt.dmin))then
c  ...                                  No mud in current cell but mud to south
              tti = ti(ks)
              ttb = tbed(ks)
              drhoms = 0.561*(cmud(ks)-CST)
              ddv = dt/(dms*(rhow+drhoms))
              gdv = g/(rhow+drhoms)
              eta = dd - hh
              etas = ds - hs
c  NB dmm = 0
              etam = - hh
              etams = dms - hs
              diffv = RHOW1*(eta - etas) + drhomS*(etam - etams) -
     1              0.5*dms*drhoms
              vm(k) = (vv -gdv*dtbydx*diffv -
     1             omega*uu*dt + ddv*tti*v(k))/(1.0 + ddv*(ttb+tti))
c  ...  Don't allow mud to flow south
              if (vm(k).lt.0.0) vm(k) = 0.0
            endif
c
          endif
c
        endif
c end of v velocity section
c-----------------------------------------------------------------------
c  ...                        end of loop over kij
 100  continue
c
      return
c
      end
c
c-----------------------------------------------------------------------
```

Appendix 4: Program Listing for the Author's Simple Numerical Model to Represent the Effects of Turbulence Damping

A SIMPLE NUMERICAL MODEL TO REPRESENT THE EFFECTS OF TURBULENCE DAMPING

```
C     PROGRAM TO DETERMINE EFFECTS OF DAMPING OF TURBULENCE
C     COPYRIGHT M.CRAPPER 1995
C
      REAL MASS(100), C(100), WS(100), USTAR(100), G(100), FLUX(100)
      REAL NEWMASS(100),UPFLUX(100),DNFLUX(100),OTM,NTM
      REAL U, CSTART, DZ, DT, WS1, WS2, WS3, WS4, WS5, WSMIN
      REAL PSI, DEPTH, SIMTIME, MINSOUT, MINS, KALPHA, KBETA
      INTEGER K, NKSTEPS, I
      INTEGER*4 T,NTSTEPS, NOUTS, NSTEPS
C
      OPEN (UNIT=5, FILE='U09030.PRN')

      DO I = 1,100
            MASS(I)=0
            C(I)=0
            WS(I)=0
            USTAR(I)=0
            G(I)=0
            FLUX(I)=0
            NEWMASS(I)=0
            UPFLUX(I)=0
            DNFLUX(I)=0
      END DO

      U = 0.09
      CSTART = 30.0
      DZ = .005
      DT = .01
      WS1 = 5.657E-08
      WS2 = 1.291
      WS3 = .002137
      WS4 = .155
      WS5 = -.45
      WSMIN = .00004
C     KALPHA = 0.2 - (0.002*CSTART)
      KALPHA = 0.2
C     KBETA = 0.0
      KBETA = -0.002
C     MUST BE NEGATIVE FOR DAMPING OF TURBULENCE
      PSI = 0.1143
      DEPTH = .05
      SIMTIME = 10
      NKSTEPS = IFIX((DEPTH / DZ)+0.5)
C     NTSTEPS = IFIX((SIMTIME * 60 / DT)+0.5)
      NTSTEPS = 360000
      MINSOUT = 0.5
C     NOUTS = INT((MINSOUT * 60 / DT) + .5)
      NOUTS = 60000

      DO K = 1,NKSTEPS
            MASS(K) = CSTART * DZ
            C(K) = CSTART
            USTAR(K) = U * (KALPHA + (KBETA * C(K)))
      END DO

C     WRITE OUT INITIAL CONDITION

      MINS=0
      WRITE (2,9999) MINS
      WRITE (5,9999) MINS
      DO K = 1,NKSTEPS
            HEIGHT = ((K - 1) * DZ)
            WRITE (2,9998) HEIGHT, USTAR(K),
```

```
     1                    C(K)
            WRITE (5,9998) HEIGHT, USTAR(K),
     1                    C(K)
      END DO

C     START TIME LOOP

      NSTEPS = 0
      DO T = 1,NTSTEPS
            MINS = (T - 1) * DT / 60
            NSTEPS = NSTEPS + 1

C     LOOP THROUGH WATER COLUMN CALCULATING UPWARD AND DOWNWARD
FLUXES

            DO K = 1,NKSTEPS
                  IF (C(K).LT.4) THEN
                        WS(K) = WS1 * ((C(K) * 1000) ** WS2)
                  ELSE IF (C(K).LT.15.3) THEN
                        WS(K) = WS3
                  ELSE
                        WS(K) = WS4 * ((C(K) * 1000) ** WS5)
                  END IF
                  IF (WS(K).LT.WSMIN) WS(K) = WSMIN
                  USTAR(K) = U * (KALPHA + (KBETA * C(K)))
                  IF (USTAR(K).LT.0) USTAR(K) = 0
                  DNFLUX(K)=DT*WS(K)*C(K)
                  UPFLUX(K)=DT*PSI*USTAR(K)*C(K)
                  FLUX(K)=UPFLUX(K)-DNFLUX(K)
C                 WRITE (2,*) K,UPFLUX(K), DNFLUX(K), FLUX(K)
                  IF (ABS(FLUX(K)).GT.MASS(K)) THEN
                        UPFLUX(K)=MASS(K)*UPFLUX(K)/FLUX(K)
                        DNFLUX(K)=MASS(K)*DNFLUX(K)/FLUX(K)
                        FLUX(K)=UPFLUX(K)-DNFLUX(K)
                  END IF
            END DO

C     CALCULATE EXCHANGE OF MASS DUE TO FLUXES

            NEWMASS(1)=MASS(1)-UPFLUX(1)+DNFLUX(2)
            IF (NEWMASS(1).LT.0) NEWMASS(1)=0
            DO K=2, NKSTEPS-1
                  NEWMASS(K)=MASS(K)+UPFLUX(K-1)-UPFLUX(K)+
     1            DNFLUX(K+1)-DNFLUX(K)
                  IF (NEWMASS(K).LT.0) NEWMASS(K)=0
            END DO
            NEWMASS(NKSTEPS)=MASS(NKSTEPS)+UPFLUX(NKSTEPS-1)-
     1            DNFLUX(NKSTEPS)
            IF (NEWMASS(NKSTEPS).LT.0) NEWMASS(NKSTEPS)=0
            OTM=0
            NTM=0
            DO K=1, NKSTEPS
                  OTM=OTM+MASS(K)
                  NTM=NTM+NEWMASS(K)
                  MASS(K)=NEWMASS(K)
                  C(K)=MASS(K)/DZ
            END DO
C           WRITE (2,*) OTM, NTM

C     ON OUTPUT LOOP, WRITE OUT NEW CONDITION

            IF (NSTEPS.LT.NOUTS) GOTO 100
            WRITE (2,9999)  MINS
            WRITE (5,9999)  MINS
            DO K = 1,NKSTEPS
                  HEIGHT = ((K - 1) * DZ)
                  WRITE (2,9998) HEIGHT, USTAR(K),
```

```
     1                    C(K)
                    WRITE (5,9998) HEIGHT, USTAR(K),
     1                    C(K)
             END DO
             NSTEPS = 0

C      END TIME LOOP

100    END DO
       STOP
9999   FORMAT(1X,F5.1)
9998   FORMAT(1X,F5.3,2H M,1X,F10.8,4H M/S,1X,F9.4,4H G/L)
       END
```

Appendix 5: Equations of Motion and Methods of Solution in the Fluent Computational Fluid Dynamics Software version 4.2.2

A5.1 The *Fluent* Software As Applied to the Simulation of Flows in the Race Track Flume

The following sections describe the *Fluent* software version 4.2.2, as used to obtain the simulation results described in chapter 3 of this thesis. The *Fluent* package is in fact very extensive, allowing a whole range of liquid and gas flow, heat transfer, chemical reaction and combustion processes to be simulated as well as the basic laminar and turbulent flow of water. In this section, only the theory on which the software is founded and the specific options used in the current investigation are discussed. For a full discussion of the package's capabilities, the reader should consult the *Fluent User's Guide* (Fluent Incorporated 1993).

A5.2 Basic Equations of Motion

The basic equations of motion used in *Fluent* are in fact the Navier-Stokes equations. The continuity equation is:

$$\frac{\partial \rho}{\partial t} + \frac{\partial}{\partial x_i}(\rho u_i) = 0 \qquad \text{(A5.1)}$$

whilst conservation of momentum in the ith direction is described by:

$$\frac{\partial}{\partial t}(\rho u_i) + \frac{\partial}{\partial x_j}(\rho u_i u_j) = \frac{\partial p}{\partial x_i} + \frac{\partial \tau_{ij}}{\partial x_j} + \rho g_i \qquad \text{(A5.2)}$$

In these equations, ρ represents the fluid density, t x_i and u_i the distance and velocity in the ith direction, p the fluid pressure and g_i the acceleration due to gravity (or other body forces) in the ith direction. τ_{ij} is the shear stress tensor.

It will be noted that equations A5.1 and A5.2 do not include any source/sink terms. This is because for water flow in the Race Track Flume, both mass and momentum are conserved within the water. In fact, the *Fluent* software does allow the souring or sinking of mass and momentum due to exchange with another phase, for example due to combustion or chemical reactions. However, these features were not used in the author's application of the software.

A5.3 Evaluation of Shear Stresses and the Modelling of Turbulence

In laminar flow, the shear stress tensor τ_{ij} is dependent solely on the viscous properties of the fluid as per the derivation of the Navier-Stokes equations (see for example Curle and Davies 1968). In turbulent flow such as that in the Race Track Flume, however, viscous shear stresses are small compared with those resulting from turbulent fluctuations in the flow.

At present, it is not possible to simulate fluid turbulence directly, and *Fluent* therefore evaluates turbulent shear stresses as time averaged values, with closure of the equations being achieved by relating time averaged turbulent shear stresses to mean flow properties. *Fluent* can do this in various different ways, but in the author's application of the software use was made of the Reynolds Stress Model, as mentioned in section 3.11, chapter 3. The following section gives only a brief overview of the Reynolds Stress Model equations; the reader wishing a fuller explanation of this aspect of the *Fluent* package should consult either Launder et al (1975) and Launder and Spalding (1973).

In turbulent flow, the ith direction velocity at any instant is represented by the formulation

$$u_i = [u_i] + u'_i \qquad \text{(A5.3)}$$

where the primes indicate a turbulent fluctuation of a mean flow property and the square brackets refer to a temporal average, over a timescale sufficiently long to

encompass many turbulent fluctuations, of the quantity they enclose. It follows from this notation that the time averaged stress tensor τ_{ij} can be expressed by:

$$\tau_{ij} = \rho [u'_i u'_j] \tag{A5.4}$$

which can be inserted into the second term on the right hand side of the momentum equation A5.2 without affecting any of the other terms except to replace all the u_i parameters by their temporal means $[u_i]$.

The correlation $[u_i'u_j']$ in equation A5.4 has six unique terms which in the Reynolds Stress Model are evaluated in terms of mean flow properties by solving equation A5.5:

$$\frac{\partial [u'_i u'_j]}{\partial t} + [u_k] \frac{\partial [u'_i u'_j]}{\partial x_k} = \frac{\partial}{\partial x_k} \left(\frac{\mu_t}{\sigma_k} \frac{\partial [u'_i u'_j]}{\partial x_k} \right) + P_{ij} + \Phi_{ij} - \epsilon_{ij} + R_{ij} \tag{A5.5}$$

Here, P_{ij} represents the production of turbulence, Φ_{ij} is a source sink term due to the pressure/strain correlation in the fluid, ε_{ij} is the viscous dissipation corrected for directional influences in non-isotropic turbulence and R_{ij} is a rotational term. The parameter μ_t is a turbulent eddy viscosity and σ_k is an empirical Prandtl number governing the diffusion of turbulent kinetic energy.

The turbulent eddy viscosity μ_t is computed from:

$$\mu_t = \rho C_\mu \frac{k^2}{\epsilon} \tag{A5.6}$$

where C_μ is a constant and k is the turbulent kinetic energy derived from equation A5.7:

$$k = \frac{1}{2}\sum_{i}[u_i^2] \qquad \text{(A5.7)}$$

The parameter ε in equation A5.6 represents isotropic viscous dissipation, and is determined by means of a number of empirically based assumptions.

In equation A5.5, the production term P_{ij} is computed directly, without the use of any assumptions:

$$P_{ij} = \left([u'_i u'_j] \frac{\partial u_j}{\partial x_k} + [u'_j u'_k] \frac{\partial u_i}{\partial x_k} \right) \qquad \text{(A5.8)}$$

However, Φ_{ij}, ε_{ij} and R_{ij} are variously derived according to the modelling assumptions inherent in the Reynolds Stress Model (Fluent Incorporated 1993).

A5.4 Wall Boundary Conditions in Fluent

In regions close to wall boundaries, *Fluent* applies the log-law of the wall to compute the wall shear stress:

$$\frac{u}{u*} = \frac{1}{\kappa}\log\left(9.8\frac{\rho u* y}{\mu}\right) \qquad \text{(A5.9)}$$

where $u^* = \sqrt{(\tau_w/\rho)}$, τ_w is the wall shear stress, κ is von Kárman's constant and y is the distance from the wall. The factor of 9.8 applies to a smooth wall condition, which is a fair approximation for the smooth steel or glass of the walls of the Race Track Flume.

The solution grid used by *Fluent* must be set up in such a way as to ensure that the grid line closest to the wall falls within the region where equation A5.9 is valid. Thus the user must ensure that:

$$25 \leq \frac{\rho y_{gr} u*}{\mu} \leq 300 \; to \; 500 \qquad \text{(A5.10)}$$

where y_{gr} is the distance from the wall to the first grid line.

The near-wall value of isotropic turbulent dissipation ε is calculated from an empirically based formulation (Fluent Incorporated 1993).

A5.5 Finite Difference Scheme used by Fluent

The equations describing the flow field are solved in *Fluent* by means of a finite difference scheme in which differential equations are converted to algebraic equations. This is done by quantifying the values of the properties in the equations at discreet points on a grid of known dimensions. The grid structure is illustrated schematically in figure A5.1. Values of velocity, pressure and turbulent properties are stored at the centre of each grid cell, and the solution of the model equations then depends on relating the values at each face of the grid cell to the values at the centres of all the neighbouring cells, so as to determine the fluxes between cells.

Fluent provides various alternative methods for actually carrying out the interpolation of properties at cell faces; in the author's application of *Fluent* the most basic option, the Power Law Scheme, was used. This provided an adequately rapid solution for the Race Track Flume, meaning there would have been no point in utilising the additional computing resources required by the optional, higher order interpolation schemes.

The Power Law Scheme interpolates the face value of a variable, ϕ, by means of an exact solution to a one-dimensional advection-diffusion equation:

$$\frac{\partial}{\partial x}(\rho u \phi) = \frac{\partial}{\partial x}\Gamma\frac{\partial \phi}{\partial x} \qquad \text{(A5.11)}$$

in which ρu and the diffusivity parameter Γ are assumed to be constant over the interval ∂x. This equation can be integrated to give the solution:

$$\frac{\phi(x) - \phi_0}{\phi_l - \phi_0} = \frac{e^{\left(\frac{\rho u x}{\Gamma}\right)} - 1}{e^{\left(\frac{\rho u L}{\Gamma}\right)} - 1} \qquad \text{(A5.12)}$$

where $\phi_0 = \phi|_{x=0}$ and $\phi_L = \phi|_{x=L}$.

The value of the term $\rho uL/\Gamma$ governs the relative importance of advection and diffusion and is known as the Peclet number. Clearly, the value of Γ used in the solution of equation A5.12 depends upon the property represented by the variable ϕ (Patankar 1981).

A5.6 Solution of the Discretised Equations

Having discretised the continuity and momentum equations, a position is arrived at where the discretised equations must be solved so as to give an acceptable balance between values stored at the cell centres and the resulting inter-cell fluxes. In *Fluent*, this procedure is carried out iteratively and progressed line-by line across the finite difference grid. This iterative approach represents a considerably more efficient approach to the use of computer resources than would a simultaneous solution of the equations across the full flow field.

The basic iterative solution procedure is illustrated below by consideration of a one-dimensional momentum equation. A discretised form of this equation, developed as described in the previous section, can be written as:

$$A_P u_P = \sum_{NB} A_{NB} u_{NB} + (p_W - P_E)A + S \qquad \text{(A5.13)}$$

in which A_P and A_{NB} are coefficients containing the convection and diffusion contributions to the momentum equation. The subscript $_P$ refers to the current point of interest in the solution, whilst the subscript $_{NB}$ refers to 'neighbour' points, which are specifically described by the subscripts $_W$ (West) and $_E$ (East).

The solution starts by the substitution of a guessed pressure field, p_G, into equation A5.13, which can then be used to determine a guessed velocity field, u_G. The guessed pressure and velocity fields are now related to the actual fields according to equation A5.14:

$$\begin{aligned} p &= p_G - p' \\ u &= u_G + u' \end{aligned} \qquad \text{(A5.14)}$$

p, p_G, p', u, u_G and u' are of course general expressions for the pressure and velocity fields. At a specific point they become p_W, p^*_W, p'_W etc. Equation A5.14 can be substituted back into A5.13 to yield a 'momentum balance' equation in terms of the velocity and pressure corrections u' and p'. This leads to the equation

$$u'_P = \frac{1}{A_P}(p'_W - p'_E)A \qquad \text{(A5.15)}$$

expressing the velocity correction in terms of pressure corrections.

A similar process to that described above is used on the continuity equation so as to derive an expression for the pressure correction p'. This leads to:

$$-(\rho A)_W \left(\frac{1}{A_P}\right)_W \left(p'_W - p'_P\right) = 0 \qquad \text{(A5.16)}$$

This equation can be solved to give the correction for the pressure field, which can then be used in equation A5.15 to determine the velocity correction. Thus, the whole flow field can ultimately be solved (Patankar 1981, Fluent Incorporated 1993).

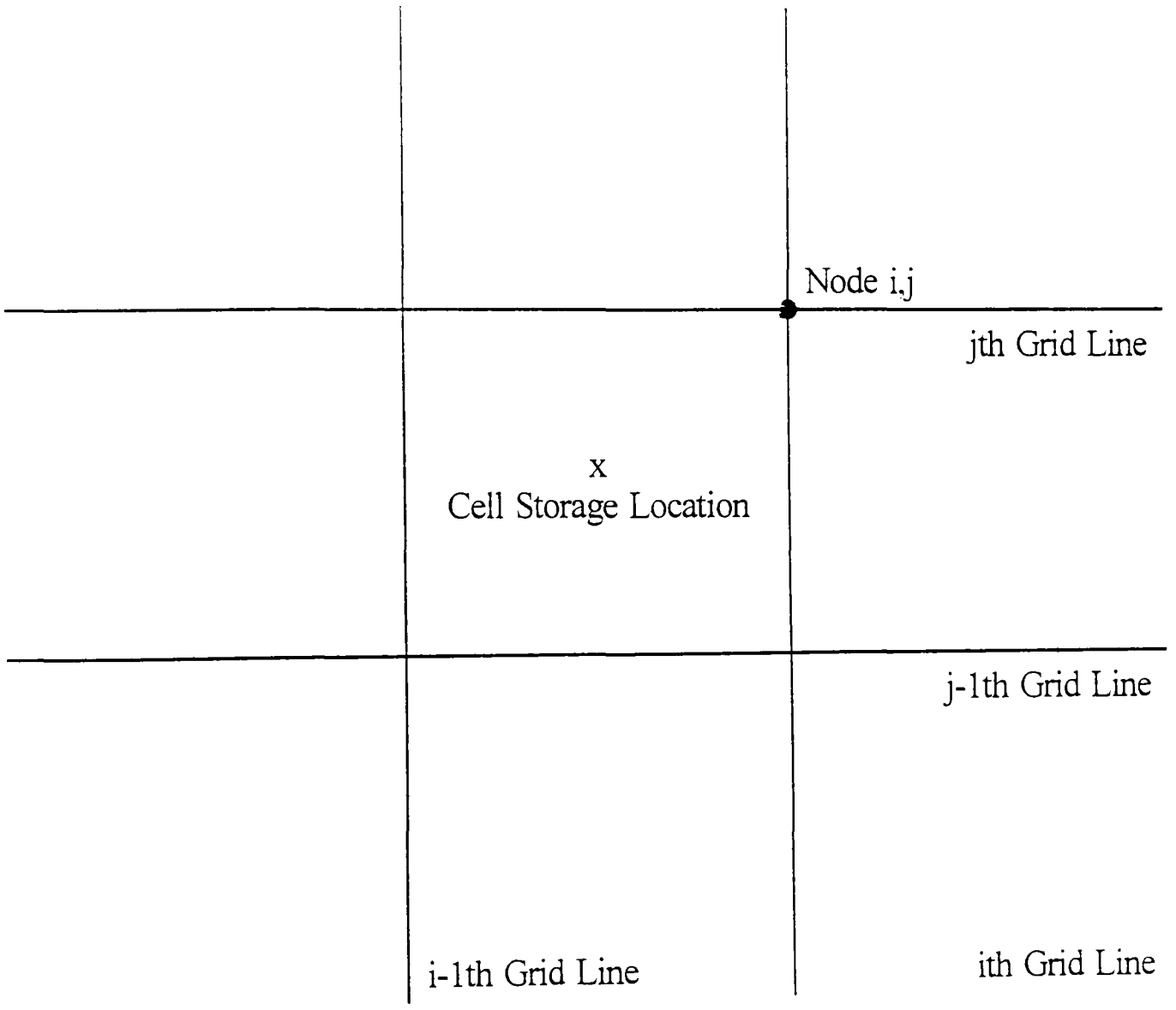

Figure A5.1: Schematic of *Fluent* Grid Structure